BỘ GIÁO DỤC VÀ ĐÀO TẠO

TRƯỜNG ĐẠI HỌC SƯ PHẠM KỸ THUẬT TP.HCM

PHẠM ĐÌNH THÁI

DANH MỤC BÀI BÁO ĐÃ CÔNG BỐ LIÊN QUAN ĐẾN ĐỀ TÀI LUẬN ÁN

1. **T. D. Pham**, T. T. Nguyen, and L. C. Kien, "Minimization of total costs for distribution systems with battery energy storage systems and renewable energy sources," *Scientific Reports*, vol. 15, no. 1, 17147, 2025. (**SCIE, Q1, IF=3.9**).
2. **T. D. Pham**, T. T. Nguyen, and L. C. Kien, "Minimize renewable distributed generator costs while achieving high levels of system uniformity and voltage regulation," *Ain Shams Engineering Journal*, vol. 15, 102720, 2024. (**SCIE, Q1, IF=6.0**).
3. **T. D. Pham**, "Integration of Photovoltaic Units, Wind Turbine Units, Battery Energy Storage System, and Capacitor Bank in the Distribution System for Minimizing Total Costs Considering Harmonic Distortions," *Iranian Journal of Science and Technology, Transactions of Electrical Engineering*, vol. 47, pp. 1265-1282, 2023. (**SCIE, Q2, IF=2.4**).
4. **T. D. Pham**, T. T. Nguyen, and L. C. Kien, "Optimal Placement of Photovoltaic Distributed Generation Units in Radial Unbalanced Distribution Systems Using MATLAB and OpenDSS-Based Cosimulation and a Proposed Metaheuristic Algorithm," *International Transactions on Electrical Energy Systems*, pp. 1-21, 2022. (**SCIE, Q2, IF=2.3**).
5. **T. D. Pham**, T. D. Nguyen, and L. C. Kien, "An Improved Equilibrium Optimizer for Optimal Placement of Distributed Generators in Distribution Systems considering Harmonic Distortion Limits," *Complexity*, pp. 1-23, 2022. (**SCIE, Q2, IF=2.3**).
6. **T. D. Pham**, H. D. Nguyen, and T. T. Nguyen, "Reduction of emission cost, loss cost and energy purchase cost for distribution systems with capacitors, photovoltaic distributed generators, and harmonics," *Indonesian Journal of Electrical Engineering and Informatics*, vol. 11, pp. 36-49, 2023. (**Scopus, Q4**).
7. **T. D. Pham**, L. C. Kien, and T. H. Tinh, "Optimization Planning Method of Renewable distributed Generation in Radial Distribution Systems," *VNUHCM Journal of Science and Technology Development*, vol. 26, pp. 2776-2790, 2023.

TP. HỒ CHÍ MINH – năm 2025

scientific reports

Check for updates

OPEN

Minimization of total costs for distribution systems with battery energy storage systems and renewable energy sources

Thai Dinh Pham[1], Thang Trung Nguyen[2]✉ & Le Chi Kien[1]

The penetration of renewable energy distributed generation units in the distribution systems has become widespread due to its many techno-economic and environmental benefits. However, avoiding the unwanted effects of unplanned integration and maximizing the resulting benefits is challenging. Thus, this research introduces a powerful method called modified coyote optimization algorithm (MCOA) for identifying the optimal installation of wind turbine farms (WFs), photovoltaic farms (PVFs), and battery energy storage systems (BESS) in IEEE 123-bus unbalanced distribution system (UDS) and Nha Be 55-bus balanced distribution system (BDS) in Nha Be District, Ho Chi Minh City, Vietnam to minimize total costs. The considered costs include (1) investment, operation, and maintenance (O&M) costs of WFs, PVFs, and BESS; (2) imported energy cost for loads and power losses from the main power grid; and (3) generated emission cost from conventional power plants considering time-varying generation and consumption. Besides, this work also suggests an open-source simulator (OpenDSS) for addressing the power flow problem and develops a co-simulation between two active software (OpenDSS and MATLAB) through the component object model (COM) interface for addressing the continuous optimization problems. The proposed solution by MCOA has demonstrated superiority over other methods through total cost savings of up to 24.13% and 27.46% in IEEE 123-bus UDS and 55-bus BDS, while the values are only 23.11% and 26.50% for salp swarm algorithm (SSA) and 23.76% and 26.78% for coyote optimization algorithm (COA), respectively, as compared to the original cases. Besides, the optimal solution also satisfied the declared constraints as well as the standards for bus voltage, line current, and harmonic distortions.

Keywords Modified coyote optimization algorithm, Battery energy storage system, Photovoltaic farms, Unbalanced distribution system, Wind turbine farms

List of symbols

$\Delta I_{b,a,o}$	Penalty amount for the *b*th current branch at the *o*th solution from the *a*th pack
$\Delta V_{s,a,o}, \Delta IHD_{s,a,o}, \Delta THD_{s,a,o}$	Penalty amounts for voltage, IHD and THD at the *s*th bus from the *o*th solution of the *a*th pack
$E^{Rated}_{BESS,k}, E^{Min}_{BESS}, E^{Max}_{BESS}$	The rated capacity of the *k*th BESS, min and max installing capacity of BESS
N_H, N_{Hr}, N_Y	Number of considering hours, harmonic orders and years
$\mathrm{THD}_{\mathrm{s,h,y}}$	Total harmonic distortion of the *s*th bus at the *h*th hour and the *y*th year
$C^{Cap}_{WF}, C^{Cap}_{PVF}, C^{Cap}_{BESS}$	Capital cost of WFs, PVFs and BESS of the BESS ($/MW)
$C^{O\&M}_{WF}, C^{O\&M}_{PVF}, C^{O\&M}_{BESS}$	O&M cost of WFs ($/MWh), PVFs ($/MWh) and BESS ($/MW-year)
$En^{Rated}_{BESS,k}$	Rated energy of the *k*th BESS
$IHD^{Hr}_{s,h,y}$	Individual harmonic distortion of the *Hr*th order from the *s*th bus of the *h*th hour and the *y*th year

[1]Faculty of Electrical and Electronics Engineering, Ho Chi Minh City University of Technology and Education, Ho Chi Minh City, Vietnam. [2]Power System Optimization Research Group, Faculty of Electrical and Electronics Engineering, Ton Duc Thang University, Ho Chi Minh City, Vietnam. ✉email: nguyentrungthang@tdtu.edu.vn

$L^{Max}_{WF,i}, L^{Max}_{PVF,j}, L^{Max}_{BESS,k}$	Maximum location for connecting the *i*th WF, the *j*th PVF and the *k*th BESS
$L^{Min}_{WF,i}, L^{Min}_{PVF,j}, L^{Min}_{BESS,k}$	Minimum location for connecting the *i*th WF, the *j*th PVF and the *k*th BESS
$N_{BESS}, N_{WF}, N_{PVF}$	Number of BESSs, WFs and PVFs
N_{bh}, N_{bs}, N_{ρ}	Number of branches, buses and phases in the system
N_a, N_o	Number of packs in population and number of coyotes from each pack
$P^{Sub}_{h,y}, Q^{Sub}_{h,y}$	Active and reactive powers from main grid at the *h*th hour and the *y*th year
$P^{DisCh}_{BESS,k,h,y}, P^{Ch}_{BESS,k,h,y}$	Discharging and charging active power of the *k*th BESS from the *h*th hour and the *y*th year
$P^{Min}_{BESS,k,h}, P^{Max}_{BESS,k,h}$	Minimum and maximum capacities for connecting the *k*th BESS at the *h*th hour
$P^{Min}_{PVF}, P^{Max}_{PVF}$	Minimum and maximum installed capacity of each PVF
$P^{Gen}_{WF,i,h,y}, P^{Gen}_{PVF,j,h,y}$	Real active power of the *i*th WF and the *j*th PVF at the *h*th hour and the *y*th year
$P^{Max}_{WF,i}, P^{Max}_{PVF,j}$	Maximum capacity for connecting the *i*th WF and the *j*th PVF
$P^{Min}_{WF,i}, P^{Min}_{PVF,j}$	Minimum capacity for connecting the *i*th WF and the *j*th PVF
$P^{Rated}_{WF,i}, P^{Rated}_{PVF,j}, P^{Rated}_{BESS,k}$	Rated active power of the *i*th WF, the *j*th PVF and the *k*th BESS
$P^{Min}_{WF}, P^{Max}_{WF}$	Minimum and maximum installed capacity of each WF
$Q^{DisCh}_{BESS,k,h,y}, Q^{Ch}_{BESS,k,h,y}$	Discharging and charging reactive power of the *k*th BESS from the *h*th hour and the *y*th year
$Q^{Gen}_{WF,i,h,y}, Q^{Gen}_{PVF,j,h,y}$	Real reactive power of the *i*th WF and the *j*th PVF from the *h*th hour and the *y*th year
$Q^{ls}_{b,h,y}, P^{ls}_{b,h,y}$	Reactive and active powers of the *b*th loss from the *h*th hour and the *y*th year
$Q^{ld}_{l,h,y}, P^{ld}_{l,h,y}$	Reactive and active powers of the *l*th load from the *h*th hour and the *y*th year
$Fit_{a,o}$	The fitness values from the *o*th solution of the *a*th pack
V^{Min}, V^{Max}	Minimum and maximum phase voltage values
$\mathcal{X}_{best\_pk,a}, \mathcal{X}_{best\_pn}$	The best solutions from the *a*th pack and the current population, respectively
$\mathcal{X}_{best\_pk,r1}, \mathcal{X}_{best\_pk,r2}, \mathcal{X}_{best\_pk,r3}$	The randomly selected best solutions in the packs
$\mathcal{X}_{r1,a}, \mathcal{X}_{r2,a}$	The randomly selected solutions in the *a*th pack
$\alpha_I, \alpha_V, \alpha_{IHD}, \alpha_{THD}$	Penalty factors of branch current, voltage bus, IHD and THD
dc	Discount rate in the present value factor (9%)
ite^{Max}, ite	The maximum and current iteration numbers
$r, r_1, r_2, r_3, r_4, r_5, \lambda$	Randomly generated numbers in the range between 0 and 1

Gradual depletion of fossil fuel sources and constantly increasing demand have strongly contributed to promoting the penetration of distributed generation resources, especially renewable energies, in meeting electricity demand as well as improving the efficiency and flexibility of the networks[1,2]. According to published data by the U.S. Energy Information Administration in 2017, 17% of the electricity supply for the total energy demand of the United States is from renewable energy sources, and this proportion is estimated to increase sharply in the future[3]. Some other large countries, such as India and China, have also reported significant penetration. The Indian government has stated that 175 GW will be generated by renewable energy resources in 2022, including 100 GW for solar energy and 60 GW for wind energy, and a penetration of 227 GW by 2027 will be considered an energy target[4]. In addition, China also generated up to 94 GW from solar energy in 2017, aiming for non-fossil energy to be 20% of total energy demand by 2030[3]. Due to the enormous economic and technical benefits gained, the penetration of distributed generation units (DGUs) is increasing rapidly. However, unplanned connections can seriously affect the power grid, such as increased branch power loss, changed bus voltage, voltage transients, and reduced reliability[5]. Therefore, integration of DGUs requires careful consideration to maximize welfare and avoid negative impacts.

Previous studies have proposed different approaches to determine the suitable connection of distributed generation units in the distributed system. As[6–8], studies have applied particle swarm optimization (PSO) as an optimum technique to solve the problem of DGU installation for minimizing losses on distribution branches and improving the voltage at the buses. PSO is one of the most popular meta-heuristic algorithms used to optimization problems in the real world. PSO stands out for its simple structure and few control parameters. Its most significant disadvantage is early convergence in the local regions, which leads to poor performance. Similarly, another popular method is the artificial bee colony (ABC) algorithm, which is inspired by the behavior of bees from nature. While the authors in[9] applied ABC to reduce both total power loss and improve the voltage sag index in the system through connecting distributed generators, the authors[10] used ABC for minimizing voltage deviation index, line loading and branch power losses in the distribution systems by using BESS. The authors significantly enhanced the distribution system's performance by identifying a suitable installation that could improve the voltage profile, mitigate line loading, and reduce total loss. ABC is a relatively good method, but its algorithm structure is complicated. Moreover, there are three phases of onlooker bee, employed bee and scout bee, which are implemented in the model, so it takes a lot of time to process data. Besides, other studies such as[11,12] also introduced ant lion optimization algorithm (ALOA) to minimize total power loss and

maximize the net savings thanks to installing renewable energy units in several distribution systems. Like the stochastic algorithms, ALOA handles optimization problems by iteratively trying to improve the quality of solutions. Although ALOA is considered a friendly method, its biggest drawback is instability. It is more likely to fall into local optima, so it is limited to solving problems with the large search space. With the same objective function for the above optimization problem, the authors in[13,14] suggested applying an adaptive biogeography-based optimization (BBO) method. BBO is known to be a helpful method for solving various complex problems. However, the processing speed of BBO is quite slow, and its performance is mainly affected by the control parameters. Additionally, for reducing energy losses, some authors[15] have also successfully found a suitable installation of BESS in the balanced system considering the duck curve phenomenon by using whale optimization algorithm (WOA), firefly algorithm (FA), and PSO. The results obtained show that WOA performs better than the compared methods. Similarly, research[16] suggested a coyote optimization algorithm (COA) to compare with WOA, FA, and PSO in determining the optimal allocation and sizing of the lithium-ion BESS in cases without and with photovoltaic units. Energy loss reduction has increased significantly by integrating BESS and photovoltaic generation units simultaneously. In that study, COA also proved outstanding in solving optimization problems compared to others. In addition to the mentioned methods, many other approaches are applied to optimize the installation of DGUs in distribution power network, such as the modified moth flame optimization (MMFO) algorithm[17], garra rufa optimization (GRO)[18], improved decomposition based evolutionary algorithm (I-DBEA)[1], harmony search (HS) algorithm[19], genetic algorithm (GA)[20], harris hawks optimizer (HHO)[21], Kalman filter algorithm (KFA)[22] and intelligent water drop (IWD) algorithm[23]. Most of these studies have only focused on reducing total power loss on the branches as well as enhancing voltage profile as the primary target. However, to fully evaluate the effectiveness of an integrated system, it is most important to consider the total costs of operating the system for a long time, and only a few studies in the past have taken this into account[24,25]. Those studies have calculated the associated costs, including investment costs, operation, and maintenance of grid-connected units. However, the authors applied optimization algorithms that are less efficient in terms of performance and stability, such as ABC[24] and water cycle algorithm (WCA)[25]. On the other hand, total costs are only considered at the peak load level. Therefore, the found global solutions are uneconomical at different loads. Several researchers have recently considered the time-varying generation and consumption to enhance the quality of the optimal solution. Specifically, study[26] looks at a 24-h variation of photovoltaic, wind turbines, and load demand to cut the long-term costs of operating the distribution system using a mixed-integer program (MIP). Similarly, research[27] sought the optimal strategy for integrating BESS with high penetration from wind turbines and photovoltaic units considering 24-time segments. By applying an efficient algorithm, which has been published in recent years, called the salp swarm algorithm (SSA), this research has succeeded in minimizing costs incurred in the operating system, preventing reverse power flow and peak shaving in the balanced distribution system. Generally, most studies in the past were only implemented in the balanced three-phase distribution systems with objectives related to total costs that have not been fully considered. However, unbalanced three-phase distribution systems are more complicated than balanced three-phase distribution systems, and it has received very little attention from researchers[28]. In addition, integrating renewable energy resources into distribution systems will significantly increase the harmonic distortions due to applied inverters. However, harmonic generation from inverter-based renewable energy sources has yet to be considered much in the published papers. A summary of previous relevant studies and existing gaps is also presented as Table 1.

Previous studies have successfully determined the optimal solution for connecting DGUs to the distribution grid to minimize losses and enhance the voltage profile. However, to implement a project for integrating generation sources into the existing grid, it is necessary to comprehensively consider the economic-technical-environmental aspects in the long term of the entire project life cycle. As referenced from the past studies in the introduction section, previous studies have many limitations such as (1) poorly established constraints, (2) simple objective functions (mostly only concerned with technical factors), (3) applied algorithms are inefficient, (4) test systems are small and often consider balanced distribution systems (rarely consider unbalanced systems), (5) little consideration is given to harmonics from nonlinear loads and power converters, and (6) little attention is paid to considering load and generation changes over time. Therefore, this study is conducted to overcome the shortcomings of past studies. This paper considers the integration of wind farms (WFs), photovoltaic farms (PVFs), and battery energy storage systems (BESS) simultaneously into IEEE 123-bus UDS with devices such as capacitors, switches, and voltage regulators[29] and 55-bus BDS in Nha Be District, Ho Chi Minh City, Vietnam[30]. The paper's main objective is to (1) minimize the total costs of investment and O&M of WFs, PVFs, and BESS, (2) cut the electricity purchasing cost for load demand and branch losses from the primary grid through the substation, and (3) reduce the emissions cost from electricity production of the traditional power plants. Furthermore, this study proposes a co-simulation from OpenDSS and MATLAB to solve power flow problems in frequency domains. This is considered a powerful tool for flexibly and quickly calculating complex distribution systems. On the other hand, this paper also introduces an effective algorithm that was recently published for solving the optimization problem, named modified coyote optimization algorithm (MCOA)[31]. MCOA is considered an enhanced version modified in COA's new solution generation equations, leading to more efficiency in MCOA. The achieved results by applying MCOA are compared with the original method and another robust method for the same objective function and technical constraints. In summary, the primary contribution of this research is briefly presented below:

1. This study proposed the optimal solution for simultaneous installation of WFs, PVFs, and BESSs to two gird types of unbalanced and balanced distribution networks to minimize total costs, including (1) investment as well as O&M costs for connected units, (2) the cost of purchasing electricity from the primary grid through the substation and (3) the emissions cost from the traditional power plants.

No	Applied method	Connected units	Objective function			Test system	Shortcomings
1	PSO [1]	DGUs	Power loss minimization	Voltage enhancement	Costs reduction	26-bus BDS	Premature convergence
2	PSO [2]	DGUs	Yes	No	No	34-bus BDS	Limited number of constraints
3	PSO [3]	DGUs and DSTATCOM	Yes	Yes	No	12-bus, 34-bus and 69-bus BDSs	Simple objective with only considered loss
4	ABC [4]	DGUs	Yes	Yes	No	69-bus BDS	Lack of comparison with other methods
5	ABC [5]	BESS	Yes	Yes	No	33-bus BDS	Slow convergence Poor reliability when performed on a test system
6	ALOA [6,7]	DGUs	Yes	Yes	No	33-bus and 69-bus BDSs	Complex algorithm structure No consideration of uncertainty for renewables
7	BBO [8]	DGUs	Yes	Yes	No	33-bus and 69-bus BDSs	Performance was highly dependent on initial parameters Lack of comparison with other implemented methods under the same initial conditions The speed to achieve convergence was relatively slow
8	BBO [9]	DGUs	Yes	Yes	No	69-bus BDS	
9	WOA [10]	BESS	Yes	No	No	48-bus BDS	Low and unstable convergence The main goal was quite simple The constraints for the problem were not fully considered
10	COA [11]	BESS	Yes	No	No	48-bus BDS	Lack of implementation on different scale systems The considered target was simple
11	SOS [12]	DGUs	Yes	No	No	33-bus, 69-bus and 118-bus BDSs	Complex algorithm structure The considered constraints were limited Uncertain convergence
12	GRO [13]	DGUs	Yes	Yes	No	14-bus and 30-bus BDSs	Limited constraints Lack of implementation on large scale systems Slow convergence speed
13	I-DBEA [14]	DGUs	Yes	Yes	No	33-bus, 69-bus and 199-bus BDSs	Lack of comparison with other implemented methods under the same initial conditions Unstable convergence
14	HS [15]	DGUs	Yes	Yes	No	69-bus BDS	
15	AGA [16]	DGUs	Yes	Yes	No	33-bus and 52-bus BDSs	Limited constraints Lack of implementation on large scale systems
16	HHO [17]	DGUs	Yes	Yes	No	33-bus and 69-bus BDSs	Complex algorithm structure No consideration of operating power factor of DGUs Restricted Constraints
17	KFA [18]	DGUs	Yes	No	No	30-bus BDS	Simple objective Lack of comparison with other methods Uncertain convergence
18	IWD [1]	DGUs	Yes	No	No	10-bus, 33-bus and 69-bus BDS	The applied algorithm had many initial parameters Performance was greatly affected by the setting values
19	ABC [19]	DGUs	Yes	Yes	Yes	33-bus and 69-bus BDSs	Limited number of constraints Lack of comparison with other implemented methods under the same initial conditions Lack of considering the operating power factor of DGUs
20	WCA [20]	DGUs and CBs	Yes	Yes	Yes	33-bus and 69-bus BDSs	Lack of comparison with other implemented methods under the same initial conditions
21	MIP [21]	DGUs	Yes	Yes	Yes	33-bus BDS	The test system was small Lack of comparison with other methods
22	SSA [22]	DGUs and BESS	Yes	Yes	Yes	33-bus and 69-bus BDSs	Limited constraints Lack of considering the operating power factor of DGs Unbalanced power systems were not considered
23	IPSO [23]	DGUs	Yes	Yes	Yes	37-bus UDS	Test system was small Balanced systems were not tested Harmonic distortions of renewables were not considered Lack of comparison with other methods

Table 1. Summary of shortcomings of previous studies.

2. This paper has contributed to considering harmonic distortions from nonlinear loads and power conversion devices of distributed sources to keep the harmonic indices to IEEE Std. 519.
3. The study analyzed the impact of the simultaneous penetration of WFs, PVFs, and BESSs on the distribution system. Notably, the BESS's strategy of suitable charging and discharging energy over time has significantly contributed to reducing operating costs and improving system efficiency. These findings have practical implications for the design and operation of power networks, highlighting the relevance of this research.
4. The research has successfully developed a co-simulation from OpenDSS and MATLAB software. This co-simulation created a robust platform for tackling quick and convenient optimization problems in various distribution systems. This supports the enhancement of the research capabilities.
5. The study also introduced a novel method with high performance and stability compared to other meta-heuristic algorithms to address optimization problems in IEEE 123-bus UDS and 55-bus BDS in Ho Chi Minh

City, Vietnam. The results from the suggested method (MCOA) are shown to be more effective than other methods (SSA and COA).

The rest of the paper consists of the following sects: "Problem formulation" section gives the objective function and constraints; "Modified coyote optimization algorithm" section introduces modified coyote optimization algorithms; "Introduced method in solving the considering problem" section describes the suggested method's application for handling the optimization problem; "Simulation results" section shows the simulation results and the analysis; And "Conclusions" section summarizes the paper.

Problem formulation

In this work, the optimal integration for distributed generation units, including photovoltaic farms, wind turbine farms, and battery energy storage systems in IEEE 123-bus unbalanced and 55-bus balanced distribution systems, is determined to minimize total costs while still satisfying the technical criteria. This integrated distribution system is briefly illustrated in Fig. 1. In this model, WFs and PVFs are connected to the primary power grid to supply energy for the loads and losses through power conversion devices. If the amount of generated power is insufficient, electricity from the primary grid will be imported. Besides, to improve the system efficiency, BESS is also integrated into the grid to charge and discharge power at each time by the electricity price to save on operating the system.

The objective function of the study

This paper considers cutting total cots by integrating WFs, PVFs, and BESS as the objective function for the balanced and unbalanced distribution networks. These costs should be minimized and expressed in the mathematical equation like follows:

$$\text{Minimize } TC^{OF} = TC^{Inv\&OM}_{WF-PVF-BESS} + TC^{Sub}_{Purch\_Elec} + TC^{Sub}_{Emission} \quad (1)$$

where TC^{OF} is the total costs of the considered system; $TC^{Inv\&OM}_{WF-PVF-BESS}$ is the costs of the investment, O&M of WFs, PVFs and BESS; $TC^{Sub}_{Purch\_Elec}$ is the cost of importing electricity for consumption; $TC^{Sub}_{Emission}$ is defined as the cost of generating emissions (CO_2, SO_2 and NO_X) from traditional power plants.

Costs for the investment, O&M of PVFs, WFs and BESS

$TC^{Inv\&OM}_{PVF-WF-BESS}$ is an important economic factor that needs to be identified for building a suitable strategy for connecting distributed generation units. It includes investment cost and O&M cost for WFs, PVFs and BESS.

$$TC^{Inv\&OM}_{WF-PVF-BESS} = TC_{WF} + TC_{PVF} + TC_{BESS} \quad (2)$$

In the Eq. (2),TC_{WF}, TC_{PVF} and TC_{BESS} are the costs of WFs, PVFs and BESS, and they can be calculated by applying below equations, respectively[32].

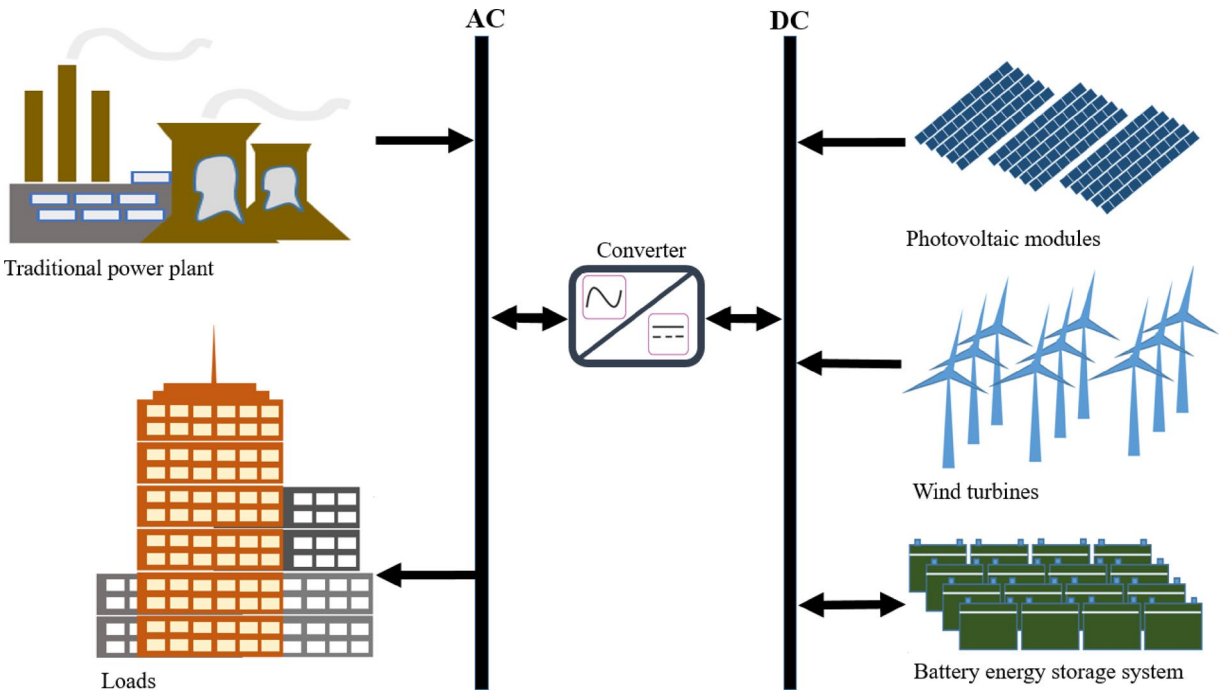

Fig. 1. The integrated system of distributed generation units.

$$TC_{WF} = \sum_{i=1}^{WF} \left(C_{WF}^{Cap}.P_{WF,i}^{Rated}\right) + 365 \times \sum_{y=1}^{20}\sum_{h=1}^{24}\sum_{i=1}^{N_{WF}} \left(\tau_y.C_{WF}^{O\&M}.P_{WF,i,h,y}^{Gen}\right) \quad (3)$$

$$TC_{PVF} = \sum_{j=1}^{N_{PVF}} \left(C_{PVF}^{Cap}.P_{PVF,j}^{Rated}\right) + 365 \times \sum_{y=1}^{20}\sum_{h=1}^{24}\sum_{j=1}^{N_{PVF}} \left(\tau_y.C_{PVF}^{O\&M}.P_{PVF,j,h,y}^{Gen}\right) \quad (4)$$

$$TC_{BESS} = \sum_{k=1}^{N_{BESS}} \left(C_{BESS}^{Cap}.En_{BESS,k}^{Rated}\right) + \sum_{y=1}^{20}\sum_{k=1}^{N_{BESS}} \left(\tau_y.C_{BESS}^{O\&M}.En_{BESS,k,y}^{Rated}\right) \quad (5)$$

This study assumes the project's lifetime is 20 years. A year has 365 days, and a day is represented by 24 h to show the change in consumption and generation during the year. As a result, the system's O&M cost will vary from year to year, so τ_y is added and defined as the present value factor, which can be determined by[26]. The cost is presented in the following sections.

Electricity purchasing cost

The electricity purchasing cost for supplying the loads and branch losses from the primary grid will be paid to the electric power company if the energy generation from distributed units is insufficient. This cost must be computed as follows:

$$TC_{Purch\_Elec}^{Sub} = 365 \times \sum_{y=1}^{20}\sum_{h=1}^{24} \left(\tau_y.EP_{h,y}^{Sub}.P_{h,y}^{Sub}\right) \quad (6)$$

where $EP_{h,y}^{Grid}$(\$/MWh) and $P_{h,y}^{Grid}$(MW) are, respectively, the electricity price announced by the electric power company and the active power that is supplied by the primary grid from the *h*th hour and the *y*th year.

Emissions cost for traditional power plants

The operation of traditional power plants that use fossil fuel sources emits large amounts of CO_2, SO_2 and NO_X. Therefore, the consumption that uses power from the above plants needs to pay a bill of emissions cost, and it is determined as[33]:

$$TC_{Emission}^{Sub} = 365 \times \sum_{y=1}^{20}\sum_{h=1}^{24} \left[\left(\tau_y.P_{h,y}^{Sub}\right) \times \left(EP_{h,y}^{CO}.EF_{h,y}^{CO} + EP_{h,y}^{SO}.EF_{h,y}^{SO} + EP_{h,y}^{NO}.EF_{h,y}^{NO}\right)\right] \quad (7)$$

where $EP_{h,y}^{CO}\&EF_{h,y}^{CO}$, $EP_{h,y}^{SO}\&EF_{h,y}^{SO}$, and$EP_{h,y}^{NO}\&EF_{h,y}^{NO}$ are the emission prices (\$/t) & emission factors ($gkWh^{-1}$) of CO_2, SO_2 and NO_X from the *h*th hour and the *y*th year, respectively.

Constraints of the study

Power balance constraints

BESS which is connected to the system, can operate in charging or discharging mode. Hence, the balance equation for active power should be included two stages of above modes as Eqs. (8) and (9), respectively[34]:

$$P_{h,y}^{Sub} + \sum_{i=1}^{N_{WF}} P_{WF,i,h,y}^{Gen} + \sum_{j=1}^{N_{PVF}} P_{PVF,j,h,y}^{Gen} = \sum_{b=1}^{N_{bh}} P_{b,h,y}^{ls} + \sum_{l=1}^{N_{ld}} P_{l,h,y}^{ld} + \sum_{k=1}^{N_{BESS}} P_{BESS,k,h,y}^{Ch} \quad (8)$$

$$P_{h,y}^{Sub} + \sum_{i=1}^{N_{WF}} P_{WF,i,h,y}^{Gen} + \sum_{j=1}^{N_{PVF}} P_{PVF,j,h,y}^{Gen} + \sum_{k=1}^{N_{BESS}} P_{BESS,k,h,y}^{DisCh} = \sum_{b=1}^{N_{bh}} P_{b,h,y}^{ls} + \sum_{l=1}^{N_{ld}} P_{l,h,y}^{ld} \quad (9)$$

The reactive power balance equation can be expressed by Eqs. (10) and (11):

$$Q_{h,y}^{Sub} + \sum_{i=1}^{N_{WF}} Q_{WF,i,h,y}^{Gen} + \sum_{j=1}^{N_{PVF}} Q_{PVF,j,h,y}^{Gen} = \sum_{b=1}^{N_{bh}} Q_{b,h,y}^{ls} + \sum_{l=1}^{N_{ld}} Q_{l,h,y}^{ld} + \sum_{k=1}^{N_{BESS}} Q_{BESS,k,h,y}^{Ch} \quad (10)$$

$$Q_{h,y}^{Sub} + \sum_{i=1}^{N_{WF}} Q_{WF,i,h,y}^{Gen} + \sum_{j=1}^{N_{PVF}} Q_{PVF,j,h,y}^{Gen} + \sum_{k=1}^{N_{BESS}} Q_{BESS,k,h,y}^{DisCh} = \sum_{b=1}^{N_{bh}} Q_{b,h,y}^{ls} + \sum_{l=1}^{N_{ld}} Q_{l,h,y}^{ld} \quad (11)$$

Constraint of the feeder

The loading at each phase of branches should not exceed the distribution system's acceptable limit[17].

$$S_{\rho,b,h,y} \le S_{\rho,b}^{Max}; \rho \forall N_\rho \ \text{ and } \ b \forall N_{bh} \quad (12)$$

Constraints of the phase voltage
Phase voltage values from all buses should be kept between upper and lower bounds as follows:

$$V^{Max} \geq V_{\rho,s,h,y} \geq V^{Min}; \rho \forall N_{\rho} \text{and} s \forall N_{bs} \tag{13}$$

The limits are set to 1.05 pu and 0.95 pu for this work, respectively[31].

Constraints of charging power and discharging power
The charging and discharging power limits by BESS are constrained as[35]:

$$0 \leq P^{Ch}_{BESS,k,h} \leq \varepsilon^{Ch}.P^{Rated}_{BESS}; \;\; h \forall N_H \;\; \text{and} \;\; k \;\; \forall \, N_{BESS} \tag{14}$$

$$0 \geq P^{DisCh}_{BESS,k,h} \geq -P^{Rated}_{BESS}.\varepsilon^{DisCh}; \;\; h \forall N_H \text{ and } \; k \, \forall \, N_{BESS} \tag{15}$$

In the Eqs. (14, 15), ε^{DisCh} and ε^{Ch} are the efficiencies of discharging and charging stages; $P^{DisCh}_{BESS,k,h}$ and $P^{Ch}_{BESS,k,h}$ are discharging power and charging power at the *k*th BESS during the *h*th hour, respectively.

Constraints of the harmonic voltage distortions
In this paper, the maximum values of total harmonic voltage distortion (THD^{Max}) and individual harmonic voltage distortion (THD^{Max}) are assigned as 5.0% and 3.0%, according to the IEEE Std. 519, respectively[36].

$$THD^{Max} \geq THD_{\rho,s,h,y}; \;\; \rho \forall N_{\rho}, s \forall N_{bs}, h \forall N_H \;\; \text{and} \;\; y \forall N_Y \tag{16}$$

$$IHD^{Max} \geq IHD^{Hr}_{\rho,s,h,y}; \;\; \rho \forall N_{\rho}, s \, \forall N_{bs}, h \forall N_H, y \forall N_Y \;\; \text{and} \;\; Hr \forall N_{Hr} \tag{17}$$

In Eqs. (16, 17), $THD_{\rho,s,h,y}$ and $IHD^{Hr}_{\rho,s,h,y}$ in percentage are computed by using Eqs. (18, 19)[36]

$$IHD^{Hr}_{\rho,s,h,y}(\%) = \left[\frac{V^{r}_{\rho,s,h,y}}{V_{\rho,s,h,y}}\right] \times 100; \; \mathrm{r} > 1 \;\; \text{and} \;\; r \forall Hr \tag{18}$$

$$\mathrm{THD}_{\rho,s,h,y}(\%) = \left[\frac{\sqrt{\sum_{r=2}^{Hr}\left(V^{r}_{\rho,s,h,y}\right)^2}}{V_{\rho,s,h,y}}\right] \times 100 \tag{19}$$

Constraints of the penetration of WFs, PVFs and BESS:
The rated capacity for each WF and each PVF, and the rated power and rated capacity for BESS should be set to the predetermined limits as follows[37]:

$$P^{Max}_{WF} \geq P^{Rated}_{WF,i} \geq P^{Min}_{WF} \& P^{Max}_{PVF} \geq P^{Rated}_{PVF,j} \geq P^{Min}_{PVF}; i \forall N_{WF}; j \forall N_{PVF} \tag{20}$$

$$P^{Max}_{BESS} \geq P^{Rated}_{BESS,k} \geq P^{Min}_{BESS} \& E^{Max}_{BESS} \geq E^{Rated}_{BESS,k} \geq E^{Min}_{BESS}; k \forall N_{BESS} \tag{21}$$

The BESS's energy at each hour must be within the limits of 20% and 90% of the rated capacity as follows[35]:

$$0.2 \times E^{Rated}_{BESS,k} \leq E_{BESS,k,h} \leq 0.9 \times E^{Rated}_{BESS,k}; \;\; k \forall N_{BESS} \;\; \text{and} \;\; h \forall N_H \tag{22}$$

Co-simulation from OpenDSS & MATLAB software

This research proposes a co-simulation by OpenDSS and MATLAB as an effective tool for solving power flow problem in frequency domains[38]. OpenDSS has many advantages of accuracy and fast processing speed in solving power flows in large and complex systems. However, it is limited in changing the control variables flexibly[28]. Therefore, this co-simulation is an excellent solution for using MATLAB to control the change of the variables from the proposed solutions in OpenDSS through the COM interface.

This basic co-simulation can be briefly shown in Fig. 2. In this model, the power grid data is described in OpenDSS, and MATLAB contains the code of the optimization algorithm. The possible solutions for the optimization problem, which are implemented in MATLAB thanks to the optimization algorithm, are transmitted to OpenDSS via the COM interface to solve power flows. Then, obtained results from OpenDSS, including bus voltage, branch current, and branch power loss will be sent back to MATLAB for calculating and evaluating the fitness of each solution. This implementation is repeated until the stopping criterion of the algorithm is satisfied and the globally optimal solution is determined.

Modified coyote optimization algorithm

The intelligent behavior of the natural phenomena from animals and plants are the most popular inspiration sources for researchers in the world to develop the optimization algorithms against which they use to solve many problems in engineering, computing, and science fields. In recent years, a positive optimization algorithm, which was developed by researchers in 2018 and named coyote optimization algorithm (COA), has attracted much attention[39]. COA is inspired from the smart behavior of coyote species (scientific name: *Canis latrans*) based on its social structure and exchange experiences. With the special characteristics of this species, the algorithm is designed with considering the coyote's social organization and adaptation to the living environment for

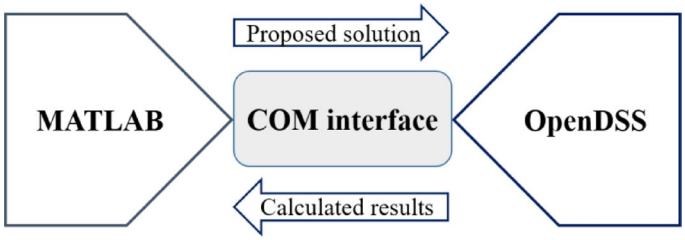

Fig. 2. The working principle of co-simulation.

addressing various real-world optimization problems effectively. In nature, the coyote population comprises many packs (N_a), and many individuals (N_o) exist in each pack. Hence, the coyote population is defined as ($N_a \times N_o$). In this algorithm, the quality of living conditions and living conditions are considered to be the two significant factors that are used to represent individuals. Here, the living condition's quality indicates the fitness of the positive solution, and the living condition presents the position of the positive solution, which is proposed for the optimization problem[39]. Although many previous studies have proven COA to be an excellent method for handling problems related to optimization[40,41], it still has many shortcomings that need to be improved. Thus, in the last year, researchers in[31] successfully modified two new solution generation processes in the original algorithm and released a modified coyote optimization algorithm (MCOA) with many outstanding features. Basically, MCOA is built on the foundation of COA, so MCOA not only inherits outstanding characteristics from original algorithm but also has positive improvements that can enhance the performance as well as the stability of the algorithm.

The first new solution generation of MCOA

Due to the stochastic characteristics of this meta-heuristic algorithm, initial solutions are created by using random generation in the predetermined range of $[\mathcal{X}^{Min}; \mathcal{X}^{Max}]$ for the control variables. The initial solutions' equation can be described as Eq. (23)[39]:

$$\mathcal{X}_{a,o} = \mathcal{X}^{Min} + r.\left(\mathcal{X}^{Max} - \mathcal{X}^{Min}\right); a\forall N_a \text{ and } o\forall N_o \tag{23}$$

In the first stage of MCOA, the new solution generation is described as the below mathematical equation[31]:

$$\mathcal{X}_{a,o}^{New} = \mathcal{X}_{a,o} + r_1.\left(\mathcal{X}_{best\_pk,a} - \mathcal{X}_{r1,a}\right) + r_2.\left(\mathcal{X}_{best\_pn} - \mathcal{X}_{r2,a}\right); \quad a\forall N_a \text{ and } o\forall N_o \tag{24}$$

Obviously, the new solutions are generated by two increased intervals: $[r_1.\left(\mathcal{X}_{best\_pk,a} - \mathcal{X}_{r1,a}\right)]$ and $[r_2.\left(\mathcal{X}_{best\_pn} - \mathcal{X}_{r2,a}\right)]$. The comer is responsible for finding new quality solutions close the best current solution of each pack, and the latter supports to the search orientation of the new solutions around the best solution of the found current population. This brings many advantages in exploiting potential solutions around high-quality solutions, such as $\mathcal{X}_{best\_pk,a}$ and $\mathcal{X}_{best\_pn}$, and found optimal solutions are positive for various optimization problems. As a result, the solution's quality in the next generation is significantly improved.

The second new solution generation of MCOA

In this step, only one solution is generated in each pack by using Eq. (25) or Eq. (26) through considering the condition of selecting the equation accordingly[31].

$$\mathcal{X}_a^{New} = \mathcal{X}_{best\_pn} + r_3.\left(\mathcal{X}_{best\_pn} - \mathcal{X}_{best\_pk,r1}\right) + r_4.\left(\mathcal{X}_{best\_pn} - \mathcal{X}_{best\_pk,r2}\right) \tag{25}$$

$$\mathcal{X}_a^{New} = \mathcal{X}_{best\_pn} + r_3.\left(\mathcal{X}_{best\_pn} - \mathcal{X}_{best\_pk,r1}\right) + r_4.\left(\mathcal{X}_{best\_pn} - \mathcal{X}_{best\_pk,r2}\right) + r_5.\left(\mathcal{X}_{best\_pn} - \mathcal{X}_{best\_pk,r3}\right) \tag{26}$$

Clearly, the equations above differ in the number of increased intervals. Two increased intervals in Eq. (25) contribute a high enough change to find new solutions far from the best quality solutions in the current population for avoiding local traps. Besides, to limit missing good solutions, Eq. (26) is suggested by adding one more increased interval, which is determined by using the same way with two previously increased intervals in Eq. (25). Equation (26) significantly contributes to the expansion of the search space for exploiting new solutions to enhance the efficiency of the discovered solution. However, it is essential for determining the possibility to apply the effective equation at this generation. Therefore, Eq. (27) is calculated to compare with a predefined threshold (γ) through the survey for selecting a suitable equation of the second new solution generation.

$$\} = \frac{\phi}{\phi^{Max}} \tag{27}$$

In Eq. (27), $\}$ is considered as the ratio of the numbers of close couple solution (ϕ) to the maximum couple solution (ϕ^{Max}). If $\}$ in Eq. (27) is less than the threshold γ, Eq. (25) is applied to produce the new solution at this stage, and vice versa.

Introduced method in solving the considering problem

Initializing for the population

Control variables of newly created solutions should be kept within predefined limits between χ^{Min} and χ^{Max}. The values between them are search space of the control variables, and they are determined as follows:

$$[\chi^{Min};\chi^{Max}]=[L^{Min}_{WF,i},P^{Min}_{WF,i},L^{Min}_{PVF,j},P^{Min}_{PVF,j},L^{Min}_{BESS,k},P^{Min}_{BESS,k,h};L^{Max}_{WF,i},P^{Max}_{WF,i},L^{Max}_{PVF,j},P^{Max}_{PVF,j},L^{Max}_{BESS,k},P^{Max}_{BESS,k,h}] \quad (28)$$

Evaluating the fitness for each solution

Each generated solution is evaluated via the calculation of the fitness function, which is determined as follows:

$$Fit_{a,o}=TC^{OF}_{a,o}+\alpha_I.\sum_{b=1}^{N_{bh}}\Delta I^2_{b,a,o}+\alpha_V.\sum_{s=1}^{N_{bs}}\Delta V^2_{s,a,o}+\alpha_{IHD}.\sum_{s=1}^{N_{bs}}\Delta IHD^2_{s,a,o}+\alpha_{THD}.\sum_{s=1}^{N_{bs}}\Delta THD^2_{s,a,o} \quad (29)$$

where $TC^{OF}_{a,o}$ is the value from objective function at the *o*th solution in the *a*th pack, which is shown in Eq. (1). Other terms on the right-hand side of Eq. (29) can be obtained by referring to[31].

Adjusting and updating new solutions

Control variables of each newly produced solution should be checked for correcting their permissible limits if they violate their predetermined limits shown in Eq. (28). The correction process is simple: Set control variables that are lower than the lower limits to the lower limits and higher than the upper limits to the upper limits. Then, the new solutions are evaluated by finding the value of the fitness function. The excellent quality solutions, as well as their fitness, are retained through comparison by applying Eqs. (30) and (31).

$$\chi_{a,o}=\begin{cases}\chi^{New}_{a,o} & if\ \ Fit^{New}_{a,o}<Fit_{a,o}\\ \chi_{a,o} & else\end{cases}\ ;\ a\forall N_a\ \text{ and }\ o\forall N_o \quad (30)$$

$$Fit_{a,o}=\begin{cases}Fit^{New}_{a,o} & if\ \ Fit^{New}_{a,o}<Fit_{a,o}\\ Fit_{a,o} & else\end{cases}\ ;\ a\forall N_a\ \text{ and }\ o\forall N_o \quad (31)$$

The flowchart for considering problem

This study considers the simultaneous integration of WFs, PVFs, and BESS in IEEE 123-bus unbalanced and 55-bus balanced distribution networks. The optimal solution is determined using MCOA as an optimization algorithm, and co-simulation (MATLAB & OpenDSS) is used as an effective computing platform for determining power flows in the frequency domains. The flowchart for determining the optimal solution is presented in Fig. 3.

Simulation results

This study solved the optimization problem from installing WFs, PVFs, and BESS using the suggested method (MCOA) and other robust methods, such as SSA and COA, to minimize total costs in IEEE 123-bus unbalanced and 55-bus balanced distribution systems. As mentioned, this study considers the generation from renewable energy sources, including wind energy and solar energy. The output of these renewable sources is highly dependent on natural conditions, so it is important to consider the uncertainty of these sources. Several studies have applied different methods, such as Weibull and Beta distribution probability density functions, to consider uncertainty by predicting wind speed and solar radiation based on historical data in the real area[42,43]. From there, the corresponding output power for wind turbines and photovoltaic modules is calculated[42]. As assumed, this study applies the results obtained in[44] to determine the power output of wind and solar energy sources. Therefore, the power generation from each renewable will depend on the coefficients of each output curve, as shown in Fig. 4. Besides, the load changing model is also plotted in this figure[44]. For the simulation of implemented methods, the maximum number of iterations (Ite^{Max}) for each independent trial is 150 for IEEE 123-bus UDS and 120 for 55-bus BDS to ensure complete convergence, and the trial running number (N_{Trial}) is selected as 40. To model both MCOA and COA, the individual number for each pack (N_o) equals the number of packs in the community (N_a), and it is 4. Besides, the threshold (γ) is chosen to be 0.2 through the survey. For applying SSA, the population (N_{pop}) is chosen as 20, and their remaining parameters are also referenced from the studies in[45,46]. The implemented methods are simulated on MATLAB ver-2017 from a desktop PC with 16.0 GB RAM and a 3.70 GHz Processor. As mentioned, this study considers harmonic sources emitted from nonlinear loads and inverters of WFs, PVFs, and BESS. In the IEEE 123-bus system, Type-1 nonlinear loads are located at buses 55, 68, and 84, and Type-2 nonlinear loads are considered at buses 10, 32, and 111 as supposed. For the 55-bus system, the loads connected at buses 3, 20, 25, 44, and 55 are assumed to be Type-1 nonlinear loads, and buses 19, 22, 35, 43, and 54 are Type-2 nonlinear loads. The detailed information of harmonic sources is also presented in Table 2[47,48].

This work has assumed that two wind farms, two photovoltaic farms and one battery energy storage system are integrated into the distribution systems by applying inverters with a fixed 0.9 lagging power factor[31]. Minimum and maximum numbers of the WFs and PVFs are 2 and 15 wind turbines, and 2,000 and 10,000 photovoltaic modules, respectively. The rated power is assumed as 100 kW for each wind turbine and 75 W for each PV module[30]. Moreover, a BESS is considered for connection to IEEE 123-bus and Nha Be 55-bus distribution systems with maximum rated capacity and maximum rated power assumed to be 4.0 MWh and 1.0 MW, respectively. In this case, the initial stored energy from this BESS is also supposed as 1.0 MWh. The efficiency of energy charge (ε^{Ch}) and discharge (ε^{DisCh}) of BESS is chosen to be 90% for lead-acid batteries. In addition, the parameters for computing total costs of connecting WFs, PVFs, and BESS are also listed in Table 3.

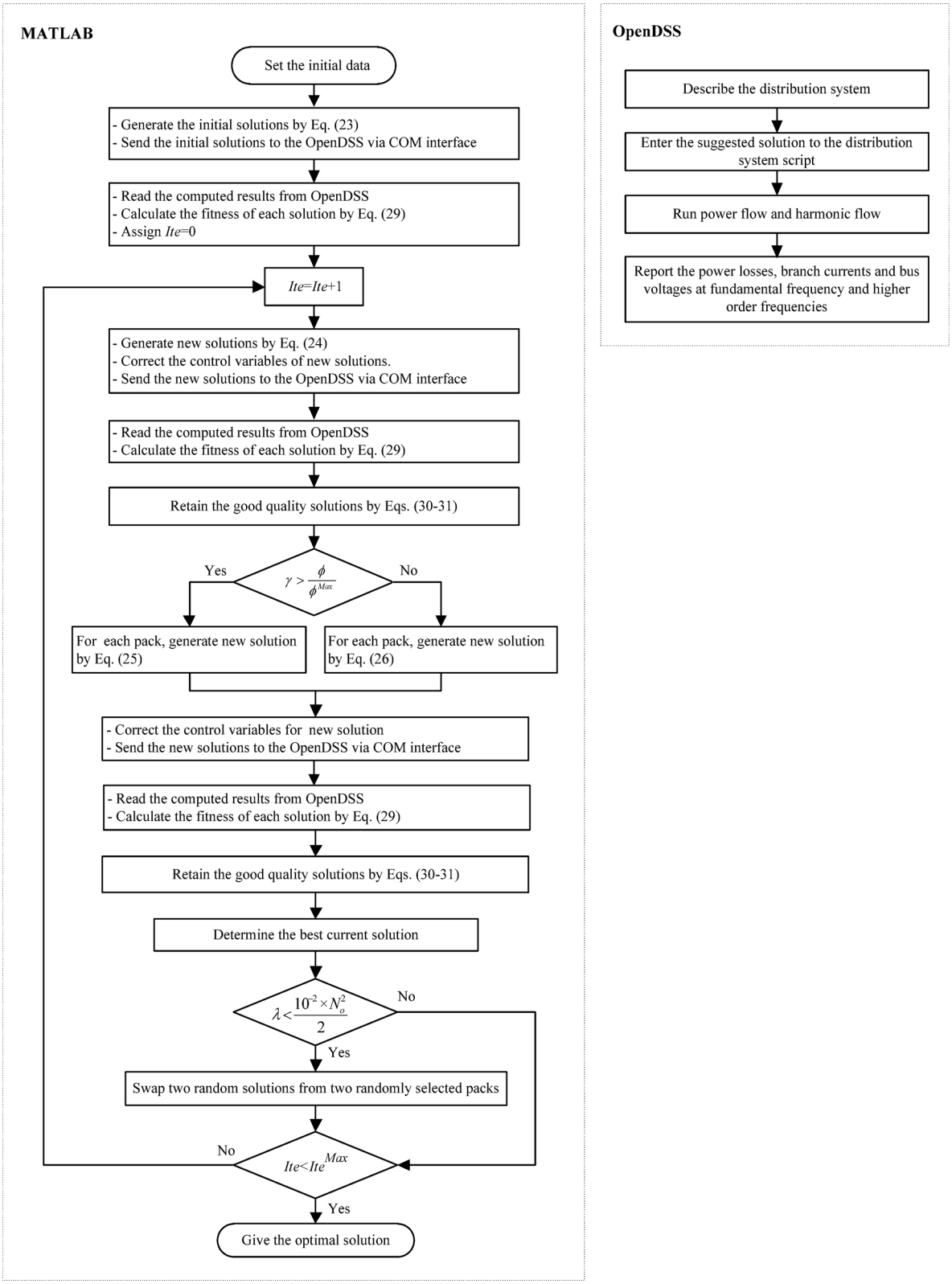

Fig. 3. The flowchart for determining the global optimal solution.

Realistically, if distributed generation units (WFs, PVFs, and BESS) do not have enough power to supply the loads due to high demand and low generation, purchasing electrical energy from the traditional power plants through the substation at the slack node is necessary. However, the electricity price is different, and it is

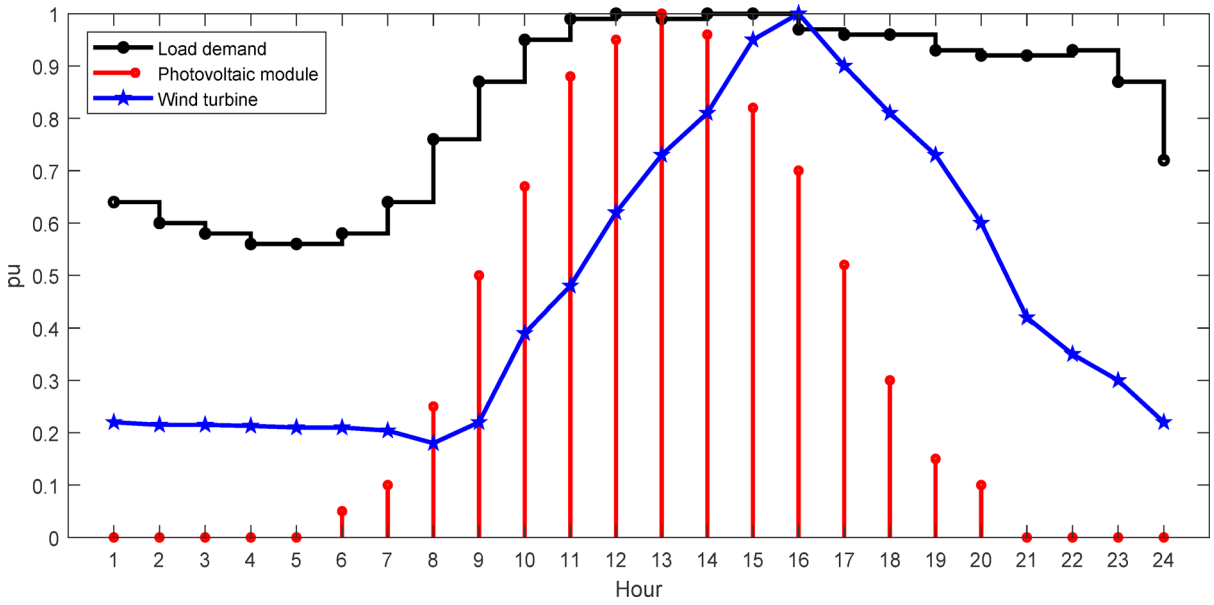

Fig. 4. The output curves of load demand, WFs and PVFs.

Harmonic sources	Harmonic order	Magnitude (%)	Angle (°)
Type-1 nonlinear loads	1, 3, 5, 7, 9, 11, 13, 15	100, 0, 19.2, 13.1, 0, 7.2, 5.6, 0	0, 0, 0, 0, 0, 0, 0, 0
Type-2 nonlinear loads	1, 3, 5, 7, 9, 11, 13, 15	100, 0, 20, 14.3, 0, 9.1, 7.7, 0	0, 0, 0, 0, 0, 0, 0, 0
Inverter-based wind turbine and PV module	1, 3, 5, 7, 9, 11, 13, 15	100, 0, 4, 4, 0, 2, 2, 0	0, 0, 0, 0, 0, 0, 0, 0
Inverter-based BESS	1, 3, 5, 7, 9, 11, 13, 15	100, 1.8, 2.3, 0.6, 0.4, 0.2, 0.25, 0.1	0, 0, 0, 0, 0, 0, 0, 0

Table 2. Harmonic spectrum.

Item	Value
C_{WF}^{Cap} and $C_{WF}^{O\&M}$ [49]	1,882,000 $/MW and 10.0 $/MWh
C_{PVF}^{Cap} and $C_{PVF}^{O\&M}$ [50]	770,000 $/MW and 10.0 $/MWh
C_{BESS}^{Cap} and $C_{BESS}^{O\&M}$ [51]	200,000 $/MW and 7000 $/MWyear
EF^{co}, EF^{so} and EF^{no} [33]	220 gkWh^{-1}, 1.08 gkWh^{-1} and 0.45 gkWh^{-1}
EP^{co}, EP^{so} and EP^{no} [52]	4 $/t, 5700 $/t and 5700 $/t

Table 3. Used parameters in calculating total costs.

divided into three stages including peak, standard and off-peak hours. Therefore, this study assumed the hourly electricity price (EP_h^{Sub}), which the utility company declares according to Fig. 5[35].

Case 1: IEEE 123-bus UDS

IEEE 123-bus unbalanced distribution system, which operates at a voltage level of 4.16 kV with grid-connected devices such as switches, capacitors, and voltage regulators, is used as a test system in this case. At peak load, this network has total power consumption of 3.448 MW and 1.358 MVar and a total power loss of 96.7 kW and 193.8 kVAr. The system data are clearly described in[29], and the single-line diagram is also shown in Fig. 6.

With the stochastic characteristics of applied methods, 40 trials are implemented to determine the most suitable location and capacity of WFs, PVFs, and BESS, and the best results from the implemented methods are presented in Table 4, and their convergence characteristics are presented as shown in Fig. 7. Obviously, at the 46th iteration, the convergence is almost achieved for MCOA, while it is the 63rd iteration for COA and the 70th iteration for SSA. Besides, each fitness point on the convergence curve of MCOA is always lower than that of SSA and COA. In other words, MCOA has better local trap avoidance than others. Not only that, the average processing time for the MCOA's simulation takes 5275.8 min, and it is slightly faster than that of SSA and COA, which are 1.054 times and 1.014 times, respectively. This shows that the suggested method not only has better convergence characteristics but also faster data processing speed than others.

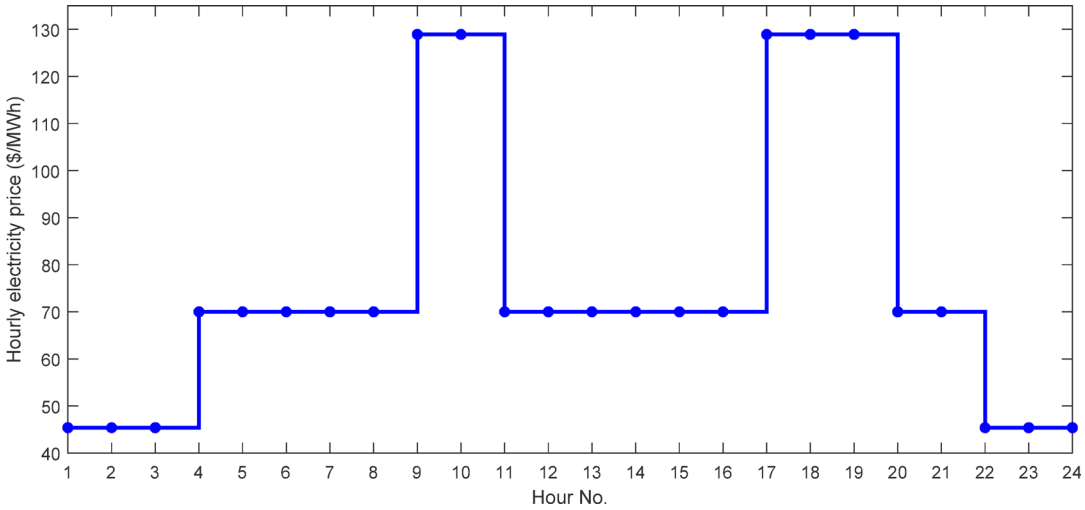

Fig. 5. Electricity prices at different hours in a day.

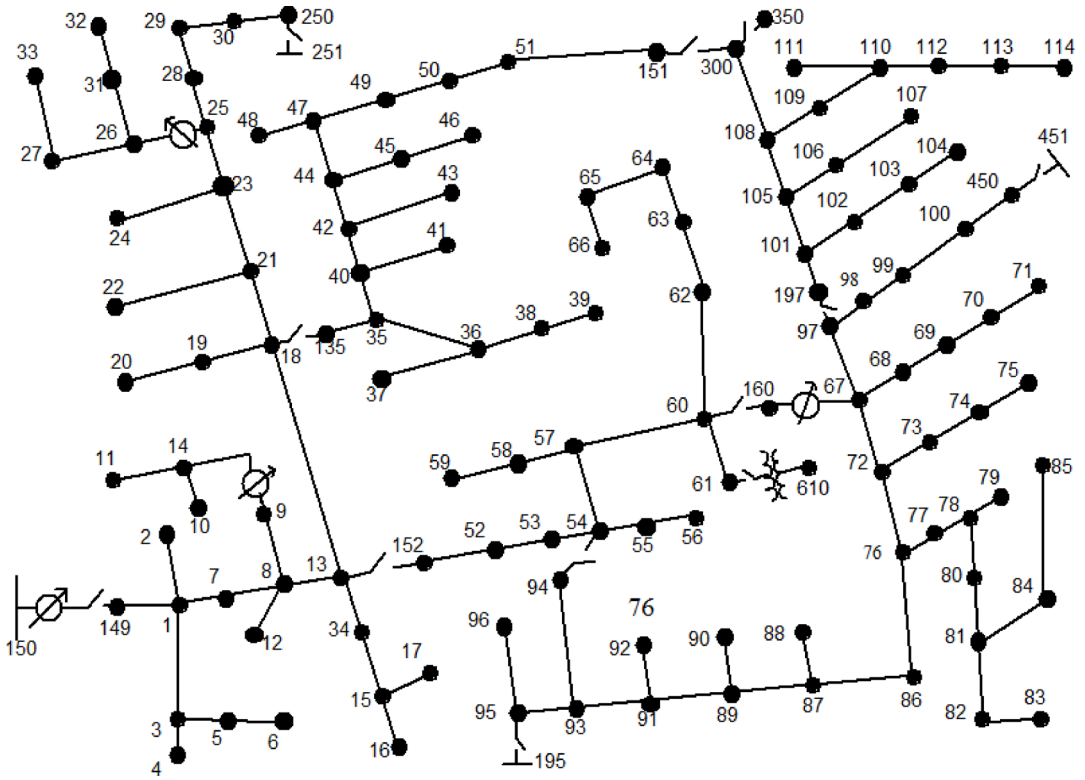

Fig. 6. The IEEE 123-bus UDS.

From the optimal solutions of methods, the associated costs are calculated and shown in detail in Table 5. As indicated in this table, total costs of MCOA are the lowest, with $15.4660 million, while SSA and COA are $15.6739 million and $15.5410 million, respectively. Although the costs from investment and O&M of MCOA ($7.3186 million) are slightly higher than COA ($7.3185 million), they are much lower than those of SSA ($7.9153 million). Besides, considering the cost of importing energy from the primary grid if WFs, PVFs, and BESS do not have enough capacity to supply energy for demand, the cost of MCOA is only $7.1663 million, it is lower than that of COA with $7.2367 million. However, it is higher than the remaining method of $6.8195 million. Lastly, the cost of emissions from power plants that use fossil energy is the highest for COA ($0.9858 million), followed by MCOA ($0.9811 million) and SSA ($0.9390 million). In summary, the optimal solution from MCOA is more economical than others, so the suggested method is the best of the three implemented

Method	WFs	PVFs	BESS
SSA	Bus: 16–15 wind turbines (1-Phase) Bus: 112–14 wind turbines (1-Phase)	Bus: 49–8408 photovoltaic modules (3-Phase) Bus: 106–4257 photovoltaic modules (1-Phase)	Bus: 15 0.554 MW/1.488 MWh (1-Phase)
COA	Bus: 05–15 wind turbines (1-Phase) Bus: 113–09 wind turbines (1-Phase)	Bus: 6–10,000 photovoltaic modules (1-Phase) Bus: 22–10,000 photovoltaic modules (1-Phase)	Bus: 5 0.539 MW/1.341 MWh (1-Phase)
MCOA	Bus: 05–15 wind turbines (1-Phase) Bus: 113–09 wind turbines (1-Phase)	Bus: 6–10,000 photovoltaic modules (1-Phase) Bus: 23–10,000 photovoltaic modules (3-Phase)	Bus: 5 0.486 MW/1.342 MWh (1-Phase)

Table 4. The best solution in 40 trial runs from three implemented methods.

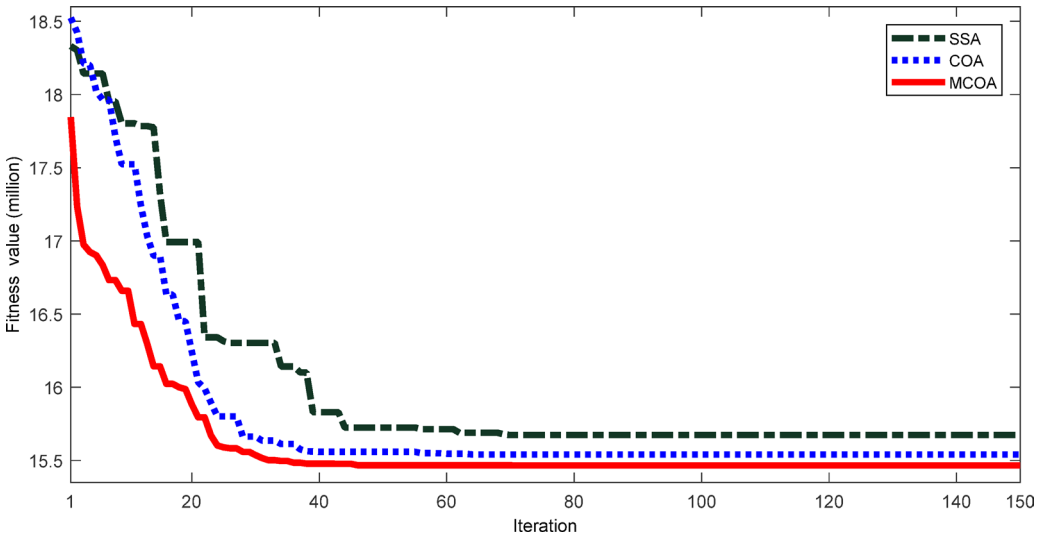

Fig. 7. The convergence curves of applied methods.

Item	Original system	SSA	COA	MCOA
TC^{OF},$ million	20.3836	15.6739	15.5410	15.4660
$TC^{Inv\&OM}_{WF-PVF-BESS}$,$ million	–	7.9153	7.3185	7.3186
$TC^{Sub}_{Purch\_Elec}$,$ million	18.1606	6.8195	7.2367	7.1663
$TC^{Sub}_{Emission}$,$ million	2.2230	0.9390	0.9858	0.9811
Saving cost, $ million	–	4.7097	4.8426	4.9176
Saving cost, %	–	23.11	23.76	24.13

Table 5. Comparision for involved costs of implemented methods.

methods. In other words, the modifications in the equations for generating new solutions for MCOA are more effective than the original method (COA) and powerful method (SSA).

On the other hand, determining the optimal solution for installing WFs, PVFs, and BESS into the distribution system also provides a huge benefit over the original system without integration. Specifically, applying the suggested method's solution can save up to $4.9176 million, equivalent to 24.13% compared to the base system. The saving cost in the percentage of MCOA is also higher than others, such as SSA and COA, with 23.11% and 23.76%, respectively, as presented in Table 5. The results indicate that suitable integration of WFs, PVFs, and BESS can provide excellent economic benefits compared to the non-integrated system.

Multiple benefits have been achieved thanks to the appropriate penetration of renewables and BESS. Specifically, as shown in Fig. 8, the total power generation in a day to the grid from renewables is 38.7978 MW, including 69.26% coming from wind energy and 30.74% coming from solar energy. Moreover, BESS has flexible charging and discharging stages according to the hourly electricity price to save operating costs by reducing the cost of importing electricity from the main grid. For a typical day, the total discharging power from the BESS is 1.4332 MW, and the total charging power is 1.7694 MW. Therefore, the total power generation to the grid from these units is 38.4616 MW, while the demand of the loads is 69.1300 MW, so the main grid will provide the energy deficit. As plotted in Fig. 9, during hours with favorable natural conditions (strong wind and high solar radiation), the distributed sources supply high power to the grid and almost enough to supply the entire demand

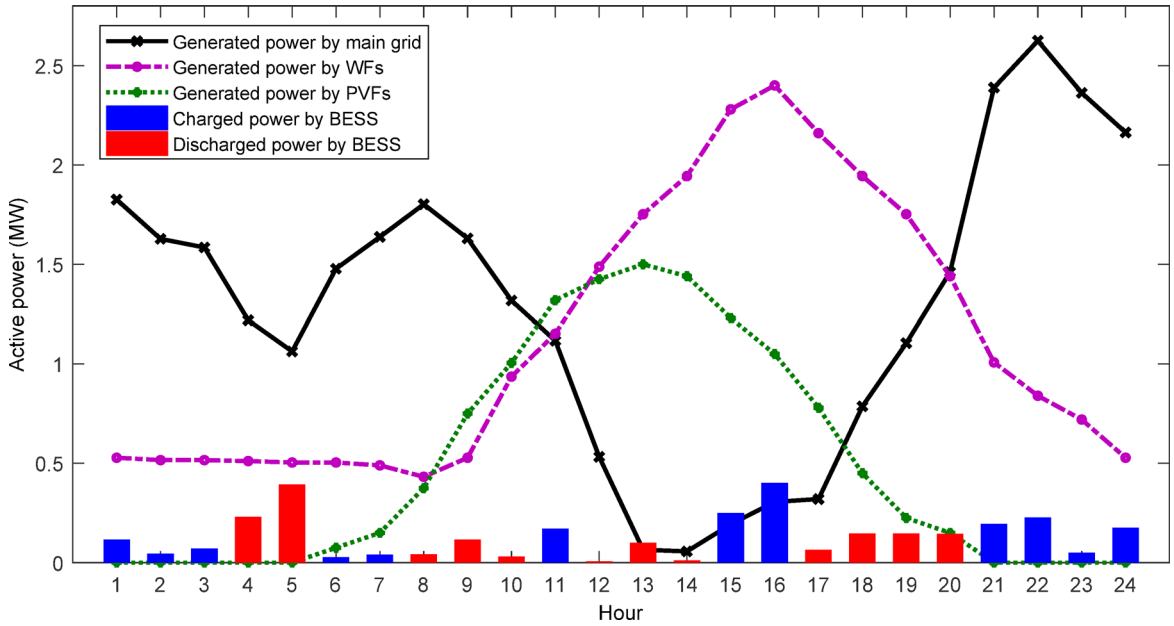

Fig. 8. The consumed and generated power of each distributed unit in power grid.

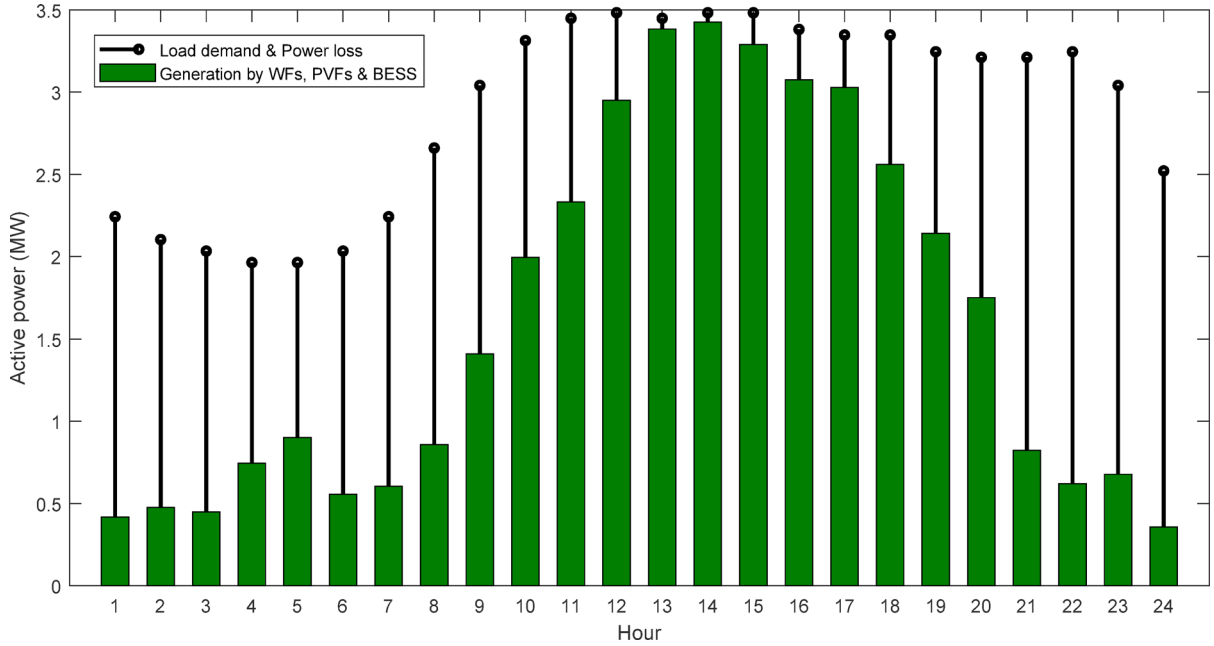

Fig. 9. The total consumption (loads and losses) and generation of all units.

of the system. On the contrary, during times when natural conditions are not favorable for the operation of these sources, the main power supply for load demand is still electricity from the main grid. Therefore, building a suitable power generation strategy for renewable sources and a charging/discharging strategy for BESS is important in optimizing grid operation to minimize costs while still ensuring the satisfaction of technical constraints. As mentioned, BESS is integrated to deploy a reasonable charging/discharging strategy to increase the system operating cost saving, as shown in Figs. 10 and 11. Figure 10 indicates the energy storage capacity, and Fig. 11 plots the charging and discharging stages after connecting BESS to the system. Generally, BESS tends to save energy during the light load periods and the off-peak hours due to the cheapest electricity price. BESS releases energy into the grid during the heavy load periods and the peak hours due to the highest electricity price at these hours. For the remaining hours, BESS has a reasonable strategy of charging and discharging energy to save money from purchasing energy of the primary grid. Optimally charging and discharging energy has contributed significantly to saving costs for operating the distribution network. Besides, the operating process of

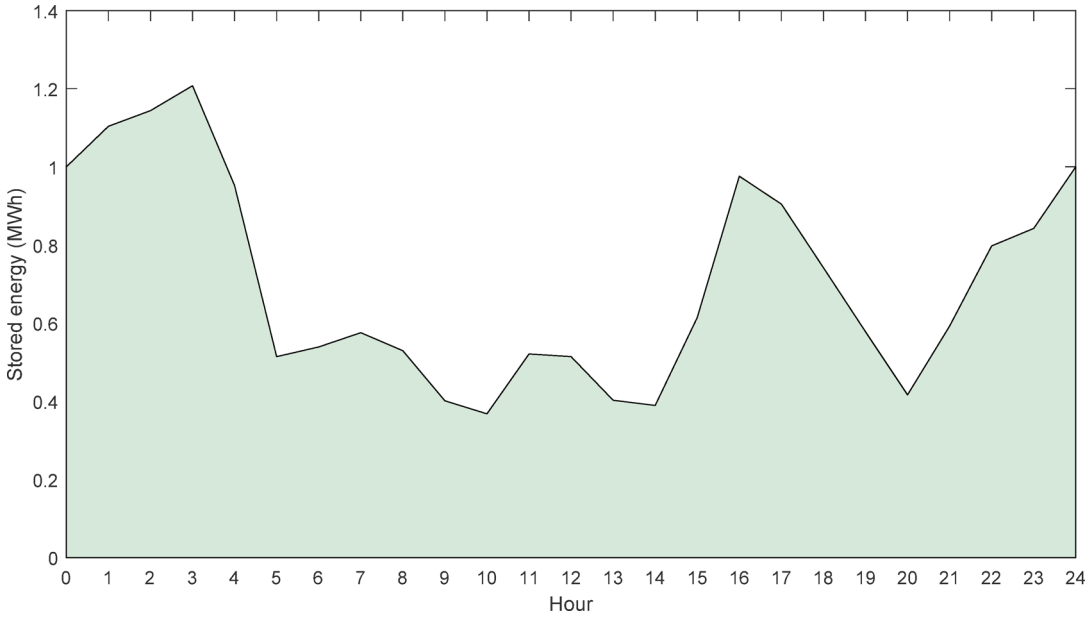

Fig. 10. The energy storage capacity from BESS.

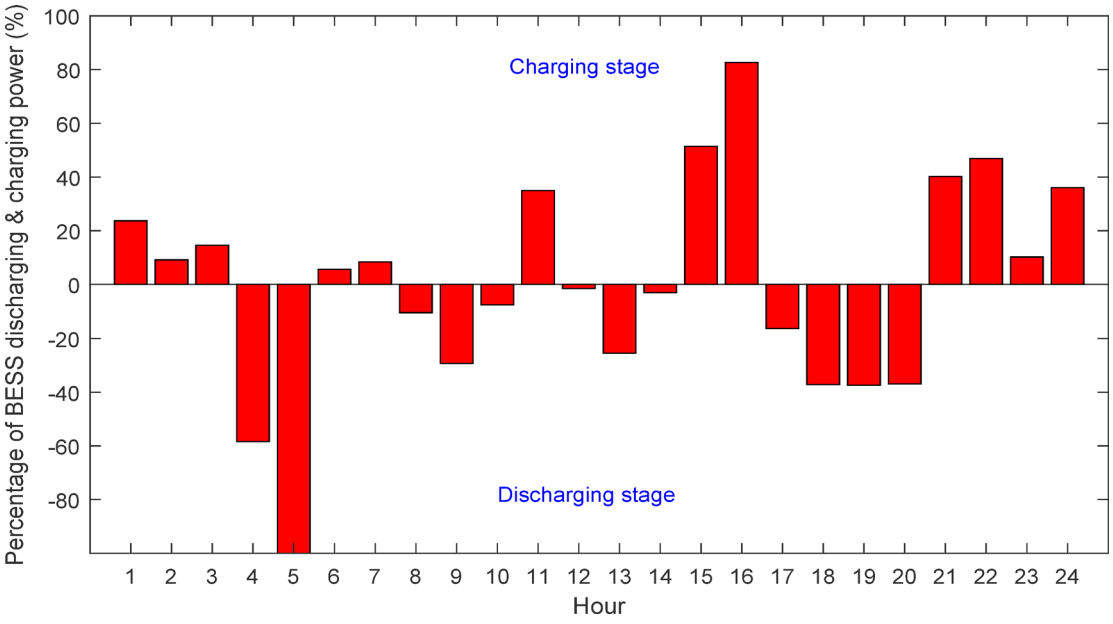

Fig. 11. The charging and discharging stages from BESS.

BESS completely also satisfies the constraints of discharging and charging limits for BESS with 20% and 90% of the rated capacity, respectively. For an example, with a rated capacity of BESS of 0.486 MW/1.342 MWh as the obtained solution from the suggested method, BESS can store up to 1.208 MWh as fully charged and vice versa, BESS down to 0.268 MWh; it will stop generating energy.

As mentioned, one of the great benefits of integrating WFs, PVFs, and BESS is power loss reduction in distribution branches. Precisely, as indicated in Fig. 12, total power loss of the distribution system is enormously cut from 1.6578 to 1.2976 MW in one day after connecting the grid-connected units, corresponding to a 21.73% loss reduction. Besides, thanks to the distributed connection of generation sources on the grid, the voltage drop at the buses, especially the weak buses, which are located far from the main power source, has also been significantly enhanced. The appropriate placement and generation of distribution sources brought great voltage profile improvement. Specifically, before connecting the WFs, PVFs, and BESS, the voltage values of phases in the system are within the range of [0.9265, 1.0031] (pu) throughout all times. However, after integration of WFs, PVFs, and BESSs into the system, the phase voltage improved drastically with fluctuating values within the range

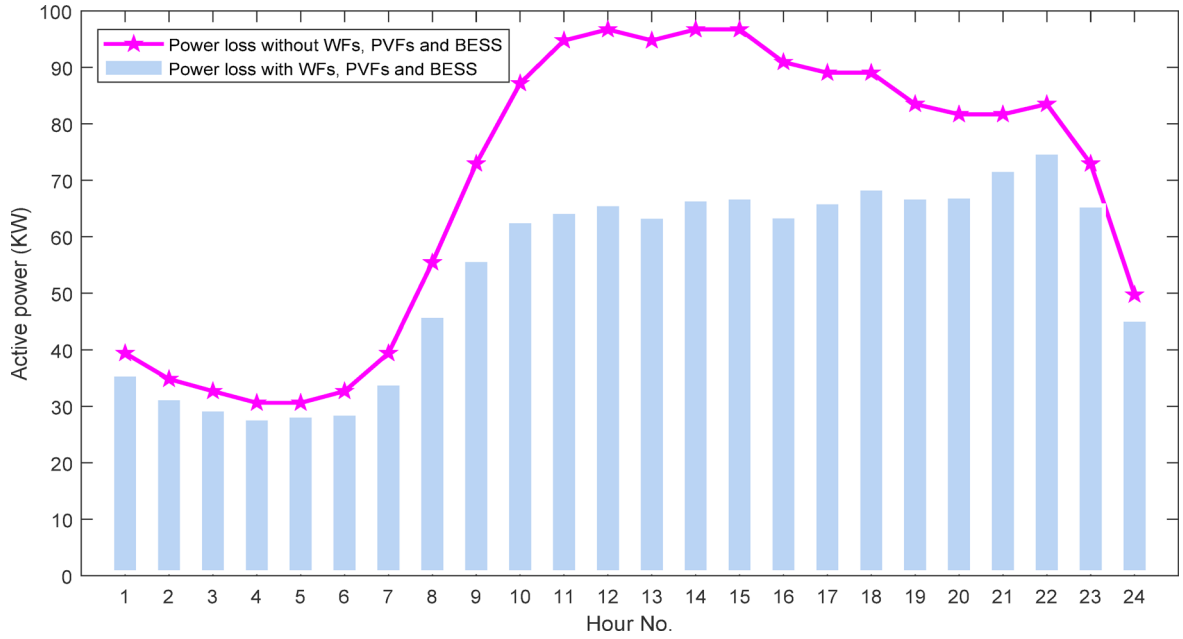

Fig. 12. The power loss of the system before and after integrating PVFs, WFs and BESS.

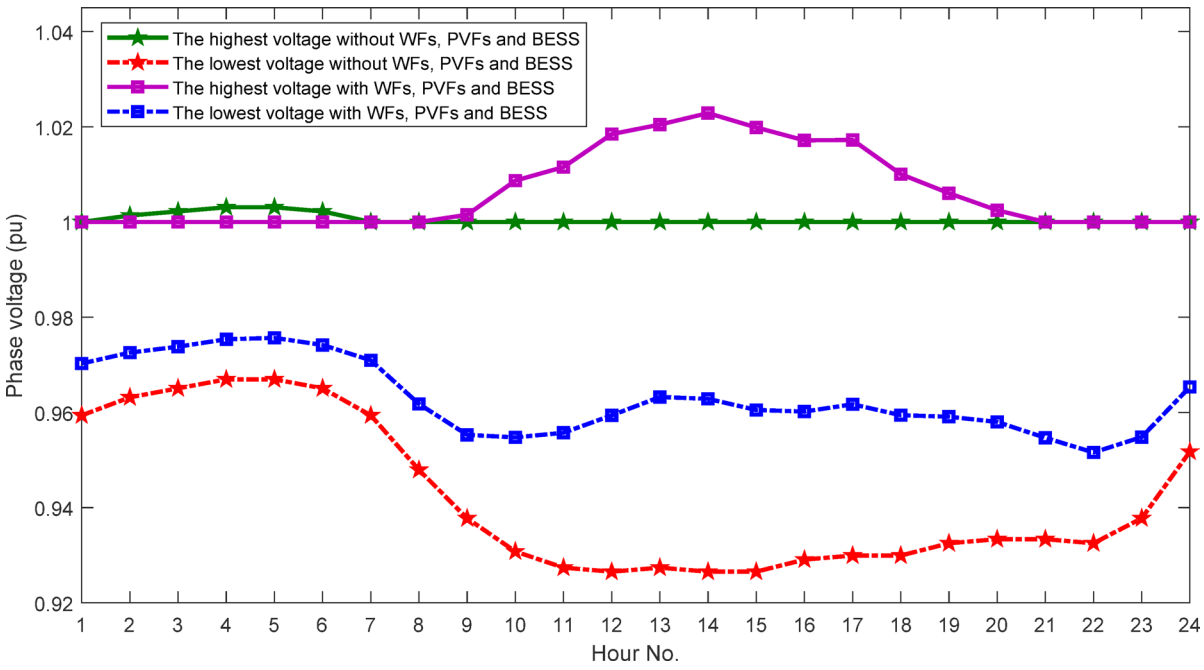

Fig. 13. The lowest and highest voltages before and after connecting PVFs, WFs and BESS.

of [0.9516, 1.0229] (pu) like plotted in Fig. 13, and this satisfies the voltage constraints of [0.950, 1.050] (pu). This shows the great benefit of properly connecting WFs, PVFs, and BESS in reducing power loss and enhancing voltage profile of the distribution system.

Moreover, this study also considers harmonic distortions caused by nonlinear loads and inverters of WFs, PVFs, and BESS. Nonlinear loads generated harmonics in the original system with the highest THD values at every hour are shown in Fig. 14, in which the highest value is 1.453% at the peak load hours. However, after connecting distributed units, their inverters significantly increased the harmonics of the system to 2.853% for the maximum value of THD. This indicates that the use of power conversion devices contributes mainly to increasing the harmonic distortions in the power grid, and it is necessary to keep the harmonic indices not exceeding the allowable limits. Like the obtained results from this study, all values of THD after integration of

units are lower than the limit of 3%, so IHD values do not exceed 3%, and thus, harmonic indices in this scenario completely satisfy the IEEE Std. 519.

Case 2: Nha Be 55-bus BDS

This study selects a real case with a 55-bus BDS in Nha Be District, Ho Chi Minh City, Vietnam, operating at 22 kV as a test system. At peak load, total consumption is 7.630 MW and 2.342 MVar with total power loss of 51.2 kW and 72.1 kVAr. Line and load data are also shown in Table S1 and Table S2 in Supplementary Material, and the system's single-line diagram is plotted in Fig. 15.

Similarly, in this case, 40 independent trials are implemented for each method to find the best results. The best solutions for the executed algorithms are indicated in Table 6, and convergence curves are also shown in Fig. 16. At the 36th iteration, MCOA achieved convergence, while SSA and COA obtained convergence at the 42nd and 60th iteration, respectively. The fitness points on the curve of MCOA through 120 iterations are always better than those of SSA and COA. On the other hand, the average processing time for the MCOA's simulation is 2485.2 min, and it is also a little faster than SSA (1.025 times) and COA (1.011 times). This indicates that the suggested method has better convergence properties and convergence speed than other methods.

On the other hand, the relevant costs from the optimal solutions are also calculated and shown in Table 7. Obviously, the found TC^{OF} value of MCOA is the lowest at \$32.3283 million compared to \$32.7566 million of SSA and \$32.6309 million of COA. Although $TC^{Inv\&OM}_{WF-PVF-BESS}$ of MCOA is \$13.9730 million and higher than that of SSA and COA (\$13.8673 million and \$12.2049 million), $TC^{Sub}_{Purch\_Elec}$ of MCOA is more economical than the two compared methods with the difference of \$0.4848 million and \$1.3746 million for SSA and COA, respectively. Not only that, the $TC^{Sub}_{Emission}$ value of MCOA is \$2.2240 million, and also smaller than that of SSA and COA (\$2.2733 million and \$2.4354 million). The above results have shown that the optimal solution from MCOA is economically better than the compared methods, including SSA and COA.

Furthermore, the optimal solutions from integrating distributed generation units such as WFs, PVFs, and BESS also bring great benefits compared to the non-integrated system. In the base system, total costs are very high and equal to \$44.5685 million. On the contrary, the total costs are significantly smaller in the modified system. MCOA, COA, and SSA found solutions with total costs of \$32.3283 million, \$32.6309 million, and \$32.7566 million. Those costs are smaller than the base systems by 27.46%, 26.78%, and 26.50%. The values conclude that installing WFs, PVFs, and BESS in the distribution networks is essential, and selecting the location and size to work for these devices by using robust algorithms is also extremely important.

By applying the optimal solution from the suggested method, total power generation from WFs, PVFs, and BESS in 24 h is also presented. As plotted in Fig. 17, the total daily generation capacity from renewables is 82.4821 MW, including 53.84% from solar power and 46.16% from wind power. Additionally, with the appropriate charging/discharging strategy of BESS, the total daily discharging power from BESS is 2.5933 MW, and the total daily charging power is 3.2016 MW. Therefore, the total daily grid injected power of these sources is 81.8738 MW, while the total demand is 151.3970 MW. Therefore, the deficit will also be compensated by the main grid. As shown in Fig. 18, the compensation amount from the main grid will depend on the generation capacity of the grid-connected distributed units. At each time of the day, the generation capacity of the renewables will vary depending on the weather conditions. During periods of good weather for renewables operation, the amount of electricity taken from the main grid will be low and vice versa. Besides, BESS, with a reasonable energy charging/discharging strategy according to each electricity price period, also greatly saves

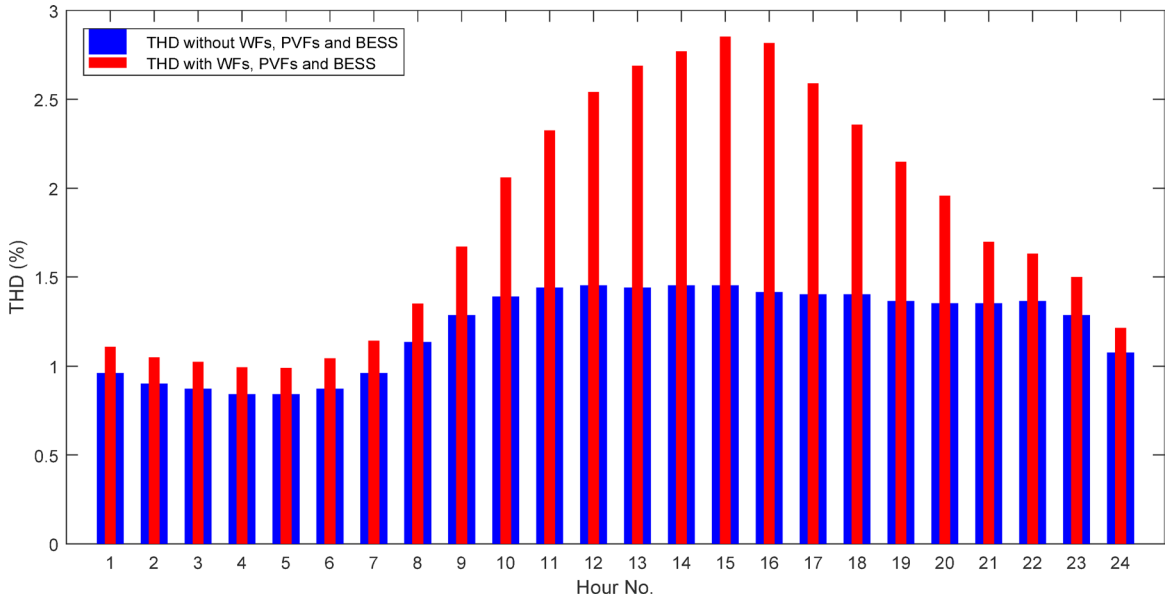

Fig. 14. THD's maximum value from each hour with and without connecting PVFs, WFs and BESS.

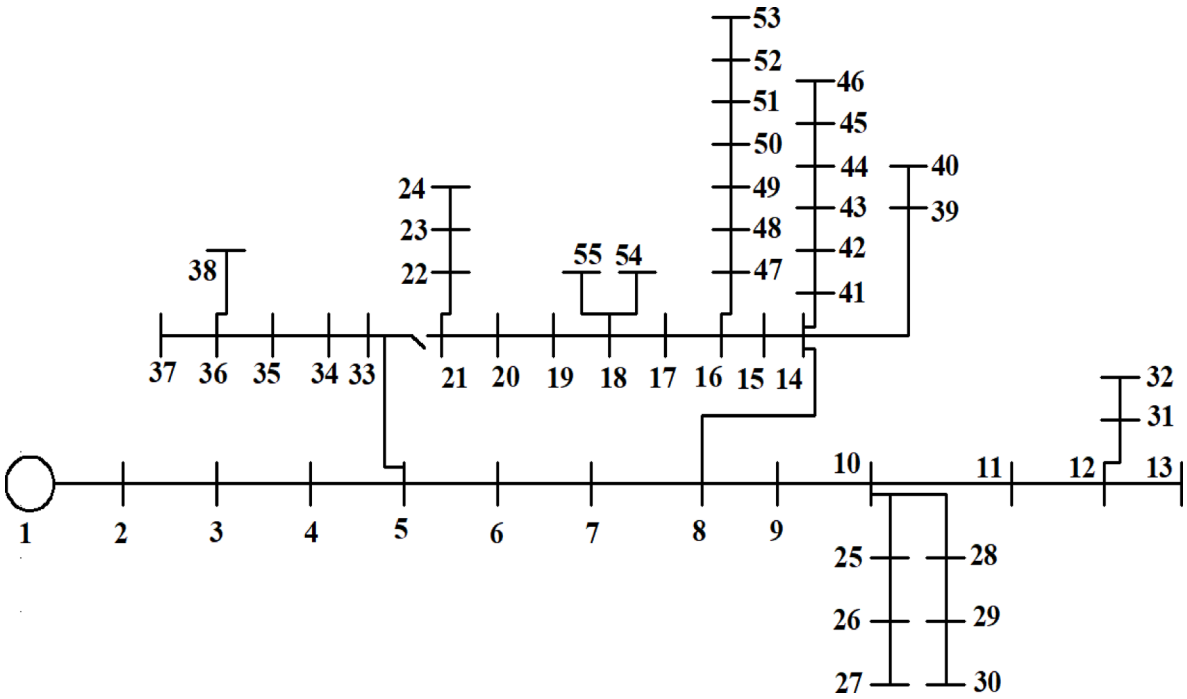

Fig. 15. The 55-bus BDS.

Method	WFs	PVFs	BESS
SSA	Bus: 04–20 wind turbines Bus: 15–17 wind turbines	Bus: 23–40,000 photovoltaic modules Bus: 53–26,034 photovoltaic modules	Bus: 03 0.504 MW/1.509 MWh
COA	Bus: 18–20 wind turbines Bus: 32–05 wind turbines	Bus: 41–39,775 photovoltaic modules Bus: 18–40,000 photovoltaic modules	Bus: 29 0.545 MW/1.423 MWh
MCOA	Bus: 25–16 wind turbines Bus: 49–18 wind turbines	Bus: 05–34,486 photovoltaic modules Bus: 03–40,000 photovoltaic modules	Bus: 28 0.805 MW/1.987 MWh

Table 6. The best solution in 40 trial runs from three implemented methods.

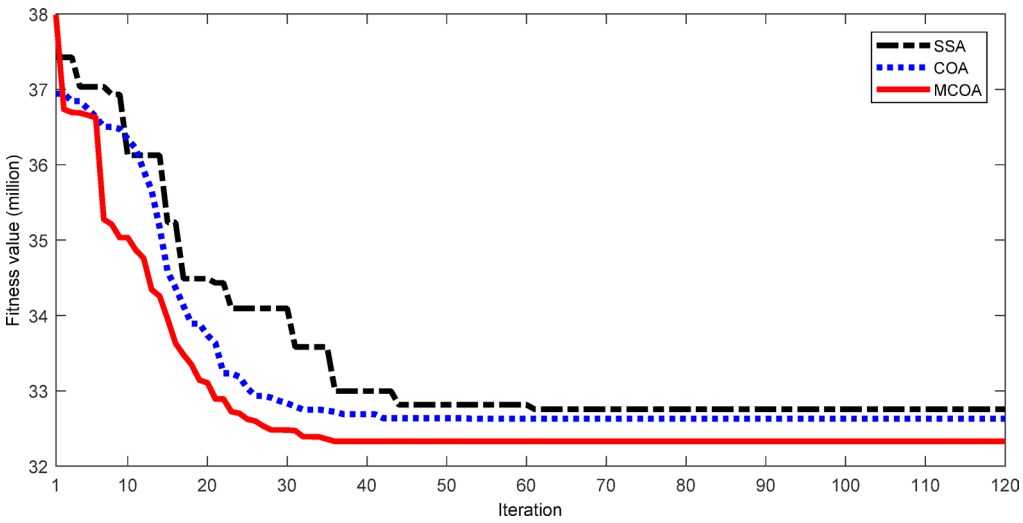

Fig. 16. The convergence curves of applied methods.

Item	Original system	SSA	COA	MCOA
TC^{OF},$ million	44.5685	32.7566	32.6309	32.3283
$TC^{Inv\&OM}_{WF-PVF-BESS}$,$ million	–	13.8673	12.2049	13.9730
$TC^{Sub}_{Purch\_Elec}$,$ million	39.7089	16.6160	17.9906	16.1312
$TC^{Sub}_{Emission}$,$ million	4.8596	2.2733	2.4354	2.2240
Saving cost, $ million	–	11.8119	11.9376	12.2402
Saving cost, %	–	26.50	26.78	27.46

Table 7. Comparision for involved costs of implemented methods.

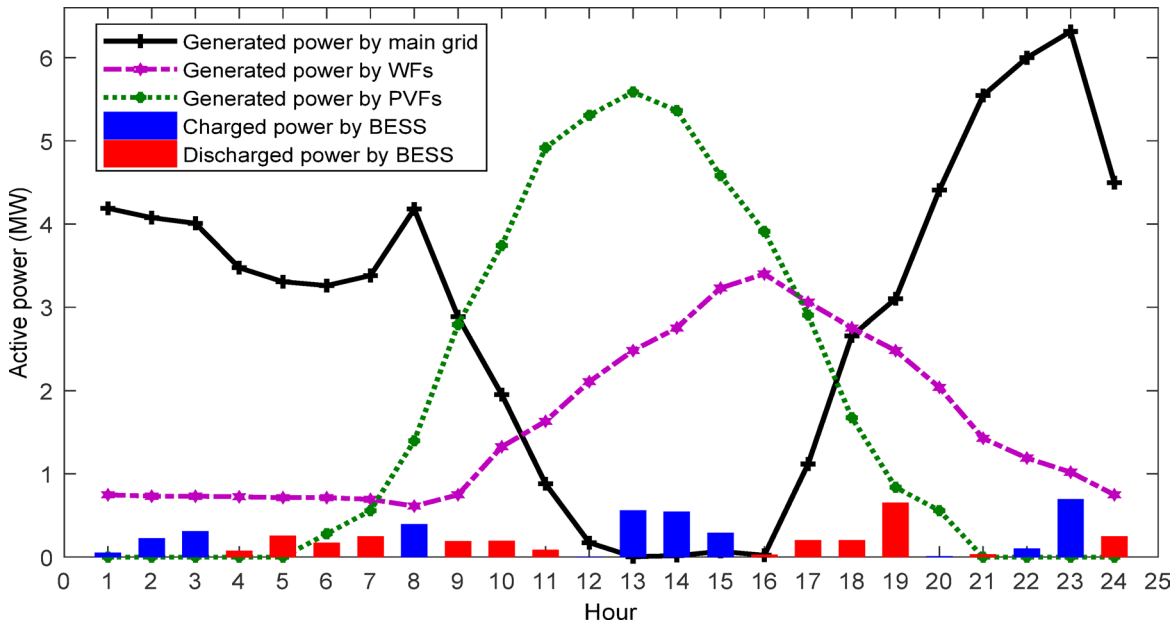

Fig. 17. The consumed and generated power of each distributed unit in power grid.

operating costs. It can also be affirmed that determining the appropriate operating strategy for units is necessary to maximize the received benefits. In addition, to further elucidate the operation of BESS, Fig. 19 also shows the energy storage process of BESS throughout 24 h of a day. As a typical example, in this system, BESS's rated energy is 1.9871 MWh with a rated charging and discharging power of 0.8049 MW. In other words, BESS can store up to 1.7884 MWh, which is considered full energy, and the remaining energy of 0.3974 MWh is considered exhausted energy. This completely satisfies the constraints of 90% and 20% for BESS's charging and discharging limits to avoid physical damage to the battery banks. Besides, Fig. 20 also plots the appropriate charging and discharging power of BESS at each time. Clearly, BESS tends to charge power at low electricity price periods and generate power at high electricity price periods to reduce total cost of importing electricity.

One of the positive points of determining the optimal connection of distributed generation sources in the distribution network is power loss minimization. Thanks to the proper integration of WFs, PVFs, and BESS, total power loss on the branches has been cut noticeably from 878.6491 to 364.3910 kW, corresponding to a 58.53% loss reduction as shown in Fig. 21. This reduction of 514.2581 kW has contributed significantly to cutting costs in operating the integrated system. Furthermore, thanks to the decentralized connection of the power sources, the bus voltage is supported significantly, especially for buses located far from the main power source. There is no integration of distributed generation units; the system phase voltage is within the range of [0.989, 1.000] (pu). However, this voltage range is sharply raised to [0.991, 1.001] (pu) after the integration of WFs, PVFs, and BESS, as shown in Fig. 22. Lastly, as mentioned, this study considers harmonic sources emitted by nonlinear loads and inverters of WFs, PVFs, and BESS. In this case, the maximum THD value in the system with nonlinear loads is 1.01%. However, this value has increased to 1.70% with the penetration of distributed units. This indicates that the connection of inverter-based wind turbines, photovoltaic modules, and BESS can strongly inject harmonics into the grid. Therefore, it is recommended that the harmonic indices satisfy the IEEE Std. 519. Like Fig. 23, the maximum THD value at each time of the day is less than 3%, so all IHD values are also less than 3%, completely satisfying the given constraints.

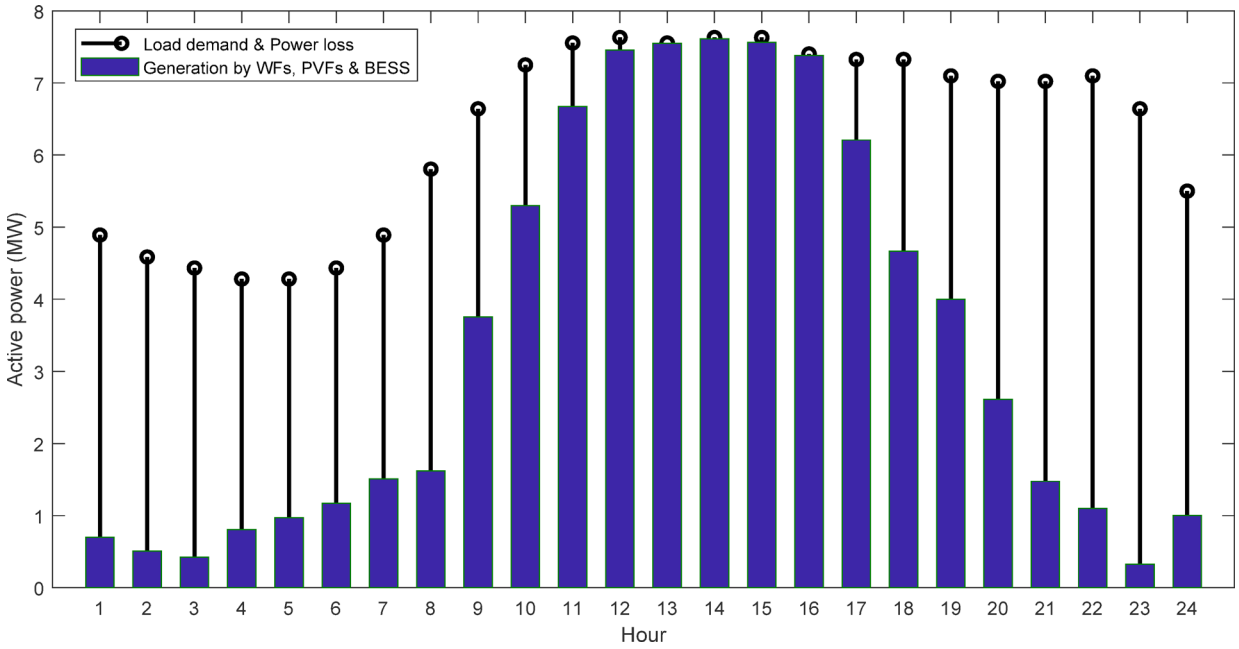

Fig. 18. The total consumption (loads and losses) and generation of all units.

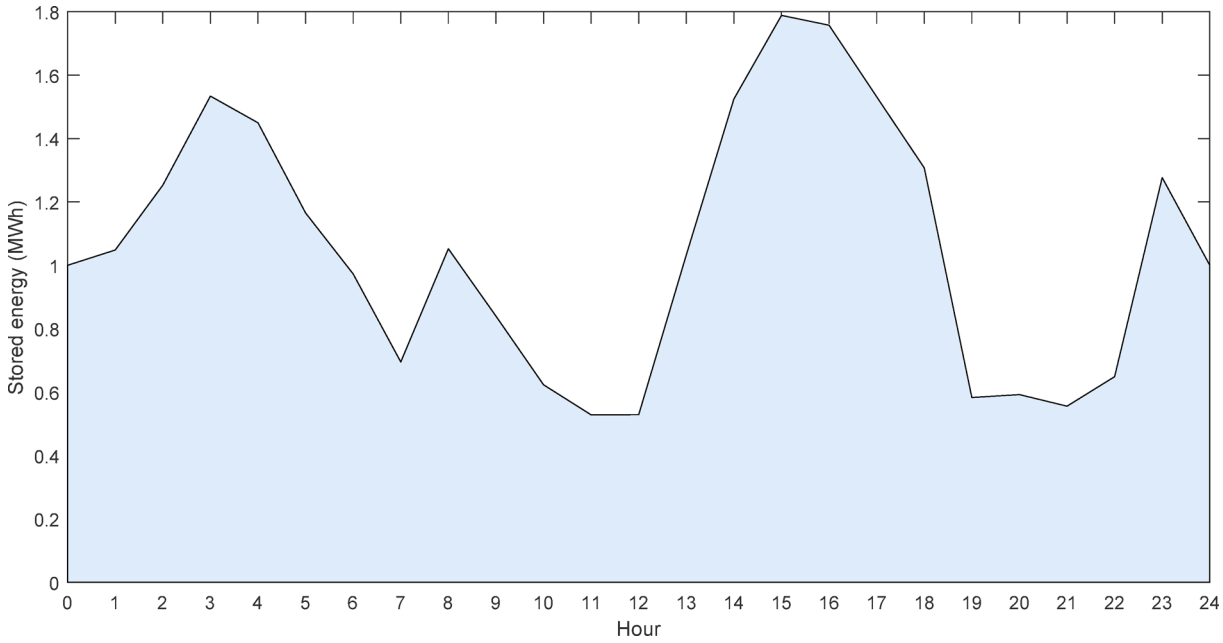

Fig. 19. The energy storage capacity from BESS.

Conclusions

This work introduced a novel high-performance meta-heuristic algorithm named the modified coyote optimization algorithm to determine the suitable location and sizing of WFs, PVFs, and BESS in both IEEE 123-bus unbalanced and Nha Be 55-bus balanced distribution systems. The study considered harmonics that are caused by nonlinear loads, and inverters of WFs, PVFs, and BESS to keep measurement values of the harmonics in compliance with IEEE Std. 519. Additionally, the research also successfully developed co-simulation of OpenDSS and MALAB through COM. This co-simulation has brought significant advantages in solving power flow problems in frequency domains flexibly and quickly. The primary objective of this work is to minimize the total costs considering environmental, technical, and economic aspects. The results obtained show that the optimal solution for integrating WFs, PVFs, and BESS could save up to 24.33% and 27.46% compared to the initial system for the 20-year project period. Besides, total power loss is also decreased by 21.73% and 58.53%

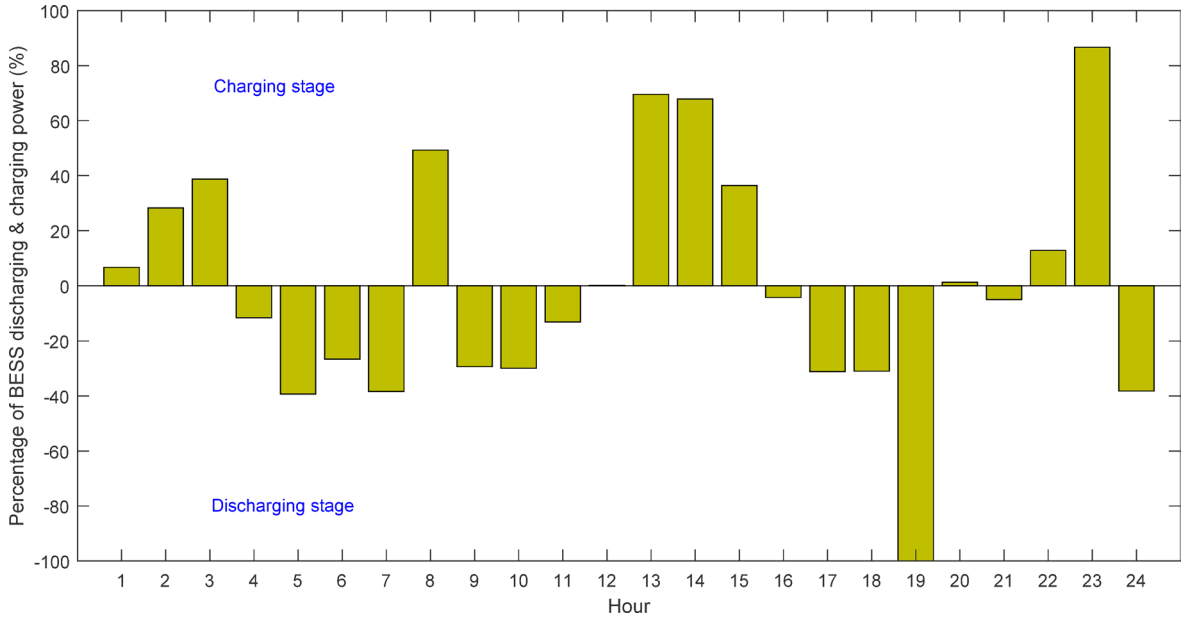

Fig. 20. The charging and discharging stages from BESS.

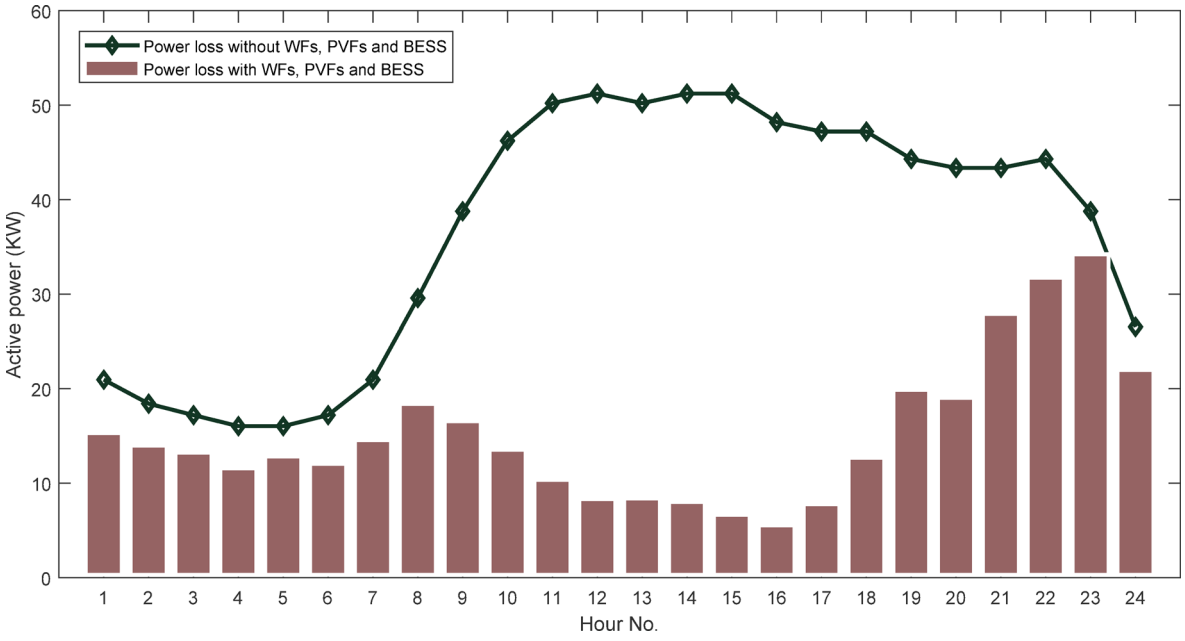

Fig. 21. The power loss before and after integrating PVFs, WFs and BESS.

in loss reduction, and the voltage profile is also enhanced from [0.9265, 1.0031] to [0.9516, 1.0229] and from [0.989, 1.000] to [0.991, 1.001] under the satisfaction of IEEE Std. 519 on harmonics for IEEE 123-bus and 55-bus distribution systems, respectively. Finally, MCOA has also proven its superior performance for addressing various optimization problems compared to strong methods of SSA and COA with the same objective function and technical constraints.

Although this study has successfully considered harmonics from nonlinear loads and renewable energy sources, the presence of supraharmonics has not been evaluated. Hence, this will be implemented in future work. Moreover, to increase the welfare, the smart inverters that are capable of setting Volt/VAR and Volt/Watt functions to increase the penetration of renewables without violating the constraint will be integrated. In addition, charging stations for electric vehicles, as well as harmonics from their power converters, will also be considered in the future.

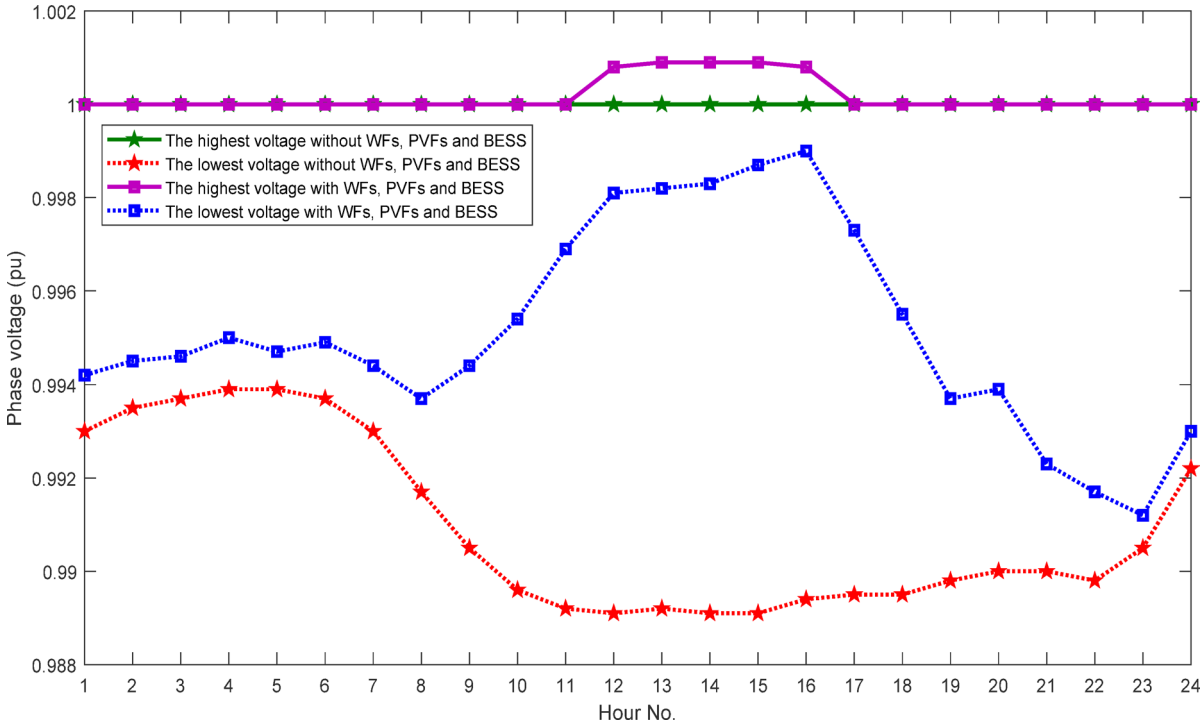

Fig. 22. The lowest and highest phase voltages without and with connecting PVFs, WFs and BESS.

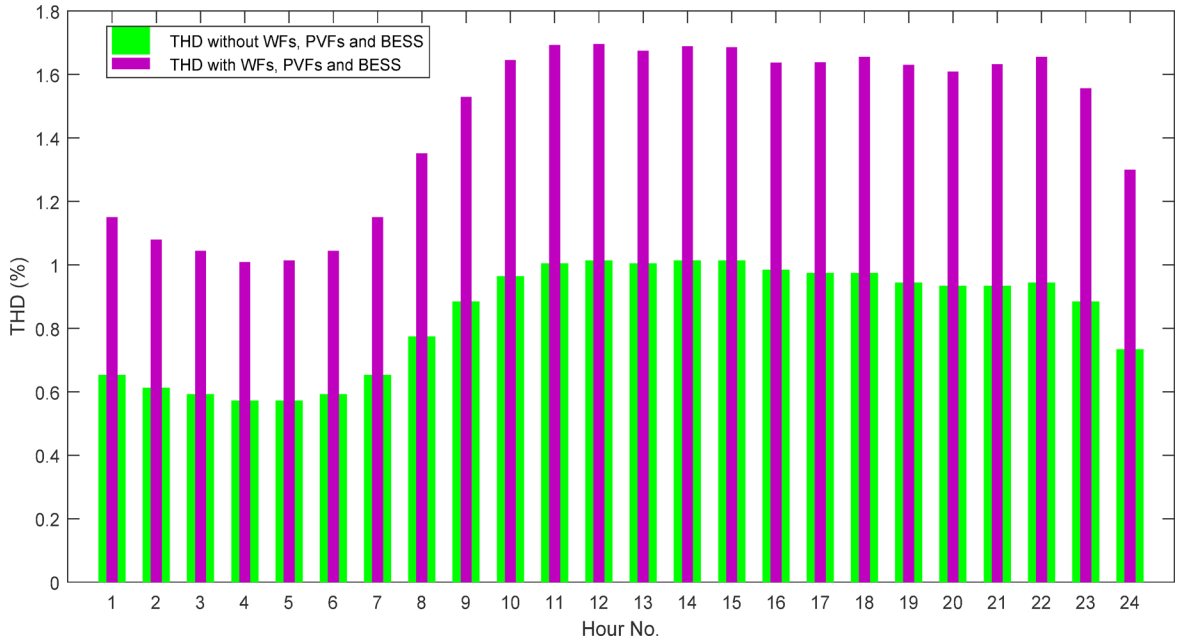

Fig. 23. Maximum THD value from each hour without and with connecting PVFs, WFs and BESS.

Data availability

Data from the study can be shared, and readers can contact Thai Dinh Pham to request the data.

Received: 5 February 2025; Accepted: 9 May 2025
Published online: 17 May 2025

References

1. Ali, A., Keerio, M. U. & Laghari, J. A. Optimal site and size of distributed generation allocation in radial distribution network using multi-objective optimization. *J. Mod. Power Syst. Clean Energy* **9**(2), 404–415 (2020).
2. Mahmoud, K. & Lehtonen, M. Simultaneous allocation of multi-type distributed generations and capacitors using generic analytical expressions. *IEEE Access* **7**, 182701–182710 (2019).
3. Gielen, D. et al. The role of renewable energy in the global energy transformation. *Energ. Strat. Rev.* **24**, 38–50 (2019).
4. Singh, K. et al. India's renewable energy research and policies to phase down coal: Success after Paris agreement and possibilities post-Glasgow climate pact. *Biomass Bioenergy* **177**, 106944 (2023).
5. Salimon, S. A., Adepoju, G. A., Adebayo, I. G. & Adewuyi, O. B. Comparative assessment of techno-economic and environmental benefits in optimal allocation of distributed generators in distribution networks. *Sci. Afr.* **19**, e01546 (2023).
6. Bhumkittipich, K. & Phuangpornpitak, W. Optimal placement and sizing of distributed generation for power loss reduction using particle swarm optimization. *Energy Procedia* **34**, 307–317 (2013).
7. Adepoju, G. A., Aderemi, B. A., Salimon, S. A. & Alabi, O. J. Optimal placement and sizing of distributed generation for power loss minimization in distribution network using particle swarm optimization technique. *Eur. J. Eng. Technol. Res.* **8**(1), 19–25 (2023).
8. Devi, S. & Geethanjali, M. Optimal location and sizing determination of distributed generation and DSTATCOM using particle swarm optimization algorithm. *Int. J. Electr. Power Energy Syst.* **62**, 562–570 (2014).
9. Murthy, G. V. K., Sivanagaraju, S., Satyanarayana, S. & Rao, B. H. Optimal placement of DG in distribution system to mitigate power quality disturbances. *Int. J. Electr. Comput. Eng.* **7**(2), 266–271 (2014).
10. Das, C. K., Bass, O., Kothapalli, G., Mahmoud, T. S. & Habibi, D. Optimal placement of distributed energy storage systems in distribution networks using artificial bee colony algorithm. *Appl. Energy* **232**, 212–228 (2018).
11. Ali, E. S., Abd Elazim, S. M. & Abdelaziz, A. Y. Ant lion optimization algorithm for optimal location and sizing of renewable distributed generations. *Renew. Energy* **101**, 1311–1324 (2017).
12. Ali, E. S., Abd Elazim, S. & Abdelaziz, A. Y. Ant lion optimization algorithm for renewable distributed generations. *Energy* **116**, 445–458 (2016).
13. Ravindran, S. & Victoire, T. A. A. A bio-geography-based algorithm for optimal siting and sizing of distributed generators with an effective power factor model. *Comput. Electr. Eng.* **72**, 482–501 (2018).
14. Gill, A. & Singh, P. Optimal penetration of distributed generation system in radial distribution network using adaptive scheme. *J. Phys. Conf. Ser.* **1914**(1), 012027 (2021).
15. Wong, L. A., Ramachandaramurthy, V. K., Walker, S. L. & Ekanayake, J. B. Optimal placement and sizing of battery energy storage system considering the duck curve phenomenon. *IEEE Access* **8**, 197236–197248 (2020).
16. Yuan, Z., Wang, W., Wang, H. & Yildizbasi, A. A new methodology for optimal location and sizing of battery energy storage system in distribution networks for loss reduction. *J. Energy Storage* **29**, 101368 (2020).
17. Nguyen, T. P. & Vo, D. N. Optimal number, location, and size of distributed generators in distribution systems by symbiotic organism search based method. *Adv. Electr. Electron. Eng.* **15**(5), 724–735 (2018).
18. Chillab, R. K., Jaber, A. S., Smida, M. B. & Sakly, A. Optimal DG location and sizing to minimize losses and improve voltage profile using Garra Rufa optimization. *Sustainability* **15**(2), 1156 (2023).
19. Nekooei, K., Farsangi, M. M., Nezamabadi-Pour, H. & Lee, K. Y. An improved multi-objective harmony search for optimal placement of DGs in distribution systems. *IEEE Trans. Smart Grid* **4**(1), 557–567 (2013).
20. Ganguly, S. & Samajpati, D. Distributed generation allocation on radial distribution networks under uncertainties of load and generation using genetic algorithm. *IEEE Trans. Sustain. Energy* **6**(3), 688–697 (2015).
21. Habib, H. U. R. et al. Optimal placement and sizing problem for power loss minimization and voltage profile improvement of distribution networks under seasonal loads using Harris Hawks optimizer. *Int. Trans. Electr. Energy Syst.* **7**, 1–49 (2022).
22. Lee, S. H. & Park, J. W. Selection of optimal location and size of multiple distributed generations by using Kalman filter algorithm. *IEEE Trans. Power Syst.* **24**(3), 1393–1400 (2009).
23. Prabha, D. R., Jayabarathi, T., Umamageswari, R. & Saranya, S. Optimal location and sizing of distributed generation unit using intelligent water drop algorithm. *Sustain. Energy Technol. Assess.* **11**, 106–113 (2015).
24. Al-Ammar, E. A. et al. ABC algorithm based optimal sizing and placement of DGs in distribution networks considering multiple objectives. *Ain Shams Eng. J.* **12**(1), 697–708 (2021).
25. Abou El-Ela, A. A., El-Sehiemy, R. A. & Abbas, A. S. Optimal placement and sizing of distributed generation and capacitor banks in distribution systems using water cycle algorithm. *IEEE Syst. J.* **12**(4), 3629–3636 (2018).
26. Wang, Z., Chen, B., Wang, J., Kim, J. & Begovic, M. M. Robust optimization based optimal DG placement in microgrids. *IEEE Trans. Smart Grid* **5**(5), 2173–2182 (2014).
27. Khunkitti, S., Boonluk, P. & Siritaratiwat, A. Optimal location and sizing of BESS for performance improvement of distribution systems with high DG penetration. *Int. Trans. Electr. Energy Syst.* **9**, 1–16 (2022).
28. Amini, F. & Kazemzadeh, R. Distributed generations optimal placement and sizing in unbalanced distribution systems with respect to uncertainties. *Int. J. Renew. Energy Res.* **7**(2), 1–11 (2017).
29. Schneider, K. P. et al. Analytic considerations and design basis for the IEEE distribution test feeders. *IEEE Trans. Power Syst.* **33**(3), 3181–3188 (2017).
30. Minh, C. D. Optimal installation of solar power sources for the distribution grid in Ho Chi Minh City. Master thesis, Ton Duc Thang University, Vietnam (2022).
31. Pham, T. D. Integration of photovoltaic units, wind turbine units, battery energy storage system, and capacitor bank in the distribution system for minimizing total costs considering harmonic distortions. *Iran. J. Sci. Technol. Trans. Electr. Eng.* **6**, 1–18 (2023).
32. Oda, E. S. et al. Stochastic optimal planning of distribution system considering integrated photovoltaic-based DG and DSTATCOM under uncertainties of loads and solar irradiance. *IEEE Access* **9**, 26541–26555 (2021).
33. Nazari, S. et al. Experimental determination and analysis of CO2, SO2 and NOx emission factors in Iran's thermal power plants. *Energy* **35**(7), 2992–2998 (2010).
34. Hung, D. Q., Mithulananthan, N. & Bansal, R. C. Integration of PV and BES units in commercial distribution systems considering energy loss and voltage stability. *Appl. Energy* **113**, 1162–1170 (2014).
35. Nguyen, T. T., Nguyen, T. T. & Le, B. Artificial ecosystem optimization for optimizing of position and operational power of battery energy storage system on the distribution network considering distributed generations. *Expert Syst. Appl.* **208**, 118127 (2022).
36. Motling, B., Paul, S. & Dey, S. H. N. Siting and sizing of DG unit to minimize loss in distribution network in the presence of DG generated harmonics. In *2020 International Conference on Emerging Frontiers in Electrical and Electronic Technologies (ICEFEET)* 1–5 (2020).
37. Prakash, R., Lokeshgupta, B. & Sivasubramani, S. Multi-objective bat algorithm for optimal placement and sizing of DG. In *2018 20th National Power Systems Conference (NPSC)* 1–6 (2018).
38. Pukhrem, S., Conlon, M. F., Sunderland, K. & Basu, M. Analysis of voltage fluctuation and flicker on distribution networks with significant PV installations. In *31st European Photovoltaic Solar Energy Conference and Exhibition* 1–6 (2015).
39. Pierezan, J. & Coelho, L. D. S. Coyote optimization algorithm: a new metaheuristic for global optimization problems. In *2018 IEEE Congress on Evolutionary Computation (CEC)* 1–8 (2018).
40. Chin, V. J. & Salam, Z. Coyote optimization algorithm for the parameter extraction of photovoltaic cells. *Sol. Energy* **194**, 656–670 (2019).

41. Roeva, O., Zoteva, D. & Vassilev, P. Generalized net model of coyote optimization algorithm. *Int. J. Bioautom.* **26**(4), 353 (2022).
42. Ramadan, A., Ebeed, M., Kamel, S., Agwa, A. M. & Tostado-Véliz, M. The probabilistic optimal integration of renewable distributed generators considering the time-varying load based on an artificial gorilla troops optimizer. *Energies* **15**(4), 1302 (2022).
43. Hassan, A. S., Sun, Y. & Wang, Z. Water, energy and food algorithm with optimal allocation and sizing of renewable distributed generation for power loss minimization in distribution systems (WEF). *Energies* **15**(6), 2242 (2022).
44. Hung, D. Q., Mithulananthan, N. & Bansal, R. C. Analytical strategies for renewable distributed generation integration considering energy loss minimization. *Appl. Energy* **105**, 75–85 (2013).
45. Mirjalili, S. et al. Salp swarm algorithm: A bio-inspired optimizer for engineering design problems. *Adv. Eng. Softw.* **114**, 163–191 (2017).
46. Faris, H., Mirjalili, S., Aljarah, I., Mafarja, M. & Heidari, A.A. Salp swarm algorithm: Theory, literature review, and application in extreme learning machines. In *Nature-Inspired Optimizers: Theories, Literature Reviews and Applications* 185–99 (2020).
47. Milovanović, M., Tasić, D., Radosavljević, J. & Perović, B. Optimal placement and sizing of inverter-based distributed generation units and shunt capacitors in distorted distribution systems using a hybrid phasor particle swarm optimization and gravitational search algorithm. *Electr. Power Comp. Syst.* **48**(6–7), 543–557 (2020).
48. Su, C. L., Chen, L. Y. & Yu, J. T. April harmonics measurements and analysis of battery energy storage systems in microgrids. In *2019 IEEE 2nd International Conference on Power and Energy Applications (ICPEA)* 163–66 (2019).
49. Zou, K., Agalgaonkar, A. P., Muttaqi, K. M. & Perera, S. Distribution system planning with incorporating DG reactive capability and system uncertainties. *IEEE Trans. Sustain. Energy* **3**(1), 112–123 (2011).
50. Gampa, S. R. & Das, D. Optimum placement and sizing of DGs considering average hourly variations of load. *Int. J. Electr. Power Energy Syst.* **66**, 25–40 (2015).
51. Mongird, K. et al. An evaluation of energy storage cost and performance characteristics. *Energies* **13**(13), 3307 (2020).
52. Truong, A. H., Ha-Duong, M. & Tran, H. A. Economics of co-firing rice straw in coal power plants in Vietnam. *Renew. Sustain. Energy Rev.* **154**, 111742 (2022).

Author contributions

T.D.P: Writing—original draft, Methodology, Simulation, Formal analysis, Data collection; T.T.N: Conceptualization, Methodology, administration, Writing—review & editing, Supervision, Conceptualization; L.C.K: review & editing, Supervision.

Funding

Thai Dinh Pham was funded by the Master, PhD Scholarship Programme of Vingroup Innovation Foundation (VINIF), code VINIF.2023.TS.106.

Declarations

Competing interests

The authors declare no competing interests.

Additional information

Supplementary Information The online version contains supplementary material available at https://doi.org/10.1038/s41598-025-01972-6.

Correspondence and requests for materials should be addressed to T.T.N.

Ain Shams Engineering Journal 15 (2024) 102720

Contents lists available at ScienceDirect

Ain Shams Engineering Journal

journal homepage: www.sciencedirect.com

Full Length Article

Minimize renewable distributed generator costs while achieving high levels of system uniformity and voltage regulation

Thai Dinh Pham [a], Le Chi Kien [a], Thang Trung Nguyen [b,*]

[a] Faculty of Electrical and Electronics Engineering, Ho Chi Minh City University of Technology and Education, Ho Chi Minh City, Vietnam
[b] Power System Optimization Research Group, Faculty of Electrical and Electronics Engineering, Ton Duc Thang University, Ho Chi Minh City, Vietnam

ARTICLE INFO

Keywords:
Modified coyote optimization algorithm
Photovoltaic module
Wind turbine
Power loss
Voltage profile

ABSTRACT

This research facilitates the placement of solar and wind-powered distributed generators (RDGs) in an unbalanced 3-phase IEEE 25-node distribution system intended to minimize the total expense of buying electricity from the grid and releasing carbon dioxide over twenty years. The probability distribution functions of Beta and Rayleigh are employed to attain solar illumination and wind velocity in a particular region. Unbalanced voltage deviation (UVD) and harmonic flows (HFs) from non-ideal loads and RDGs are considered. Metaheuristic methods are coded in MATLAB to find RDGs' location and capacity, and then OpenDSS is used to calculate power and harmonic issues. As a result, the total expenses can be reduced to $1.4141 million, which is 10.7% of the base system's. Additionally, HFs and UVDs at every node follow the IEEE Std. 519 and the IEEE Std. 45-2002, respectively. So, the placement of RDGs has a beneficial position in unbalanced distribution systems.

1. Introduction

The continuous development of various energy conversion technologies besides the energy crisis has created many major breakthroughs in integrating distributed generators (DGs) in the distribution system to contribute to reducing dependence on traditional concentrated energy sources [1–3]. DGs are often proposed to be installed closer to the consumption and provide energy to meet a part of the total demand. However, DG penetration needs to be carefully considered to avoid undesirable effects on the grid, such as fault currents, voltage sags, voltage flickers, harmonics, etc., in the system [4,5]. Therefore, identifying the suitable installation of DGs plays an important role, and this can bring great benefits technically and economically. Many studies have indicated that properly connecting DGs can enormously minimize power losses on the distribution branches [6,7]. This significantly contributes to a cut in operating costs due to loss cost reduction. On the other hand, the system's power quality is also enhanced by supporting the voltage at the nodes to the best zone and mitigating harmonic distortions, according to the IEEE Std. 519 [8,9]. Other researchers have also demonstrated improved capacity limit for transferring energy on distribution branches and enhanced system reliability through connecting DGs accordingly [10,11].

In previous studies, authors often focused on minimizing power loss and enhancing voltage profile as the main objectives [12,13]. By applying optimization algorithms, the obtained results from the simulation showed excellent technical–economic benefits in improving loss reduction and voltage profile after integrating DGs into the original system. However, these targets are not enough to consider for connecting DGs in the distribution systems, and it is necessary to determine other essential factors, such as the penetration level of DGs, the emissions and total investment costs, and operation and maintenance of the DGs in the integrated systems over the project life cycle [14]. Besides, once DGs were connected to the system, the power converters generated harmonic flows affecting the grid, especially for high penetration levels of DGs over the allowable standard [15]. Most of the past studies only implemented the peak demand of loads, and generation output was constant throughout the project period in the distribution systems [16,17]. Therefore, the achieved solutions could be more optimal at variable loads and fluctuating generation sources. In addition, the unbalanced three-phase distribution systems usually exist in reality with different characteristics of unequal loading between phases compared to the balanced system. However, it has yet to receive much attention from researchers [18]. Moreover, for solving the optimization problem of determining the allocation of DGs in distributed systems, various popular methods were applied, such as genetic algorithm (GA) [19], particle swarm optimization (PSO) [20,21], ant colony algorithm (ACA) [22] and artificial bee colony algorithm (ABC) [23,24]. These algorithms

* Corresponding author.
E-mail addresses: thaipd.ncs@hcmute.edu.vn (T.D. Pham), kienlc@hcmute.edu.vn (L.C. Kien), nguyentrungthang@tdtu.edu.vn (T.T. Nguyen).

https://doi.org/10.1016/j.asej.2024.102720
Received 22 September 2023; Received in revised form 7 January 2024; Accepted 16 February 2024
Available online 2 March 2024

List of symbols

$CO_{TotalCosts}$ The objective function of total costs
$CO_{Inv}, CO_{OM}, CO_{Emis}$ Components in the objective function of investment, O&M and emission costs
CO_{Grid} Component in the objective function of electricity purchase cost from grid
Pr_{PF}, Pr_{WF}, Initial investment cost of PF and WF ($/MW)
$AP_{PF}^{Rated}, AP_{WF}^{Rated}$ Rated power of PF and WF
$Pr_{PF}^{OM}, Pr_{WF}^{OM}$ Operation and maintenance cost for PF and WF ($/MWh)
$AP_{PF,H,Y}, AP_{WF,H,Y}$ Actual active power of PF and WF at the H^{th} hour of the Y^{th} year
$RP_{PF,H,Y}, RP_{WF,H,Y}$ Actual reactive power of PF and WF at the H^{th} hour of the Y^{th} year
θ_Y The function for calculating present value factor with interest rate of 9%
$RP_{Sub,H,Y}, RP_{PF,H,Y}, RP_{WF,H,Y}$ Reactive power injections from the main grid, PF and WF at the H^{th} hour of the Y^{th} year, respectively
$AP_{load,d,H,Y}, RP_{load,d,H,Y}$ Active and reactive powers from the d^{th} load, at the H^{th} hour of the Y^{th} year
$AP_{loss,b,H,Y}^{Aft}, RP_{loss,b,H,Y}^{Aft}$ Active and reactive power losses from the b^{th} branch at the H^{th} hour of the Y^{th} year after connecting DGs
$I_b^{Max}, I_{b,k}$ Maximum allowable current limit and the current magnitude at the b^{th} branch and the k^{th} phase
N_k, N_s, N_b, N_d The phase, node, branch and load numbers, respectively
V_s^k The voltage magnitude at the k^{th} phase of the s^{th} node
V^{Max}, V^{Min} Maximum and minimum allowable voltage limits
THD_V^{Max}, IHD_V^{Max} Maximum limits of total and individual voltage harmonic distortions
$THD_{V,s,k}$ Total voltage harmonic distortion at the s^{th} node and the k^{th} phase
$IHD_{V,s,k}^h$ Individual voltage harmonic distortion of the h^{th} order at the s^{th} node and the k^{th} phase
$AP_{loss,b,H,Y}^{Bef}, RP_{loss,b,H,Y}^{Bef}$ Active and reactive power losses from the b^{th} branch at the H^{th} hour of the Y^{th} year before connecting DGs
$AP_{PF}^{Max}, AP_{PF}^{Min}$ Maximum and minimum active power limits of PF
$AP_{WF}^{Max}, AP_{WF}^{Min}$ Maximum and minimum active power limits of WF
$N_{Mem}^{Coy}, N_{Group}^{Coy}$ The coyote numbers in each group and the group numbers in population
Num_{Trial} The trial running numbers of the algorithm
L^{Cur}, Num_{Iter} The current and maximum iteration numbers of the algorithm
$Sl_{G,M}^{New}$ and $Sl_{G,M}$ The M^{th} new solution and the M^{th} current solution in the G^{th} group
$Sl_{G,r_{d1}}, Sl_{G,r_{d2}}$ The random solutions which are taken from random groups
r_d, r_{d1}, r_{d2} and r_{d3} Randomly produced numbers in the range from 0 to 1
Num^{Max} and Num^{Clo} The numbers of maximum and close couple solutions, respectively

were widely used because of their simple structure. However, their biggest disadvantage is that they easily fall into the local optimum region in high-dimensional space and with a low convergence rate. On the other hand, approaches that had better performance were also suggested, including improved particle swarm optimization (IPSO) [25], equilibrium optimizer (EO) [26], whale optimization algorithm (WOA) [27], sunflower optimization algorithm (SFA) [28], ant lion optimization algorithm (ALOA) [29], cuckoo search algorithm (CSA) [30], shuffled frog leap algorithm (SFLA) [31], mutated salp swarm algorithm (MSSA) [32] and coyote optimization algorithm (COA) [33]. Although these methods had strengths in finding global solutions, but they mainly depended on the setting parameters of algorithms and randomization, so the determination of the initial values should be investigated. Not only that, but the implementation was also complicated, and the convergence speed was relatively slow. In addition to meta-heuristic methods, mixed-integer nonlinear programming (MINLP) [34] and mixed-integer linear programming (MILP) [35] are also introduced to solve the same problem. However, the calculation process of these methods was complicated but less effective, so they were not commonly applied.

To overcome the mentioned limitations of previous papers, we introduce an effective algorithm with high stability for determining optimal solutions to the problem of installing renewable distributed generators in the unbalanced three-phase distribution system that exists universally in the real world, considering technical–economic aspects. The study focused on minimizing total costs over a 20-year project cycle with various constraints such as power balance, branch current, phase voltage, unbalanced voltage deviation, voltage harmonic distortions, degradation of power loss, and DG penetration levels. Not only that, but the research also develops a flexible simulation tool that coordinates two different software for power flow analysis quickly. The novelties of this study can be listed as follows:

– This work seeks the optimal solution for the location and sizing of photovoltaic farms and wind turbine farms, which are integrated simultaneously into the system to minimize total costs, including (1) investment cost, (2) operation and maintenance (O&M) cost, (3) cost of purchasing electricity from the grid for the load demand and (4) cost of emissions from conventional power plants. This is like a comprehensive consideration of both economic and technical aspects.
– The paper simulates an unbalanced three-phase distribution system considering the load demand and generation sources' output power vary with time. The study collects actual data on solar irradiance and wind speed in three years of 2019, 2020, and 2021 from Southern Vietnam region (Can Gio district, Ho Chi Minh city). Besides, Beta and Rayleigh probability distribution functions (pdfs) are suggested to simulate the solar irradiance and wind speed at the above search area for estimating the output power of photovoltaic modules and wind turbines, respectively.
– Furthermore, a recently published efficient method named modified coyote optimization algorithm (MCOA) [36] is applied to solving the considering problem. This powerful method has outstanding fast convergence features, high performance, and great stability. Besides, the study also develops co-simulation between MATLAB and OpenDSS software for solving problems related to analysis of power flow and harmonic flow with multiple harmonic sources. This is considered a novelty because very few previous studies have implemented this work successfully.

Based on the results obtained, the contributions of this work can be briefly summarized as follows:

– The study considered not only the harmonics that are generated by the nonlinear loads but also from the inverters-based DGs. The results indicated that the values representing harmonic distortions are within the allowable limits of IEEE Std. 519. Besides, the unbalanced voltage deviation index, which showed the voltage difference between the phases due to unequal loading, is also calculated to keep them according to IEEE Std. 45-2002.

– Moreover, another significant contribution of this study was the successful development of a co-simulation tool between MATLAB and OpenDSS software. This flexible platform has provided many advantages regarding flexibility and speed for solving power and harmonic flow problems.
– The optimal solutions by the introduced method (MCOA) for determining the appropriate DG installation can save much money compared to the original system. The loss reduction on branches, voltage profile, and unbalanced voltage deviation satisfy the technical constraints and are better than the base system. Besides, MCOA is also compared relatively under the same conditions with other positive metaheuristic methods such as IPSO [25], CSA [30], and COA [33] to demonstrate the superior performance of the suggested method.

The remaining parts of this paper can be divided into sections: Section 2 presents the problem formulation, Section 3 describes the applied method to solve the optimization problem, Section 4 analyzes the obtained results, and Section 5 summarizes the whole paper.

2. Problem formulation

2.1. Objective function

In this study, PF and WF are considered for simultaneous integration in unbalanced radial distribution system for minimizing total costs while satisfying all constraints. It includes the investment cost, O&M cost, electricity purchase cost from main grid and emissions cost. The objective can be expressed by the following mathematical formula [37]:

$$Minimize \;\; CO_{TotalCosts} = CO_{Inv} + CO_{OM} + CO_{Grid} + CO_{Emis} \;\; (\$) \tag{1}$$

where

$$CO_{Inv} = Pr_{PF}\cdot AP_{PF}^{Rated} + Pr_{WF}\cdot AP_{WF}^{Rated} \;\; (\$) \tag{2}$$

$$CO_{OM} = 30.4167 \times \sum_{Y=1}^{20}\sum_{H=1}^{288} \theta_Y \cdot \left(Pr_{PF}^{OM}\cdot AP_{PF,H,Y} + Pr_{WF}^{OM}\cdot AP_{WF,H,Y}\right) \;\; (\$) \tag{3}$$

$$CO_{Grid} = 30.4167 \times \sum_{Y=1}^{20}\sum_{H=1}^{288} \theta_Y \cdot \left(Pr_{H,Y}^{Grid}\cdot AP_{Sub,H,Y}\right) \;\; (\$) \tag{4}$$

$$CO_{Emis} = 30.4167 \times \sum_{Y=1}^{20}\sum_{H=1}^{288} \theta_Y \cdot \left(Pr_{Emis}\cdot G_{Emis}\cdot AP_{Sub,H,Y}\right) \;\; (\$) \tag{5}$$

In Eqs. (1)–(3), the symbols are specifically defined in the list of symbols. For Eq. (4), $Pr_{H,Y}^{Grid}$ and $AP_{Sub,H,Y}$ are electric purchase price from the main grid ($/MWh) and received power of the main grid which is injected through substation at the H^{th} hour of the Y^{th} year (MW). Besides, Pr_{Emis} and G_{Emis} at Eq. (5) are also called as emissions cost ($/kg) and total generated emissions (kg/MWh) from the main grid by using fossil fuels-based generators, respectively.

The study considers a project life cycle of 20 years with 365 days per year and 24 h per day. Each day represents a month and 288 results from the multiplication of 12 days and 24 h. The coefficient of 30.4167 in Eqs. (3)–(5) results from the ratio of 8760 h of a year to 288. Besides, to facilitate the evaluation of the economic efficiency of the project, all its costs that are paid in the future should be converted to present values, so function of θ_Y is added to the formulas for calculating CO_{OM}, CO_{Grid} and CO_{Emis}, and θ_Y is clearly defined in [38].

2.2. Operational constraints

2.2.1. Constraints for the power balances

Active and reacitve power demand of loads must be satisfied at each hour over the 20-year project as the priority requirement. However, generation from the main grid and renewable generators must equals the demands and the line losses as follows [39]:

$$AP_{Sub,H,Y} + AP_{PF,H,Y} + AP_{WF,H,Y} = \sum_{d=1}^{N_d} AP_{load,d,H,Y} + \sum_{b=1}^{N_b} AP_{loss,b,H,Y}^{Aft} \tag{6}$$

$$RP_{Sub,H,Y} + RP_{PF,H,Y} + RP_{WF,H,Y} = \sum_{d=1}^{N_d} RP_{load,d,H,Y} + \sum_{b=1}^{N_b} RP_{loss,b,H,Y}^{Aft} \tag{7}$$

2.2.2. Constraint of branch current

The current magnitude on each distribution branch should not exceed its maximum allowable thermal limit as [40]:

$$I_b^{Max} \geq I_{b,k}, \;\; b = 1,\cdots,N_b \;\; \& \;\; k = 1,\cdots,N_k \tag{8}$$

2.2.3. Constraints of node voltage

In this study, the phase voltage magnitude at each node is kept within the best operating range of V^{Min} (0.95 pu) and V^{Max} (1.05 pu) [39,40].

$$V^{Min} \leq \left|V_s^k\right| \leq V^{Max}, \;\; s = 1,\cdots,N_s \;\; \& \;\; k = 1,\cdots,N_k \tag{9}$$

2.2.4. Constraint of unbalanced voltage deviation

This work considers unbalanced three-phase distribution system, so the voltage at each phase of nodes will have difference. The unbalanced voltage deviation ($UV_{dev,s}$) should be kept within the constraint according to IEEE Std. 45-2002 [41]:

$$UV_{dev,s} \;\; (\%) \leq UVD_{Std}^{Max} \;\; (\%) \tag{10}$$

where

$$UV_{dev,s} \;\; (\%) = 100 \times \frac{V_{dif,s}^{Max}}{V_{un,s}^{Mean}}, \;\; s = 1,\cdots,N_s \tag{11}$$

In Eq. (11), UVD_{Std}^{Max} is the maximum allowable limit of unbalanced voltage deviation, which is selected to be 3% [41]. $V_{un,s}^{Mean}$ and $V_{dif,s}^{Max}$ are the average phase voltage value and maximum voltage difference from the average phase voltage value at the s^{th} node. The two factors are presented in detail in item A.1 of Appendix.

2.2.5. Constraints of total and individual harmonic distortions

The two factors should not exceed the maximum acceptable limits as indicated in the IEEE Std. 519 [37]. So, the following constraints are applied to satisfy the standard. In this case, THD_V^{Max} and IHD_V^{Max} are taken as 5% and 3%, respectively.

$$THD_V^{Max} \;\; (\%) \geq THD_{V,s,k} \;\; (\%) \tag{12}$$

$$IHD_V^{Max} \;\; (\%) \geq IHD_{V,s,k}^{h} \;\; (\%) \tag{13}$$

2.2.6. Degradation of power loss

In the study, distributed generators are integrated into the unbalanced system to reduce power loss. Therefore, the total losses on all branches after connecting DGs must be less than those before connecting DGs [40].

$$\sum_{b=1}^{N_b} AP_{loss,b,H,Y}^{Bef} > \sum_{b=1}^{N_b} AP_{loss,b,H,Y}^{Aft} \tag{14}$$

$$\sum_{b=1}^{N_b} RP_{loss,b,H,Y}^{Bef} > \sum_{b=1}^{N_b} RP_{loss,b,H,Y}^{Aft} \tag{15}$$

2.2.7. Constraints of DGs installation

The allowable installation limits of DGs should be within predefined lower and upper bounds as follows [38]:

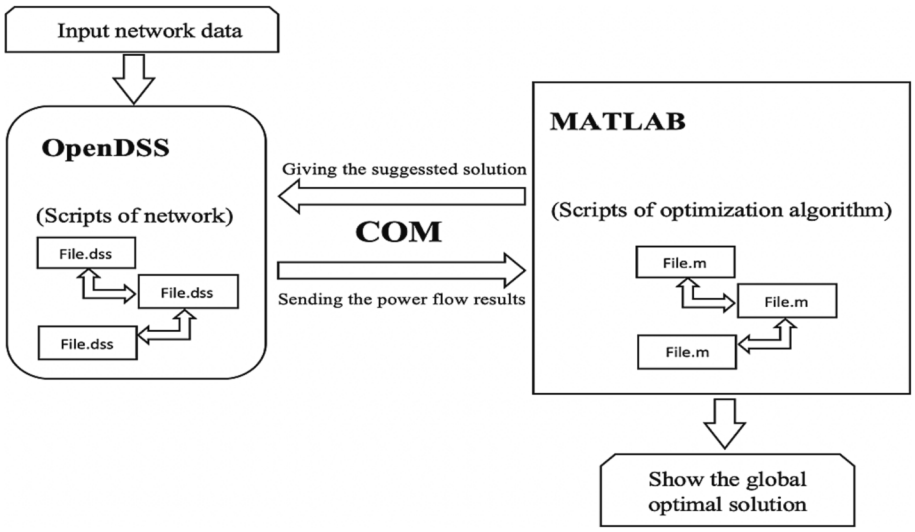

Fig. 1. Basic operating principle of OpenDSS and MATLAB.

$$AP_{PF}^{Min} \le AP_{PF}^{Rated} \le AP_{PF}^{Max} \tag{16}$$

$$AP_{WF}^{Min} \le AP_{WF}^{Rated} \le AP_{WF}^{Max} \tag{17}$$

$$AP_{PF,H,Y} + AP_{WF,H,Y} \le \sum_{d=1}^{N_d} AP_{load,d,H,Y} + \sum_{b=1}^{N_b} AP_{loss,b,H,Y}^{Aft} \tag{18}$$

3. Applied methods

3.1. Simulation tools

In this study, OpenDSS software is applied. It is an open-source version of the distribution system simulator (DSS), which was introduced by the Electric Power Research Institute (EPRI) for support simulation and analysis of power systems in the frequency domain [42]. This is a powerful tool for building a research platform with flexibility and efficiency for solving complex load flow problems quickly and accurately, especially the distributed generation sources integrated systems. OpenDSS was built to allow interaction with other environments, such as PYTHON, C#, VBA, MATLAB, etc., through the windows component objective model (COM). The combination of OpenDSS and other software created a useful simulation tool to overcome gaps in previous analysis tools.

For this work, OpenDSS and MATLAB are combined as a co-simulation tool, and its general principle is shown in Fig. 1. Remarkably, the coded optimization algorithm in MATLAB proposes the possible solution for solving the considering problem, and this solution is transferred to OpenDSS through COM. After receiving the solution, OpenDSS which contains the system description, is responsible for solving the power flow problem, and the obtained results, such as voltage, current, power loss, etc., are sent back to MATLAB for computing and evaluating the quality of the proposed solution. Users define the process of controlling the operation of OpenDSS through written code in MATLAB. This co-simulation has created a flexible platform for solving problems related to power system analysis.

3.2. Modified coyote optimization algorithm

In this research, the modified coyote optimization algorithm (MCOA) is suggested to solve the optimization problem of installing PF and WF to minimize the total costs. MCOA is a modified version of COA that is inspired from the *Canis latrans* behavior in nature [43]. MCOA was recently published, and it demonstrated higher stability and efficiency than other meta-heuristic algorithms [36]. This algorithm is based on the operating principle of COA, so it inherits the outstanding advantages of the original algorithm. Besides, it has modifications in the new generation equations to enhance the algorithm's efficiency. In coyote species, the community is divided into N_{Group}^{Coy} groups and each group has N_{Mem}^{Coy} members. So, the population of the species is the product of $(N_{Group}^{Coy} \times N_{Mem}^{Coy})$. In this algorithm, individuals' positions are considered as potential solutions to the optimization problem. The process of natural selection and their movement with the cultural tendency in the community to find better living conditions are called new solution generation [43]. Application of the suggested method for solving the considered problem can be presented by following steps:

Step 1: Initial parameters setting, including N_{Group}^{Coy}, N_{Mem}^{Coy}, Num_{Iter} and Num_{Trial}.

Step 2: MCOA produces the initial solutions randomly within predetermined lower bound (Sl^{Min}) and upper bound (Sl^{Max}). The mathematic method for creating the initial solutions at the initial stage is presented in Eq. (19) [33]:

$$Sl_{G,M} = Sl^{Min} + r_d.\left(Sl^{Max} - Sl^{Min}\right);\ \ G = 1,\cdots,N_{Group}^{Coy}\ \ \&\ \ M = 1,\cdots,N_{Mem}^{Coy} \tag{19}$$

Step 3: The proposed solutions from the developed algorithm in MATLAB are transferred to OpenDSS (OpenDSS scripts contain the described system) via COM for solving power and harmonic flows. The obtained results are collected and sent back to MATLAB by COM for evaluating the fitness of the solutions based on the objective function. The best current solution in each group will be determined through comparing their fitness values.

Step 4: Like mentioned, each generated coyote is a viable solution. Specifically, the newly created M^{th} coyote in the G^{th} group is considered as a new solution ($Sl_{G,M}^{New}$). In this stage, $Sl_{G,M}^{New}$ are produced according to Eq. (20) [36]:

$$Sl_{G,M}^{New} = Sl_{G,M} + r_{d1}.\left(Sl_{G}^{GrBest} - Sl_{G,r_{d1}}\right) + r_{d2}.\left(Sl^{PoBest} - Sl_{G,r_{d2}}\right);\ \ G = 1,\cdots,N_{Group}^{Coy}\ \ \&\ \ M = 1,\cdots,N_{Mem}^{Coy} \tag{20}$$

where Sl_{G}^{GrBest} and Sl^{PoBest} are the best solutions of the G^{th} group and the whole population, respectively. Besides, $Sl_{G,r_{d1}}$ and $Sl_{G,r_{d2}}$ are defined as randomly chosen solutions in the G^{th} group. The control variables of newly generated solutions are checked and adjusted to always keep them within predetermined allowable limits.

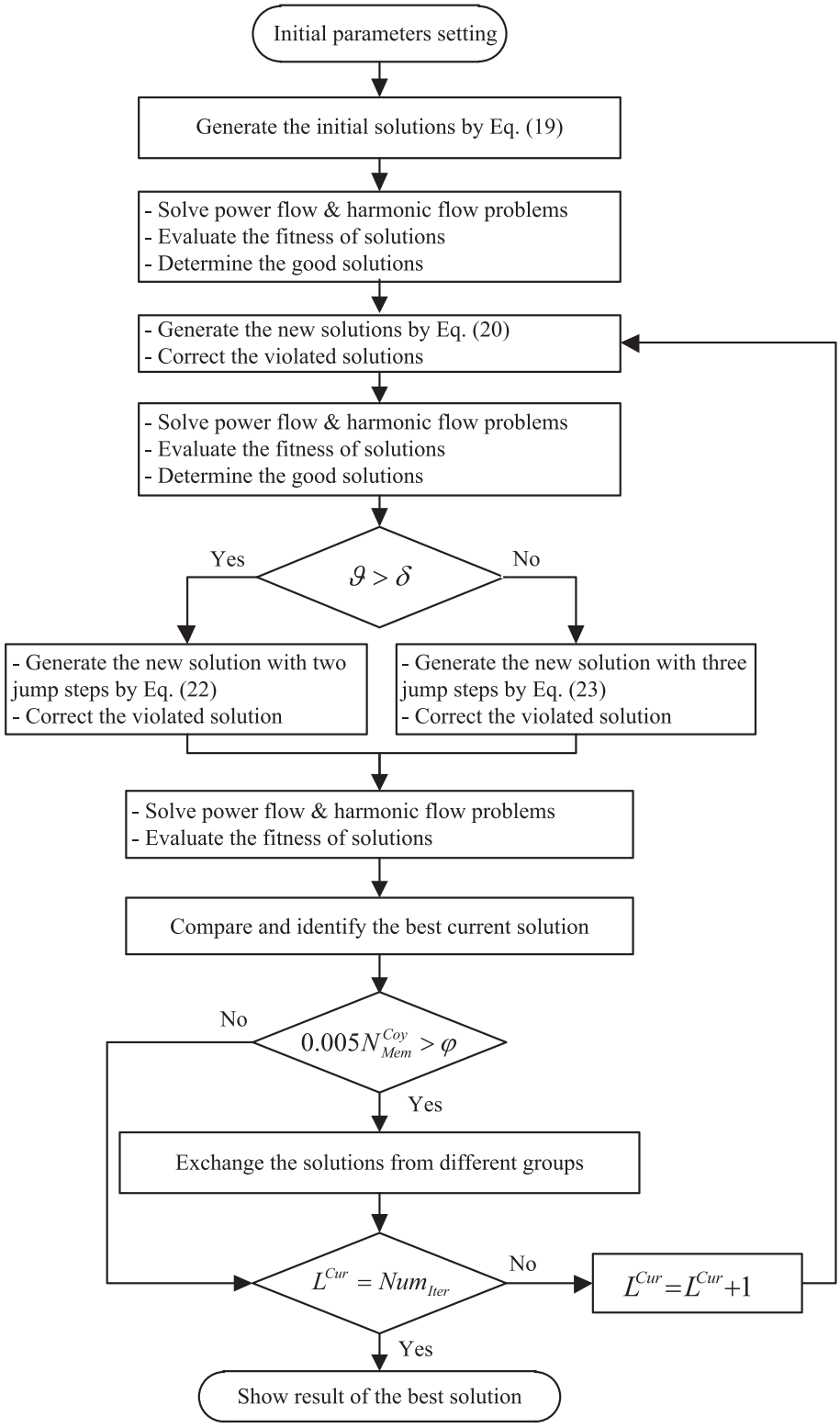

Fig. 2. The flowchart of MCOA for determining the optimal solutions.

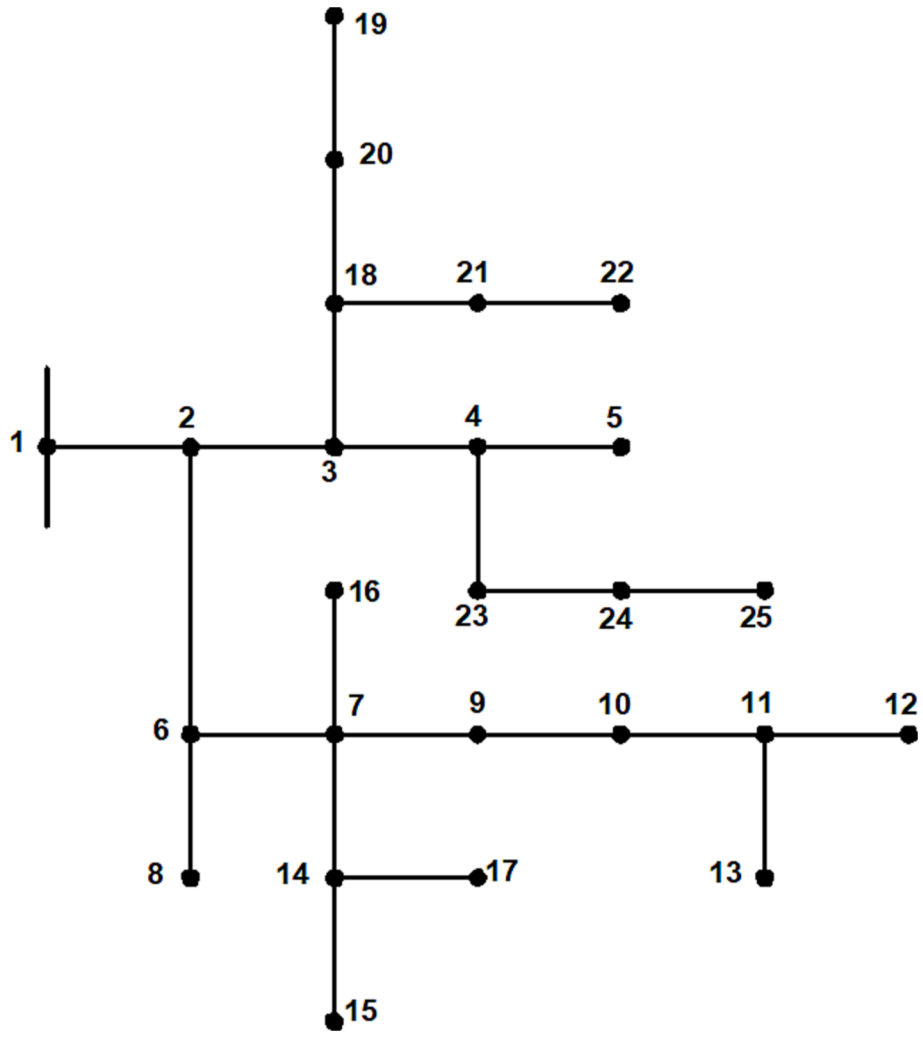

Fig. 3. The 25-node unbalanced radial distribution system.

Step 5: Step 3 is repeated for computing and evaluating the fitness of the found solutions.

Step 6: Calculate the factor δ, as shown in Eq. (21):

$$\delta = \frac{Num^{Clo}}{Num^{Max}} \tag{21}$$

If δ is less than the coefficient (ϑ), Eq. (22) is selected to generate a new solution for each group. Otherwise, the new solution is obtained by using Eq. (23) [36].

$$Sl_G^{New} = Sl^{PoBest} + r_{d1}\cdot\left(Sl^{PoBest} - Sl_{G,r_1}^{GrBest}\right) + r_{d2}\cdot\left(Sl^{PoBest} - Sl_{G,r_2}^{GrBest}\right) \tag{22}$$

$$Sl_G^{New} = Sl^{PoBest} + r_{d1}\cdot\left(Sl^{PoBest} - Sl_{G,r_{d1}}^{GrBest}\right) + r_{d2}\cdot\left(Sl^{PoBest} - Sl_{G,r_{d2}}^{GrBest}\right) + r_{d3}\cdot\left(Sl^{PoBest} - Sl_{G,r_{d3}}^{GrBest}\right) \tag{23}$$

where $Sl_{G,r_{d1}}^{GrBest}$, $Sl_{G,r_{d2}}^{GrBest}$, $Sl_{G,r_{d3}}^{GrBest}$ are the best current solutions in each group which are taken at random.

Step 7: Step 3 is repeated to compute and evaluate the fitness of the found solution.

Step 8: Select the best solution with the smallest fitness function in the current population.

Step 9: Swapping two solutions in each two randomly selected groups is implemented, if the result of $0.005 \times N_{Mem}^{Coy}$ is greater than φ(where φ is number randomly generated in the range of [0,1]). This exchange mainly depends on the number of individuals in each group.

Step 10: If the maximum iteration is reached, the best solution is determined and the iterative algorithm is terminated. Otherwise, the computation process moves to the next iteration by implementing Step 4.

The above steps for finding the optimal solution can be also briefly illustrated through the flowchart as Fig. 2.

4. Simulation results and discussions

In this study, PF and WF with inverters that can operate at the power factor of 0.9 (lagging) [44] are considered for simultaneous integration into the distribution system to minimize the total costs. The unbalanced three-phase distribution system exists widely in the real world, with the voltage difference between phases due to unequal loading and asymmetric line parameters. In this case, the 25-node UDS, which characterizes the type of unbalanced system, is selected for the simulation. This system operates at 4.16 kV with a load demand of 3.3466 MW and 2.5267 MVar. The single-line diagram of the system is drawn in Fig. 3, and the node and line data are clearly presented in [45].

The minimum and maximum numbers of photovoltaic modules for PF are (3,000 and 30,000 modules), and the numbers of wind turbines for WF are (3 and 30 turbines), respectively. The main parameters of the selected photovoltaic module and wind turbine are also described in Tables A.1 and A.2 in Appendix A. In this work, the research area is Southern Vietnam, with a latitude of 10.508 and a longitude of 106.863

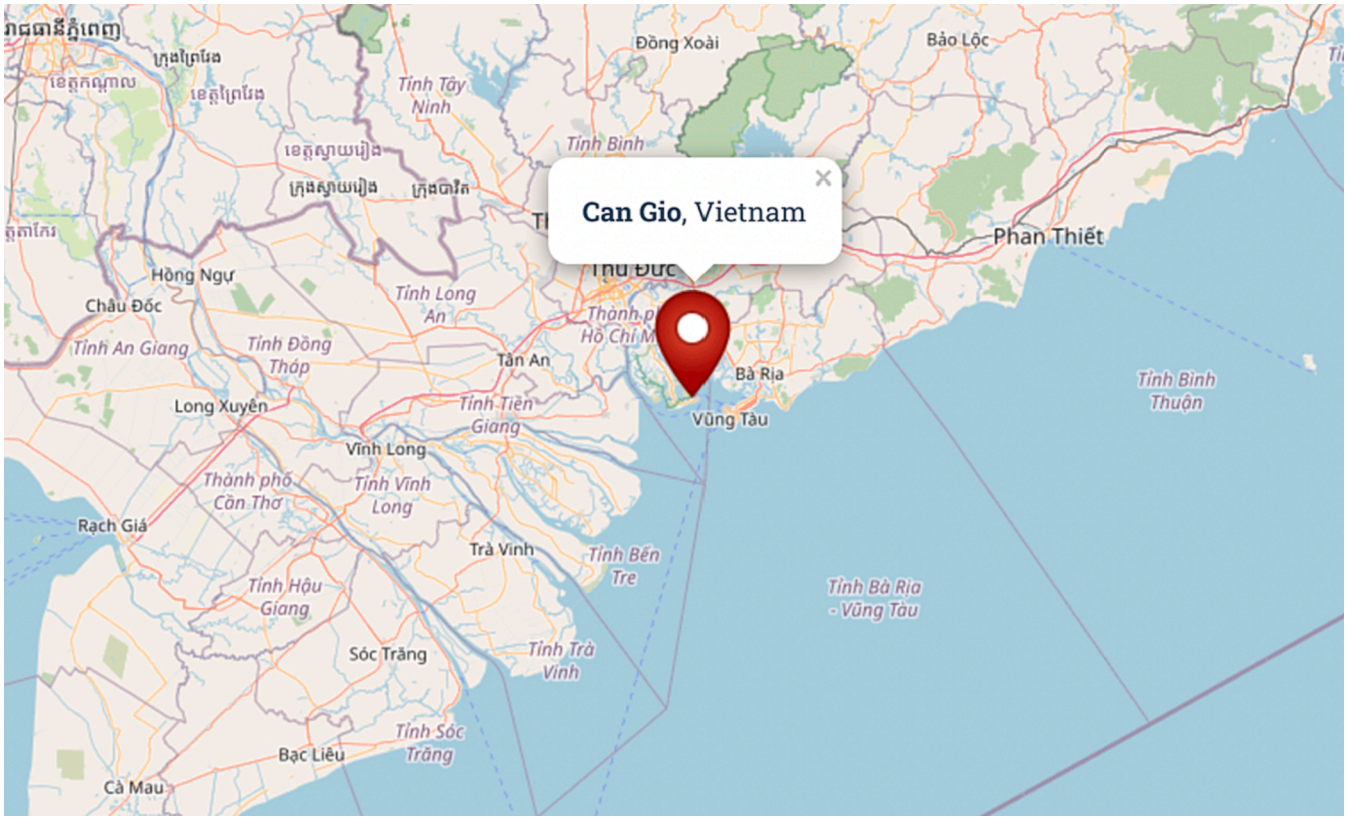

Fig. 4. The research region (Can Gio district, Ho Chi Minh city).

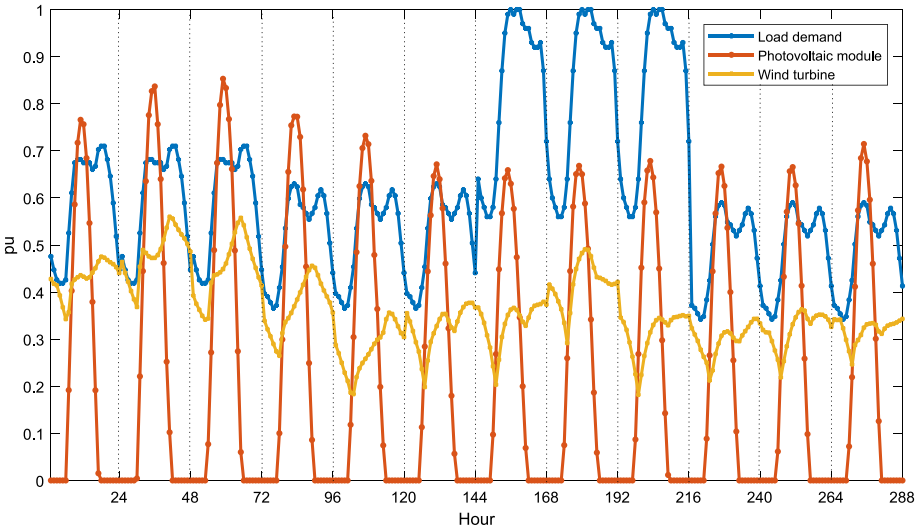

Fig. 5. Output curves of generation sources and load demand over time.

Table 1
Harmonic spectrum of nonlinear loads and inverter-based DGs.

Harmonic order		1	5	7	11	13	17	19	23	25	29	31
Nonlinear loads	Magnitude (%) for six-pulse (type 1) at node 13 and node 23	100	20.0	14.3	9.1	7.7	5.9	5.3	4.3	4.0	3.4	3.2
	Magnitude (%) for six-pulse (type 2) at node 08 and node 19	100	19.1	13.1	7.2	5.6	3.3	2.4	1.2	0.8	0.2	0.2
Inverters	Magnitude (%) for inverters-based DGs	100	4.0	4.0	2.0	2.0	1.5	1.5	0.6	0.6	0.6	0.6

(Can Gio district, Ho Chi Minh City), as shown in Fig. 4 [46]. This area has great potential for developing renewable energy sources such as solar and wind power. Besides, the used data for calculating the power output of PF and WF is collected over three years (2019, 2020, and 2021) from the above region. Specifically, values of solar irradiance and wind speed vary over time, with 288 data points used to show 12 months

Table 2
The best result in 30 trial runs for solving the optimization problem.

Method	Optimal solution PF & WF	CO_{Inv} ($ million)	CO_{OM} ($ million)	CO_{Grid} ($ million)	CO_{Emis} ($ million)	$CO_{TotalCosts}$ ($ million)
Base	–	–	–	12.7520	0.4683	13.2203
IPSO	Node 05 – 2,1440 modules Node 09 – 18 turbines	4.6258	0.8002	6.2105	0.2302	11.8667
CSA	Node 03 – 1,9933 modules Node 09 – 20 turbines	4.9151	0.8384	5.9170	0.2185	11.8890
COA	Node 07 – 2,2916 modules Node 10 – 16 turbines	4.3346	0.7617	6.4827	0.2412	11.8201
MCOA	Node 15 – 2,3317 modules Node 10 – 16 turbines	4.3577	0.7669	6.4418	0.2397	11.8062

in 1 year (24 h of a day represent one month), and these data points are the average values of the dataset for three years. In this case, Beta pdf and Rayleigh pdf [47] are applied to simulate the solar irradiance and wind speed to predict the output powers from photovoltaic modules and wind turbines, respectively. Besides, for simulating the load demand of the system, 288 data points are applied to show changes in loads, and they are referred to [47]. The output curves of generation and consumption are also clearly plotted in Fig. 5. As mentioned, harmonic distortions which are generated from nonlinear loads and inverters of photovoltaic modules and wind turbines, are fully considered. This study assumed that the nonlinear loads at nodes 13 and 23 emit harmonics of six-pulse converter (type 1), and the nonlinear loads at nodes 08 and 19 emit harmonics of six-pulse converter (type 2). The harmonic spectrum of harmonic sources from these nonlinear loads as well as inverters- based DGs are also presented in detail as Table 1 [15].

In this paper, MCOA, IPSO, CSA, and COA are performed to demonstrate the outstanding performance of the suggested method. For the IPSO's simulation, the population is selected to be 25, and the acceleration factors C_{1i}, C_{2i}, C_{1f} and C_{2f} are selected to be 2.5, 0.5, 0.5 and 2.5, respectively. In addition, the inertia weight factors are chosen as follows: $\alpha = 0.9$ and $\beta = 0.5$ [25]. In implementing CSA, the population (N) is set to 25 and the alien egg discovery probability ($P\alpha$) is selected to be 0.25 [30]. For running both COA and MCOA, the coefficient (ϑ) is surveyed and selected to be 0.2, and the number of groups (N_{Group}^{Coy}) and the number of individuals in each group (N_{Mem}^{Coy}) are set to 5 and 4, respectively. For the fair comparison, the number of iterations (Num_{Iter}) is surveyed and selected as 80 and the number of trial runs (Num_{Trial}) is 30 for all implemented methods. On the other hand, the maximum values of harmonic distortions (THD_V^{Max} and IHD_V^{Max}) are set to 5% and 3% according to IEEE Std. 519 [9]. The unbalanced voltage deviation (UVD_{Std}^{Max}) is selected to be 3% to satisfy IEEE Std. 45-2002 [41] and the established voltage range for this study is [0.95, 1.05] (pu) [39]. Furthermore, the involved parameters to calculate cost functions, such as Pr_{PF}, C_{PF}^{OM}, Pr_{WF} and C_{WF}^{OM}, are set to 770,000 ($/MW), 10.0 ($/MWh), 1,882,000 ($/MW) and 10.0 ($/MWh), respectively [48,49]. Pr_{Emis} is chosen as 0.004 ($/kg) and G_{Emis} is 724 (kg/MWh) for generating emissions from conventional power plants [50]. Besides, the electricity prices ($Pr_{H,Y}^{Grid}$) at the peak hours, the standard hours and the off-peak hours, which are declared by the power company, are 128.9 $/MWh, 70.0 $/MWh, and 45.4 $/MWh, respectively [51].

As mentioned, IPSO, CSA, COA and MCOA are implemented to minimize total costs, including investment, O&M, purchasing electricity, and emissions. The best results in trials with the random generation of initial population are presented in Table 2. With the found optimal solution by MCOA, the total costs ($CO_{TotalCosts}$) went down sharply from $13.2203 million to $11.8062 million. It saved up to $1.4141 million, equivalent to 10.70% compared to the base system. This indicates that connecting proper DGs to the distribution system can reduce the costs significantly. Additionally, MCOA can provide lower total costs than IPSO, COA and CSA. $CO_{TotalCosts}$ of MCOA is only $11.8062 million, whereas it is $11.8667 million, $11.8890 million, and $11.8201 million for IPSO, CSA and COA, respectively. For considering

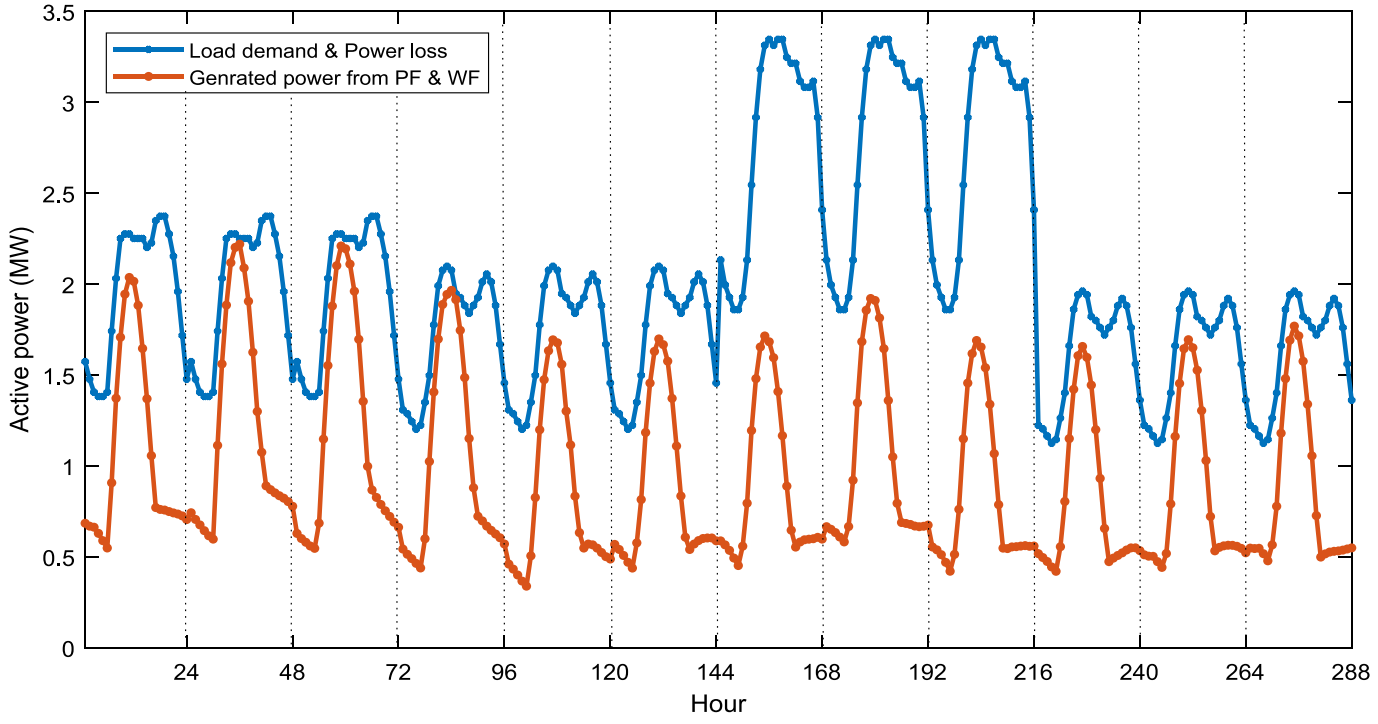

Fig. 6. Total active power of consumption and generation over time.

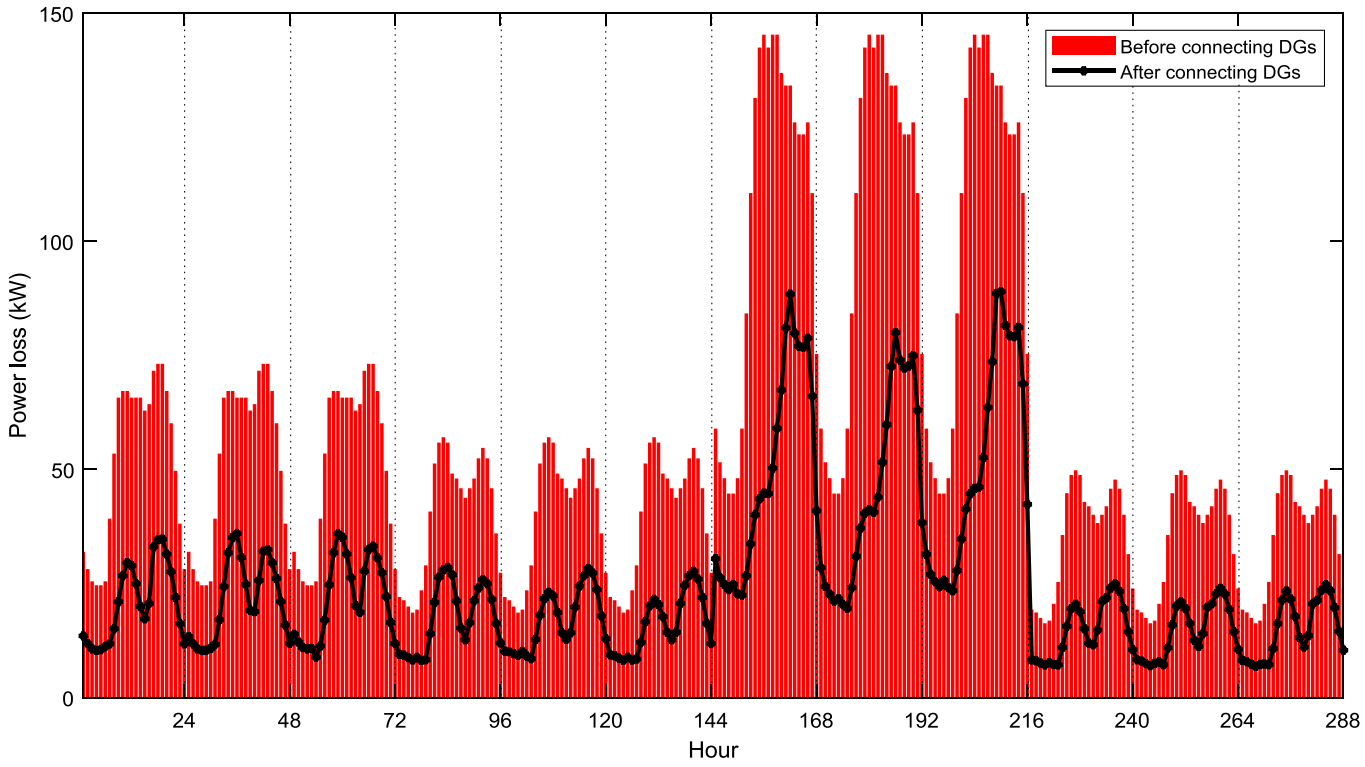

Fig. 7. Total power loss before and after integrating DGs.

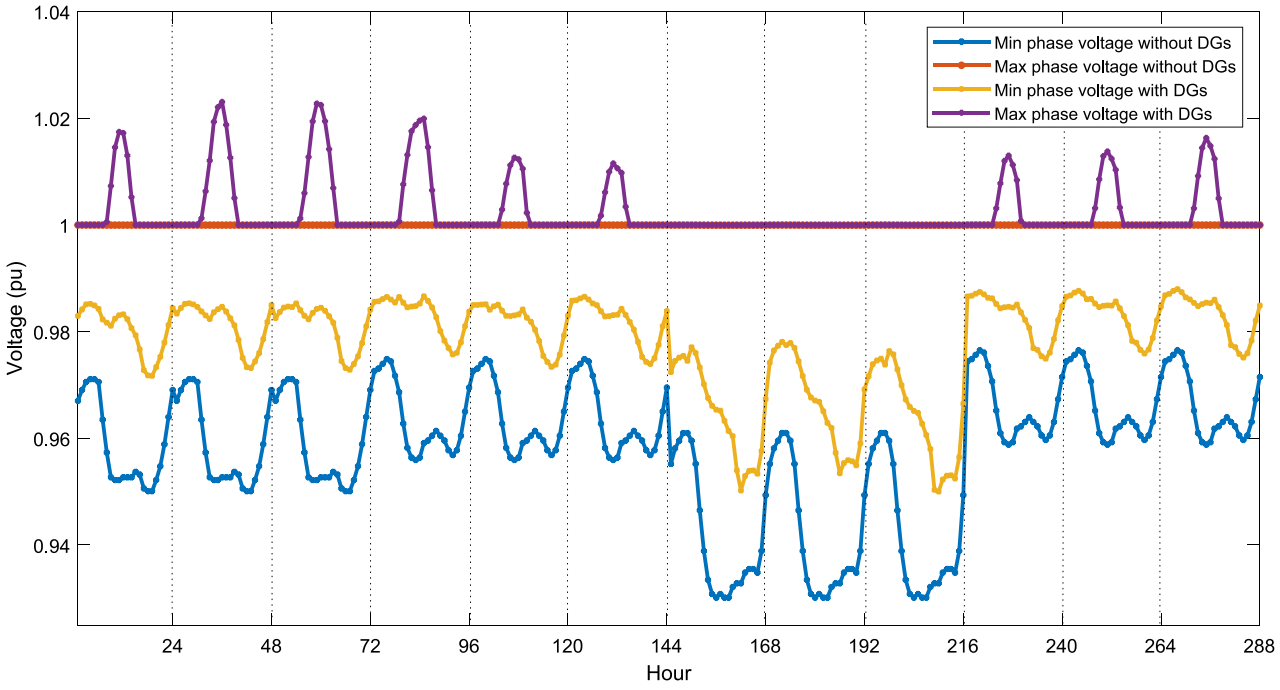

Fig. 8. Maximum and minimum phase voltage values at each hour before and after integrating DGs.

components in total costs, the costs of investment (CO_{Inv}) and O&M (CO_{OM}) from MCOA are ($4.3577 million and $0.7669 million), which are lower than ($4.6258 million and $0.8002 million) of IPSO and ($4.9151 million and $0.8384 million) of CSA, but slightly higher than ($4.3346 million and $0.7617 million) of COA. This shows that the costs of investment, operation and maintenance from MCOA are more economical than those of IPSO and CSA, but worse than those of COA. Remaining components of the objective function are the cost of buying electricity from the main grid (CO_{Grid}) and the cost of emissions from conventional power plants (CO_{Emis}). These costs of MCOA ($6.4418 million and $0.2397 million) are more benefits than COA ($6.4827 million and $0.2412 million), but they are worse than the other methods such as CSA ($5.9170 million and $0.2185 million) and IPSO ($6.2105 million and $0.2302 million). In short, through the summary of Table 2, MCOA is the method that can find the solution with the best total costs in compared methods for solving same optimization problem.

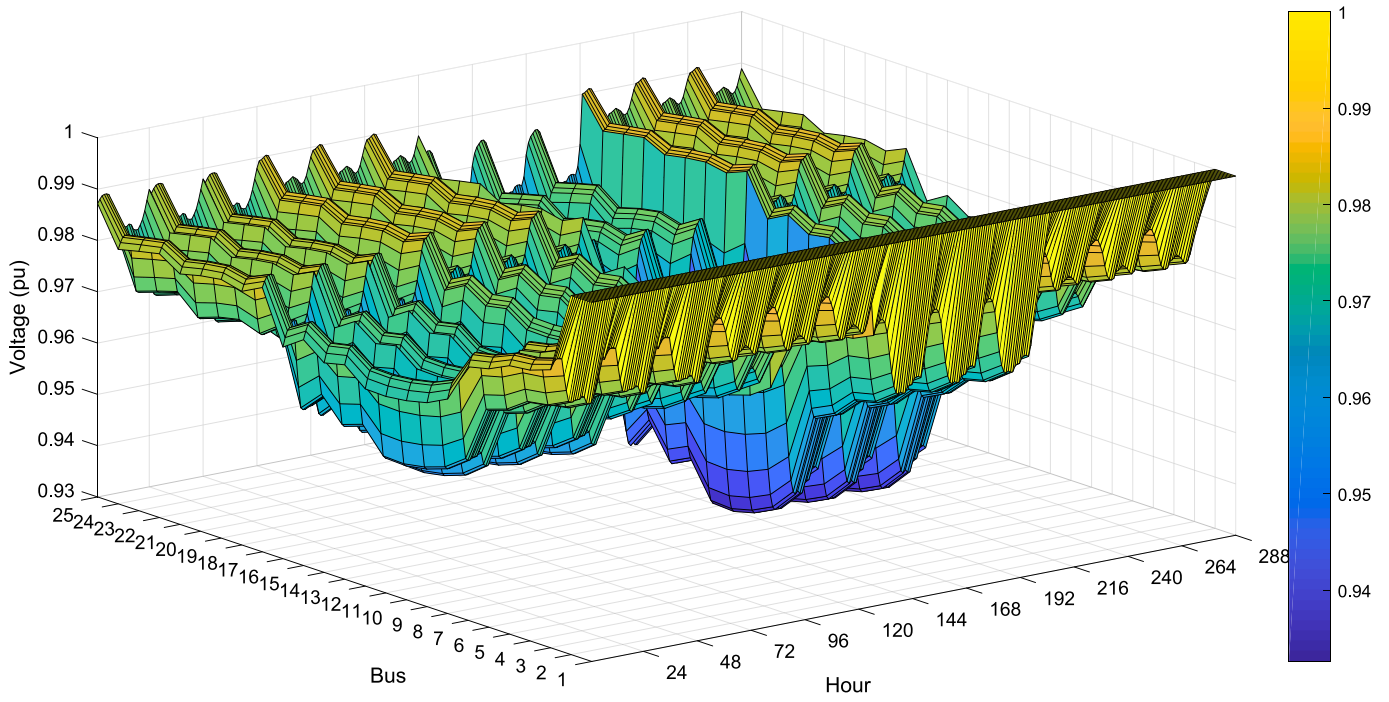

Fig. 9. The mean phase voltage profile before integrating DGs.

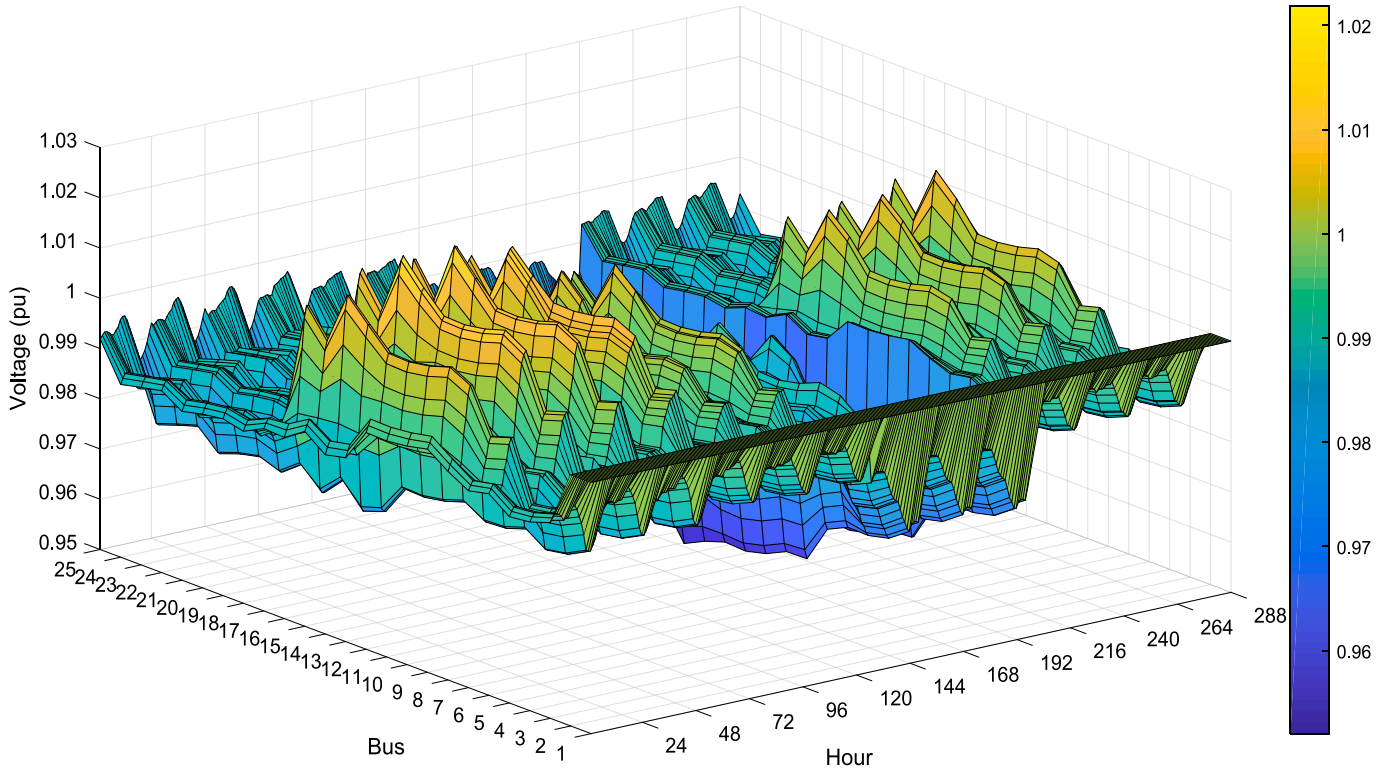

Fig. 10. The mean phase voltage profile after integrating DGs.

In this research, the power generation from renewable distributed generators and the consumption, including load demand and branch losses, is clearly illustrated in Fig. 6. Total consumption at 288 data points, which represent a year, is 582.437 MW, but the total generation is only 276.199 MW, equivalent to 47.42%. It shows that the penetration of DGs, in this case, can supply almost half of the total consumption, and the main grid will provide the remaining demand through the substation. Additionally, as mentioned, one of the great benefits of connecting DGs in the system is reduced losses in the distribution branches, and the total power loss before and after having DGs is shown in Fig. 7. The total loss is firmly down from 16.61 MW to 7.27 MW, equal to 56.23% for power loss reduction as calculated. This dramatically reduces costs for operating the DGs integrated distribution system in the long term.

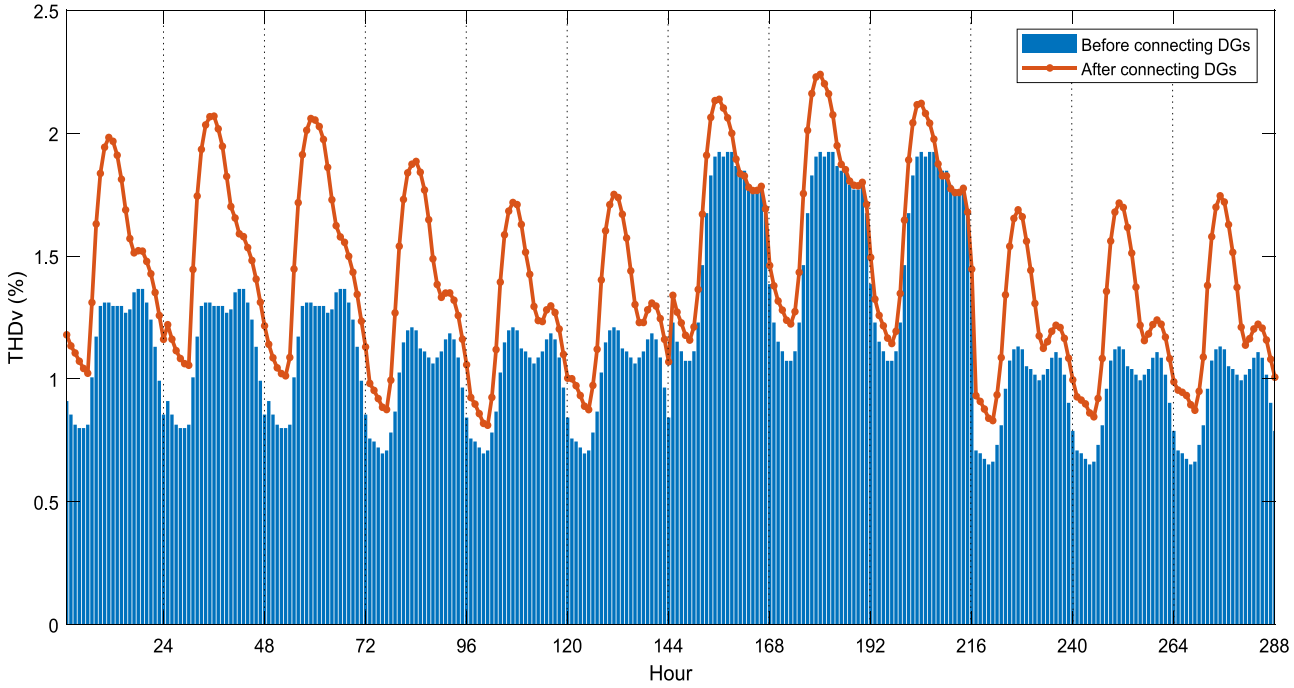

Fig. 11. Maximum value of THD_V at each hour before and after integrating DGs.

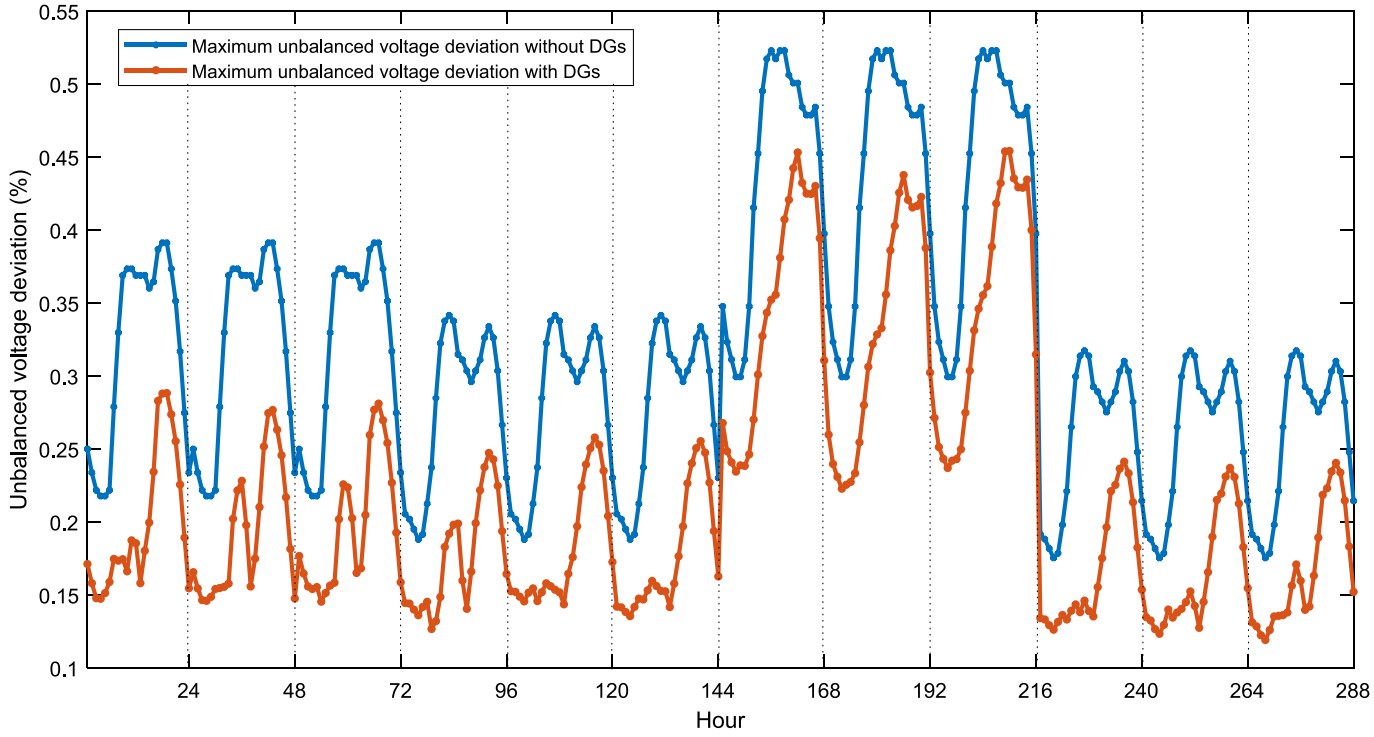

Fig. 12. Maximum unbalanced voltage deviation at each hour before and after integrating DGs.

Due to the nature of an unbalanced three-phase distribution system, the voltage values between phases in the same node may be different. Therefore, it is necessary to consider the voltage of each phase to ensure they meet the constraints. As shown in Fig. 8, the minimum and maximum phase voltages for the base system are 0.93 pu and 1.00 pu, but these values are raised to 0.950 pu and 1.023 pu by suitable integration of DGs, respectively. Besides, each time period's average phase voltage profiles are clearly illustrated. As plotted in Fig. 9, the phase voltage values at the hours near and equal to the peak load have violated the allowable limit of this study, and the average phase voltage region has fluctuated in the range of [0.93, 1.00] (pu) for the original system. Nevertheless, this was successfully overcome up to [0.952, 1.022] (pu) with DGs, as presented in Fig. 10. Specifically, the lowest mean phase voltage is 0.930 pu at peak load in the base system, and it is strongly improved up to 0.952 pu due to the penetration of DGs. In general, all phase voltages at each hour have satisfied the acceptance limits with the range of [0.95, 1.05] (pu) from the appropriate installation of DGs. This is seen as one of the great benefits of penetrating distributed energy

Table A.1
The specification of photovoltaic module.

Peak watt	Open circuit volt	Short circuit current	Current at maximum power	Current temp. coefficient	Voltage at maximum power	Volt temp. coefficient	Nominal cell operating temp.
75.0 W	21.98 V	5.32 A	4.76 A	1.22 mA/°C	17.32 V	14.4 mV/°C	43.0 °C

Table A.2
The specification of wind turbine.

Item	Parameters
Rated power	100 kW
Rated wind speed	10 m/s
Cut-in wind speed	3 m/s
Cut-out wind speed	20 m/s

sources in the distribution systems.

As stated, besides harmonic sources from nonlinear loads, this study uses inverters-based DGs, which are also capable of generating harmonics for the system. Therefore, it is essential to consider harmonic generation sources from nonlinear loads and inverters. As plotted in Fig. 10, the maximum values of THD_V at each hour before and after integrating DGs into the system are 1.92% and 2.24%, respectively. Clearly, the harmonic distortions have increased up and they depended on the penetration level of DGs. Because the THD_V index does not exceed 3%, so the IHD_V^h index is always within the allowable limit. This shows that THD_V and IHD_V^h values that represent the influence of harmonics are compliant with IEEE Std. 519 after placing the suitable DGs. Moreover, this study uses the unbalanced three-phase distribution system as a test case. Thus, the phase voltage values at each node are different. As shown in Fig. 11, the maximum values of unbalanced voltage deviation after connecting DGs not only satisfy IEEE Std. 45-2002 of 3%, but these values are also better than the original system. Specifically, the maximum unbalanced voltage deviation of the base system is 0.523%, but this value dropped to 0.454% with integrating DGs. Adding DGs into the distribution system in reducing unbalanced voltage deviation has proven to be an additional benefit (Fig. 12).

5. Conclusions

This research utilized a successful method, the modified coyote optimization algorithm (MCOA), to determine the location and capacity of renewable distributed generators in the unbalanced distribution system. The research has also succeeded in developing a co-simulation between MATLAB and OpenDSS dedicated to quickly addressing power and harmonic problems with high accuracy. Because of the application of the obtained optimal solution from MCOA, the total costs, including the investment cost, the O&M cost, the electricity purchase cost, and the emissions cost, were reduced by up to 10.7% (corresponding to $1.4141 million) compared to the original system that generated nearly 50% of the total demand. This research considered harmonious sources derived from nonlinear loads and harmonious inverter-based DGs within the permitted range of 5% (for THD_V) and 3% (for IHD_V^h). The average phase voltage profile also increased from [0.93, 1.00] to [0.952, 1.022]. The voltage deviation at each node that was not balanced not only met the 3% goal but was also superior to the original system; the power loss in the branches was reduced by 56.23% due to the proper integration of DGs in the unbalanced distribution system. This demonstrated the great value of DG integration, and the profit gained primarily depends on the strategy used to install DG in the distribution system. Ultimately, for the expansion of this research, future work will implement system reconfiguration and consider adding the integration of other devices, such as capacitors and voltage regulators, for maximum benefits.

CRediT authorship contribution statement

Thai Dinh Pham: Conceptualization, Coding and simulations, Writing - original draft preparation. **Le Chi Kien:** Data acquisition, Formal analysis, Resources. **Thang Trung Nguyen:** Methodology, Writing - review and editing, Supervision.

Declaration of competing interest

The authors declare that they have no known competing financial interests or personal relationships that could have appeared to influence the work reported in this paper.

Appendix

A.1. The computing process for $V_{un,s}^{Mean}$ and $V_{un,s}^{Max}$ from Eq. (11) can be presented as belows:

$$V_{un,s}^{Mean} = \frac{V_s^1 + V_s^2 + V_s^3}{3}, \quad s = 1, \cdots, N_s \tag{A.1}$$

where V_s^1, V_s^2 and V_s^3 are the voltage magnitude values of phase A, B and C at the s^{th} node, respectively.

$$V_{un,s}^{\Delta A} = |V_{un,s}^{Mean} - V_s^1|, \quad s = 1, \cdots, N_s \tag{A.2}$$

$$V_{un,s}^{\Delta B} = |V_{un,s}^{Mean} - V_s^2|, \quad s = 1, \cdots, N_s \tag{A.3}$$

$$V_{un,s}^{\Delta C} = |V_{un,s}^{Mean} - V_s^3|, \quad s = 1, \cdots, N_s \tag{A.4}$$

where $V_{un,s}^{\Delta A}$, $V_{un,s}^{\Delta B}$ and $V_{un,s}^{\Delta C}$ are defined as the voltage magnitude difference between phase A and mean voltage values, between phase B and mean voltage values, and between phase C and mean voltage values at the s^{th} node, respectively. Finally, the maximum value of voltage magnitude difference ($V_{dif,s}^{Max}$) can be determined by:

$$V_{dif,s}^{Max} = \max\left[V_{un,s}^{\Delta A}, V_{un,s}^{\Delta B}, V_{un,s}^{\Delta C}\right], \quad s = 1, \cdots, N_s \tag{A.5}$$

See Tables A.1 and A.2.

References

[1] Zhan H, Wang C, Wang Y, Yang X, Zhang X, Wu C, et al. Relay protection coordination integrated optimal placement and sizing of distributed generation sources in distribution networks. IEEE Trans Smart Grid 2015;7(1):55–65.
[2] Smaisim GF, Abed AM, Shamel A. Investigation and optimization of solar collector and geothermal pump hybrid system for cogeneration of heat and power with exergy-economic approach. Clean Energy 2023;7(3):571–81.
[3] Smaisim GF, Abed AM, Alavi H. Analysis of pollutant emission reduction in a coal power plant using renewable energy. Int J Low-Carbon Technol 2023;18:38–48.
[4] Kumawat M, Gupta N, Jain N, Bansal RC. Optimal planning of distributed energy resources in harmonics polluted distribution system. Swarm Evol Comput 2018;39:99–113.
[5] Purlu M, Turkay BE. Optimal allocation of renewable distributed generations using heuristic methods to minimize annual energy losses and voltage deviation index. IEEE Access 2022;10:21455–74.
[6] Smaisim GF, Abed AM, Hadrawi SK, Majdi HS, Shamel A. Modelling and optimization of combined heat and power system in microgrid based on renewable energy. Clean Energy 2023;7(4):735–46.
[7] Mahmoud K, Yorino N, Ahmed A. Optimal distributed generation allocation in distribution systems for loss minimization. IEEE Trans Power Syst 2015;31(2):960–9.
[8] Muttaqi KM, Le AD, Negnevitsky M, Ledwich G. An algebraic approach for determination of DG parameters to support voltage profiles in radial distribution networks. IEEE Trans Smart Grid 2014;5(3):1351–60.
[9] Pandi VR, Zeineldin HH, Xiao W. Determining optimal location and size of distributed generation resources considering harmonic and protection coordination limits. IEEE Trans Power Syst 2012;28(2):1245–54.
[10] Parizad A, Khazali A, Kalantar M. Optimal placement of distributed generation with sensitivity factors considering voltage stability and losses indices. In: 2010 18th Iranian conference on electrical engineering. IEEE; 2010. p. 848–55.
[11] Razavi SE, Rahimi E, Javadi MS, Nezhad AE, Lotfi M, Shafie-khah M, et al. Impact of distributed generation on protection and voltage regulation of distribution systems: a review. Renew Sustain Energy Rev 2019;105:157–67.
[12] Sanjay R, Jayabarathi T, Raghunathan T, Ramesh V, Mithulananthan N. Optimal allocation of distributed generation using hybrid grey wolf optimizer. IEEE Access 2017;5:14807–18.
[13] Adepoju GA, Aderemi BA, Salimon SA, Alabi OJ. Optimal placement and sizing of distributed generation for power loss minimization in distribution network using particle swarm optimization technique. Eur J Eng Technol Res 2023;8(1):19–25.
[14] Ramavat SR, Jaiswal SP, Goel N, Shrivastava V. Optimal location and sizing of DG in distribution system and its cost–benefit analysis. In: Applications of artificial intelligence techniques in engineering: SIGMA 2018, vol. 1. Springer Singapore; 2019. p. 103–12.
[15] Milovanović M, Tasić D, Radosavljević J, Perović B. Optimal placement and sizing of inverter-based distributed generation units and shunt capacitors in distorted distribution systems using a hybrid phasor particle swarm optimization and gravitational search algorithm. Electr Power Compon Syst 2020;48(6–7):543–57.
[16] Gallego Pareja LA, López-Lezama JM, Gómez CO. A mixed-integer linear programming model for the simultaneous optimal distribution network reconfiguration and optimal placement of distributed generation. Energies 2022;15(9):3063.
[17] Prabha DR, Jayabarathi T, Umamageswari R, Saranya S. Optimal location and sizing of distributed generation unit using intelligent water drop algorithm. Sustainable Energy Technol Assess 2015;11:106–13.
[18] Zheng Y, Dong ZY, Meng K, Yang H, Lai M, Wong KP. Multi-objective distributed wind generation planning in an unbalanced distribution system. CSEE J Power Energy Syst 2017;3(2):186–95.
[19] Ayodele TR, Ogunjuyigbe ASO, Akinola OO. Optimal location, sizing, and appropriate technology selection of distributed generators for minimizing power loss using genetic algorithm. J Renew Energy 2015.
[20] Bhumkittipich K, Phuangpornpitak W. Optimal placement and sizing of distributed generation for power loss reduction using particle swarm optimization. Energy Procedia 2013;34:307–17.
[21] Devi S, Geethanjali M. Optimal location and sizing determination of distributed generation and DSTATCOM using particle swarm optimization algorithm. Int J Electr Power Energy Syst 2014;62:562–70.
[22] Ogunsina AA, Petinrin MO, Petinrin OO, Offornedo EN, Petinrin JO, Asaolu GO. Optimal distributed generation location and sizing for loss minimization and voltage profile optimization using ant colony algorithm. SN Appl Sci 2021;3:1–10.
[23] Abu-Mouti FS, El-Hawary ME. Optimal distributed generation allocation and sizing in distribution systems via artificial bee colony algorithm. IEEE Trans Power Delivery 2011;26(4):2090–101.
[24] Al-Ammar EA, Farzana K, Waqar A, Aamir M, Haq AU, Zahid M, et al. ABC algorithm based optimal sizing and placement of DGs in distribution networks considering multiple objectives. Ain Shams Eng J 2021;12(1):697–708.
[25] Xu L, Song B, Cao M. An improved particle swarm optimization algorithm with adaptive weighted delay velocity. Syst Sci Control Eng 2021;9(1):188–97.
[26] Zhang W, Wang S. Optimal placement and sizing of distributed generators based on equilibrium optimizer. Front Energy Res 2022;10:936566.
[27] Reddy PDP, Reddy VV, Manohar TG. Whale optimization algorithm for optimal sizing of renewable resources for loss reduction in distribution systems. Renewables: Wind Water Sol 2017;4:1–13.
[28] Shaheen MA, Hasanien HM, Mekhamer SF, Talaat HE. Optimal power flow of power systems including distributed generation units using sunflower optimization algorithm. IEEE Access 2019;7:109289–300.
[29] Ali ES, Abd Elazim SM, Abdelaziz AY. Ant lion optimization algorithm for optimal location and sizing of renewable distributed generations. Renew Energy 2017;101:1311–24.
[30] Yuvaraj T, Ravi K, Devabalaji KR. Optimal allocation of DG and DSTATCOM in radial distribution system using cuckoo search optimization algorithm. Modell Simulat Eng 2017.
[31] Bagherinasab A, Khalid SA, Jahangere H, Kiani M, Zadebagheri M, Yousefpour A. Optimal DG placement in distribution networks using shuffled frog leap algorithm. EasyChair 2022.
[32] Gholami K, Parvaneh MH. A mutated salp swarm algorithm for optimum allocation of active and reactive power sources in radial distribution systems. Appl Soft Comput 2019;85:105833.
[33] Chang GW, Chinh NC. Coyote optimization algorithm-based approach for strategic planning of photovoltaic distributed generation. IEEE Access 2020;8:36180–90.
[34] Pruitt KA, Leyffer S, Newman AM, Braun RJ. A mixed-integer nonlinear program for the optimal design and dispatch of distributed generation systems. Optim Eng 2014;15:167–97.
[35] Rueda-Medina AC, Franco JF, Rider MJ, Padilha-Feltrin A, Romero R. A mixed-integer linear programming approach for optimal type, size and allocation of distributed generation in radial distribution systems. Electr Pow Syst Res 2013;97:133–43.
[36] Pham TD. Integration of photovoltaic units, wind turbine units, battery energy storage system, and capacitor bank in the distribution system for minimizing total costs considering harmonic distortions. Iran J Sci Technol Trans Electr Eng 2023:1–18.
[37] Pham TD, Nguyen TT, Kien LC. An improved equilibrium optimizer for optimal placement of distributed generators in distribution systems considering harmonic distortion limits. Complexity 2022.
[38] Prakash R, Lokeshgupta B, Sivasubramani S. Multi-objective bat algorithm for optimal placement and sizing of DG. In: 2018 20th National Power Systems Conference (NPSC). IEEE; 2018. p. 1–6.
[39] Dehghani M, Montazeri Z, Malik OP. Optimal sizing and placement of capacitor banks and distributed generation in distribution systems using spring search algorithm. Int J Emerg Electr Power Syst 2020;21(1):20190217.
[40] Ouali A, Cherkaoui A. Optimal allocation of combined renewable distributed generation and capacitor units for interconnection cost reduction. J Electr Comput Eng 2020:1–11.
[41] Sinuraya EW, Soemantri M, Rafif IR. Evaluation and mitigation of voltage and current unbalance at MSTP Undip Jepara. J Phys: Conf Ser 2022;2406(1):012013.
[42] Dugan R. Opendss, introductory training, level 1. Palo Alto (California): Electric Power Research Institute; 2009.
[43] Pierezan J, Coelho LDS. Coyote optimization algorithm: a new metaheuristic for global optimization problems. In: 2018 IEEE Congress on Evolutionary Computation (CEC). IEEE; 2018. p. 1–8.
[44] Hung DQ, Mithulananthan N, Lee KY. Determining PV penetration for distribution systems with time-varying load models. IEEE Trans Power Syst 2014;29(6):3048–57.
[45] Subrahmanyam JBV, Radhakrishna C. Distributed generator placement and sizing in unbalanced radial distribution system. Int J Electr Comput Eng 2009;3(4):753–60.
[46] Available online: https://power.larc.nasa.gov/data-access-viewer/.
[47] Atwa YM, El-Saadany EF, Salama MMA, Seethapathy R. Optimal renewable resources mix for distribution system energy loss minimization. IEEE Trans Power Syst 2009;25(1):360–70.
[48] Gampa SR, Das D. Optimum placement and sizing of DGs considering average hourly variations of load. Int J Electr Power Energy Syst 2015;66:25–40.
[49] Zou K, Agalgaonkar AP, Muttaqi KM, Perera S. Distribution system planning with incorporating DG reactive capability and system uncertainties. IEEE Trans Sustain Energy 2011;3(1):112–23.
[50] Alam MS, Arefifar SA. Cost & emission analysis of different DGs for performing energy management in smart grids. In: 2018 IEEE international conference on Electro/information Technology (EIT). IEEE; 2018. p. 0667–72.
[51] Nguyen TT, Nguyen TT, Le B. Artificial ecosystem optimization for optimizing of position and operational power of battery energy storage system on the distribution network considering distributed generations. Expert Syst Appl 2022;208:118127.

Thai Dinh Pham He received M.S.E.E degree with an outstanding academic record from National Chung Cheng University in Taiwan, R.O.C in 2017. He is currently pursuing the Ph.D degree in electrical engineering with HCMC University of Technology and Education in Ho Chi Minh City, Vietnam. His favorite research areas include power quality, power system optimization and renewable energies.

Le Chi Kien He received the M.Eng. and Ph.D. degrees in electrical engineering from Nagaoka University of Technology, Japan in 2002 and 2005. From 2015, he serves as an Associate Professor of the Faculty of Electrical and Electronics Engineering, Ho Chi Minh City University of Technology and Education. His research interests include optimization algorithms in power systems and Magnetohydrodynamic power generation system. Currently, he is the Vice Dean, Faculty of Electrical and Electronics Engineering, Ho Chi Minh City University of Technology and Education, Vietnam.

Thang Trung Nguyen (corresponding author) He was born in Binh Thuan province, Vietnam. He received his M.Sc. and PhD degree from Ho Chi Minh City University of Technology and Education in 2010 and 2018. His research interests include optimization problems in power systems, optimization renewable energies in power systems, and optimization algorithms. Now, he is working at Ton Duc Thang University, and he is the head of Power System Optimization Research Group, Faculty of Electrical and Electronics Engineering.

Iranian Journal of Science and Technology, Transactions of Electrical Engineering
https://doi.org/10.1007/s40998-023-00691-w

CORRECTION

Correction: Integration of Photovoltaic Units, Wind Turbine Units, Battery Energy Storage System, and Capacitor Bank in the Distribution System for Minimizing Total Costs Considering Harmonic Distortions

Thai Dinh Pham[1]

Correction to: Iranian Journal of Science and Technology, Transactions of Electrical Engineering (2023) 47:1265–1282
https://doi.org/10.1007/s40998-023-00613-w

In the original publication of the article, the author had identified few errors which should have been corrected as below.

No.	Place of error	The current version	The corrected version
1	Introduction section, the second paragraph, 3rd cited reference	Nguyen et al. (2022b, c, a)	Nguyen et al. (2022a)
2	Introduction section, the second paragraph, 5th cited reference	Kumar et al. 2017b, a	Kumar et al. 2017b
3	Introduction section, the second paragraph, 11th cited reference	Nguyen et al. 2022b, c, a	Nguyen et al. 2022b
4	Introduction section, the second paragraph, 21st cited reference	Kumar et al. 2017b, a	Kumar et al. 2017a
5	In the 2.2 Constraints, at item of 2.2.1 Power Balance Constraints, 1st cited reference	Hung et al. 2014a, b	Hung et al. 2014a
6	In the 2.2 Constraints, at item of 2.2.1 Power Balance Constraints, 4th cited reference	Hung et al. 2014a, b	Hung et al. 2014b
7	In the 2.2.6 Capacity Limits of BESS, 1st cited reference	Nguyen et al. 2022b, c, a	Nguyen et al. 2022c
8	In the Simulation Results section, in the second paragraph, 1st cited reference	Nguyen et al. 2022b, c, a	Nguyen et al. 2022c
9	Simulation results section, the first three references in Table 1	Nguyen et al. 2022b, c, a	Nguyen et al. 2022c
10	Simulation results section, in Table 4 at the 4th column and the last line	Bus: 05 – 0.979 MW/2.495 MWh	Bus: 05 – 1.088 MW/2.495 MWh

The original article can be found online at https://doi.org/10.1007/s40998-023-00613-w.

✉ Thai Dinh Pham
thaipd.ncs@hcmute.edu.vn

[1] Faculty of Electrical and Electronics Engineering, Ho Chi Minh City University of Technology and Education, Ho Chi Minh City, Vietnam

Published online: 01 February 2024

Iranian Journal of Science and Technology, Transactions of Electrical Engineering (2023) 47:1265–1282
https://doi.org/10.1007/s40998-023-00613-w

RESEARCH PAPER

Integration of Photovoltaic Units, Wind Turbine Units, Battery Energy Storage System, and Capacitor Bank in the Distribution System for Minimizing Total Costs Considering Harmonic Distortions

Thai Dinh Pham[1]

Received: 14 November 2022 / Accepted: 16 April 2023 / Published online: 20 May 2023

Abstract

This paper presents an effective method, named modified coyote optimization algorithm (MCOA), for determining the optimal integration of photovoltaic units (PVs), wind turbine units (WTs), battery energy storage system (BESS), and capacitor bank (CB) in the IEEE 69-bus radial distribution system. This research is developed with the goal of minimizing the total costs of investment, operation and maintenance (O&M) for PVs, WTs, BESS, and CB as well as energy purchase cost from the main grid considering time-varying load demand and generation units. The simulation results demonstrate total costs in operating the integrated system can be significantly minimized by the proper connection of PVs, WTs, BESS, and CB. On the other hand, the study also considers the test system under the condition of many nonlinear loads, and the approach has been successful in mitigating harmonics to the IEEE Std. 519. In addition, the proposed method (MCOA) is also compared with the original coyote optimization algorithm (COA) and slime mould algorithm (SMA) to prove its effectiveness in solving the optimization problems.

Keywords Modified coyote optimization algorithm · Wind turbine units · Photovoltaic units · Capacitor bank · Battery energy storage system · Harmonic flows

List of Symbols

$\Delta I_{bh,pk,ce}, \Delta V_{j,pk,ce}$	Amount of penalty of current at the *bh*th branch and voltage at the *j*th bus of the *ce*th solution in the *pk*th pack
$\Delta\text{THD}_{j,pk,ce}, \Delta\text{IHD}_{j,pk,ce}$	Amount of penalty of the total harmonic voltage distortion (THD) and individual harmonic voltage distortion (IHD) at the *j*th bus of the *ce*th solution in the *pk*th pack
$C_{\text{PV}}^{\text{Cal}}, C_{\text{WT}}^{\text{Cal}}, C_{\text{BESS}}^{\text{Cal}}, C_{\text{BESS}}^{\text{Aux}}$	The capital costs of the photovoltaic units (PVs), wind turbine units (WTs), battery energy storage system (BESS), and components of the power conversion system (PCS), and balance of plant (BOP) in BESS, respectively ($/MW)
$C_{\text{PV}}^{\text{OM}}, C_{\text{WT}}^{\text{OM}}, C_{\text{BESS}}^{\text{OM}}$	The operation and maintenance (O&M) cost of PVs and WTs ($/MWh), and BESS ($/MWyear), respectively
$E_{\text{BESS}}^{\text{Rated}}$	The rated capacity of BESS
$I_{bh,pk,ce}$	The *bh*th branch current of the *ce*th solution in the *pk*th pack
$\text{IHD}_{j,pk,ce}$	The IHD value at *j*th bus of the *ce*th solution in the *pk*th pack
$L_p^{\text{Max}}, L_w^{\text{Max}}, L_{\text{BESS},bs}^{\text{Max}}, L_c^{\text{Max}}$	The maximum place of the *p*th PV, the *w*th WT, the *bs*th BESS, and the *c*th capacitor bank (CB)

✉ Thai Dinh Pham
thaipd.ncs@hcmute.edu.vn

[1] Faculty of Electrical and Electronics Engineering, Ho Chi Minh City University of Technology and Education, Ho Chi Minh City, Vietnam

$L_p^{\text{Min}}, L_w^{\text{Min}}, L_{\text{BESS},bs}^{\text{Min}}, L_c^{\text{Min}}$ The minimum place of the pth PV, the wth WT, the bsth BESS, and the cth CB

$\text{Loc}_{\text{Cap}}, C_{\text{Cap}}^{\text{Cal}}$ The installation cost (\$/location) and the capital cost of CB (\$/MVAr)

$N_{ld}, N_{bh}, N_{bu}, N_{va}$ The number of loads, branches, buses, and control variables, respectively

$N_{\text{PV}}, N_{\text{WT}}, N_{\text{Cap}}, N_{\text{BESS}}$ The number of PVs, WTs, CB and BESS, respectively

$P_{\text{BESS},bs,hr,yr}^{\text{DisCh}}, P_{\text{BESS},bs,hr,yr}^{\text{Char}}$ The discharge and charge powers of the bsth BESS at the hrth hour in the yrth year

P_{lo}^{ld}, P_{bh}^{ls} The active power of the loth load and the active power loss of the bhth branch

$P_{\text{PV}}^{\text{Gen}}, P_{\text{WT}}^{\text{Gen}}$ The actual active power of PVs and WTs, respectively

$P_{\text{PV}}^{\text{Min}}, P_{\text{PV}}^{\text{Max}}$ The minimum and maximum active powers of PVs

$P_{\text{PV}}^{\text{Rated}}, P_{\text{WT}}^{\text{Rated}}, P_{\text{BESS}}^{\text{Rated}}$ The rated active power of PVs, WTs, and BESS, respectively

$P_{\text{WT}}^{\text{Min}}, P_{\text{WT}}^{\text{Max}}$ The minimum and maximum active powers of WTs

$Q_{\text{Cap}}^{\text{Min}}, Q_{\text{Cap}}^{\text{Max}}$ The minimum and maximum reactive powers of CB

$Q_{\text{Cap}}^{\text{Rated}}$ The rated reactive power of CB

Q_{lo}^{ld}, Q_{bh}^{ls} The reactive power of the loth load and reactive power loss of the bhth branch

$Q_{\text{PV}}^{\text{Gen}}, Q_{\text{WT}}^{\text{Gen}}, Q_{\text{Cap}}^{\text{Gen}}, Q^{\text{Grid}}$ The reactive power of PVs, WTs, CB, and main grid, respectively

$S_{\text{bestPk},pk}, S_{\text{cent},pk}$ The best solution of the pkth pack and the central solution of the pkth pack

S_{bestPop} The best solution of the population

$S_{rd1,pk}, S_{rd2,pk}$ The randomly taken solutions from the pkth packs

$\text{SF}_{pk,ce}, \text{TC}_{pk,ce}$ The fitness and the objective function values of the ceth solution in the pkth pack

$\text{THD}_{j,hr,yr}, \text{IHD}_{j,hr,yr}^{Hr}$ THD and IHD values of the jth bus at the hrth hour in the yrth year

$\text{THD}_{j,pk,ce}$ THD value at jth bus of the ceth solution in the pkth pack

$V_{j,hr,yr}, I_{bh,hr,yr}$ The jth bus voltage and the bhth branch current at the hrth hour in the yrth year

$V_{j,hr,yr}^{1}$ The jth bus voltage at the fundamental frequency at the hrth hour in the yrth year

$V_{j,hr,yr,hc}$ The jth bus voltage at the hcth order frequency at the hrth hour in the yrth year

$V_{j,pk,ce}$ The jth bus voltage of the ceth solution in the pkth pack

$\sigma_V, \sigma_I, \sigma_{\text{THD}}, \sigma_{\text{IHD}}$ Penalty coefficient of bus voltage, branch current, THD, and IHD, respectively

H The maximum number of considering harmonic orders

$\text{It}, \text{It}^{\text{Max}}$ The current iteration and the maximum iteration numbers, respectively

1 Introduction

In recent years, concerns related to the uncertainties of fossil fuel prices, the worsening of environmental pollution, and the liberalization of the electricity market have increased sharply (Hung et al. 2013). These factors have greatly contributed to promoting the development of distributed generation units (DGUs), especially renewable energy sources. However, the installation of DGUs requires appropriate strategies to limit unwanted impacts and to maximize the economic and technical benefits (Elattar and Elsayed 2020; Chang and Chinh 2020).

In studies by Lee and Park (2013), Mahmoud et al. (2015), and Nguyen et al. (2022b, c, a), the authors demonstrated the benefits of DGUs in reducing power loss and improving voltage quality. DGUs are also effective in enhancing system reliability, mitigating harmonic distortion, and reducing costs in purchasing energy from the main grid (HassanzadehFard and Jalilian 2018; Kumar et al. 2017b, a; Pham et al. 2021). Conversely, poorly planned integration of DGUs can lead to negative effects such as increased power loss, overvoltage, and reverse power flows (Sgouras et al. 2017; Gupta et al. 2020). Most of the previous studies were interested in determining the location and sizing of the DGUs for minimizing the power loss on the branches (Mohandas et al. 2015; Wong et al. 2019; Nguyen et al. 2022b, c, a; Ogunsina et al. 2021). These researchers focused on developing different optimization algorithms to improve power loss reduction. However, the biggest drawback in these studies is that they only consider the optimal installation of DGUs at the peak

load. This is not feasible in practice with the load variation and output power uncertainties of DGUs. Therefore, their proposed solution for placement and sizing of DGUs cannot be optimal at different load levels. Various methods such as mixed integer programming (Rueda-Medina et al. 2013; Sandhu et al., 2018), an analytical approach (Elsaiah et al. 2014; Viral and Khatod 2015), and heuristic algorithms (Pemmada et al. 2021; Sanjay et al. 2017; Nguyen et al. 2020) have been implemented for solving related optimization problems of DGU integration in the distribution systems. Only a few researchers have resolved the optimal connection of DGUs considering the uncertainties of the load demand and the generation units (Ganguly and Samajpati 2015; Kumar et al. 2017b, a). However, these studies also only focused on the aspect of power loss reduction and voltage enhancement, while ignoring the most important issue of total costs of operating the system, including the costs of DGUs and the costs of purchasing electricity for load demand. Besides, most of the studies in the past considered DGUs that only transmit active power and used older methods for solving the optimization problem (Ayodele et al. 2015; Hassan et al. 2020). This leads to underappreciated efficiency.

This paper overcomes the disadvantages of previous studies. Firstly, the study considers the simultaneous integration of PVs, WTs, BESS, and CB into distribution systems under conditions of many nonlinear loads for minimizing the total costs in operating the system. Secondly, the CB are optimally positioned for supporting reactive power to the distribution system without penalty. Thirdly, BESS is integrated into the system for charging and discharging energy reasonably according to different periods of electricity price and load demand. Finally, this research proposes a novel optimization algorithm called the modified coyote optimization algorithm (MCOA) for determining DGU installation under time-varying load demand and generation. Not only that, the power factor of an individual generation unit is also mentioned. Generally, the proposed method (MCOA) has demonstrated outstanding efficiency in solving the optimization problem as compared to original COA (Pierezan and Coelho 2018) and slime mould algorithm (SMA) (Li et al. 2020).

Overall, the significant contribution of the study can be briefly presented as follows:

- The study considers total costs of investment, operation, and maintenance for PVs, WTs, BESS, and CB, and energy purchase cost from the main grid for load demand and power loss on the branches in the distribution system. This can help to evaluate the effectiveness of the project comprehensively.
- The research proposes a novel algorithm with high efficiency and good stability which is named modified coyote optimization algorithm (MCOA). The obtained results demonstrate the superiority of MCOA over other compared methods such as the original coyote optimization algorithm (COA) and slime mould algorithm (SMA). This novel algorithm greatly contributes in improving the quality of the possible solutions in solving real-world optimization problems.
- The paper successfully shows the best solution of placement and capacity of PVs, WTs, BESS, and CB in the distribution system for minimizing the total costs while still satisfying the set criteria. The best obtained solution from the proposed method can save up to \$4.662 million compared to the original scenario, corresponding to 22.422% over the 20-year project life. Besides, power loss is also strongly reduced, with the power loss reduction reaching 78.692%. Not only that, the voltage profile improvement and harmonic distortion mitigation are also significantly enhanced with satisfied constraints.

The rest of the paper is structured as follows: Sect. 2 presents the objective function and constraints. Section 3 focuses on describing the proposed method. Section 4 shows the application of the proposed method for solving the optimization problem. Section 5 presents the simulation results along with the analysis. Finally, Sect. 6 is the conclusions for the whole paper.

2 Problem Formulation

2.1 Objective Function

Total costs for operating the system that have integrated PVs, WTs, BESS, and CB include (1) investment, maintenance, and operation costs for PVs, WTs, BESS, and CB, and (2) the cost of purchasing electricity from the main grid for load demand and power loss. These costs should be minimized and described mathematically as

$$\text{Minimize TC} = \text{Cost}^{\text{Inv\&OM}}_{\text{PV-WT-BESS-Cap}} + \text{Cost}^{\text{Purch}}_{\text{Grid}} \ (\$) \quad (1)$$

where TC is total costs; $C^{\text{Inv\_OM}}_{\text{PV-WT-BESS-Cap}}$ is the cost of the investment, operation, and maintenance of PVs, WTs, BESS, and CB; and $C^{\text{purch}}_{\text{grid}}$ is the cost of purchasing energy from the main grid.

2.1.1 Investment and O&M Costs of PVs, WTs, BESS, and CB

$C^{\text{Inv\&OM}}_{\text{PV-WT-BESS-Cap}}$ is an economically important term to determine the installation strategy for distributed generation sources which are integrated into the distribution system. In this case, it includes the one-time investment

cost at the early stage of the project and O&M cost of connected components throughout the lifetime of the project. This can be expressed as (Beck et al. 2017)

$$\mathrm{Cost}^{\mathrm{Inv\&OM}}_{\mathrm{PV-WT-BESS-Cap}} = \mathrm{Cost}_{\mathrm{PV}} + \mathrm{Cost}_{\mathrm{WT}} + \mathrm{Cost}_{\mathrm{BESS}} + \mathrm{Cost}_{\mathrm{Cap}}\ (\$) \tag{2}$$

where $\mathrm{Cost}_{\mathrm{PV}}$, $\mathrm{Cost}_{\mathrm{WT}}$, $\mathrm{Cost}_{\mathrm{BESS}}$ and $\mathrm{Cost}_{\mathrm{Cap}}$ are the costs of PVs, WTs, BESS, and CB, respectively. These costs can be determined by

$$\mathrm{Cost}_{\mathrm{PV}} = \sum_{p=1}^{N_{\mathrm{PV}}}\left(C^{\mathrm{Cal}}_{\mathrm{PV}}.P^{\mathrm{Rated}}_{\mathrm{PV},p}\right) + 365 \times \sum_{yr=1}^{20}\sum_{hr=1}^{24}\sum_{p=1}^{N_{PV}}\left(\gamma_{yr}.C^{\mathrm{OM}}_{\mathrm{PV}}.P^{\mathrm{Gen}}_{\mathrm{PV},p,hr,yr}\right)\ (\$) \tag{3}$$

$$\mathrm{Cost}_{\mathrm{WT}} = \sum_{w=1}^{N_{\mathrm{WT}}}\left(C^{\mathrm{Cal}}_{\mathrm{WT}}.P^{\mathrm{Rated}}_{\mathrm{WT},w}\right) + 365 \times \sum_{yr=1}^{20}\sum_{hr=1}^{24}\sum_{w=1}^{N_{\mathrm{WT}}}\left(\gamma_{yr}.C^{\mathrm{OM}}_{\mathrm{WT}}.P^{\mathrm{Gen}}_{\mathrm{WT},w,hr,yr}\right)\ (\$) \tag{4}$$

$$\mathrm{Cost}_{\mathrm{BESS}} = \sum_{bs=1}^{N_{\mathrm{BESS}}}\left(C^{\mathrm{Cal}}_{\mathrm{BESS}}.E^{\mathrm{Rated}}_{\mathrm{BESS},bs}\right) + \sum_{yr=1}^{20}\sum_{bs=1}^{N_{\mathrm{BESS}}}\left(\gamma_{yr}.C^{\mathrm{OM}}_{\mathrm{BESS}}.E^{\mathrm{Rated}}_{\mathrm{BESS},bs,yr}\right) + \sum_{bs=1}^{N_{\mathrm{BESS}}}\left(C^{\mathrm{Aux}}_{\mathrm{BESS}}.P^{\mathrm{Rated}}_{\mathrm{BESS},bs}\right)\ (\$) \tag{5}$$

$$\mathrm{Cost}_{\mathrm{Cap}} = \sum_{c=1}^{N_{\mathrm{Cap}}}\left(C^{\mathrm{Cal}}_{\mathrm{Cap}}.Q^{\mathrm{Rated}}_{\mathrm{Cap},c}\right) + \sum_{c=1}^{N_{\mathrm{Cap}}}\left(\mathrm{Loc}_{\mathrm{Cap},c}\right)\ (\$) \tag{6}$$

This work assumed a project period of 20 years with consideration of the time-varying load demand and generation units in a typical day (i.e., 24 h) and a year with 365 days. However, the O&M cost is paid differently over the years, so the function (γ_{yr}) is added to the O&M cost, and this function can be computed by (Prakash et al. 2018)

$$\gamma_{yr} = \left(\frac{1}{1+\mathrm{d}r}\right)^{yr} \tag{7}$$

where yr is the considered year in the lifetime of the project, and dr is the discount rate.

2.1.2 Cost of Purchasing Energy from the Main Grid

If the generation from the distributed sources is not enough to meet the load demand and power loss on the branches in the system, then it is necessary to pay the bill to the power company for the power injected at the substation. This cost is expressed as follows (Oda et al. 2021):

$$\mathrm{Cost}^{\mathrm{Purch}}_{\mathrm{Grid}} = 365 \times \sum_{yr=1}^{20}\sum_{hr=1}^{24}\left(\gamma_{yr}\cdot \mathrm{Price}^{\mathrm{Grid}}_{hr,yr}\cdot P^{\mathrm{grid}}_{hr,yr}\right)(\$) \tag{8}$$

where $P^{\mathrm{Grid}}_{hr,yr}$ (MW) is the active power which is supplied by the main grid at the substation at the hrth hour in the yrth year; and $\mathrm{Price}^{\mathrm{Grid}}_{hr,yr}$ ($/MWh) is the electricity price that is declared by the power company and which is subject to change according to the specific time.

2.2 *Constraints*

2.2.1 Power Balance Constraints

In this paper, BESS can be in a state of charging or discharging energy to the system (Hung et al. 2014a, b; Khunkitti et al. 2022). Thus, the active power balance equation should be divided into two equations for two states of BESS and is shown as follows:

The active power balance equation for the discharging state of BESS:

$$P^{\mathrm{Grid}}_{hr,yr} + \sum_{p=1}^{N_{\mathrm{PV}}}P^{\mathrm{Gen}}_{\mathrm{PV},p,hr,yr} + \sum_{w=1}^{N_{\mathrm{WT}}}P^{\mathrm{Gen}}_{\mathrm{WT},w,hr,yr} + \sum_{bs=1}^{N_{\mathrm{BESS}}}P^{\mathrm{DisCh}}_{\mathrm{BESS},bs,hr,yr} = \sum_{lo=1}^{N_{ld}}P^{ld}_{lo,hr,yr} + \sum_{bh=1}^{N_{bh}}P^{ls}_{bh,hr,yr} \tag{9}$$

The active power balance equation for charging state of BESS:

$$P^{\mathrm{Grid}}_{hr,yr} + \sum_{p=1}^{N_{\mathrm{PV}}}P^{\mathrm{Gen}}_{\mathrm{PV},p,hr,yr} + \sum_{w=1}^{N_{\mathrm{WT}}}P^{\mathrm{Gen}}_{\mathrm{WT},w,hr,yr} = \sum_{lo=1}^{N_{ld}}P^{ld}_{lo,hr,yr} + \sum_{bh=1}^{N_{bh}}P^{ls}_{bh,hr,yr} + \sum_{bs=1}^{N_{\mathrm{BESS}}}P^{\mathrm{Char}}_{\mathrm{BESS},bs,hr,yr} \tag{10}$$

The reactive power balance equation is presented as

$$Q^{\mathrm{Grid}}_{hr,yr} + \sum_{w=1}^{N_{\mathrm{WT}}}Q^{\mathrm{Gen}}_{\mathrm{WT},w,hr,yr} + \sum_{p=1}^{N_{\mathrm{PV}}}Q^{\mathrm{Gen}}_{\mathrm{PV},p,hr,yr} + \sum_{c=1}^{N_{\mathrm{Cap}}}Q^{\mathrm{Gen}}_{\mathrm{Cap},c,hr,yr} = \sum_{lo=1}^{N_{ld}}Q^{ld}_{lo,hr,yr} + \sum_{bh=1}^{N_{bh}}Q^{ls}_{bh,hr,yr} \tag{11}$$

In the above equation, $Q^{\mathrm{Gen}}_{\mathrm{PV},p,hr,yr}$ and $Q^{\mathrm{Gen}}_{\mathrm{WT},w,hr,yr}$ can be found by (Hung et al. 2014a, b)

$$Q^{\mathrm{Gen}}_{\mathrm{PV},p,hr,yr} = P^{\mathrm{Gen}}_{\mathrm{PV},p,hr,yr} \times \beta_{\mathrm{PV},p};\quad \text{where, } \beta_{\mathrm{PV},p} = \pm\tan\left(\cos^{-1}\left(\mathrm{PF}_{\mathrm{PV},p}\right)\right) \tag{12}$$

$$Q^{\text{Gen}}_{\text{WT},w,hr,yr} = P^{\text{Gen}}_{\text{WT},w,hr,yr} \times \beta_{\text{WT},w};\ \text{where, } \beta_{\text{WT},w} = \pm \tan\left(\cos^{-1}\left(\text{PF}_{\text{WT},w}\right)\right) \quad (13)$$

In Eqs. (12, 13), $\text{PF}_{\text{PV},p}$ and $\text{PF}_{\text{WT},w}$ are defined as the operating power factors for inverter-based PVs and WTs, respectively. In addition, $\beta_{\text{PV},p}$ and $\beta_{\text{WT},w}$ can be negative values (or positive values) for reactive power absorption (or reactive power injection) (Hung et al. 2014a, b).

2.2.2 Bus Voltage Limits

The bus voltage is constrained in lower and upper limits (V^{Min}andV^{Max}) of 0.95 pu and 1.05 pu as (Kien et al. 2022):

$$V^{\text{Min}} \le V_{j,hr,yr} \le V^{\text{Max}}, j = 1, 2, 3\ldots, N_{bu} \quad (14)$$

2.2.3 Branch Current Limit

The branch current should not exceed the maximum allowable limit at each branch (Kien et al. 2022):

$$I_{bh,hr,yr} \le I^{\text{Max}}_{bh}; bh = 1, 2, 3\ldots, N_{bh} \quad (15)$$

2.2.4 Harmonic Voltage Distortion Limits

According to the IEEE Std. 519, the maximum allowable limits of total harmonic voltage distortion (THD^{Max}) and individual harmonic voltage distortion (IHD^{Max}) are 5% and 3%, respectively (Nguyen et al. 2020). Therefore, this standard is applied to become constraints for harmonic distortions (Lakum and Mahajan 2021):

$$\text{THD}_{j,hr,yr} \le \text{THD}^{\text{Max}};\ j = 1, 2, 3\ldots, N_{bu} \quad (16)$$

$$\text{IHD}^{H}_{j,hr,yr} \le \text{IHD}^{\text{Max}};\ j = 1, 2, 3\ldots, N_{bu} \quad (17)$$

$$\text{where} \quad \text{THD}_{j,hr,yr} = \left[\frac{\sqrt{\sum_{hc=2}^{H}\left(V_{j,hr,yr,hc}\right)^2}}{V^{1}_{j,hr,yr}}\right] \times 100(\%) \quad (18)$$

$$\text{IHD}^{H}_{j,hr,yr} = \left[\frac{V_{j,hr,yr,hc}}{V^{1}_{j,hr,yr}}\right] \times 100(\%) \quad (19)$$

2.2.5 Charging and Discharging Power Limits

The charging and discharging power limits should be followed (Peng et al. 2021):

$$P^{\text{Rated}}_{\text{BESS}} \times \mu^{\text{Char}} \ge P^{\text{Char}}_{\text{BESS},bs,hr} \ge 0 \quad (20)$$

$$-P^{\text{Rated}}_{\text{BESS}} \times \mu^{\text{DisCh}} \le P^{\text{DisCh}}_{\text{BESS},bs,hr} \le 0 \quad (21)$$

where μ^{Char} and μ^{DisCh} are the charging and discharging efficiencies of BESS, respectively; and $P^{\text{Char}}_{\text{BESS},hr}$ and $P^{\text{DisCh}}_{\text{BESS},hr}$ are the charging power and discharging power at the hrth hour of the bsth BESS, respectively.

2.2.6 Capacity Limits of BESS

The capacity of BESS at the hrth hour ($\left(E_{\text{BESS},hr}\right)$) should be determined in the minimum and maximum limits ($E^{\text{Min}}_{\text{BESS}}$ and$E^{\text{Max}}_{\text{BESS}}$) of BESS. It must be set at 20% and 90% of the rated capacity (Nguyen et al. 2022b, c, a):

$$E^{\text{Min}}_{\text{BESS}} \le E_{\text{BESS},hr} \le E^{\text{Max}}_{\text{BESS}} \quad (22)$$

Besides, the energy at the beginning of the day or the initial energy ($\text{E}_{\text{BESS},0}$) should be equal to the energy at the end of the day ($\text{E}_{\text{BESS},24}$) to ensure that BESS can continue its operation on the next day without any violation (Khunkitti et al. 2022).

$$E_{\text{BESS},0} = E_{\text{BESS},24} \quad (23)$$

2.2.7 Penetration of PVs, WTs, and CB

The installed capacity of each unit should be bound within the predefined limits as (Pham et al. 2021; Kumar et al. 2017b, a):

$$P^{\text{Min}}_{\text{PV}} \le P^{\text{Rated}}_{\text{PV},p} \le P^{\text{Max}}_{\text{PV}}; p = 1, 2, 3\ldots, N_{\text{PV}} \quad (24)$$

$$P^{\text{Min}}_{\text{WT}} \le P^{\text{Rated}}_{\text{WT},w} \le P^{\text{Max}}_{\text{WT}}; w = 1, 2, 3\ldots, N_{\text{WT}} \quad (25)$$

$$Q^{\text{Min}}_{\text{Cap}} \le Q^{\text{Rated}}_{\text{Cap},c} \le Q^{\text{Max}}_{\text{Cap}}; c = 1, 2, 3\ldots, N_{\text{Cap}} \quad (26)$$

3 Modified Coyote Optimization Algorithm

3.1 The First Modification

In recent years, an efficient meta-heuristic algorithm has been published by Pierezan and Coelho (2018) called the coyote optimization algorithm (COA). This algorithm is inspired by the coyote species, and it has the ability to balance exploration and exploitation for searching the global optimal solution (Chang and Chinh 2020). Based on the nature characteristics of the coyote community, it is divided into many packs (N_{pk}) and has coyote members (N_{ce}) in each pack. Thus, ($N_{pk} \times N_{ce}$) is considered as the coyote population. In COA, the living condition and quality of living condition are the two main factors that characterize individuals. While the living condition

represents the solution for the optimization problem, the quality of the living condition reports the fitness of that solution.

As other stochastic algorithms, the initial solutions $S_{pk,ce}$ can be randomly generated by (Pierezan and Coelho 2018)

$$S_{pk,ce} = S^{\text{Min}} + rd.\left(S^{\text{Min}} + S^{\text{Max}}\right); pk = 1, 2, 3 \ldots N_{pk} \& ce = 1, 2, 3 \ldots, N_{ce} \tag{27}$$

where S^{Min} and S^{Max} are defined as the minimum and maximum values of the control variables in the proposed solution for the optimization problem, respectively; and rd is a random number in the interval of [0, 1].

In the first generation of the original COA, new solutions were updated according to the following mathematical equation (Pierezan and Coelho 2018):

$$S^{New}_{pk,ce} = S_{pk,ce} + rd.\left(S_{bestPk,pk} - S_{rd1,pk}\right) + rd.\left(S_{cent,pk} - S_{rd2,pk}\right);\ pk = 1,\ 2,\ 3 \ldots,\ N_{pk}\ \&\ ce = 1,\ 2,\ 3 \ldots,\ N_{ce} \tag{28}$$

In the above equation, there are two jumps which are implemented for generating the new solutions. Clearly, at the first jump, $rd.\left(S_{\text{best}Pk,pk} - S_{rd1,pk}\right)$ tends to search for the best solution in the pack, and at the second jump, $rd.\left(S_{\text{cent},pk} - S_{rd2,pk}\right)$ searches for the central solution of the pack. This is effective in solving optimization problems that have a near-zero global solution like the benchmark functions that COA solved (Pierezan and Coelho 2018). However, the global optimal solution is not always the zero solution in the real cases. Thus, this update equation is not efficient in the variety of optimization problems. To overcome the above drawback, the central solution is replaced by the best solution in the current population. This opens the door for better opportunities to search possible solutions for solving complex optimization problems, leading to enhanced performance of the proposed algorithm. The modified equation of creating new solutions at the first generation can be expressed in the mathematical model as

$$S^{New}_{pk,ce} = S_{pk,ce} + rd.\left(S_{bestPk,pk} - S_{rd1,pk}\right) + rd.\left(S_{bestPop} - S_{rd2,pk}\right);\ pk = 1,\ 2,\ 3 \ldots,\ N_{pk}\ \&\ ce = 1,\ 2,\ 3 \ldots,\ N_{ce} \tag{29}$$

3.2 The Second Modification

In COA, the second new solution generation equation produces only one new solution per pack by applying a randomization mechanism (Pierezan and Coelho 2018):

$$S^{\text{New}}_{pk} = \begin{cases} S_{pk,rd1}, & \text{if} \quad rd < 1/N_{va} \\ S_{pk,rd2}, & \text{if} \quad 1/N_{va} \le rd < 1/2 + 1/N_{va} \\ S_{pk,rd}, & \text{otherwise} \end{cases} \tag{30}$$

Explicitly, in Eq. (30), there are three solutions which are randomly generated. $S_{p,rd1}$ and $S_{p,rd2}$ are two solutions generated in each pack that are randomly selected from taking available variables in random packs. This random selection significantly affects the quality of the found solution, and finding a good quality solution is very rare. Besides, $S_{pk,rd}$ is also randomly produced within the allowable limits of S^{Min} and S^{Max}. Clearly, all three solutions hardly follow any trend to find the good solutions. As a result, the created solution at each group by applying Eq. (30) is likely to be of poor quality, especially in solving complex problems with a large search space. In each pack, after a new solution is created, it is compared with the worst solution in that pack, and the better one will be kept. However, this is inefficient and also consumes a lot of time in comparison to keep good solutions. To overcome this remaining drawback, it should be suggested to determine positive directions to increase the possibility of generating a new solution with good quality for each pack. Therefore, Eq. (30) is terminated and replaced by using Eqs. (31, 32):

$$S^{\text{New}}_{pk} = S_{\text{best Pop}} + rd.\left(S_{\text{bestPop}} - S_{\text{best},r1}\right) + rd.\left(S_{\text{bestPop}} - S_{\text{best},r2}\right) \tag{31}$$

$$S^{\text{New}}_{pk} = S_{\text{bestPop}} + rd.\left(S_{\text{bestPop}} - S_{\text{best},r1}\right) + rd.\left(S_{\text{bestPop}} - S_{\text{best},r2}\right) + rd.\left(S_{\text{bestPop}} - S_{\text{best},r3}\right) \tag{32}$$

While S_{bestPop} is the current best solution of the population, $S_{\text{best},r1}$, $S_{\text{best},r2}$ and $S_{\text{best},r3}$ are the best solutions in each pack that is randomly selected from the available packs. Choosing the best solution from each pack for Eqs. (31, 32) offers the better chances than taking a random solution as suggested by Eq. (30) of the original algorithm. Thus, newly created solutions tend to move around the best solution in the current population for finding the possible solutions. This has greatly contributed in enhancing the quality of the new solution in general. In addition, to avoid falling into the local traps as much as possible, the new solution generation equation at this stage is divided into two equations with different number of jumps, as Eq. (31) and Eq. (32). While Eq. (31) uses only two jumps, Eq. (32) again suggests using an extra jump to locate far enough from the global solution $\left(S_{\text{bestPop}}\right)$. This can open new opportunities for searching for new solutions in the positive large search region and avoids missing good-quality solutions. Thus, it is important to determine the condition to choose the appropriate equation of new solution generation for enhancing the performance of the algorithm. For

deciding the suitable time to apply the equation of the second generation, a ratio of the close solution couple number (N_C) to the maximum solution couple number (N_M) is set. The calculated value of this ratio is compared with a predefined threshold (δ). If the result of N_C/N_M is less thanδ, then Eq. (31) is selected, and in other cases, Eq. (32) is used.

4 Applying the Proposed Method for the Optimization Problem

4.1 Population Initialization

The generated initial solutions must be constrained within the limits of S^{Min} and S^{Max}, and are presented as

$$S^{\text{Min}} = \left[L_p^{\text{Min}}, S_p^{\text{Min}}, L_w^{\text{Min}}, S_w^{\text{Min}}, L_{\text{BESS},bs}^{\text{Min}}, P_{\text{BESS},bs,h}^{\text{Min}}, L_c^{\text{Min}}\right] \tag{33}$$

$$S^{\text{Max}} = \left[L_p^{\text{Max}}, S_p^{\text{Max}}, L_w^{\text{Max}}, S_w^{\text{Max}}, L_{\text{BESS},bs}^{\text{Max}}, P_{\text{BESS},bs,h}^{\text{Max}}, L_c^{\text{Max}}\right] \tag{34}$$

For the generation of initial solutions, the control variables in each solution are randomly produced within the given limits as Eqs. (33, 34). Then, the forward–backward sweep technique (FW-BWST) (Teng and Chang 2007) is applied to solve power flow and harmonic flow problems for determining the objective function value and the penalty terms. Finally, the fitness function value for each solution is found by applying Eq. (35).

$$\begin{aligned}\text{SF}_{pk,ce} = \text{TC}_{pk,ce} &+ \sigma_V \cdot \sum_{j=1}^{N_{bu}} \Delta V_{j,pk,ce}^2 + \sigma_I \cdot \sum_{bh=1}^{N_{bh}} \Delta I_{bh,pk,ce}^2 \\ &+ \sigma_{\text{THD}} \cdot \sum_{j=1}^{N_{bu}} \Delta \text{THD}_{j,pk,ce}^2 + \sigma_{\text{IHD}} \cdot \sum_{j=1}^{N_{bu}} \Delta \text{IHD}_{j,pk,ce}^2\end{aligned} \tag{35}$$

In Eq. (35), the amount of penalty of bus voltage, branch current, THD, and IHD can be calculated as Eqs. (36–39), respectively:

$$\Delta V_{j,pk,ce} = \begin{cases} V_{j,pk,ce} - V^{\text{Max}} \text{ if } V_{j,pk,ce} > V^{\text{Max}} \\ V^{\text{Min}} - V_{j,pk,ce} \text{ if } V_{j,pk,ce} < V^{\text{Min}} \\ 0 \text{ else} \end{cases} \tag{36}$$

$$\Delta I_{bh,pk,ce} = \begin{cases} I_{bh,pk,ce} - I_{bh}^{\text{Max}} \text{ if } I_{bh,pk,ce} > I_{bh}^{\text{Max}} \\ 0 \text{ else} \end{cases} \tag{37}$$

$$\Delta \text{THD}_{j,pk,ce} = \begin{cases} \text{THD}_{j,pk,ce} - \text{THD}^{\text{Max}} \text{ if } \text{THD}_{j,pk,cec} > \text{THD}^{\text{Max}} \\ 0 \text{ else} \end{cases} \tag{38}$$

$$\Delta \text{IHD}_{j,pk,ce} = \begin{cases} \text{IHD}_{j,pk,ce} - \text{IHD}^{\text{Max}} \text{ if } \text{IHD}_{j,pk,ce} > \text{IHD}^{\text{Max}} \\ 0 \text{ else} \end{cases} \tag{39}$$

4.2 Correcting New Solutions

The control variables ($CV_{va,pk,ce}^{\text{New}}$) in new solutions which are produced at the first solution generation stage using Eq. (29) and the second solution generation state using Eqs. (31, 32) are checked and corrected within the predetermined limits of S^{Min} and S^{Max}. This can be shown in the following model (Pham et al. 2021):

$$\begin{aligned}\text{CV}_{va,pk,ce}^{\text{New}} &= \begin{cases} \text{CV}_{va}^{\text{Min}} \text{ if } \text{CV}_{va,pk,ce}^{\text{New}} < \text{CV}_{va}^{\text{Min}} \\ \text{CV}_{va}^{\text{Max}} \text{ if } \text{CV}_{va,pk,ce}^{\text{New}} > \text{CV}_{va}^{\text{Max}} \\ \text{CV}_{va,pk,ce}^{\text{New}} \text{ else} \end{cases}; va \\ &= 1,2,3\ldots,N_{va}; pk = 1,2,3\ldots,N_{pk}; ce \\ &= 1,2,3\ldots,N_{ce}\end{aligned} \tag{40}$$

4.3 Updating the Good Solutions

After correcting the violated control variables of the new solutions, all solutions should be evaluated by applying Eq. (35), and the good solutions and their quality will be updated according to the rules as (Pham et al. 2021)

$$\begin{aligned}S_{pk,ce} &= \begin{cases} S_{pk,ce}^{New} \text{ if } \text{SF}_{pk,ce}^{New} < \text{SF}_{pk,ce} \\ S_{pk,ce} \text{ else} \end{cases}; pk \\ &= 1,\ 2,\ 3\ldots,\ N_{pk}; ce = \ 1,\ 2,\ 3\ldots,\ N_{ce}\end{aligned} \tag{41}$$

$$\begin{aligned}\text{SF}_{pk,ce} &= \begin{cases} \text{SF}_{pk,ce}^{\text{New}} \text{ if } \text{SF}_{pk,ce}^{\text{New}} < \text{SF}_{pk,ce} \\ \text{SF}_{pk,ce} \text{ else} \end{cases}; pk \\ &= 1,\ 2,\ 3\ldots,N_{pk};\ ce = \ 1,\ 2,\ 3\ldots,\ N_{ce}\end{aligned} \tag{42}$$

4.4 Flowchart for Solving the Optimization Problem

For solving the optimization problem of integration of wind turbine units, photovoltaic units, capacitor bank, and battery energy storage system to minimize total costs in the distribution system, the modified coyote optimization algorithm (MCOA) is proposed. This algorithm is performed iteratively to search for the best solution for the above problem. When the number of iterations reaches the predetermined maximum value (It^{Max}), the globally optimal solution is given. The flowchart of finding the global optimal solution is presented as Fig. 1.

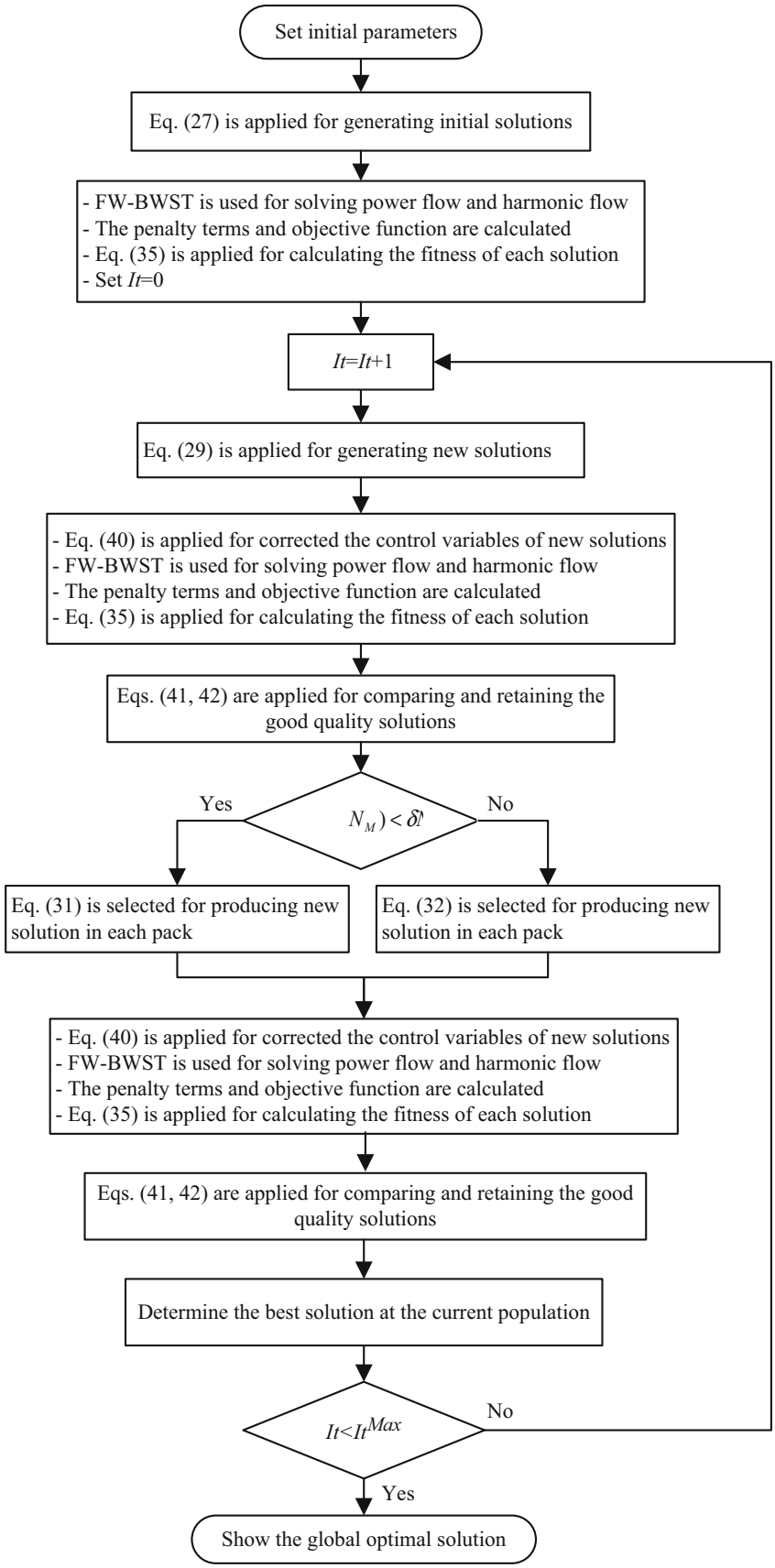

Fig. 1 The flowchart for finding the optimal solution in the considering problem

5 Simulation Results

In this study, three algorithms including SMA, COA, and MCOA are applied to find the optimal solution for the installation of WTs, PVs, BESS, and CB to minimize total costs in the IEEE 69-bus radial distribution system. For the simulation implementation, the coyote number in each pack and the pack number in the community are 5 and 4 for both COA and MCOA, and the population of SMA is selected as 25. Besides, the predefined threshold (δ) is determined based on the survey from 0.2 to 0.8 with step size of 0.2, and in the case of this study, it is 0.2. The total number of iterations is set to 300, and the number of independent trial runs for each method is taken as 40. All methods are performed on a personal computer with a 2.1 GHz processor, 16.0 GB RAM, 1.0 TB solid-state drive (SSD) in MATLAB (R2022b). In addition, other parameters for calculating the grid operating costs are reported in Table 1.

In Table 1, the peak hours are defined as 9:00 to 11:00 and 17:00 to 20:00; the standard hours are from 4:00 to 9:00, 11:00 to 17:00, and 20:00 to 22:00; the off-peak hours are the remaining hours in a day, from 22:00 to 4:00 (Nguyen et al. 2022b, c, a). Besides, a typical day is used to represent 365 days in a year, and there are 20 years for the project life. In this study, the capital cost of PVs, WTs, and CB also included the balance of the plant and supporting infrastructure cost, land cost, start-up cost, and inverter cost for PVs and WTs. Additionally, this study also referred to the obtained results of output power prediction for WTs and PVs from (Hung et al. 2013). The output curves of PVs, WTs, and load demand are plotted as Fig. 2.

Three WTs and three PVs which applied inverters with the power factor of 0.9 (lagging) (Hung et al. 2013) are integrated into the system with the maximum and minimum numbers of each being 10 turbines and two turbines, and 20,000 modules and 2000 modules, respectively. The rated capacity is assumed to be 100 kW for each wind turbine and 75 W for each photovoltaic module (Atwa et al. 2009). In addition, a BESS system using a battery of lead acid technology (Mongird et al. 2020) is considered for connection with the maximum values of rated power and rated capacity which are selected as 2.0 MW and 6.0 MWh, respectively. The initial energy $\left(E_{\mathrm{BESS},0}\right)$ is assumed as 1.0 MWh for BESS, and the charging and discharging efficiencies $\left(\mu^{\mathrm{Char}}\right.$ and $\left.\mu^{\mathrm{DisCh}}\right)$ are supposed to be 90%. Additionally, a capacitor bank is also connected to compensate for the reactive power and to keep the power factor of the system as 0.9. As mentioned, the system has integration of nonlinear loads and they are located at buses of 8, 12, 18, 22, 24, 34, 46, 55, and 65, with the harmonic spectrum as described in Table 2 (EPRI, 2014), and FW-BWST is used to solve the harmonic flows (Teng and Chang 2007). On the other hand, the IEEE 69-bus radial distribution system is also selected as the test case with a structure as presented in Fig. 3, and the system data are collected from Kadir et al. (2013).

Due to the random nature of the meta-heuristic methods, 40 trial runs were performed to evaluate the performance objectively. The best, the average, and the worst fitness values are reported in Table 3. Clearly, the found variation

Table 1 The information for calculating the cost of operating the integrated grid

Item	Value
$\mathrm{Price}_{hr}^{\mathrm{grid}}$ at the peak hours (Nguyen et al. 2022b, c, a)	128.9 $/MWh
$\mathrm{Price}_{hr}^{\mathrm{grid}}$ at the standard hours (Nguyen et al. 2022b, c, a)	70.0 $/MWh
$\mathrm{Price}_{hr}^{\mathrm{grid}}$ at the off-peak hours (Nguyen et al. 2022b, c, a)	45.4 $/MWh
ir (Elattar and Elsayed 2020)	9%
$C_{\mathrm{PV}}^{\mathrm{Cal}}$ (Gampa and Das 2015)	770,000 $/MW
$C_{\mathrm{PV}}^{\mathrm{OM}}$ (Gampa and Das 2015)	10.0 $/MWh
$C_{\mathrm{WT}}^{\mathrm{Cal}}$ (Zou et al. 2011)	1,882,000 $/MW
$C_{\mathrm{WT}}^{\mathrm{OM}}$ (Zou et al. 2011)	10.0 $/MWh
C_{Cap}^{Cal} (Thang and Minh 2017)	20,000 $/MVAr
Loc_{Cap} (Thang and Minh 2017)	1,000 $/Location
$C_{\mathrm{BESS}}^{\mathrm{Cal}}$ (Mongird et al. 2020)	200,000 $/MW
$C_{\mathrm{BESS}}^{\mathrm{OM}}$ (Mongird et al. 2020)	7,000 $/MWyear
$C_{\mathrm{BESS}}^{\mathrm{Aux}}$ (Mongird et al. 2020)	380,000 $/MW

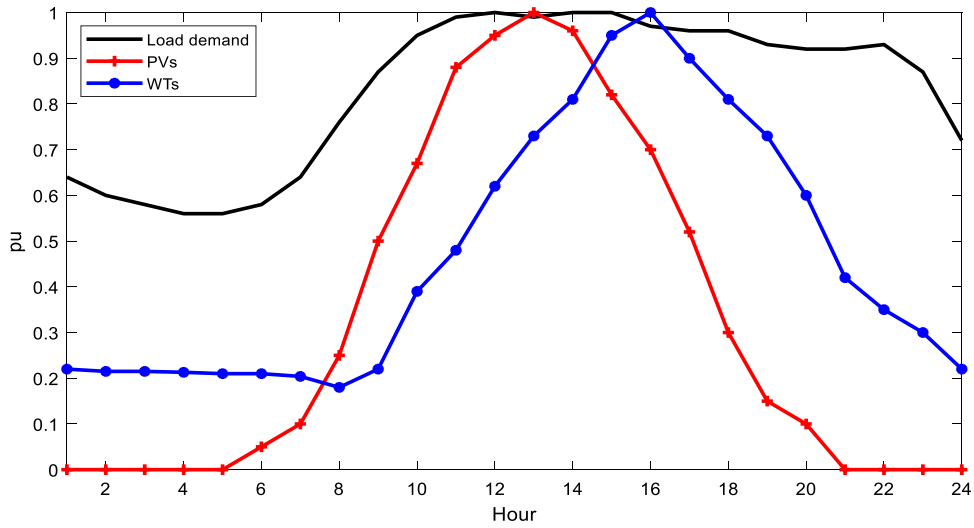

Fig. 2 The output curves of PVs, WTs, and load demand

Table 2 Harmonic spectrum

Harmonic order	Magnitude (%)	Angle (^{o})
5, 7, 11, 13, 17	76.5, 62.7, 24.8, 12.7, 7.1	28, −180, −59, 79, −253

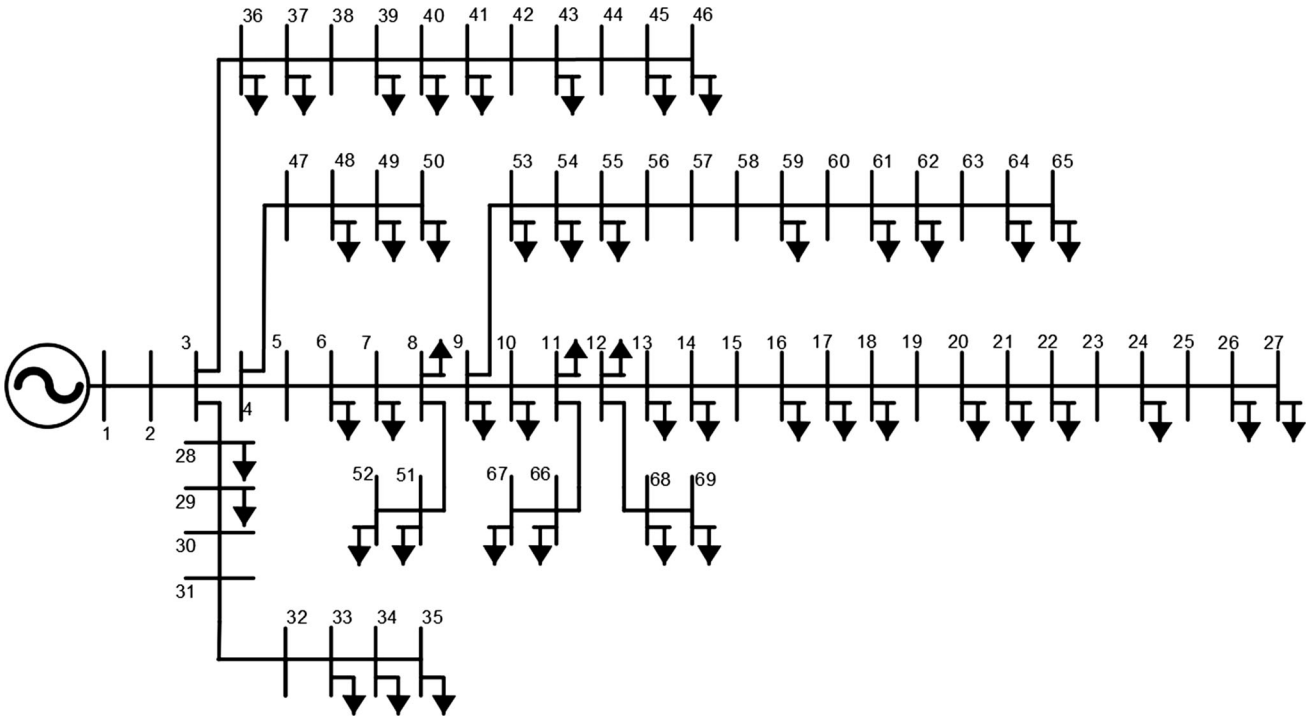

Fig. 3 The IEEE 69-bus radial distribution system

Table 3 The comparison of found fitness values and the mean running time of the three implemented methods

Implemented method	SMA	COA	MCOA
Worst fitness value	$16.723 million	$16.562 million	$16.501 million
Mean fitness value	$16.521 million	$16.314 million	$16.271 million
Best fitness value	$16.356 million	$16.148 million	$16.130 million
Mean running time	4211 s	4282 s	4277 s

of fitness values from MCOA is best with the range of [16.130, 16.501] ($ million), while the range is [16.356, 16.723] ($ million) for SMA and [16.148, 16.562] ($ million) for COA. Not only that, the average fitness value, which represents the stability of the methods over the 40 trial runs, is also calculated. Specifically, it is $16.521 million, $16.314 million, and $16,271 million for SMA, COA, and MCOA, respectively. Thereby, it indicates that MCOA not only has higher performance but also has better stability than other methods. In addition, the average running time of 40 trial runs is also compared in Table 3. The average running time per trial run of MCOA (4277 s) is slower than SMA (4211 s), but it is faster than COA (4282 s), although not significantly. However, this also contributes to proving that the improvements for MCOA are effective in enhancing the speed for solving the optimization problem.

The best optimal solution of the implemented methods is presented in detail as Table 4, including location and capacity of PVs, WTs, BESS, and CB for integration into the distribution system to achieve the minimum total costs. Besides, the calculation results for related costs in the 20-year project period of all methods are also shown in Table 5. As a result, after the components such as PVs, WTs, BESS, and CB are connected, total costs of operating the system are significantly reduced from $20.792 million to $16.356 million, $16.148 million, and $16.130 million for SMA, COA, and MCOA, respectively. Obviously, total costs from applying the proposed solution by MCOA are lower than the others. In detail, the investment and O&M costs of MCOA are $8.319 million, which is lower than $8.370 million for SMA and higher than $8.253 million for COA. In addition, thanks to the lower cost of purchasing electricity from the main grid for load demand, it is only $7.811 million for MCOA, while the remaining methods amounted to $7.986 million (SMA) and $7.895 million (COA), resulting in more money saved. As calculated, the saving costs compared to the base system of SMA, COA, and MCOA are $4.436 million, $4.644 million, and $4.662 million, corresponding to 21.335%, 22.336%, and 22.422%, respectively. In short, the money saved using MCOA is the highest, and this indicates that the proposed method is the best. Besides high efficiency and good stability, the convergence characteristic of MCOA is also compared, and it is better than other methods. Clearly, MCOA can find better quality solutions with lower fitness values than COA and SMA at the early stage, as plotted Fig. 4. The above arguments have proved that modifications in the new solution generation equations are positive and MCOA is a great method for solving the optimal installation of PVs, WTs, BESS, and CB in the distribution system.

Figure 5 shows the time-varying power consumption and power generation of PVs and WTs from the proposed method for a typical day. As presented in Fig. 5, total power generation from renewable energy sources is only 41.71 MW, while total power consumption amounts to 76.46 MW, thereby showing the energy shortage and that this amount of energy will be provided by the main grid and BESS in the most optimal strategy. The charge and discharge stages of BESS are determined and plotted in Fig. 6. Obviously, at the peak hours from 9:00 to 11:00 and 17:00 to 20:00, BESS discharges power to the distribution system to save money on purchasing power due to high electricity price at these times. On the other hand, at the off-peak hours from 22:00 to 4:00, BESS also tends to charge power for storage due to low electricity price. During the remaining hours of the day, the BESS has flexibility in charging and discharging power to minimize total costs. Similarly, Fig. 7 indicates the energy change from the charge and discharge of BESS. In this particular case, the amount of stored energy in BESS reaches 2.245 MWh; BESS is considered fully charged, and the stored energy in BESS drops to 0.499 MWh, so BESS will stop discharging to avoid damaging the battery bank. Generally, BESS tends to store energy during periods of low

Table 4 The best solution of implemented methods

Method	PVs	WTs	BESS	CB
SMA	Bus: 09 – 9432 modules	Bus: 17 – 04 turbines	Bus: 46 –	Bus: 61 – 1.29 MVAr
	Bus: 54 – 3651 modules	Bus: 65 – 10 turbines	1.092 MW/3.228 MWh	
	Bus: 69 – 14,170 modules	Bus: 63 – 08 turbines		
COA	Bus: 63 – 2162 modules	Bus: 65 – 10 turbines	Bus: 28 –	Bus: 59 – 1.11 MVAr
	Bus: 49 – 15,386 modules	Bus: 61 – 08 turbines	0.793 MW/2.681 MWh	
	Bus: 53 – 8670 modules	Bus: 21 – 05 turbines		
MCOA	Bus: 32 – 5952 modules	Bus: 15 – 07 turbines	Bus: 05 –	Bus: 61 – 1.18 MVAr
	Bus: 05 – 2000 modules	Bus: 57 – 09 turbines	0.979 MW/2.495 MWh	
	Bus: 61 – 18,814 modules	Bus: 62 – 07 turbines		

Table 5 The comparison of the costs involved in operating the system

Method	Base system	SMA	COA	MCOA
Costs of the investment, operation, and maintenance ($Cost^{Inv\&OM}_{PV-WT-BESS-Cap}$,$ million)	–	8.370	8.253	8.319
Cost of purchasing energy from the main grid ($Cost^{Purch}_{Grid}$,$ million)	20.792	7.986	7.895	7.811
Total costs (TC,$ million)	20.792	16.356	16.148	16.130
Saving cost compared to the base system ($ million)	–	4.436	4.644	4.662
Saving cost compared to the base system (%)	–	21.335	22.336	22.422

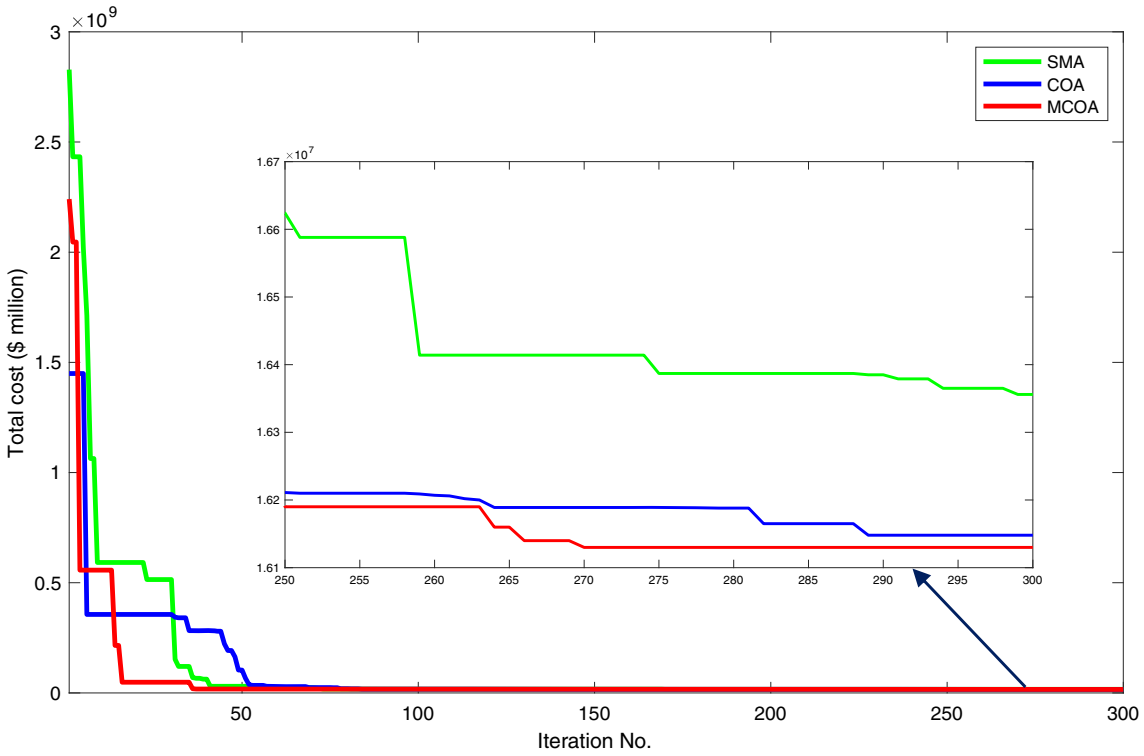

Fig. 4 The convergence curve of the implemented methods

electricity price and light loads to generate energy at periods of high electricity price and heavy loads. This has greatly contributed to reducing the cost of purchasing energy, leading to reduced costs in the operating system.

In this study, a capacitor bank is selected for the connection. The installation position of the capacitor bank is optimally determined, and the time-varying output power is calculated to keep the power factor of the system equal to or higher than 0.9 as required by many countries, and the applied formula for calculating reactive power compensation is clearly described by SACE (2008). As shown in Fig. 8, the maximum capacity found for the capacitor bank is considered as the installation capacity. Specifically, its location and rated capacity should be at bus 61 and 1.18 MVAr with the step size of 10.0 kVAr to minimize the capacitor bank cost without a reactive power penalty.

As mentioned, one of the greatest benefits of connecting suitably distributed sources is the reduction of power loss on the distribution lines. As indicated in Fig. 9, total branch losses in the typical day are cut drastically from 3.778 MW to 0.805 MW by using the optimal solution of the proposed method. In other words, the power loss reduction reaches 78.692%, and this mainly contributes to saving money for operating the system in the long-term project period. In addition, thanks to applying the appropriate solution of the proposed method for integration, the voltage profile of the system is significantly enhanced, as indicated by comparing Figs. 10 and 11. At most times, their voltage profiles drop below the allowable limit of 0.950 pu, of which the

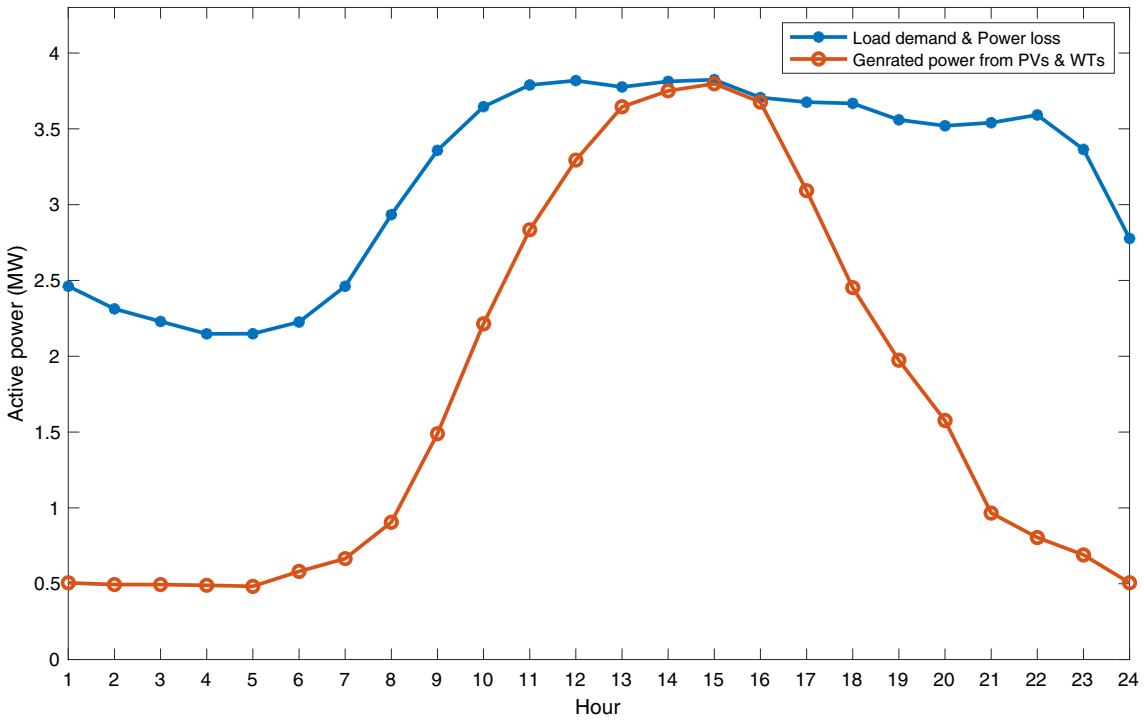

Fig. 5 The actual generated power of PVs and WTs from the proposed method

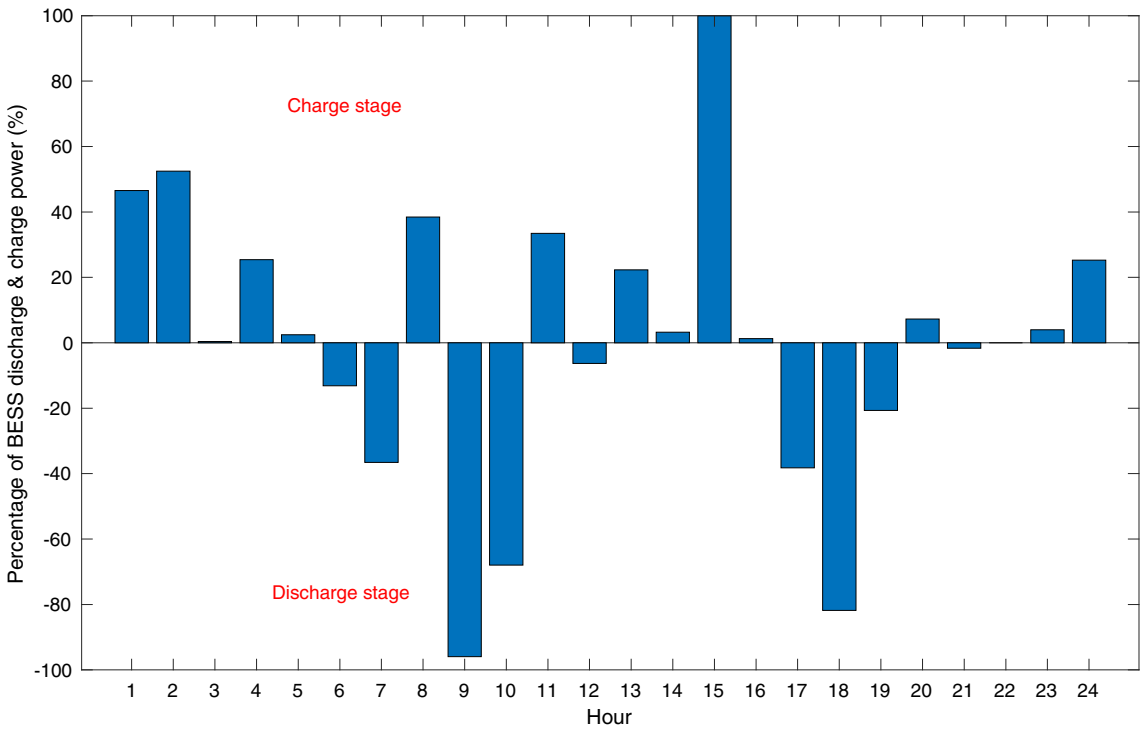

Fig. 6 The charge and discharge stages of BESS

lowest bus voltage value is 0.911 pu at the peak load stages of the base system. But after the optimal solution is used, the lowest bus voltage value and the highest bus voltage value of the whole system considering time increase strongly to 0.953 pu and 1.032 pu, respectively. This completely satisfies the voltage constraints and shows that one of the great benefits of properly connecting PVs, WTs,

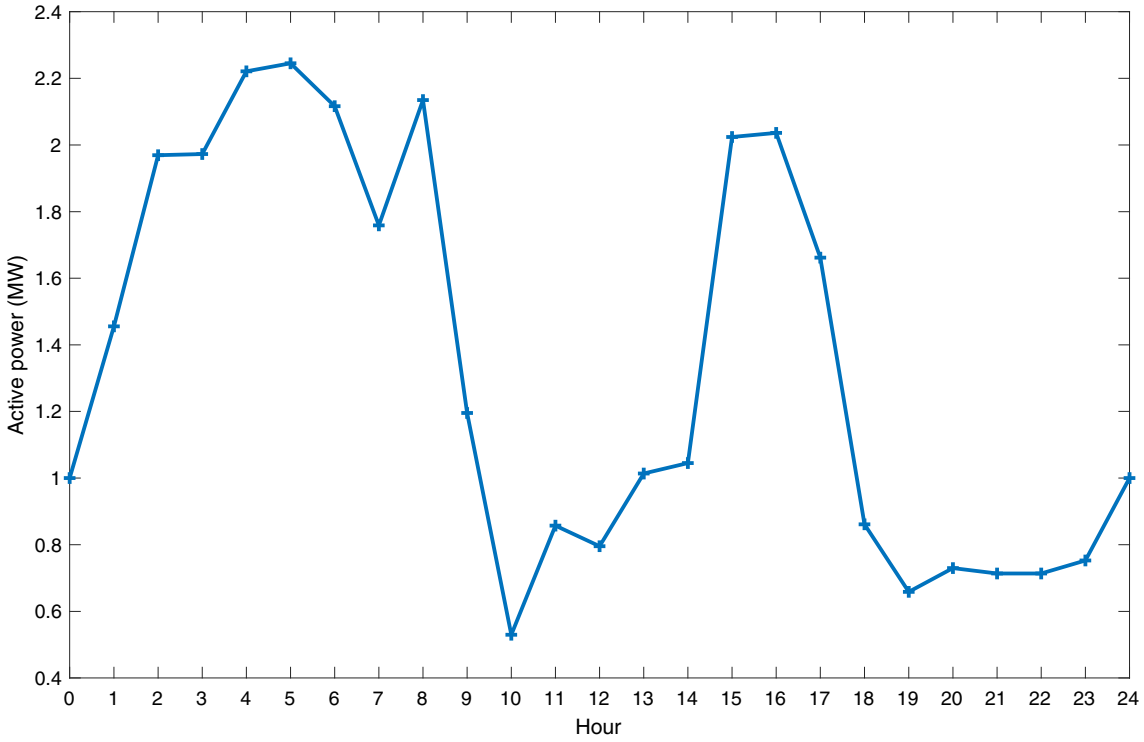

Fig. 7 The stored energy of BESS

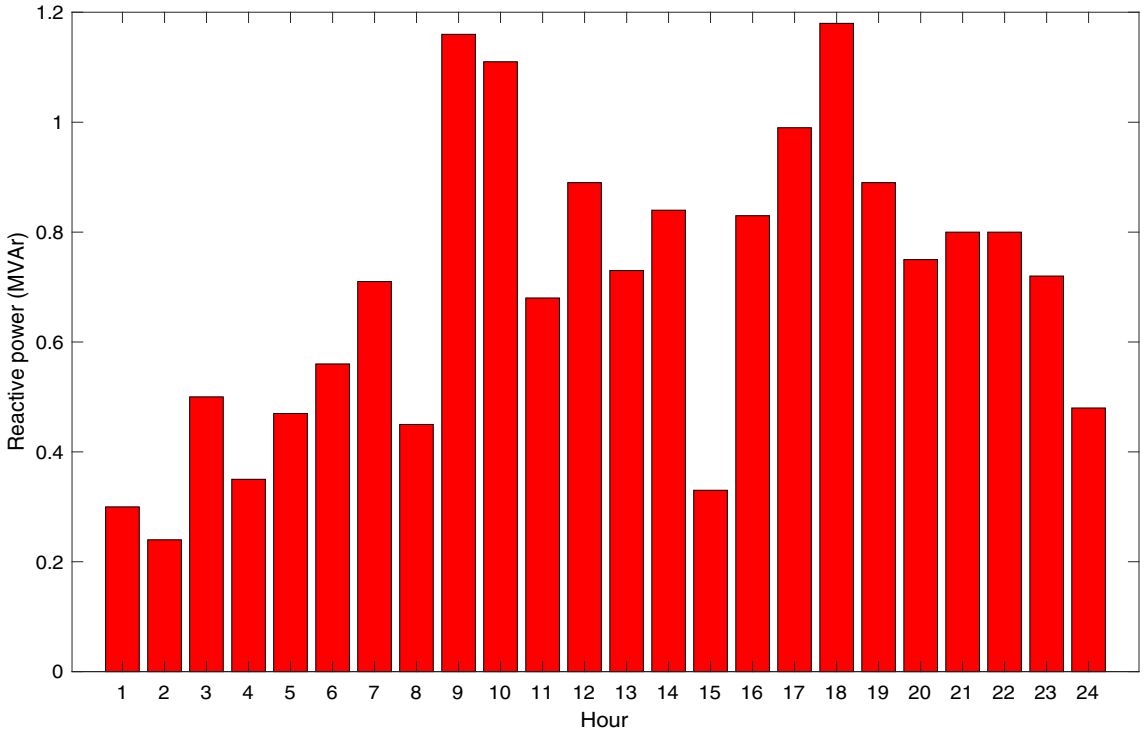

Fig. 8 The reactive power compensation of the capacitor bank

CB, and BESS is enhancement of the voltage profile in the distribution system.

As stated, the system integrates many nonlinear loads, and thus harmonic distortions exist in the system. As shown Figs. 12, there are many THD and IHD values that

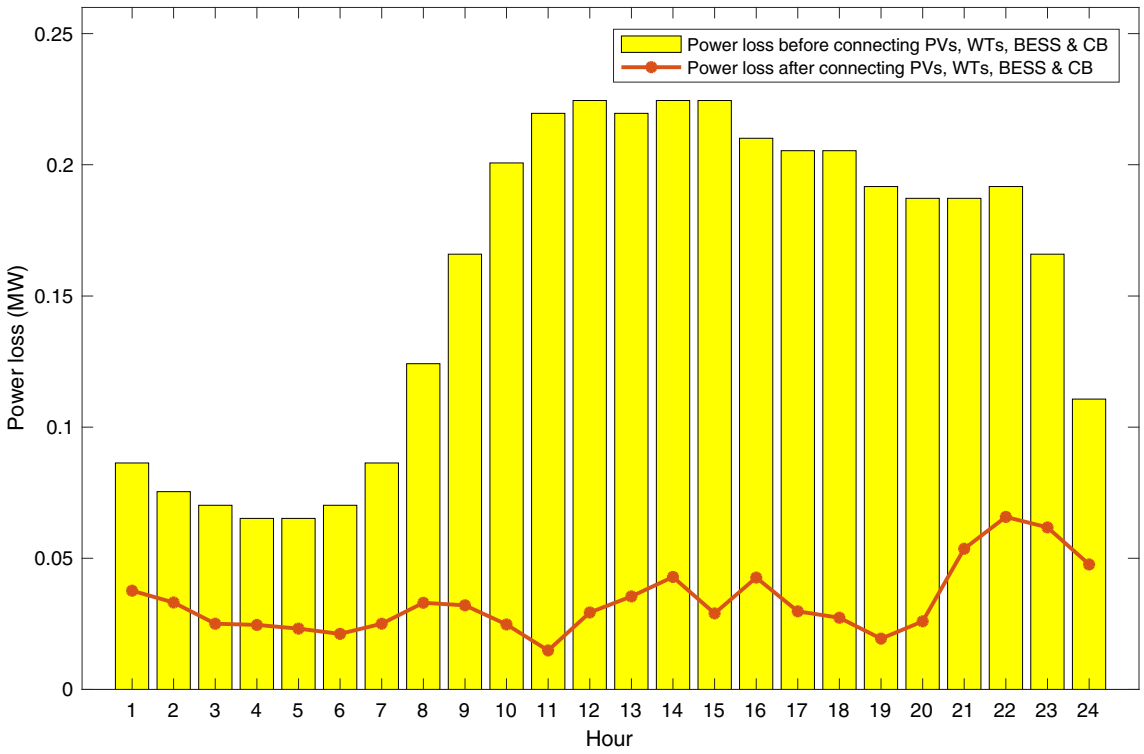

Fig. 9 The power loss of the system before and after integration

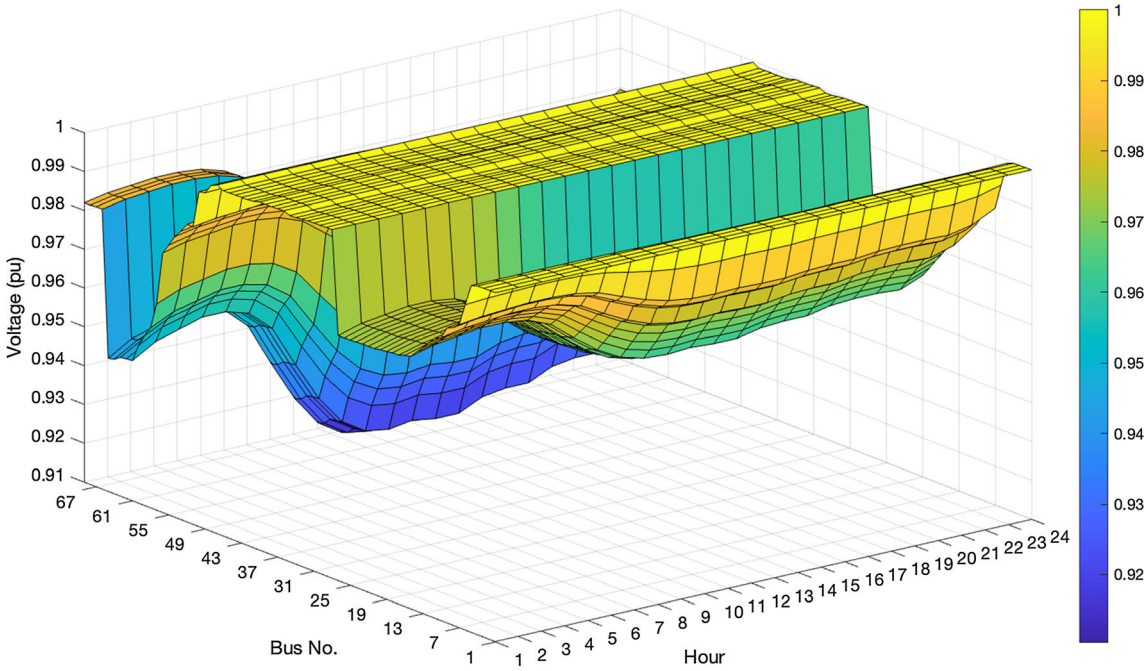

Fig. 10 The bus voltage before connecting PVs, WTs, BESS, and CB

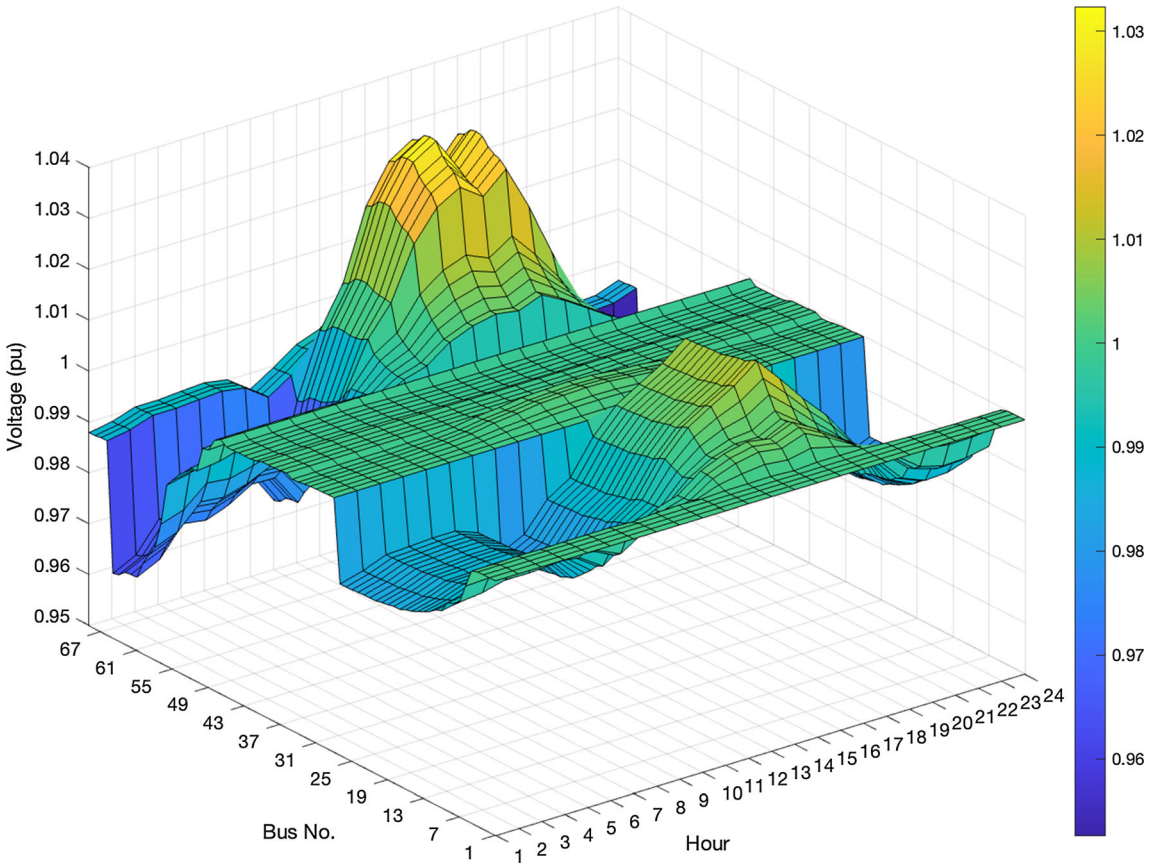

Fig. 11 The bus voltage after connecting PVs, WTs, BESS, and CB

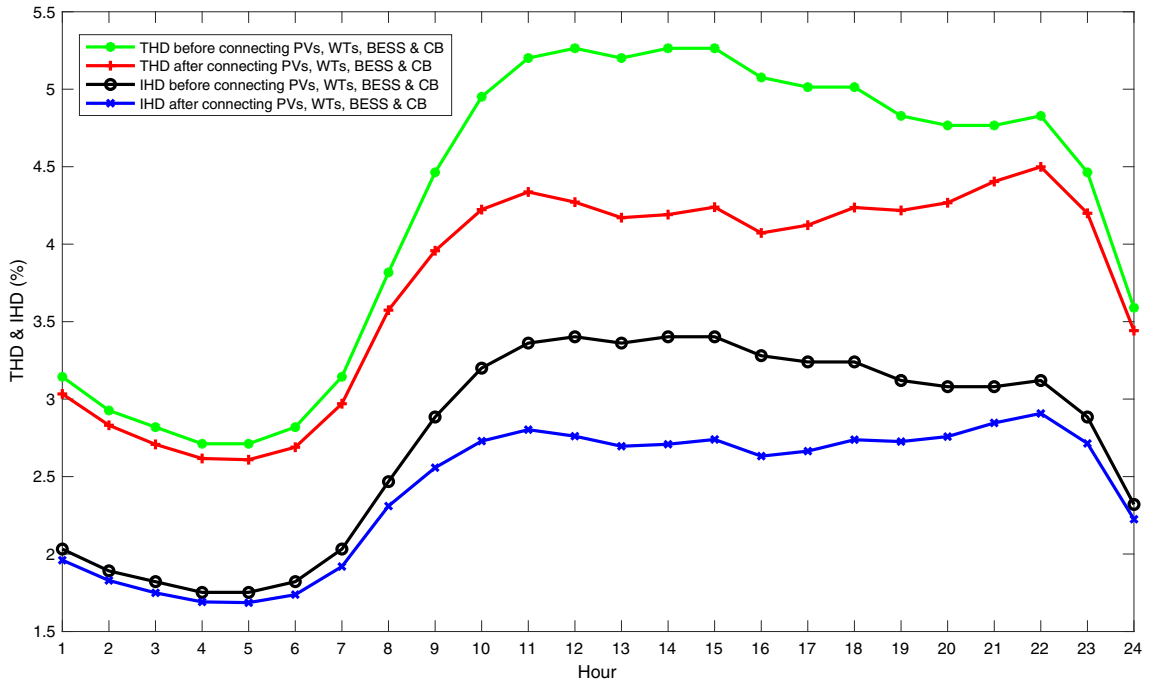

Fig. 12 The maximum THD and IHD values before and after PVs, WTs, BESS, and CB

exceed the acceptance limits of IEEE Std. 519, such as from hour no. 10 to hour no. 22. Specially, at the peak load stages of the base system such as hour no. 12, 14, and 15, THD and IHD reach the highest values with 5.265% and 3.403%, respectively. However, by applying the optimal solution of MCOA, harmonics are mitigated to 4.499% for the maximum THD value and 2.908% for the maximum IHD value. These values do not exceed the allowable limits of the IEEE Std. 519. The above obtained results have proved one more benefit in improving the power quality of the system through integrating PVs, WTs, BESS, and CB.

6 Conclusions

In this study, MCOA is proposed as a novel optimization algorithm for solving the problem of location and sizing of PVs, WTs, BESS, and CB. The main objective is to minimize the total costs of operating the distribution system considering the variation of the load demand as well as the generation of renewable energy sources. By determining the proper possible solution, the proposed method (MCOA) saved up to $4.662 million for the 20 years of the project period compared to the base system, corresponding to 22.422%. Besides, the optimal solution is found not only to satisfy the bus voltage constraints and requirement of the reactive power compensation but also complies with the standard of harmonics. In summary, this study succeeded in determining the optimal solution for installation of distributed sources as well as the proper charging and discharging strategy of BESS in the distribution system. Besides, it also proved the proposed method to be an effective method with high stability and a good convergence characteristic compared with other methods in solving optimization problems.

Acknowledgements I would like to express my great appreciation to Dr. Thang Trung Nguyen (Ton Duc Thang University, Vietnam) and Assoc. Prof. Dr. Le Chi Kien (Ho Chi Minh City University of Technology and Education, Vietnam) for helpful suggestions. The willingness to give their time for assisting me is greatly appreciated. Besides, I also acknowledge editor and reviewers for their comments to improve the quality of this paper.

Data availability The data used are included within the paper.

Declarations

Conflict of interest This paper has no conflict of interest with any other individuals or parties.

References

Atwa YM, El-Saadany EF, Salama MMA, Seethapathy R (2009) Optimal renewable resources mix for distribution system energy loss minimization. IEEE Trans Power Syst 25(1):360–370

Ayodele TR, Ogunjuyigbe ASO, Akinola OO (2015) Optimal location, sizing, and appropriate technology selection of distributed generators for minimizing power loss using genetic algorithm. J Renew Energy. https://doi.org/10.1155/2015/832917

Beck T, Kondziella H, Huard G, Bruckner T (2017) Optimal operation, configuration and sizing of generation and storage technologies for residential heat pump systems in the spotlight of self-consumption of photovoltaic electricity. Appl Energy 188:604–619

Chang GW, Chinh NC (2020) Coyote optimization algorithm-based approach for strategic planning of photovoltaic distributed generation. IEEE Access 8:36180–36190

Elattar EE, Elsayed SK (2020) Optimal location and sizing of distributed generators based on renewable energy sources using modified moth flame optimization technique. IEEE Access 8:109625–109638

Electric Power Research Institute (EPRI) (accessed in 2014) Harmonic spectrum. Available online: https://github.com/tshort/OpenDSS/blob/master/Test/indmachtest/Spectrum.DSS

Elsaiah S, Benidris M, Mitra J (2014) Analytical approach for placement and sizing of distributed generation on distribution systems. IET Gener Transm Distrib 8(6):1039–1049

Gampa SR, Das D (2015) Optimum placement and sizing of DGs considering average hourly variations of load. Int J Electr Power Energy Syst 66:25–40

Ganguly S, Samajpati D (2015) Distributed generation allocation on radial distribution networks under uncertainties of load and generation using genetic algorithm. IEEE Trans Sustain Energy 6(3):688–697

Gupta Y, Doolla S, Chatterjee K, Pal BC (2020) Optimal DG allocation and Volt-Var dispatch for a droop-based microgrid. IEEE Trans Smart Grid 12(1):169–181

Hassan AS, Sun Y, Wang Z (2020) Multi-objective for optimal placement and sizing DG units in reducing loss of power and enhancing voltage profile using BPSO-SLFA. Energy Rep 6:1581–1589

HassanzadehFard H, Jalilian A (2018) Optimal sizing and location of renewable energy based DG units in distribution systems considering load growth. Int J Electr Power Energy Syst 101:356–370

Hung DQ, Mithulananthan N, Bansal RC (2013) Analytical strategies for renewable distributed generation integration considering energy loss minimization. Appl Energy 105:75–85

Hung DQ, Mithulananthan N, Bansal RC (2014a) Integration of PV and BES units in commercial distribution systems considering energy loss and voltage stability. Appl Energy 113:1162–1170

Hung DQ, Mithulananthan N, Lee KY (2014b) Determining PV penetration for distribution systems with time-varying load models. IEEE Trans Power Syst 29(6):3048–3057

Kadir AFA, Mohamed A, Shareef H, Wanik MZC (2013) Optimal placement and sizing of distributed generations in distribution systems for minimizing losses and THD_v using evolutionary programming. Turk J Electr Eng Comput Sci 21(8):2269–2282

Khunkitti S, Boonluk P, Siritaratiwat A (2022) Optimal Location and Sizing of BESS for Performance Improvement of Distribution Systems with High DG Penetration. International Transactions on Electrical Energy Systems pp.1–16.

Kien LC, Bich Nga TT, Phan TM, Nguyen TT (2022) Coot optimization algorithm for optimal placement of photovoltaic

generators in distribution systems considering variation of load and solar radiation. Math Probl Eng. https://doi.org/10.1155/2022/2206570

Kumar M, Nallagownden P, Elamvazuthi I (2017a) Optimal placement and sizing of distributed generators for voltage-dependent load model in radial distribution system. Renew Energy Focus 19:23–37

Kumar M, Nallagownden P, Elamvazuthi I (2017b) Optimal placement and sizing of renewable distributed generations and capacitor banks into radial distribution systems. Energies 10(6):811

Lakum A, Mahajan V (2021) A novel approach for optimal placement and sizing of active power filters in radial distribution system with nonlinear distributed generation using adaptive grey wolf optimizer. Eng Sci Technol, Int J 24(4):911–924

Lee SH, Park JW (2013) Optimal placement and sizing of multiple DGs in a practical distribution system by considering power loss. IEEE Trans Ind Appl 49(5):2262–2270

Li S, Chen H, Wang M, Heidari AA, Mirjalili S (2020) Slime mould algorithm: a new method for stochastic optimization. Futur Gener Comput Syst 111:300–323

Mahmoud K, Yorino N, Ahmed A (2015) Optimal distributed generation allocation in distribution systems for loss minimization. IEEE Trans Power Syst 31(2):960–969

Mohandas N, Balamurugan R, Lakshminarasimman L (2015) Optimal location and sizing of real power DG units to improve the voltage stability in the distribution system using ABC algorithm united with chaos. Int J Electr Power Energy Syst 66:41–52

Mongird K, Viswanathan V, Balducci P, Alam J, Fotedar V, Koritarov V, Hadjerioua B (2020) An evaluation of energy storage cost and performance characteristics. Energies 13(13):3307

Nguyen TT, Pham TD, Kien LC, Van Dai L (2020) Improved coyote optimization algorithm for optimally installing solar photovoltaic distribution generation units in radial distribution power systems. Complexity 2020:1–34

Nguyen TT, Nguyen TT, Duong MQ (2022a) An improved equilibrium optimizer for optimal placement of photovoltaic systems in radial distribution power networks. Neural Comput Appl 34(8):6119–6148

Nguyen TT, Phan TM, Nguyen TT (2022b) Maximize the penetration level of photovoltaic systems and shunt capacitors in distribution systems for reducing active power loss and eliminating conventional power source. Sustain Energy Technol Assess 52:102253

Nguyen TT, Nguyen TT, Le B (2022c) Artificial ecosystem optimization for optimizing of position and operational power of battery energy storage system on the distribution network considering distributed generations. Expert Syst Appl 208:118127

NORVENTO nED100. Available online: https://www.norvento.com/en/new-ned100/

Oda ES, Abd El Hamed AM, Ali A, Elbaset AA, Abd El Sattar M, Ebeed M (2021) Stochastic optimal planning of distribution system considering integrated photovoltaic-based DG and DSTATCOM under uncertainties of loads and solar irradiance. IEEE Access 9:26541–26555

Ogunsina AA, Petinrin MO, Petinrin OO, Offornedo EN, Petinrin JO, Asaolu GO (2021) Optimal distributed generation location and sizing for loss minimization and voltage profile optimization using ant colony algorithm. SN Appl Sci 3(2):1–10

Pemmada S, Patne NR, Kumar A, Manchalwar AD (2021) Optimal planning of power distribution network by a novel modified jaya algorithm in multiobjective perspective. IEEE Syst J 16(3):4411–4422

Peng S, Gong X, Liu X, Lu X, Ai X (2021) Optimal locating and sizing of BESSs in distribution network based on multi-objective memetic salp swarm algorithm. Front Energy Res 9:1–12

Pham TD, Nguyen TT, Dinh BH (2021) Find optimal capacity and location of distributed generation units in radial distribution networks by using enhanced coyote optimization algorithm. Neural Comput Appl 33(9):4343–4371

Pierezan J, Coelho LDS (2018) Coyote optimization algorithm: a new metaheuristic for global optimization problems. In: 2018 IEEE congress on evolutionary computation (CEC) IEEE pp 1–8

Prakash R, Lokeshgupta B, Sivasubramani S (2018) Multi-objective bat algorithm for optimal placement and sizing of DG. In: 2018 20th National Power Systems Conference (NPSC) IEEE pp 1–6

Rueda-Medina AC, Franco JF, Rider MJ, Padilha-Feltrin A, Romero R (2013) A mixed-integer linear programming approach for optimal type, size and allocation of distributed generation in radial distribution systems. Electr Power Syst Res 97:133–143

SACE A (2008). Power factor correction and harmonic filtering in electrical plants. Tech Appl Pap pp 1–62

Sandhu KS (2018) Optimal location of WT based distributed generation in pool based electricity market using mixed integer nonlinear programming. Mater Today: Proc 5(1):445–457

Sanjay R, Jayabarathi T, Raghunathan T, Ramesh V, Mithulananthan N (2017) Optimal allocation of distributed generation using hybrid grey wolf optimizer. IEEE Access 5:14807–14818

Sgouras KI, Bouhouras AS, Gkaidatzis PA, Doukas DI, Labridis DP (2017) Impact of reverse power flow on the optimal distributed generation placement problem. IET Gener Transm Distrib 11(18):4626–4632

Teng JH, Chang CY (2007) Backward/forward sweep-based harmonic analysis method for distribution systems. IEEE Trans Power Deliv 22(3):1665–1672

Thang VV, Minh ND (2017) Optimal allocation and sizing of capacitors for distribution systems reinforcement based on minimum life cycle cost and considering uncertainties. Open Electr Electron Eng J 11(1):165–176

Viral R, Khatod DK (2015) An analytical approach for sizing and siting of DGs in balanced radial distribution networks for loss minimization. Int J Electr Power Energy Syst 67:191–201

Wong LA, Ramachandaramurthy VK, Walker SL, Taylor P, Sanjari MJ (2019) Optimal placement and sizing of battery energy storage system for losses reduction using whale optimization algorithm. J Energy Storage 26:100892

Zou K, Agalgaonkar AP, Muttaqi KM, Perera S (2011) Distribution system planning with incorporating DG reactive capability and system uncertainties. IEEE Trans Sustain Energy 3(1):112–123

Hindawi
International Transactions on Electrical Energy Systems
Volume 2022, Article ID 1446479, 21 pages
https://doi.org/10.1155/2022/1446479

Research Article

Optimal Placement of Photovoltaic Distributed Generation Units in Radial Unbalanced Distribution Systems Using MATLAB and OpenDSS-Based Cosimulation and a Proposed Metaheuristic Algorithm

Thai Dinh Pham,[1] **Thang Trung Nguyen**,[2] **and Le Chi Kien**[1]

[1]*Faculty of Electrical and Electronics Engineering, Ho Chi Minh City University of Technology and Education, Ho Chi Minh City, Vietnam*
[2]*Power System Optimization Research Group, Faculty of Electrical and Electronics Engineering, Ton Duc Thang University, Ho Chi Minh City, Vietnam*

Correspondence should be addressed to Thang Trung Nguyen; nguyentrungthang@tdtu.edu.vn

Received 8 July 2022; Revised 24 October 2022; Accepted 9 November 2022; Published 18 November 2022

Academic Editor: Santoshkumar Hampannavar

In this paper, an improved slime mould algorithm (ISMA) is proposed for finding the optimal location and sizing of photovoltaic distributed generation units (PVDGUs) in unbalanced distribution systems (UDSs). The proposed method is developed by changing the control variable update mechanism of the original slime mould algorithm (SMA). Total power losses on distribution lines and voltage deviation index of all buses are minimized under the consideration of various constraints. The location and sizing of PVDGUs found by ISMA are added into the cosimulation between MATLAB and OpenDSS for reaching other remaining parameters of UDSs. In addition, sunflower optimization (SFO), social-ski drive (SSD), cuckoo search algorithm (CSA), salp swarm algorithm (SSA), bonobo optimizer (BO), and SMA are also run for finding PVDGUs placement solution on the unbalanced three-phase IEEE 123-bus test feeder. As a result, the proposed ISMA can reduce the power loss up to 78.88% and cut the voltage deviation up to 1.4779 pu while that of others is from 69.10% to 78.87% and from 1.5759 to 1.4996 pu. Thus, ISMA should be used to place PVDGUs in UDSs meanwhile the cosimulation between MATLAB and OpenDSS should be applied as a power flow calculation tool for UDSs.

1. Introduction

1.1. Importance of DGUs in the Distribution System. In recent years, conventional power sources, including nuclear power plants, hydropower plants, and thermal power plants, brought terrible consequences to people and the Earth such as radiation exposure, floods, and global warming. So, the reduction of the use of these sources was implemented while renewable power sources with smaller capacity, which were known as distributed generation units (DGUs), were encouraged to be installed, especially in distribution systems.

The integration of DGUs in general and PVDGUs into distribution power networks is growing strongly with many benefits gained. Many studies have shown various benefits thanks to the integration of DGUs in the distribution system. Because of that, many countries have invested significantly in research to integrate DGUs into the electricity distribution systems to gain benefits like flexibility, reliability, environmental friendliness, economic benefits, etc [1]. Numerous studies have shown that selecting and connecting the suitable DGUs to the distribution system can achieve positive results such as reduced power losses, enhanced voltage profile, improved power quality, reduced fuel cost, and increased reliability and security of the system [2]. However, to maximize benefits, the determination of position and capacity for DGUs must be taken seriously [3].

Once the location and sizing of DGUs is predetermined incorrectly, it will cause many unwanted problems on the electrical system such as power losses, voltage sag, voltage flicker, and fault current [4]. Therefore, the determination of the optimal location and capacity of DGUs is necessary for maximizing both economic and technical benefits.

1.2. Related Work. Most studies have applied popular optimization algorithms such as genetic algorithm (GA) and particle swarm optimization algorithm (PSO) to find the location and capacity of DGUs before connecting them to the distribution system. The main purpose of this is to reduce power loss on branches and improve the voltage profile [5–9]. The authors in [5, 6] suggested GA and [7–9] applied PSO for determining the integration of DGUs with objective functions of improving voltage stability, reducing losses with the lowest investment cost. Through the application of technology-economic factors, the suitable solution of DGUs is found with the smallest generated cost. GA and PSO are fairly simple methods in operation and are popular in solving optimal problems. However, it is easily trapped in the local search space as well as the low convergence rate. In addition, another optimization tool is called the artificial bee colony (ABC) algorithm is also proposed for finding the suitable DGUs with a major role in enhancing voltage stability and decreasing losses [10, 11]. This method has a quite stable convergence and it is built based on the principle of operation of the bee colony in finding food sources. Due to going through all three phases such as employed bee, onlooker bee, and scout bee phases, the convergence speed of this method is relatively slow. Similarly, another effective method, biogeography-based optimization (BBO), is also applied in searching for the optimal installation of DGUs. BBO is created based on the study of the distribution of biological species in habitats. Reference [12] used BBO to solve the optimal problem for the connection of DGUs with considering the multiobjective function. The results showed that BBO has many advantages over compared methods. Recently, a new nature-inspired optimization method is introduced. This method is developed based on sunflower's motion and it is called the sunflower optimization algorithm (SFO) [13]. SFO is built on the natural phenomenon of the movement of sunflowers towards sunlight under consideration of pollination between adjacent sunflowers and this algorithm is stimulated by inverse square law radiation. The intensity of the radiation will depend on the distance between the sunflowers and the sun [14]. The effectiveness of the SFO method is clearly shown in [15]. The authors applied the SFO method for determining the suitable place and sizing of DGUs with the goal of decreasing power losses and increasing the voltage profile in the distribution systems. In addition, the salp swarm algorithm (SSA) is also receiving much attention recently. SSA is a metaheuristic optimization algorithm which is developed by the swarming behavior of salps in the oceans [16]. The authors in [17–19] used the SSA method for optimizing the installation of DGUs in the integrated systems. Thanks to the suitable integration of DGUs, total operating costs are minimized while power quality is significantly improved in the grid. Besides, a novel algorithm which is called social ski-driver (SSD) has been introduced. The characteristic of SSD is stochastic exploration like the roads where ski-drivers slip downhill. In this algorithm, there are four main parameters including the position of the agents, previous best position, mean global solution, and velocity of the agents. The number of parameters should be determined optimally in order to be most effective in finding the optimal solutions [20]. This method promises to be a powerful tool in solving the optimization problems. In addition, another optimization algorithm, which is named bonobo optimizer (BO), is recently published [21]. This algorithm is developed based on the social behavior and reproductive strategies of bonobos. The features of bonobos have been artificially modeled in mathematical formulas to solve optimization problems with high efficiency. Similarly, a new method for stochastic optimization is slime mould algorithm (SMA), is also introduced in [22]. SMA is inspired from the oscillation mode of slime mould in the nature. The properties of the slime mold have been constructed as a mathematical model with using adaptive weights to simulate the process of generating positive and negative feedback on a slime mold oscillation. This oscillation has been modeled to form an active method of searching and discovering food sources optimally [22, 23]. Several authors in [23] have also demonstrated the superior effectiveness of SMA through finding the optimal parameters for the solar photovoltaic system. The obtained results showed SMA is an efficient method with low data processing time in the solving optimization problems.

1.3. Proposals, Novelties and Contributions. In terms of choosing the test system, most previous studies have ignored the consideration in unbalanced distribution systems. Determining the location and capacity of DGUs in an unbalanced distribution system is more complex than a balanced distribution system due to their effects on power flow analysis [24, 25]. To further clarify this issue, the authors in [26] conducted experimental simulations on both balanced and unbalanced distribution systems with and without DGUs. The obtained results showed that the current magnitude and voltage magnitude varied according to load levels and DGU's penetration levels. Besides, the balanced and unbalanced distribution system's power flows may differ significantly. Therefore, the choice of the system for simulation and analysis is very important in connecting the device/machine into the power grid. Moreover, the authors [27] also analyzed the effects of connecting DGUs in a three-phase unbalanced secondary distribution system by using the novel sensitivity analysis (SA) method. The results have shown that a dramatic change in the integrated distribution system comes with tremendous economic and technical benefits. For the same problem with [27], the authors in [28] proposed the PSO as an optimization method and the cosimulation framework as a calculation and data processing tool. In that paper, the authors have also mentioned the superiority of using the OpenDSS analysis support tool [29] in improving calculation speed and enhancing accuracy.

Overall, the previous studies [30–32] mostly focused on the consideration of the multiobjective function. However, the effectiveness of the multiobjective function has not been clearly and accurately evaluated. The problem of trade-off in the multiobjective functions always happens and this can cause controversy in determining the best solution that meets all the stated criteria. Therefore, considering a single objective function will have more advantages in evaluation. In this paper, the single objective function is proposed to fairly evaluate the effectiveness of the proposed method and compared methods in determining the optimal location and sizing of DGUs, specifically photovoltaic distributed generation units (PVDGUs). As shown in [33], power losses depend greatly on factors such as the type of used conductors, transformers, and generators. in the distribution system. Hence, losses of the system can only be minimized by various techniques that cannot be completely removed and it is a leading factor in considering the economic and technical efficiency of the grid. Thus, total power loss minimization becomes one of the objective functions in this study. Besides, the enhancement of voltage stability is also paid much attention to a distribution system [34]. For solving this issue, the voltage improvement is considered as a single objective function in the network. In short, in this paper, the power loss reduction and the voltage improvement are proposed to be the two single objective functions under consideration of constraints such as voltage limits, current limits, and generated power limits of each PVDGU.

Generally, the optimization issues, especially the PVDGUs optimization, have been solved by the optimization methods. However, these methods are not effective and have low stability. Therefore, in this paper, an improved stochastic optimizer, called an improved slime mould algorithm (ISMA), is proposed to solve the optimization problem.

In summary, the main contributions in this paper can be listed as follows:

(1) Improved slime mould algorithm (ISMA) with the application of two proposed modifications is developed. The first modification is implemented to improve the effectiveness of the second formula of the new solution updating process; meanwhile the second modification abandons the old selection condition of SMA and applies a new condition based on a fitness function. Thanks to the simultaneous combination of the two modifications, ISMA is superior to SMA in terms of search speed and solution quality.

(2) Test system is recommended: Balanced distribution system and an unbalanced distribution system may have differences in voltage and current magnitudes. Therefore, to ensure the accuracy of power flow analysis, a complex unbalanced distribution system is proposed to be a test system, IEEE 123-bus test feeder.

(3) Cosimulation tool is suggested: conventionally, the three-phase power flow can be solved using the full rectangular coordinate and the Newton–Raphson method. However, the computational speed is relatively slow. In addition to the Newton–Raphson method, forward backward sweep method is also a popular power flow method for distribution systems. The same disadvantage of the two methods when solving unbalanced systems is to run power flow three times for three single phases. This advantage leads to the time-consuming manner for the two methods. On the contrary, the computing speed of OpenDSS is very fast. In fact, OpenDSS does not rebuild the Y matrix during iterations and it is run one time only for three unbalanced phases simultaneously. In addition, convergence and accuracy in the OpenDSS are also great. Thus, MATLAB and OpenDSS are combined as a cosimulation tool to solve the optimal problem for improving accuracy and data processing speed. This cosimulation promises to be the best cosimulation tool for solving power flow problem.

(4) Benefits of integrating the suitable PVDGUs into the distribution system are demonstrated: when PVDGUs are accordingly integrated into the system; it can help to reduce losses, improve voltage profile, enhance voltage stability, etc. Thus, the optimal location and capacity of the PVDGUs is proposed to maximize economic and technical benefits.

The structure in this paper is divided into 5 sections as follows: the objective functions and constraints are presented in problem formulation, Section 2. Next, two modifications in the second method and the condition for selecting the method in the equations of generating new solutions with simulation tools are introduced and analyzed in detail in the proposed method and simulation tools, Section 3. Then, the application of ISMA in finding suitable PVDGUs in an unbalanced distribution system is presented in the proposal of ISMA in optimizing the position and capacity of PVDGUs, Section 4. Besides, all obtained results and analysis as well as the expanded research fields are presented in simulation results, Section 5. Lastly, the summary and conclusions for the whole paper as well as exciting future works which continue this research are shown in the conclusions, Section 6.

2. Problem Formulation

In this study, the location and capacity of PVDGUs is considered to connect to an unbalanced distribution system optimally. Losses and voltage profile are the two main factors, which commonly used to evaluate the power quality as well as the economic benefits for a distribution system. Thus, minimizing losses and improving voltage with strict constraints have become the two main goals of this paper. These constraints are in place to ensure that the proposed solution meets the technical criteria in a distribution system.

2.1. Unbalanced Distribution Systems. For clarifying the characteristic of unbalanced distribution systems, a typical 123-bus system in Figure 1 is used for the analysis of loads, impedance, and voltage. The system is comprised of 123

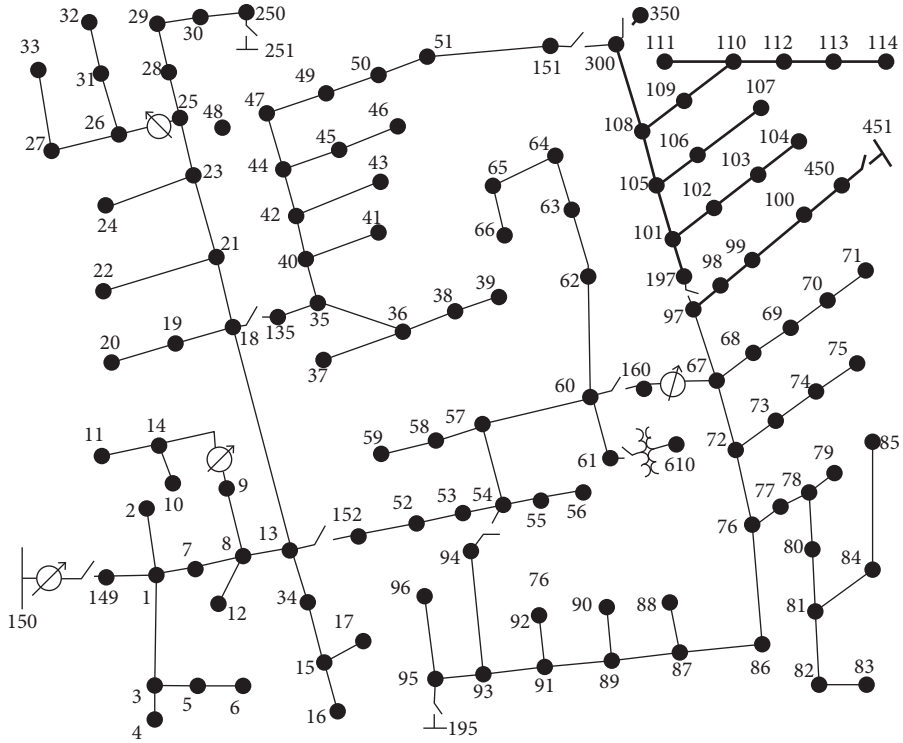

Figure 1: IEEE 123-bus test feeder.

buses, 124 lines, and 91 loads. Among the 91 loads, there are only 3 three-phase loads and 3 two-phase loads while the number of single-phase loads (N_{spl}) accounts for the highest rate with 85 loads. There are 2 balanced and 1 unbalanced three-phase loads among 3 three-phase loads and there are 2 unbalanced two-phase loads and 1 balanced two-phase loads among the 3 two-phase loads. The view on the number of loads indicates that there are three-phase, two-phase and one-phase distribution lines in the unbalanced system and the load of each phase at the same bus can be equal or totally different. The detail of the distribution lines and the loads at different buses can be clarified in the section.

Normally, a distribution line connecting Bus a and Bus b as shown in Figure 2 has three conductors with the same impedance and loads of phase A, phase B, and phase C at the receiving Bus b. The three series impedances are represented as Z_A^{ab}, Z_B^{ab} and Z_C^{ab} in which each impedance has two parts, resistance and reactance shown in equation (1). Similarly, the load of phases is represented as S_A^b, S_B^b, S_C^b at Bus b, and mathematically formulated in equation (2).

$$\begin{cases} Z_A^{ab} = R_A^{ab} + jX_A^{ab}, \\ Z_B^{ab} = R_B^{ab} + jX_B^{ab}, \\ Z_C^{ab} = R_C^{ab} + jX_C^{ab}, \end{cases} \tag{1}$$

$$\begin{cases} S_A^b = P_A^b + jQ_A^b, \\ S_B^b = P_B^b + jQ_B^b, \\ S_C^b = P_C^b + jQ_C^b. \end{cases} \tag{2}$$

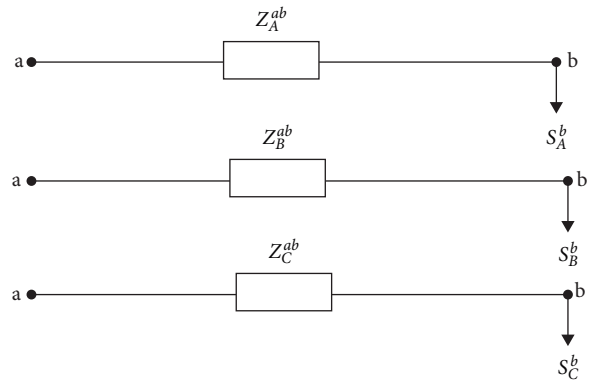

Figure 2: Three phases of a distribution line.

For unbalanced three-phase loads, there are some cases of the unbalanced power such as three unbalanced phases, and two balanced phases with one unbalanced phase. For the sake of easy understanding, the unbalanced three-phase loads at Bus b can be mathematically formulated as the following equation:

$$\begin{cases} S_A^b \neq S_B^b \neq S_C^b, \\ S_A^b = S_B^b \neq S_C^b, \\ S_B^b = S_C^b \neq S_A^b, \\ S_A^b = S_C^b \neq S_B^b. \end{cases} \tag{3}$$

In practical, the demands of three phases are not requested for some cases while one-phase loads and two-

phase loads need to be supplied. Consequently, the unbalanced distribution can be modeled in Figure 3.

As shown in Figure 3, Figure 3(a) shows a one-phase distribution line and Figure 3(b) shows a two-phase distribution line in which the one-phase distribution line supplies electricity to a single-phase load at phase A and the two-phase distribution line supplied electricity to two loads at phase A and phase B. The two figures can be mathematically formulated as follows:

$$\begin{cases} S_A^b \neq 0, \\ S_B^b = 0, \\ S_C^b = 0, \end{cases} \tag{4}$$

$$\begin{cases} S_A^b = S_B^b \neq 0, \\ \text{or } S_A^b \neq S_B^b \neq 0, \\ S_C^b = 0. \end{cases} \tag{5}$$

Equation (4) shows the case with load at phase A. So, the loads at phase B and phase C are zero. On the contrary, Equation (5) can present the characteristic of both the balanced two-phase loads and the unbalanced two-phase loads. Loads at phase A and phase B are the same for the case with balanced two-phase loads whilst the loads are different for the case with unbalanced two-phase loads. About the impedance, the distribution lines can be represented as the following formulas:

$$\begin{cases} Z_A^{ab} = R_A^{ab} + jX_A^{ab}, \\ Z_B^{ab} = \infty, \\ Z_C^{ab} = \infty, \end{cases} \quad \begin{cases} Z_A^{ab} = R_A^{ab} + jX_A^{ab}, \\ Z_B^{ab} = R_B^{ab} + jX_B^{ab}, \\ Z_A^{ab} = \infty. \end{cases} \tag{6}$$

In summary, the unbalanced distribution systems in practical are very complicated as shown in the figures and equations.

2.2. Objective Function. As mentioned, this paper focuses on two objective functions including total power loss (TPL) and voltage deviation index (VDI). The applied mathematical equations for describing those two objective functions are shown as follows.

2.2.1. Total Power Losses (TPL). Power loss reduction in a distribution system brings tremendous benefits economically and technically. Therefore, connecting appropriate PVDGUs will be a great idea for minimizing losses. The mathematical equation of total power losses (TPL) is shown as follows:

$$\text{Minimize TPL} = \sum_{f=1}^{N_f} P_{\text{Loss}}^f, \tag{7}$$

$$P_{\text{Loss}}^f = R_A^f \left(I_A^f\right)^2 + R_B^f \left(I_B^f\right)^2 + R_C^f \left(I_C^f\right)^2. \tag{8}$$

2.2.2. Voltage Deviation Index (VDI). Connecting proper PVDGUs can improve voltage quality and enhance power grid reliability. So, the voltage deviation index should be considered like a main goal and its mathematical equation is shown as follows:

$$\text{Minimize VDI} = \sum_{b=1}^{N^b} \left| V_{\text{Aver}}^b - 1 \right|. \tag{9}$$

In equation (9), V_{Aver}^b in pu is the average voltage of phases at the b^{th} bus. In the unbalanced distribution systems as explained in Section 2.1, some distribution lines have three phases but other ones may have one or two phases. So, the voltage of the end bus in the line should be the average value of the voltage of phases. For three cases with three phases, one phase, and two phases, the voltage average is calculated by the following equation:

$$\begin{aligned} V_{\text{Aver}}^b &= \frac{\left(V_A^b\right) + \left(V_B^b\right) + \left(V_C^b\right)}{3}, \\ V_{\text{Aver}}^b &= \left(V_{\text{phase1}}^b\right), \\ V_{\text{Aver}}^b &= \frac{\left(V_{\text{phase1}}^b\right) + \left(V_{\text{phase2}}^b\right)}{2}, \end{aligned} \tag{10}$$

where V_{phase1}^b and V_{phase2}^b are voltage of the first phase and the second phase at Bus b in which the first phase and the second phase are two different phases among phases A, B, and C of distribution systems.

2.3. Constraints

2.3.1. The Power Flow Balance Constraints. In this study, losses at a higher frequency are ignored due to a very tiny current flow. Therefore, losses mainly occur at the fundamental frequency. All components are calculated and considered with the same the fundamental frequency and the power flow balance constraint has the following form [12]:

$$\sum_{i=1}^{N_L} P_{\text{Load}}^i + \sum_{f=1}^{N_f} P_{\text{Loss}}^f - \sum_{k=1}^{N_{\text{DG}}} P_{\text{DG}}^k = P_{\text{Gr}}. \tag{11}$$

2.3.2. The Voltage Limits. According to IEC Std. 50160, the lower and upper bounds should be kept from 0.90 pu to 1.10 pu, respectively. However, narrowing the voltage limits is better in enhancing voltage quality for low and medium voltage distribution systems, and the best range for applying the voltage limits is suggested to be from 0.95 pu to 1.05 pu [12]. Consequently, the lower bound and upper bound of voltage, which are represented by $V_{\min}$ and $V_{\max}$, are selected to be 0.95 and 1.05 pu in the study. As suggested in [35, 36], the voltage of buses should be constrained by the following equation:

$$V_{\min} \leq V^b \leq V_{\max}, \quad b = 1, \ldots, N^b. \tag{12}$$

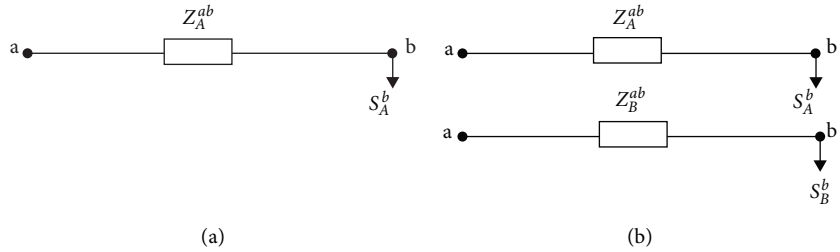

Figure 3: Distribution lines with less than three phases.

However, it should be noted that in the unbalanced distribution system, an example bus can have three values for voltage because of the presence of unbalanced loads. Hence, the constraint is modified as follows:

$$\begin{aligned} V_{\min} &\le V_{\min}^b, \quad b = 1, \ldots, N^b, \\ V_{\max} &\ge V_{\max}^b, \quad b = 1, \ldots, N^b. \end{aligned} \tag{13}$$

Here $V_{\min}^b$ and $V_{\max}^b$ are determined by the following equation:

$$\begin{aligned} V_{\min}^b &= \min\left(V_A^b, V_B^b, V_C^b\right), \quad b = 1, \ldots, N^b, \\ V_{\max}^b &= \max\left(V_A^b, V_B^b, V_C^b\right), \quad b = 1, \ldots, N^b. \end{aligned} \tag{14}$$

2.3.3. Generation Limits of Photovoltaic Distributed Generation Units. The total capacity of proposed PVDGUs should not exceed the total load demand and the capacity limit of each PVDGU is constrained as follows [28]:

$$\begin{aligned} P_{\mathrm{DG}}^{\min} &\le P_{\mathrm{DG}}^k \le P_{\mathrm{DG}}^{\max}, \\ \sum_{k=1}^{N_{\mathrm{DG}}} P_{\mathrm{DG}}^k &\le 80\% \times \sum_{i=1}^{N_L} P_{\mathrm{Load}}^i. \end{aligned} \tag{15}$$

2.3.4. The Branch Current Limits. The thermal capacity must not exceed the allowable limit of each conductor. Thus, the current limit is defined in the following model [9]:

$$\begin{aligned} \left|I^f\right| &\le I_{\mathrm{rated}}^f, \\ I^f &= \max\left(I_A^f, I_B^f, I_C^f\right), \quad f = 1, \ldots, N_f. \end{aligned} \tag{16}$$

Solving the power flow problem is one of the important steps in the process of optimizing location and size of PVDGUs in unbalance distribution networks. To evaluate the fitness function of each solution, the power flow solutions need to be evaluated to obtain parameters such as the branches' power loss, the buses' voltage, and the branches' current magnitude.

3. The Proposed Method

In 2020, Li et al. developed Slime mold algorithm (SMA) and showed its outstanding performance over many previous metaheuristic algorithms [22]. SMA reached results as expected for a set of complicated benchmark functions such as global optimums, stability, and convergence speed. However, these functions are not difficult enough because they were not comprised of complicated constraints and different search spaces for different control variables. Thus, SMA still has big limitations for such complicated problems and the placement of DGUs in unbalance distribution systems is one example. In the section, the existing shortcomings of SMA are analyzed and then modified to form an improved version, called the improved slime mold algorithm (ISMA). To implement ISMA for the problem, it should be simulated by using OpenDSS and MATLAB software. So, the connection between OpenDSS and MATLAB is also expressed in the section.

3.1. Conventional Slime Mould Algorithm. Slime mould algorithm (SMA) has been developed recently and proved to be more effective than a huge number of popular and famous metaheuristic algorithms [22]. Each particle in the population of SMA is represented as a solution Sol_m where m is from 1 to N_{ps}. Sol_m in the population is within the lower bound solution (LB) and upper bound solution (UB), and randomized as follows:

$$\mathrm{Sol}_m \in [\mathrm{LB}, \mathrm{UB}], \tag{17}$$

$$\mathrm{Sol}_m = [\mathrm{LB} + \mathrm{rdn}\,(\mathrm{UB} - \mathrm{LB})]. \tag{18}$$

SMA has one solution update technique and it updates the solution once for each iteration based on the following equation:

$$\mathrm{Sol}_m^{\mathrm{new}} = \begin{cases} \mathrm{Sol}_{sf\,\mathrm{best}} + V_A \times \left(\mathrm{Weight} \times \mathrm{Sol}_{r\,d1} - \mathrm{Sol}_{r\,d2}\right), & \text{if } \mathrm{rdn} < \mathrm{CD}, \\ V_B \times \mathrm{Sol}_m, & \text{else.} \end{cases} \tag{19}$$

In the formula, Sol_{rd1} and Sol_{rd2} are the two randomly selected solutions in the current population. V_A, V_B, and Weight are vectors with the same dimension as each solution m. V_A, V_B, and Weight are formulated as follows [22]:

$$V_A = (-A, A), \tag{20}$$

$$V_B = (-B, B), \tag{21}$$

$$\text{Weight} = \begin{cases} rd_1 \times \log\left(1 + \dfrac{Ft_{\text{best}} - Ft_m}{Ft_{\text{best}} - Ft_{\text{worst}}}\right) + 1, & \text{Condition}, \\ rd_2 \times \log\left(1 + \dfrac{Ft_{\text{best}} - Ft_m}{Ft_{\text{best}} - Ft_{\text{worst}}}\right) + 1, & \text{Other}, \end{cases} \tag{22}$$

$$A = \text{arctanh}\left(1 - \frac{C_{\text{Iter}}}{M_{\text{Iter}}}\right), \tag{23}$$

$$B = 1 - \frac{C_{\text{Iter}}}{M_{\text{Iter}}}. \tag{24}$$

In the computational formula of Weight, the Condition indicates that Ft_m represents the ranking of the first half of the population. rd_1 and rd_2 are vectors with the same dimension as solution m in which rd_1 and rd_2 denote the random numbers in the interval of [0, 1] and [−1, 0], respectively.

In addition, CD in equation (19) is obtained by the following equation:

$$\text{CD} = \tanh\left|Ft_m - Ft_{\text{best}}\right|. \tag{25}$$

After producing new solution $\text{Sol}_m^{\text{new}}$ by using (19), the new solution is verified and fixed by using the following equation:

$$\text{Sol}_m^{\text{new}} = \begin{cases} \text{LB}, & \text{if } \text{Sol}_m^{\text{new}} < \text{LB}, \\ \text{UB}, & \text{if } \text{Sol}_m^{\text{new}} > \text{UB}, \\ \text{Sol}_m^{\text{new}}, & \text{else}. \end{cases} \quad C\ D = \tanh\left|Ft_m - Ft_{\text{best}}\right|, \tag{26}$$

Fitness function of the m new solution is calculated and represented by Ft_m^{new}. Among Ft_m^{new} values (where $m = 1, \ldots, N_{ps}$), the lowest fitness value is set to Ft_{best} and the highest fitness value is set to Ft_{worst}. Then, the selection technique is implemented to retain better solutions and abandon worse solutions. The process of selection is done by the following model:

$$\text{Sol}_m = \begin{cases} \text{Sol}_m, & \text{if } Ft_m^{\text{new}} > Ft_m, \\ \text{Sol}_m^{\text{new}}, & \text{if } Ft_m^{\text{new}} \le Ft_m, \end{cases} \tag{27}$$

$$Ft_m = \begin{cases} Ft_m, & \text{if } Ft_m^{\text{new}} > Ft_m, \\ Ft_m^{\text{new}}, & \text{if } Ft_m^{\text{new}} \le Ft_m. \end{cases} \tag{28}$$

In the last step, the so-fart best fitness is determined by using the lowest fitness value of Ft_m ($m = 1, \ldots, N_{ps}$) and the so-fart best solution $\text{Sol}_{sf\text{best}}$ is obtained accordingly.

In summary, the application of the applied SMA can be described in the following steps.

Step 1: Select values for N_{ps} and M_{Iter}

Step 2: Employ (18) to get the initial population

Step 3: Calculate fitness function Ft_m

Step 4: Determine Ft_{best} and Ft_{worst}, Set $C_{\text{Iter}} = 1$

Step 5: Employ (23) and (24) to obtained A and B

Step 6: Randomly produce V_A and V_B satisfying (20) and (21)

Step 7: Employ (22) to obtain Weight

Step 8: Employ (25) to calculate CD

Step 9: Employ (19) to generate new solution $\text{Sol}_m^{\text{new}}$

Step 10: Use (26) to verify and fix $\text{Sol}_m^{\text{new}}$

Step 11: Calculate Ft_m^{new} and determine Ft_{best} and Ft_{worst} from Ft_m^{new}

Step 12: Use (27) and (28) to get Sol_{m} and Ft_m

Step 13: Select the lowest fitness value from Ft_m and determine $\text{Sol}_{sf\text{best}}$

Step 14: if C_{Iter} and M_{Iter} are equal, stop implementing SMA and reporting results. Otherwise, set C_{Iter} to $C_{\text{Iter}} + 1$ and back to Step 5.

3.1.1. Improved Slime Mould Algorithm. As shown in equation (19), SMA uses two different ways for producing new solutions. The formula of the equation is called the first method and the following one is named the second method. The advantages and disadvantages of the two methods are analyzed as follows:

(1) The first method searches around the so-far best solution with a distance by using $V_A \times (\text{Weight} \times \text{Sol}_{r\ d1} - \text{Sol}_{r\ d2})$. The first method is the effective creation of SMA through applying the fitness function (i.e., Weight factor in equation (19)) and the

creation supported SMA to have a better search method than other metaheuristic algorithms.

(2) The second method modifies the old solutions by using vector V_B and the second method using $(V_B \times \mathrm{Sol}_m)$ for updating the new solution $\mathrm{Sol}_m^{\mathrm{new}}$ is not a potential search strategy. In fact, V_B is a randomly produced vector within $-B$ and B as shown in equation (21) while B has a range from 0 (for the case $C_{\mathrm{Iter}} = M_{\mathrm{Iter}}$) to 1 ($C_{\mathrm{Iter}} = 1$) for the case as shown in equation (24). From equations (21) and (24), V_B is a vector with terms from −1 to 1. As a result, $(V_B \times \mathrm{Sol}_m)$ can be from $(-\mathrm{Sol}_m)$ to (Sol_m) and the new solution $\mathrm{Sol}_m^{\mathrm{new}}$ is equal to from $(-\mathrm{Sol}_m)$ to (Sol_m). Clearly, if $\mathrm{Sol}_m^{\mathrm{new}}$ is around Sol_m, it may be a potential new solution. But for the case that $\mathrm{Sol}_m^{\mathrm{new}}$ is close to 0 or close to $(-\mathrm{Sol}_m)$, the new solution is certainly low quality solution. Furthermore, the new solution $\mathrm{Sol}_m^{\mathrm{new}}$ is always smaller than the old one Sol_m and there are not any demonstrations that promising solutions have to be smaller than the old one. The noted issue in the second method is that B is approaching 0 when the current iteration is approaching the maximum iteration (i.e., $C_{\mathrm{Iter}} \longrightarrow M_{\mathrm{Iter}} => B \longrightarrow 0$) and V_B is also approaching 0 as a result. Thus, the new solution $\mathrm{Sol}_m^{\mathrm{new}}$ will become a Zero solution with 0 value for all control variables. In [22], benchmark functions were solved for reaching the minimum value and the global solutions for approximately all functions are Zero solution. The global solutions and the produced solution by the second method are unintentionally the same and SMA becomes a very strong method.

In this paper, control variables have a large range and the global optimum is certainly not the zero solution. This fact indicates the second method using $(V_B \times \mathrm{Sol}_m)$ to update new solutions is ineffective and it should be replaced with another method. In this section, a proposed method is developed to replace the second method in equation (19) and it is presented as follows:

$$\mathrm{Sol}_m^{\mathrm{new}} = \mathrm{Sol}_m + V_A \times (\mathrm{Weight} \times \mathrm{Sol}_{r\,d1} - \mathrm{Sol}_{r\,d2}) + \mathrm{rdn} \times (\mathrm{Sol}_{r\,d3} - \mathrm{Sol}_{r\,d4}). \tag{29}$$

Equation (29) is the first modification of the proposed ISMA. Currently, ISMA has two different methods for producing new solutions $\mathrm{Sol}_m^{\mathrm{new}}$ in which the first method is taken from the conventional SMA and the second method is taken from the first modification. However, the condition for using either the first method or the second method should not be taken from SMA. As shown in equation (19), the condition is rdn < CD where CD is calculated by using equation (25), which is $\mathrm{CD} = \tanh|Ft_m - Ft_{\mathrm{best}}|$. For the sake of simplicity, the result of $(Ft_m - Ft_{\mathrm{best}})$ is represented by x and the result of (rdn < CD) is represented by y. As showing the values of x, CD, and y, x is set the range of [0, 5] for a better view of the three factors. It is noted that $x = (Ft_m - Ft_{\mathrm{best}})$ can be much higher than 5; however, we limit the maximum value at 5 only because CD at $x = 5$ is approximately equal to 1 and CD is still one if $x > 5$ is set. On the contrary to x and CD, the values of y is either 0 (for rdn < CD) or 1 (for rdn ≥ CD). After producing the matrix with random values rdn, y is obtained by comparing rdn and CD. As a result, Figure 4 is plotted to show the values of x, CD, and y.

Observing Figure 4 seen that most values of y are 1 and few values are 0. For a better view of the influence of $x = (Ft_m - Ft_{\mathrm{best}})$ on y, x is selected to be from 5 to 1000 and Figure 5 is plotted. It is seen that y is equal to 1 for all values of x. Hence, it concludes that y is equal to 1 for approximately all values of x, and the first method in equation (19) is used for approximately all solutions over the search process with M_{Iter} iterations whereas the second method is hardly ever used. In the second modification, we propose to change the condition of using the comparison between rdn and CD by using a measured condition. The first method is to search around the best solution, so it should be applied for the old solutions with low quality. The second method is to exploit around the current old solutions, so the around searched solutions should be promising solutions and the search space around the solutions are possible to be the presence of higher quality. So the condition for selecting the first or the second method is as follows:

$$Ft_m > Ft_{\mathrm{mean}}, \tag{30}$$

where Ft_{mean} is the mean of fitness values of the whole population.

As a result, the technique for producing the new solutions of ISMA is summarized as follows:

$$\mathrm{Sol}_m^{\mathrm{new}} = \begin{cases} \mathrm{Sol}_{sf\,\mathrm{best}} + V_A \times (\mathrm{Weight} \times \mathrm{Sol}_{r\,d1} - \mathrm{Sol}_{r\,d2}), & \text{if } Ft_m > Ft_{\mathrm{mean}}, \\ \mathrm{Sol}_m + V_A \times (\mathrm{Weight} \times \mathrm{Sol}_{r\,d1} - \mathrm{Sol}_{r\,d2}) + \mathrm{rdn} \times (\mathrm{Sol}_{r\,d3} - \mathrm{Sol}_{r\,d4}), & \text{else.} \end{cases} \tag{31}$$

Generally, the first method in equation (31) just makes a jump for finding new solutions around the best solution ($\mathrm{Sol}_{sf\,\mathrm{best}}$). However, when the quality classification condition of solutions is fulfilled ($Ft_m \leq Ft_{\mathrm{mean}}$), then the second method is applied. This second method contains $(\mathrm{rdn} \times (\mathrm{Sol}_{r\,d3} - \mathrm{Sol}_{r\,d4}))$ to produce one more jumping step. So, two generated jumps in the second method are to search for new solutions far from current good quality solutions (Sol_m). This facilitates the minimization of falling into the local optimal region and opens opportunities to

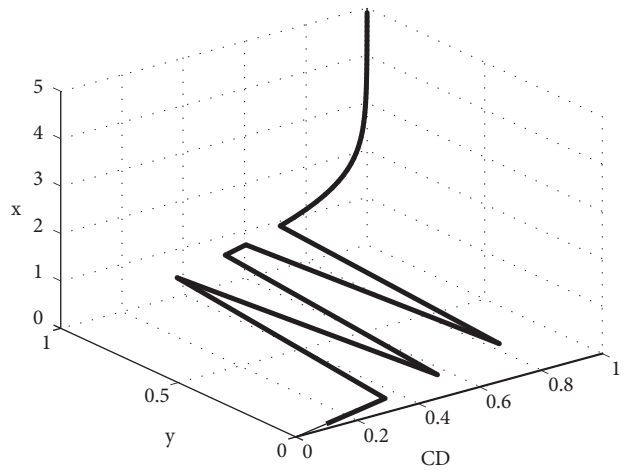

Figure 4: The survey for values of x CD and y with $x = 0 \div 5$.

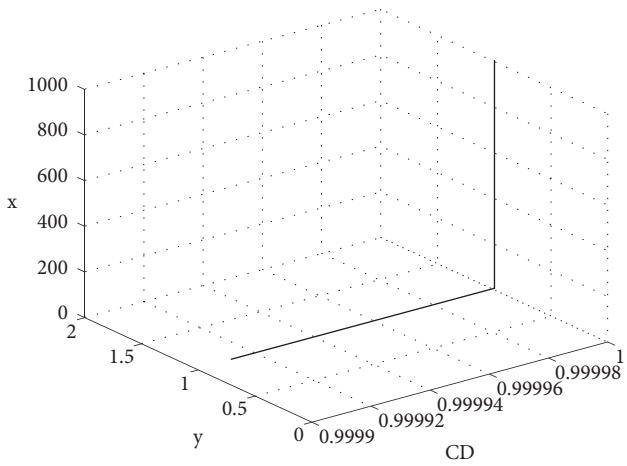

Figure 5: The survey for values of x CD and y with $x = 5 \div 1000$.

discover new solutions in the larger possible search area. In summary, in order to strike a balance between exploiting new solutions around the best solution and finding new solutions in the feasible search space, Equation (31) should be applied under the selection condition for using the first method or the second method. This combination with reasonably selected condition promises to create the great opportunities in searching the better potential solutions than the original method.

3.2. OpenDSS Software and Cosimulation between OpenDSS and MATLAB

3.2.1. OpenDSS Software. OpenDSS is the distribution system simulator (DSS), which is an open source version used to support the calculation and simulation for distribution systems in the frequency domain. This is developed by the Electric Power Research Institute (EPRI) to address the gaps of other distribution system analysis tools. Besides, it is built to create a flexible and reliable research platform that aims to serve distribution system analysis applications, especially the distribution system with the integration of distributed generation sources as a synchronous generator, photovoltaic/wind turbine generator, capacitor, etc. The general structure of this software can be briefly presented as shown in Figure 6 [37].

For this OpenDSS's structure, it allows for importing user-written code into the software. The environment in OpenDSS contains script files for circuit definition with the transformer specification, line data, load data, etc. These script files are appropriately defined by the user. Besides, OpenDSS is developed to allow interaction with other popular software such as MATLAB, PYTHON, VBA, C+, and C#. This interaction is considered as coordinated simulation and this is implemented through the windows component objective model (COM). In other words, OpenDSS allows script development or modification from other software to control the OpenDSS model via this COM server.

3.2.2. Cosimulation between OpenDSS and MATLAB. OpenDSSS can be driven by other software via the COM server as mentioned above. In this study, OpenDSS has interacted with MATLAB for coordinate simulation to perform the analysis of PVDGU impacts in the distribution system. The coordination process between OpenDSS and MATLAB is briefly summarized as Figure 7 [38].

In this study, a hybrid interface is built for necessary data transmission between two software by using the COM server. OpenDSS is limited in solving the problem that involves changing the control variable. Therefore, in this work, OpenDSS needs to coordinate with MATLAB to solve the considered problem in the distribution system. OpenDSS is a powerful tool for calculating the power flow in large distributed systems with fairly fast simulation times and using MATLAB to control the operations of OpenDSS is a great hybrid interface. For this particular case, the grid data is described in the OpenDSS. The power flow is calculated and the obtained results are sent out by OpenDSS. The required values are transferred to the MATLAB through the COM server. Besides, the written optimization algorithm in MATLAB is responsible for computing and proposing the suitable solution in distributed resource integration into the considered grid. This proposed solution is transferred to OpenDSS via the COM server for recalculating the power flow. This process is implemented at each cycle until the loop requirement is satisfied.

4. The Implementation of the Applied Method for the Problem

4.1. Improved Slime Mould Algorithm. In this paper, the implemented methods are in charge of finding the most suitable location and the best generation for installed photovoltaic systems. Hence, each solution m among the set of solutions contains the two main factors, which are represented by $L^k_{DG\,m}$ and $P^k_{DG\,m}$ (where $k = 1, \ldots, N_{\mathrm{DG}}$ and $m = 1, \ldots, N_{ps}$). The solution m Sol_m is formulated mathematically and randomly produced as follows:

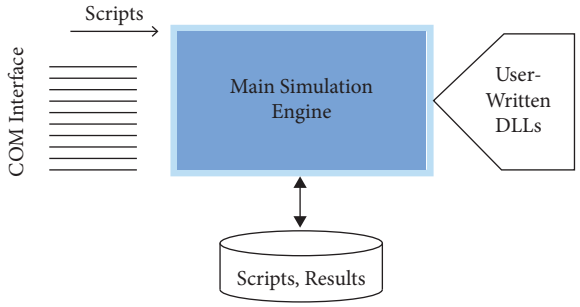

Figure 6: Distribution system simulator structure.

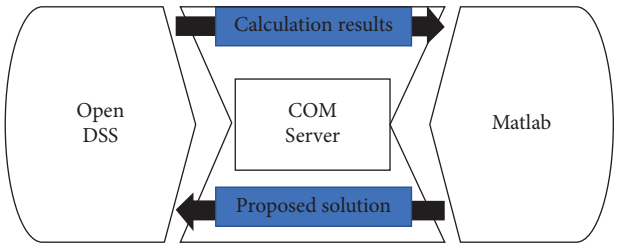

Figure 7: The base principle of cosimulation between OpenDSS and MATLAB.

$$\mathrm{Sol}_m = \left[L^k_{DG\,m}, P^k_{DG\,m}\right]; \quad k = 1, \ldots, N_{\mathrm{DG}}, \tag{32}$$

$$\mathrm{Sol}_m = \mathrm{LB} + \mathrm{rdn}\,(\mathrm{UB} - \mathrm{LB}), \tag{33}$$

where LB and UB are the minimum solution and maximum solution containing the minimum values and maximum values of the location and power generation of distribution systems. The two solutions should be defined before implementing the search process of the applied methods as the two following formulas:

$$\begin{aligned} \mathrm{LB} &= \left[L^{\min}_{\mathrm{DG}}, P^{\min}_{\mathrm{DG}}\right], \\ \mathrm{UB} &= \left[L^{\max}_{\mathrm{DG}}, P^{\max}_{\mathrm{DG}}\right]. \end{aligned} \tag{34}$$

As shown in the boundary solution, $L^{\min}_{\mathrm{DG}}$ and $L^{\max}_{\mathrm{DG}}$ are the minimum location and maximum location in the unbalanced distribution system corresponding to Bus 2 and Bus N^b. $P^{\min}_{\mathrm{DG}}$ and $P^{\max}_{\mathrm{DG}}$ are the minimum rated power and maximum rated power of each installed PVDGU. Besides, the dependent variables of the problem are comprised of I^f_A, I^f_B, and I^f_C, and V^b_A, V^b_B, and V^b_C which are the results from running OpenDSS software.

4.2. OpenDSS for Solving the Power Flow of Unbalanced Distribution System. This simulation tool is designed to simulate most analysis types of the distribution planning. It is capable of quickly and accurately solving problems related to power system analysis such as power flow, dynamic, harmonics, and short circuit calculations. The application of DSS to solve the problem of power flow analysis can be summarized briefly based on the process of building and calculating the matrix for the elements in the electrical system as Figure 8 [37].

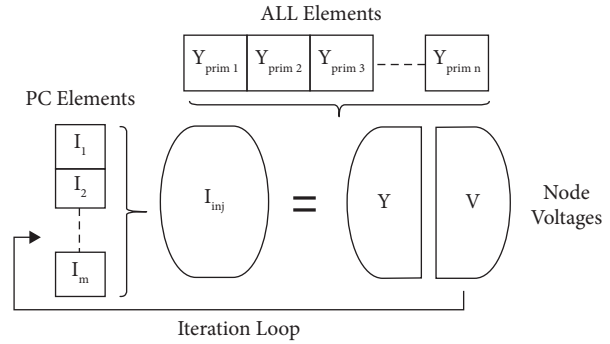

Figure 8: Proposed power flow analysis in OpenDSS.

With the initial bus data and line data from the power distribution system, a base matrix Y (or $1/Z$) is created for each element. After each element's matrix is built, the overall system admittance matrix (Y) is generated by aggregating all the matrices of the element and solving them through a sparse matrix solver. The relationship between the phase angle and voltage magnitude is appropriately established after all power delivery elements are maintained interconnection to the considered power system. Power conversion elements inject current and these currents are added appropriately to their place in the vector matrix (I_{inj}). The bus voltage and the feeder current vectors for each phase in the distribution system can be presented as follows:

$$\begin{aligned} V^b &= \begin{bmatrix} V^b_A \\ V^b_B \\ V^b_C \end{bmatrix} = \begin{bmatrix} V^{b,re}_A \\ V^{b,re}_B \\ V^{b,re}_C \end{bmatrix} + j \begin{bmatrix} V^{b,im}_A \\ V^{b,im}_B \\ V^{b,im}_C \end{bmatrix}, \\ I^f &= \begin{bmatrix} I^f_A \\ I^f_B \\ I^f_C \end{bmatrix} = \begin{bmatrix} I^{f,re}_A \\ I^{f,re}_B \\ I^{f,re}_C \end{bmatrix} + j \begin{bmatrix} I^{f,im}_A \\ I^{f,im}_B \\ I^{f,im}_C \end{bmatrix}. \end{aligned} \tag{35}$$

Subsequently, the sparse matrix will be solved to find out the phase angle and amplitude values of all voltages at each phase in the system. The voltage value at each bus is converged to the most accurate value through each iteration and stops this if the tolerance is satisfied. This convergence is processed quite quickly because the Y-matrix system is built only once in the early stage and it is not rebuilt during processing. This has contributed to reduce the processing time in the power flow analysis [38]. Besides, many researchers have also analyzed and mentioned the great accuracy of OpenDSS in solving problems in distributed systems [39]. Thereby, OpenDSS is really the best tool in solving power flow problems.

4.3. Fitness Function. The fitness function of each solution m is represented by FF_m and it is used to measure the effectiveness of the determined location and rated power of PVDGUs installed in the unbalanced systems. Before calculating the fitness value, objective function and penalty terms must be obtained. The study considers two single

objectives, including total power loss and voltage deviation index, which are obtained by employing equations (7) and (9), respectively. On the other hand, penalty terms can be calculated by comparing dependent variables and their limits as follows:

$$I^f = \begin{cases} 0, & \text{if } I^f \le I^f_{\text{rated}}, \\ \left(I^f - I^f_{\text{rated}}\right)^2, & \text{if } I^f > I^f_{\text{rated}}, \end{cases} \tag{36}$$

$$V^b = \begin{cases} 0, & \text{if } V_{\min} \le V^b_{\min} \text{ and } V^b_{\max} \le V_{\max}, \\ \left(V_{\min} - V^b_{\min}\right)^2, & \text{if } V_{\min} > V^b_{\min} \text{ and } V^b_{\max} \le V_{\max}, \\ \left(V_{\max} - V^b_{\max}\right)^2, & \text{if } V_{\min} \le V^b_{\min} \text{ and } V^b_{\max} > V_{\max}, \end{cases} \tag{37}$$

where ΔI^f and ΔV^b are the penalty terms for the violation of current in the f^{th} feeder and the violation of voltage at Bus b.

Finally, fitness functions for reduction of total power loss and reduction of voltage deviation index are, respectively, determined by the following equation:

$$FF_m = \text{TPL}_m + \sum_{b=1}^{N^b} \left(\Delta V^b\right) + \sum_{f=1}^{N^f} \left(\Delta I^f\right), \tag{38}$$

$$FF_m = \text{VDI}_m + \sum_{b=1}^{N^b} \left(\Delta V^b\right) + \sum_{f=1}^{N^f} \left(\Delta I^f\right), \tag{39}$$

where TPL_m and VDI_m are the total power loss and voltage deviation index of the m^{th} solution, respectively.

4.4. Correction of Control Variables. The proposed method generates new solutions where each new solution is comprised of the location and capacity of each PVDGU. To ensure that the new solution is always within the search limits, the position and capacity of each PVDGU is checked and modified appropriately by applying two equations as follows:

$$L^k_{DG\,m} = \begin{cases} N_b, & \text{if } L^k_{DG\,m} > N^b, \\ 2, & \text{if } L^k_{DG\,m} < 2, \\ L^k_{DG\,m}, & \text{else}, \end{cases} \tag{40}$$

$$P^k_{DG\,m} = \begin{cases} P^{\max}, & \text{if } P^k_{DG\,m} > P^{\max}, \\ P^{\min}, & \text{if } P^k_{DG\,m} < P^{\min}, \\ P^k_{DG\,m}, & \text{else}. \end{cases} \tag{41}$$

4.5. Termination Condition for Iterative Algorithm. To ensure objective comparability between the proposed method and other methods, 50 trial runs are implemented for all methods. The best solution in each trial run is saved for comparing and evaluating the effectiveness of each method. In each trial run, the maximum number of iterations is considered and appropriately selected to ensure the execution methods have converged completely.

4.6. The Cosimulation between OpenDSS and MATLAB. The implemented cosimulation between OpenDSS and MATLAB for determining the optimal position and capacity of PVDGUs in an unbalanced distribution system is briefly presented by the flowchart as Figure 9.

This implementation is carried out in two different environments. In the OpenDSS, a program is written by the user for describing the entire distribution system. It includes main circuit script and element scripts such as line modeling, load modeling, and transformer modeling. OpenDSS will be run from the main circuit script for data processing and computation to solve the power flow problem. The results obtained from this calculation (phase angle, voltage magnitude, power losses on each branch, etc) will be transferred to MATLAB via COM server for processing as MATLAB input data. MATLAB will conduct analysis and generate the possible solutions of location and sizing of PVDGUs in the search area. Proposed solutions will be sent back to OpenDSS for integrating and processing additional data as OpenDSS input data at the first iteration. The received solution will be properly added to the system's script and the power flow is resolved by using a power flow solver in OpenDSS with the integration of PVDGUs in the distribution system. Obtained results as OpenDSS output data will be transmitted through the COM server to MATLAB to process, calculate and evaluate solution quality. The optimization algorithm that is written in MATLAB will rely on the quality evaluation of existing solutions to suggest better solutions. These new solutions will also be passed over to OpenDSS to handle data at the next iteration. This process is repeated until the optimization algorithm's criterion is satisfied, i.e., the current iteration is equal to the maximum iteration. After each loop is finished, the next solution with better quality than the previous one will be updated as the best current solution and convergence will occur. As a result, the most suitable solution for the position and capacity of PVDGUs in the distribution system will be found.

5. Simulation Results

In this paper, the proposed method (ISMA) and six other methods (SFO, SSD, CSA, SSA, BO, and SMA) are implemented for finding the optimal location and capacity of three PVDGUs in IEEE 123-bus test feeder as Figure 1. The used data of the system is taken from IEEE PES [40]. For an accurate and objective evaluation, all methods are simulated in 50 trial runs with randomly generated initial solutions. MATLAB and OpenDSS are two used software and this simulation is done on a personal computer with a 4.0 GB RAM, 1.80 GHz CPU, and Intel Core i5. For all implemented methods, the main parameters have been surveyed and selected appropriately to have a fair assessment from the obtained simulation results. The total created generation numbers at each loop are surveyed from 20 to 40 with a step size of 5 and the suitable result is 30. Besides, the total

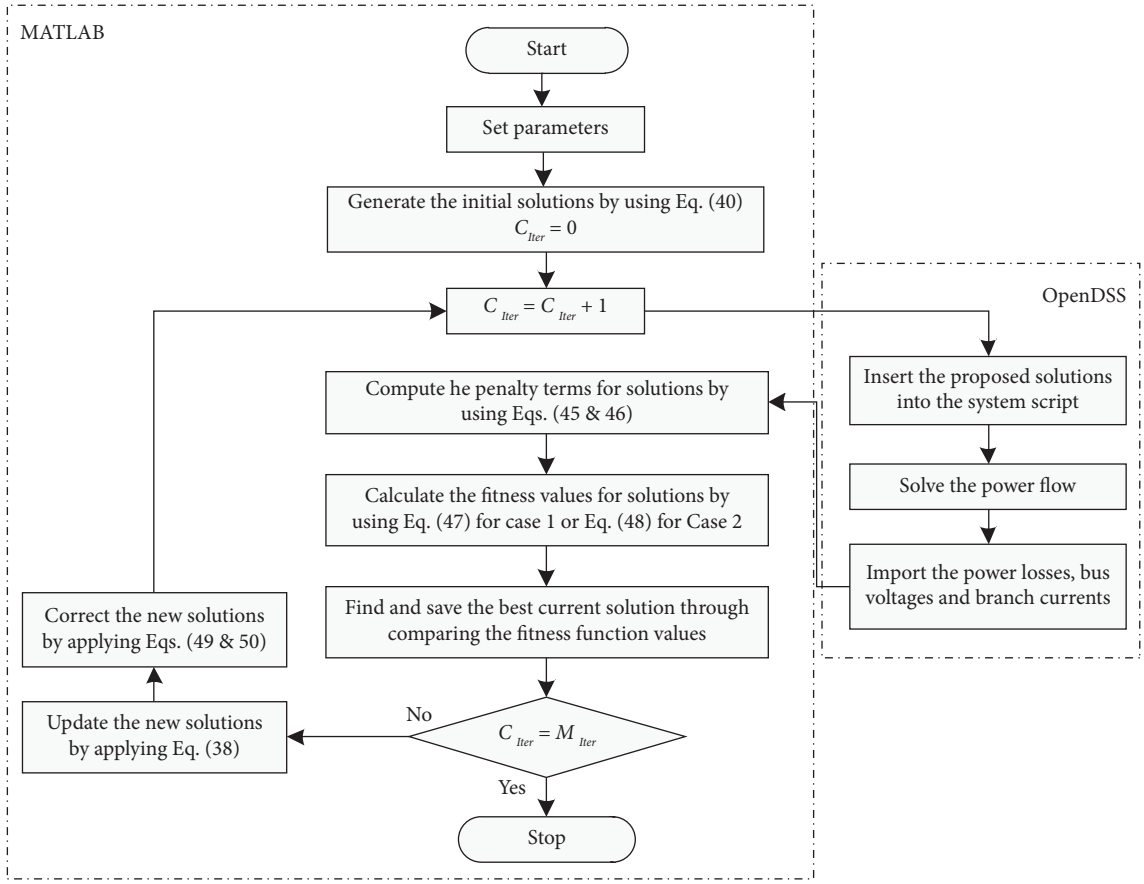

Figure 9: The detailed cosimulation between OpenDSS and MATLAB.

iteration numbers are also chosen enough to guarantee the complete convergence of algorithms with 200 loops. Other remaining parameters of SFO and SSA, SSD, CSA, and BO are taken from [20, 21, 41, 42], respectively. Moreover, for building the unbalanced distribution systems, the model of circuit elements in OpenDSS has been described in detail in [37]. As mentioned, OpenDSS is applied as software to solve the power flow problem in the unbalanced system. This software is interacted with MATLAB software through the Component Object Model server Dynamic-link library for cosimulation [43, 44]. In addition, two single objective functions are considered independently, including of minimizing the total power losses on transmission lines and improving the voltage deviation index in the distribution system while the allowable limits of the load voltage and branch current are satisfied.

5.1. Case 1: Minimizing the Total Power Losses. Power loss is one of the important factors that strongly influence the evaluation of the system quality as well as the economic benefits. Therefore, the reduction of losses on the transmission lines is a necessary matter that should be studied carefully. In this case, the total power losses are considered for reducing to a minimum under consideration of load voltage and branch current limits. Besides, in order to ensure the objectivity of the proposed method and the compared methods, the results of the 50 trial runs are collected for analysis and evaluation.

The values of the best fitness, the worst fitness, and the average fitness of the proposed method are compared in detail with others such as SFO, SSD, CSA, SSA, BO, and SMA as shown in Table 1. For the assessment between the improved method and the original method, the best fitness, the worst fitness, and the average fitness values for ISMA are 20.2221, 22.4978, and 20.7153 while for SMA are 20.2352, 23.4059, and 20.9881, respectively. These values indicate that the performance of ISMA is better than SMA. In other words, the modifications on the new control variable updating process of ISMA have reached a positive effect in enhancing performance. To clearly justify the effectiveness, the improvement level (IL) was calculated and the last three columns show the IL of the proposed ISMA over others for the mean fitness, worst fitness, and the best fitness. The three values are, respectively, 1.2998%, 3.8798%, and 0.0647% as comparing results with SMA. Similarly, ISMA is also compared with other popular methods. As obtained results, the best fitness and the worst fitness values of ISMA are better than the five remaining methods from 20.2340 to 21.7190 and from 22.6942 to 25.5408 with the levels of improvement from 0.0588% to 6.8921% and 0.8654% to 11.9143%. This shows that the solutions with the best quality and the worst quality proposed within the 50 random runs from ISMA are always more optimal and efficient than other

Table 1: The comparison among implemented methods at the first case.

Applied method	The average FF_A	The worst FF_A	The best FF_A	IL of the average FF_A (%)	IL of the worst FF_A (%)	IL of the best FF_A (%)
SFO	23.2920	25.5408	21.7190	11.0626	11.9143	6.8921
SSD	21.8733	23.1912	20.8366	5.2941	2.9899	2.9491
CSA	21.1234	22.6942	20.3081	1.9320	0.8654	0.4235
SSA	22.7907	24.316	21.4735	9.1063	7.4774	5.8276
BO	20.9122	23.0431	20.2340	0.9416	2.3664	0.0588
SMA	20.9881	23.4059	20.2352	1.2998	3.8798	0.0647
ISMA	20.7153	22.4978	20.2221	—	—	—

solutions. Moreover, in order to demonstrate the high stability of the proposed method, the calculation of the average value of the fitness function is performed. The average fitness value of 50 trial runs from ISMA is the smallest as compared to other popular methods from 20.9122 to 23.2920 with the corresponding improvement level from 0.9416% to 11.0626%. This shows that the proposed method is more stable than the other methods in finding the optimal solution in the same search area.

Figure 10 shows the fitness values of all implemented methods during the 50 trial runs with the initial solutions are randomly generated. For convenience in reviewing and evaluating the stability of the implemented methods, all fitness values are rearranged from low to high. As a result, the curve of ISMA has proved the effectiveness and stability of this method compared to other methods with the same iteration number and created generation number in each iteration. In addition, the convergence characteristic of ISMA is also better than other methods like Figure 11 presented. During the 200 iterations of the best solution, ISMA exhibited convergence fairly quickly; it found the better quality solution than others and the best solution at the 138^{th} iteration. This shows the outstanding properties of the proposed method in the process of finding the feasible solution for solving the optimization problem.

Like presented in Figure 12, by using the proposed solution from ISMA, the power losses on transmission lines are reduced as compared with the original system. Specifically, the total losses on the system are significantly reduced from 95.77 kW to 20.22 kW, corresponding to 78.88% in the loss reduction after installed suitable PVDGUs and the obtained loss of ISMA is smallest as compared to other methods. This shows that the proper installation of PVDGUs has had a strong impact on reducing losses on the transmission lines. In other words, the benefit from loss reduction depends on the quality of the optimal solution that has been proposed. All of the above-given arguments prove that ISMA is really an efficient and suitable method for solving the problem of the optimal place and sizing of PVDGUs in the unbalanced multiphase distribution system.

The best solutions of PVDGUs placement found by previous and implemented methods are presented in Table 2. As demonstrated from simulation results, the power loss reduction entirely depends on the optimal solutions that the implemented methods have proposed. Three methods (ISMA, SMA, and CSA) proposed Buses 47, 65, and 72, and they could achieve the relatively same good results for loss reduction, which is 78.88% for ISMA, 78.87% for SMA, and 78.80% for CSA. Besides, another option consisting of Buses 47, 65, and 76 found by BO could also lead to good results like the three above-given locations. BO achieved the loss reduction of 78.87%, which is approximately equal to that of the best method, 78.88%. Thereby, it shows that the two key locations to maximize the benefits in reducing power loss are Buses 47 and 65, and one remaining position is Bus 72 or Bus 76. In addition, PSO suggested the installation locations at Buses 47, 67, and 72, but it got the worst loss reduction with only 69.10%. The cause is that PSO did not properly determine good capacity for each PVDGU. In fact, BO, SMA, and ISMA proposed approximately the same total capacity, which are respectively 2809.0 kW, 2807.7 kW, and 2808.9 kW, and the capacity of each PVDGU from the three algorithms are nearly equal. On the contrary, the total capacity found by PSO was 2940.0 kW and the capacity for each PVDGU is also different from that of BO, SMA, and ISMA. Clearly, the capacity of each PVDGU obtained by PSO was not effective as others. Therefore, determining the suitable capacity for each position is extremely important and it greatly contributes to high loss reduction to distribution systems. In summary, the three best locations for this case should be Buses 47, 65, and 72, and the best capacities for them are, respectively, 907.2 kW, 341.1 kW, and 1560.6 kW.

5.2. Case 2: Minimizing the Voltage Deviation Index. In this case, the enhancement of the voltage deviation index is considered as an objective function with under the constraints of the load voltage profile and the current on the branches in the test system. In evaluating a distribution system, the voltage deviation index becomes an important criterion and it is the basis for analysis and evaluation. The consideration for improving this index will drastically enhance the quality of the voltage for the entire system. As mentioned, the proposed method is compared to six other effective methods with 50 trial runs.

The best, the worst, and the average values of the fitness function from the proposed method and other popular methods are compared in detail in Table 3. The best fitness, the worst fitness, and the average fitness values of ISMA are 1.4779, 1.6322, and 1.5523, respectively, meanwhile those values of SMA are higher and equal to 1.5036, 1.6749, and 1.5726. From the three values, it is obtained that the levels of improvement are 1.7092% for the best fitness, 2.5494% for

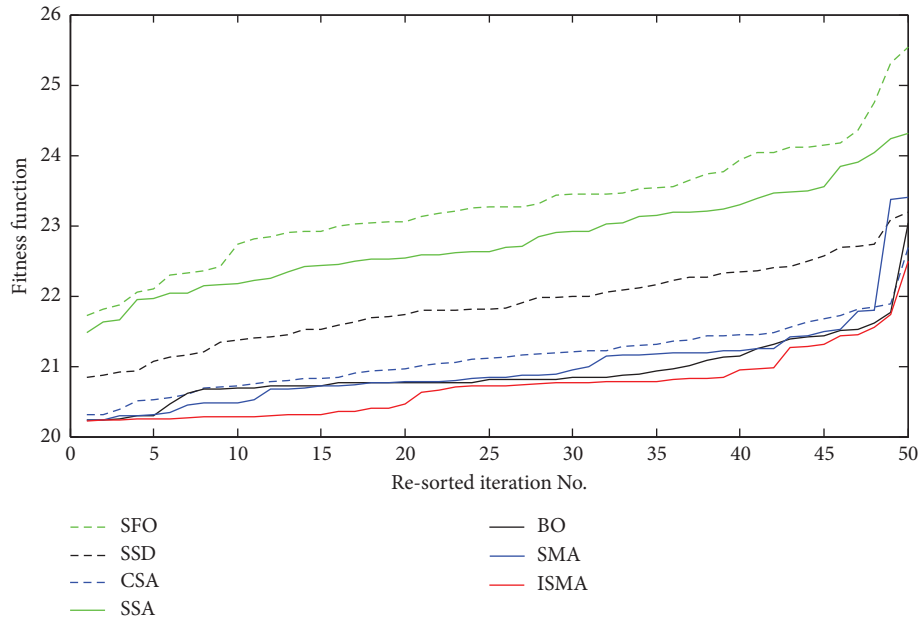

Figure 10: The fitness values of implemented methods are resorted and compared at the first case.

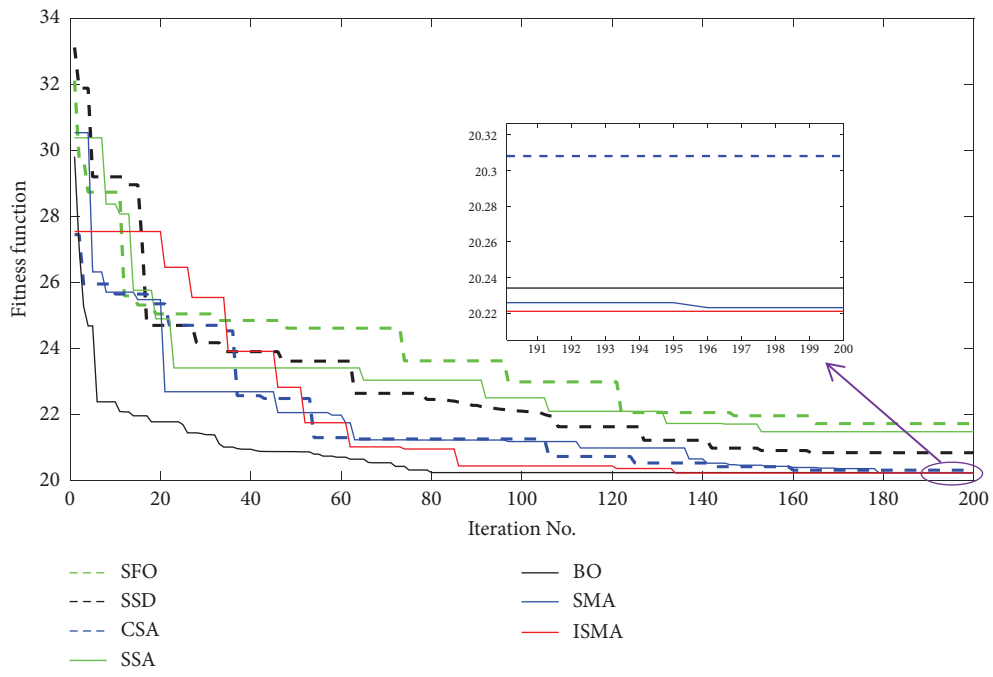

Figure 11: The convergence curve of implemented methods in the best solution at the first case.

the worst fitness, and 1.2909% for the mean fitness. The best fitness and the worst fitness of the other five remaining are, respectively, from 1.4974 to 1.5759, and 1.6327 to 1.7031. The proposed ISMA can reach the levels of improvement from 1.3023% to 6.2187% for the best fitness and from 0.0306% to 4.1630% for the worst fitness. In addition, the average fitness over 50 trial runs indicates that the proposed ISMA can reach better stability from 0.4745% to 5.0058%. In summary, the proposed ISMA is very successful in finding solutions for the problem, and it has high improvement levels over six other implemented algorithms.

Figure 13 shows the fitness function values of the proposed and compared methods in 50 trial runs, and all fitness values are rearranged from low to high for the convenience of evaluation. Most of the points of fitness values on the ISMA curve are lower than those of the original SMA and other compared methods. This represents the stability level of the methods at random trial runs. The obtained results from Figure 13 also showed that ISMA have better solution quality and stability as compared with the implemented methods. Besides, the convergence of seven methods in the best solution is also clearly presented in Figure 14. ISMA

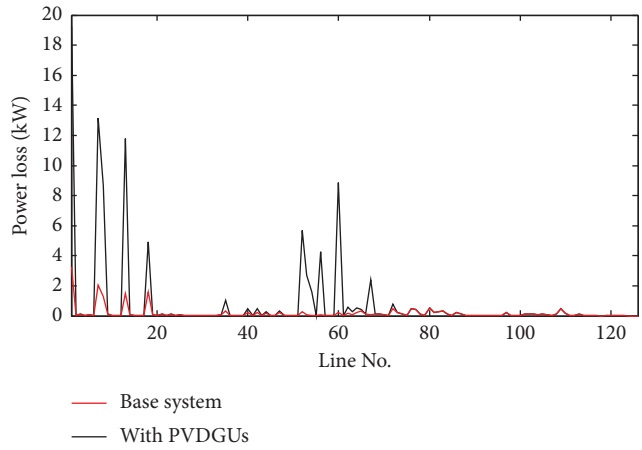

Figure 12: The power loss at each line before and after PVDGU's connection at the first case.

Table 2: The optimal solution of the proposed and the compared methods at the first case.

Applied method	The optimal solution (bus—size)	Total capacity (kW)	Power loss reduction (%)
JAYA [28]	Bus: 44–1310.0 kW; bus: 64–580.0 kW; bus: 86–1110.0 kW	3000.0	76.50
Based LII [43]	Bus: 28–200.0 kW; bus: 47–880.0 kW; bus: 67–2380.0 kW	3460.0	76.97
PSO [44]	Bus: 47–540.0 kW; bus: 67–1080.0 kW; bus: 72–1320.0 kW	2940.0	69.10
SFO	Bus: 47–775.0 kW; bus: 60–656.7 kW; bus: 76–1189.3 kW	2621.0	77.32
SSD	Bus: 47–808.7 kW; bus: 62–776.6 kW; bus: 76–1223.7 kW	2809.0	78.24
CSA	Bus: 47–943.7 kW; bus: 65–361.6 kW; bus: 72–1490.5 kW	2795.8	78.80
SSA	Bus: 42–777.2 kW; bus: 72–1779.9 kW; bus: 114–203.7 kW	2760.8	77.58
BO	Bus: 47–933.3 kW; bus: 65–370.2 kW; bus: 76–1505.5 kW	2809.0	78.87
SMA	Bus: 47–901.5 kW; bus: 65–317.0 kW; bus: 72–1589.2 kW	2807.7	78.87
ISMA	Bus: 47–907.2 kW; bus: 65–341.1 kW; bus: 72–1560.6 kW	2808.9	78.88

Table 3: The comparison among the implemented methods at the second case.

Applied method	The average FF_B	The worst FF_B	The best FF_B	IL of the average FF_B (%)	IL of the worst FF_B (%)	IL of the best FF_B (%)
SFO	1.6341	1.6837	1.5307	5.0058	3.0587	3.4494
SSD	1.5962	1.7031	1.5235	2.7503	4.1630	2.9931
CSA	1.5646	1.6327	1.5074	0.7861	0.0306	1.9570
SSA	1.6216	1.6776	1.5759	4.2736	2.7062	6.2187
BO	1.5597	1.6481	1.4974	0.4745	0.9647	1.3023
SMA	1.5726	1.6749	1.5036	1.2909	2.5494	1.7092
ISMA	1.5523	1.6322	1.4779	—	—	—

found better quality solutions than others at the 100^{nd} iteration and the best solution is also determined at 123^{th} iteration. Thereby, ISMA is a method with quite good convergence and it is an effective method in finding the optimal solution.

From obtained results, the voltage values of all phases before and after installation of PVDGUs for Case 1 and Case 2 are plotted according to distance from the substation as shown in Figures 15–17, respectively. In other words, the y-axis is the values of voltage amplitude (pu) in phases such as phase A, phase B and phase C. These voltage values are distributed in the x-axis by distance (km) calculated from the substation. Since the considered system is a multiphase system, the voltage values of the phases for each bus are different and they are clearly denoted in Figures 15–17. Due to the characteristics of the transmission line connection and the distribution of the load concentrated in phase A of the system, the system has a higher number of bus voltages in phase A than in phase B and phase C. As shown, thanks to the application of the proposed solution from ISMA, the minimum value of rms voltage is significantly improved from 0.979 pu to 0.989 pu for Case 1 and from 0.979 pu to 0.990 pu for Case 2. Not only that, the maximum value of rms voltage before and after the installing PVDGUs also changed positively from 1.037 pu to 1.030 pu approximately for Case 2 and that value has no improvement after connecting PVDGUs in Case 1.

Besides, the voltage deviation of the system has been greatly enhanced as Figure 18 after optimally integrating the position and capacity of the PVDGUs into the system. The smaller this deviation, the voltage quality of the system will be more stable. Specifically, the sum of voltage deviation

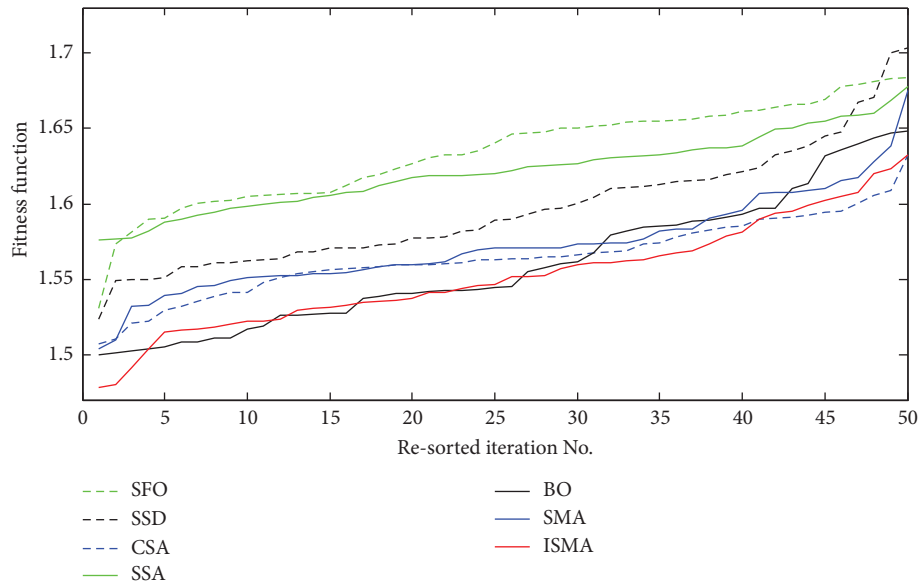

Figure 13: The fitness values of implemented methods are resorted and compared at the second case.

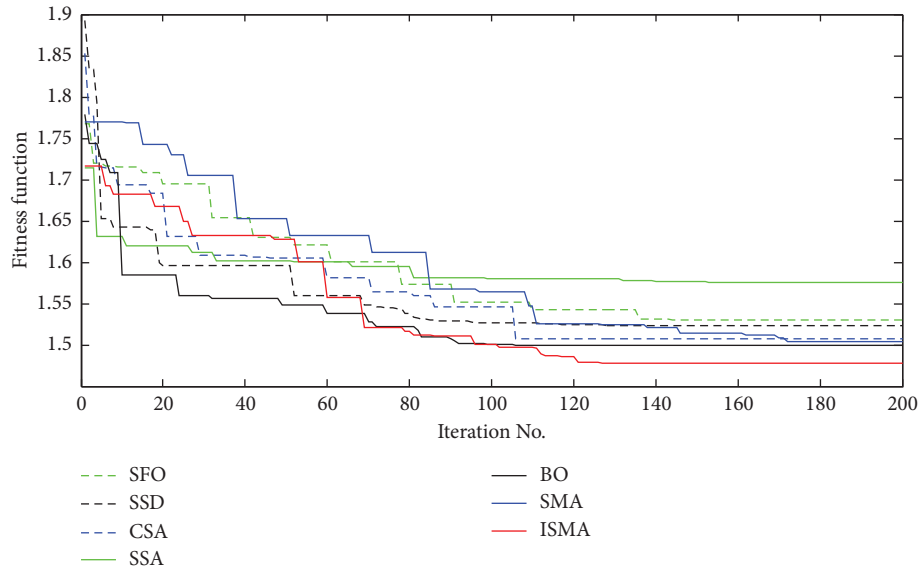

Figure 14: The convergence curve of the implemented methods in the best solution at the second case.

values for all buses without PVDGUs connection is 2.2035 pu. However, after the integration of three suitable PVDGUs into this system with the two single goals of reducing the total power loss and minimizing the voltage deviation index, the total voltage deviation values at the buses drop to 1.8523 pu and 1.4779 pu, respectively. As a result, Figure 18 shows the concrete evidence of the positive change of voltage deviation at each bus in the distribution system. Generally, the voltage deviation of the buses with suitable PVDGU's connection in the second objective function is better than in the other two cases of no PVDGU connection and PVDGU's connection in the first objective function. This shows that, when properly connected PVDGUs into the system, the voltage deviation values are significantly reduced and this contributes to enhance voltage quality for an unbalanced multiphase distribution system. In other words, the well-being of the voltage depends strongly on the optimization of the solution as well as on the efficiency of the proposed method. Like all things proved, ISMA provides the optimal solution for the place and sizing of PVDGUs in the unbalanced multiphase distribution system with higher quality and more stability than other methods under the same conditions.

The most appropriate position and capacity of PVDGUs of all implemented methods are presented in Table 4. As shown in the table, ISMA is the best method in improving the voltage profile with the lowest VDI of 1.4779 by proposing Buses 46, 67, and 106, whereas the second-best method, BO reaches the VDI of 1.4974 by proposing Buses 22, 46 and 67. Although the two methods did not use the

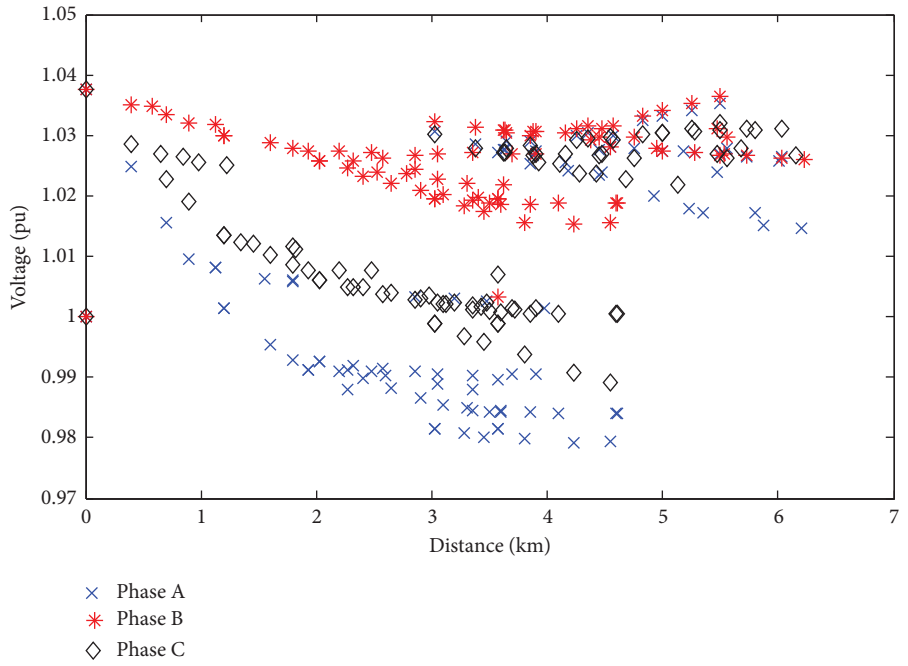

Figure 15: The voltage profile without any PVDGU.

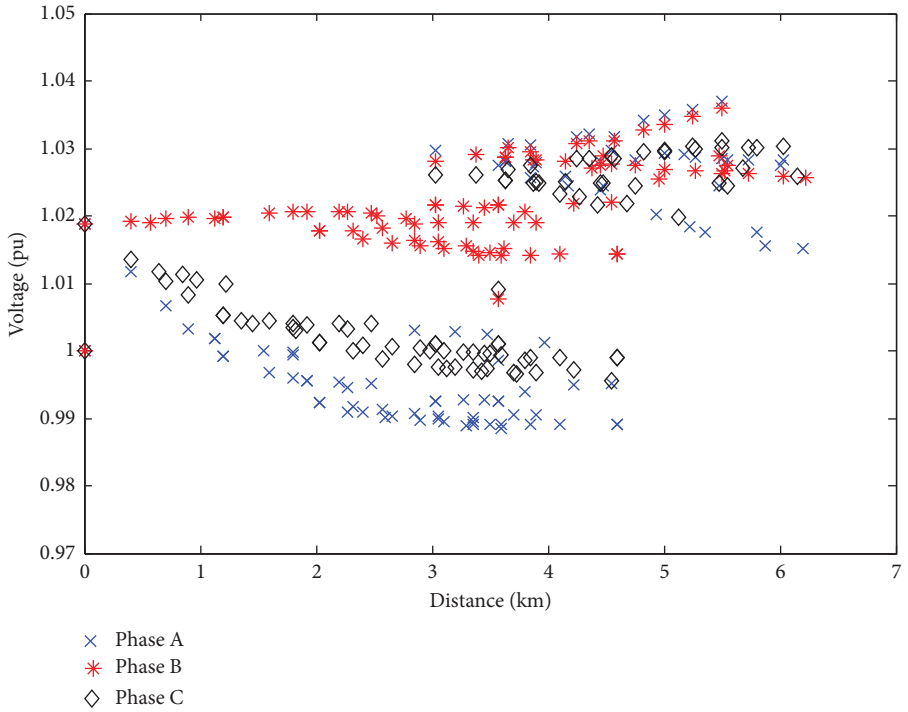

Figure 16: The voltage profile with PVDGUs for Case 1.

same locations, the total capacity of the three PVDGUs is approximately the same, 2767.1 kW for BO and 2767.0 for ISMA. Focusing on the locations and total capacity of the third-best method (SMA) and the worst method (SSA) indicates that different locations and different capacity were used. SMA used Buses 38, 45, and 67 and the total capacity of 2777.4 kW. SSA used Buses 48, 69, and 97, and capacity of 2735.0 kW. Among the three proposed locations of other remaining methods, only one or two buses are identical to those of ISMA. On the other hand, the total capacity from these methods is also much different from that of ISMA. In summary, the best position and the best capacity of three PVDGUs for reaching the best voltage profile are Buses 46, 67, and 106, and 813.8 kW, 1900.0 kW, and 53.2 kW.

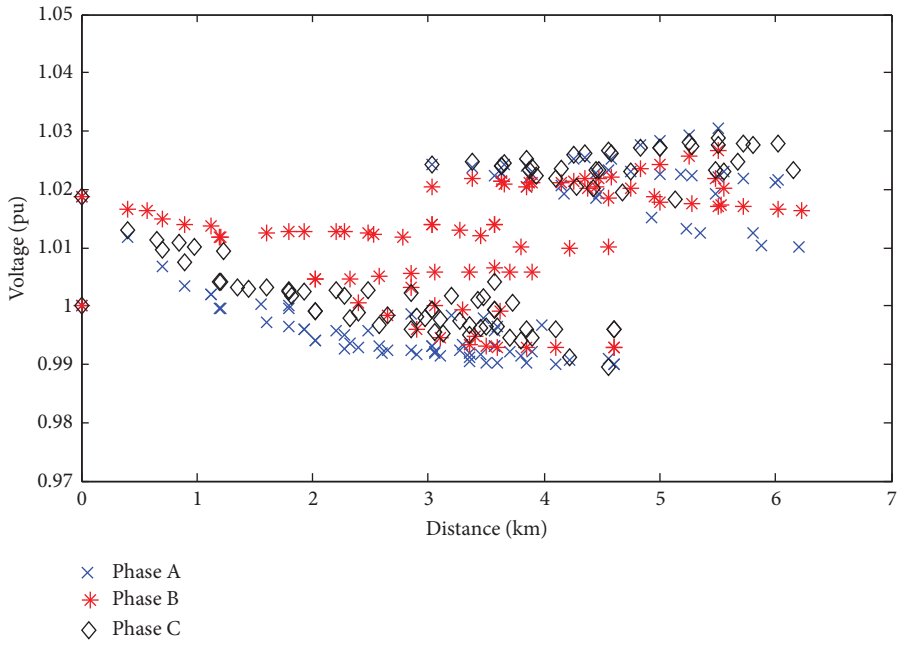

Figure 17: The voltage profile with PVDGUs for Case 2.

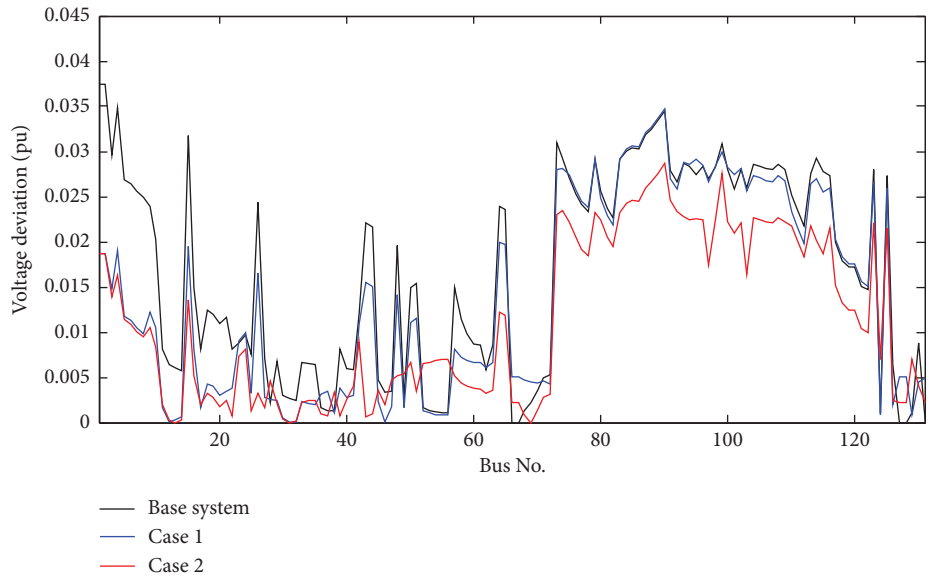

Figure 18: The voltage deviation before and after connecting PVDGUs with two cases.

5.3. Discussion on the Objective Functions and Expanded Research Fields. In this study, we suggested the use of two single objective functions in the two cases for determining the optimal location and sizing of photovoltaic distributed generation units. The reduction of the total power loss on the branches is an important criterion regarding the economic problem of the distribution system. The reduced loss will contribute greatly in saving the operating cost of the system [45]. Thus, Case 1 focuses on minimizing power losses (TPL). In addition, the phase voltages at each bus of the system in this case have also been constrained within the allowable limits to avoid overvoltage by high penetration of PVDGUs. In addition, to improve the voltage quality, another important factor, which is the voltage deviation index (VDI), is also considered [46]. Hence, this index minimization is assigned as the goal of Case 2.

Figures 15–17 indicate the voltage profiles of the based system without PVDGUs and hybrid systems with PVDGUs for Case 1 and Case 2, respectively. Although all cases have voltages within the permissible limits of 0.95 pu and 1.05 pu, the voltage range between the cases differs significantly. In detail, the phase voltages at buses are in the range of [0.979, 1.037] pu for base system without PVDGUs, while this range is [0.989 1.037] pu for Case 1 and [0.990, 1.030] pu for Case 2. Obviously, Case 2 has a better voltage profile than others because all values are close to 1.0 pu. On the other hand,

Table 4: The optimal solution of the proposed and the compared methods at the second case.

Applied method	The optimal solution (bus—size)	Total capacity (kW)	VDI
SFO	Bus: 36–822.9 kW; bus: 45–248.0 kW; bus: 67–1572.8 kW	2643.7	1.5307
SSD	Bus: 46–751.0 kW; bus: 49–949.6 kW; bus: 67–874.1 kW	2574.7	1.5235
CSA	Bus: 46–771.7 kW; bus: 67–1950.5 kW; bus: 65–10.5 kW	2732.7	1.5074
SSA	Bus: 48–972.7 kW; bus: 69–722.3 kW; bus: 97–1040.0 kW	2735.0	1.5759
BO	Bus: 22–47.7 kW; bus: 46–773.7 kW; bus: 67–1945.7 kW	2767.1	1.4974
SMA	Bus: 38–73.9 kW; bus: 45–754.5 kW; bus: 67–1949.0 kW	2777.4	1.5036
ISMA	Bus: 46–813.8 kW; bus: 67–1900.0 kW; bus: 106–53.2 kW	2767.0	1.4779

Figure 18 sees the voltage deviation of Case 2 is the smallest. On the other hand, the sum of voltage deviation values for all buses for the base case is 2.2035 pu, but the result is much smaller in Case 1 and Case 2, which are, respectively, 1.8523 pu and 1.4779 pu. In summary, different objective functions can result in different achievements and we can choose the most appropriate objective function for our purpose. If we are interested in the economic aspect and ignore voltage quality improvement, Case 1 will be a more suitable choice than the remaining cases. On the contrary, if we need a very good voltage profile, Case 2 should be applied. This indicates the advantage of the single objective function in facilitating the appropriate selection by purpose.

On the other hand, the two single objectives can be reached simultaneously by using a multiobjective function [47], but it cannot reach a solution with the same total power loss and the same voltage profile as Case 1 and Case 2. Normally, there are two cases for the solution with the two objectives. In the first case, total power loss is better, but voltage is worse. In the second case, the results are the opposite. To solve the multiobjective problem, two weight factors are associated with each objective and higher values of the weight factor are set for a more important objective [2]. The two weight factors are constrained to be within 0 and 1 and their sum should be always 1.0. For the problem, the application of ISMA or other algorithms is like the study with two single objectives.

6. Conclusions

This paper proposes ISMA for determining the optimal location of PVDGUs in the unbalanced distribution system, IEEE 123-bus test feeder for minimizing the power loss and improving the voltage quality. Besides, the study also proposed a cosimulation combining MATLAB and OpenDSS for solving the considered problem. This combination offers many advantages in improving the speed of data processing and enhancing the accuracy of power flow computation in the unbalanced distribution system. Confidently, it is the best cosimulation tool for solving the power flow problems. In addition, by applying the solutions for optimal installation of PVDGUs, the power loss and voltage deviation index in the system have dropped significantly to 20.222 kW (corresponding to 78.88%) and 1.4779 pu for ISMA, while these values are 20.235 kW (corresponding to 78.87%) and 1.5036 pu for SMA, respectively. Thereby, the improvement in ISMA is more efficient than the original SMA. The proposed method is also better than other implemented methods such as SFO, SSD, CSA, SSA, and BO, and other published methods such as PSO and JAYA. Like the obtained results, the solution of ISMA is better than others from 69.10% to 78.87% in the power loss reduction and from 1.5759 pu to 1.4996 pu in the minimization of voltage deviation index. In short, ISMA is really effective in maximizing economic and technical welfare.

As shown previously, the study has significant contributions to unbalanced distribution systems for loss reduction, voltage improvement, and voltage deviation reduction between phases; however, there are still serious problems existing in the unbalanced distribution systems such as surplus power of PVDGUs based on renewable energies for the cases of low load demand and a high deviation between real and estimated wind speed and solar radiation. So, the placement of the battery energy store system (BESS) and smart inverters in the system can be the upcoming directions of the study. The energy storage function of BESS and the smart function of the inverter can lead to high benefits without causing adverse effects. The electric components can be located at the most suitable nodes by using the proposed ISMA or a newly developed algorithm with higher performance.

Nomenclature

TPL: Total power losses
N_f: The number of feeders in the system
P^f_{Loss}: The active power loss of the f^{th} feeder in the system
VDI: Voltage deviation index
N^b: The number of buses in the system
P^i_{Load}: The i^{th} power load in the system
P^k_{DG}: The capacity of the k^{th} PVDGU
P_{Gr}: The power is supplied by grid
$M_{\text{Iter}}, C_{\text{Iter}}$: The maximum number of iteration and the current iteration
N_{ps}: The population size or number of solutions in the sole solution set
V^b: The b^{th} bus voltage in the system
I^f_{rated}: The rated current magnitude of the f^{th} feeder
I^f: The current magnitude of the f^{th} feeder
$\text{Sol}_{rd1}, \text{Sol}_{rd2}$: The randomly generated integer numbers in the range from 1 to number of search agents
$\text{Sol}_{rd3}, \text{Sol}_{rd4}$: The randomly generated integer numbers in the range from 1 to number of search agents
$V_{\max}$, $V_{\min}$: The minimum and maximum voltage of the system
N_v: The number of control variables
N_L: The number of loads

I_A^f, I_B^f, I_C^f: The current magnitude of phase A, B and C at the f^{th} feeder
R_A^f, R_B^f, R_C^f: The resistance of phase A, B and C at the f^{th} feeder
N_{spl}: The number of single phase loads
N_{DG}: The number of PVDGUs
$V_{\min}^b, V_{\max}^b$: The minimum and maximum voltage of the b^{th} bus
$P_{\text{DG}}^{\min}, P_{\text{DG}}^{\max}$: The minimum and maximum of PVDGU's capacity
$R_A^{ab}, R_B^{ab}, R_C^{ab}$: The resistance of phase A, B and C
$X_A^{ab}, X_B^{ab}, X_C^{ab}$: The reactance of phase A, B and C
P_A^b, P_B^b, P_C^b: The active power of phase A, B and C at the b^{th} bus
Q_A^b, Q_B^b, Q_C^b: The reactive power of phase A, B and C at the b^{th} bus
$L_{DG\,m}^k, P_{DG\,m}^k$: The location and capacity of the k^{th} PVDGU corresponding to the m^{th} solution
$V_A^{b,re}, V_B^{b,re}, V_C^{b,re}$: The real part of voltage of phase A, B and C at the b^{th} bus
$V_A^{b,im}, V_B^{b,im}, V_C^{b,im}$: The imaginary part of voltage of phase A, B and C at the b^{th} bus
FF_A, FF_B: The fitness value of objective functions
$\text{Sol}_{sf\text{best}}$: The best solution
Ft_{best}, Ft_{worst}, Ft_m: Fitness function of the best, worst and the m^{th} solutions
rdn: A random number within 0 and 1.

Data Availability

The data used to support the study are included in the paper.

Conflicts of Interest

The authors declare that there are no conflicts of interest regarding the publication of this paper.

Acknowledgments

This research was funded by Foundation for Science and Technology Development of Ton Duc Thang University (FOSTECT), website: https://fostect.tdtu.edu.vn, under Grant no. FOSTECT.2022.10.

References

[1] M. C. V. Suresh and E. J. Belwin, "Optimal DG placement for benefit maximization in distribution networks by using dragonfly algorithm," *Renewables Wind Water and Solar*, vol. 5, pp. 2–8, 2018.

[2] T. D. Pham, T. T. Nguyen, and B. H. Dinh, "Find optimal capacity and location of distributed generation units in radial distribution networks by using enhanced coyote optimization algorithm," *Neural Computing & Applications*, vol. 33, pp. 4343–4371, 2021.

[3] A. Rathore and N. P. Patidar, "Optimal sizing and allocation of renewable based distribution generation with gravity energy storage considering stochastic nature using particle swarm optimization in radial distribution network," *Journal of Energy Storage*, vol. 35, p. 102282, 2021.

[4] P. C. Chen, V. Malbasa, Y. Dong, and M. Kezunovic, "Sensitivity analysis of voltage sag based fault location with distributed generation," *IEEE Transactions on Smart Grid*, vol. 6, no. 4, pp. 2098–2106, 2015.

[5] R. Sulistyowati, D. C. Riawan, and M. Ashari, "PV farm placement and sizing using GA for area development plan of distribution network," in *Proceedings of the 2016 International Seminar on Intelligent Technology and Its Applications (ISITIA)*, Lombok, Indonesia, July 2016.

[6] M. Kashyap, A. Mittal, and S. Kansal, "Optimal placement of distributed generation using genetic algorithm approach," *Lecture Notes in Electrical Engineering*, vol. 476, pp. 587–597, 2019.

[7] S. R. Ramavat, S. P. Jaiswal, N. Goel, and V. Shrivastava, "Optimal location and sizing of DG in distribution system and its cost-benefit analysis," *Advances in Intelligent Systems and Computing*, vol. 698, pp. 103–112, 2019.

[8] T. S Tawfeek, A. H. Ahmed, and S. Hasan, "Analytical and particle swarm optimization algorithms for optimal allocation of four different distributed generation types in radial distribution networks," *Energy Procedia*, vol. 153, pp. 86–94, 2018.

[9] S. Mirsaeidi, S. Li, S. Devkota et al., "Reinforcement of power system performance through optimal allotment of distributed generators using metaheuristic optimization algorithms," *Journal of Electrical Engineering & Technology*, vol. 17, no. 5, pp. 2617–2630, 2022.

[10] N. Mohandas, R. Balamurugan, and L. Lakshminarasimman, "Optimal location and sizing of real power DG units to improve the voltage stability in the distribution system using ABC algorithm united with chaos," *International Journal of Electrical Power & Energy Systems*, vol. 66, pp. 41–52, 2015.

[11] M. N. B. Muhtazaruddin, J. J. B. Jamian, and G. Fujita, "Determination of optimal output power and location for multiple distributed generation sources simultaneously by using artificial bee colony," *IEEJ Transactions on Electrical and Electronic Engineering*, vol. 9, no. 4, pp. 351–359, 2014.

[12] M. Duong, T. Pham, T. Nguyen, A. Doan, and H. Tran, "Determination of optimal location and sizing of solar photovoltaic distribution generation units in radial distribution systems," *Energies*, vol. 12, p. 24, 2019.

[13] G. F. Gomes, S. S. da Cunha, and A. C. Ancelotti, "A sunflower optimization (SFO) algorithm applied to damage identification on laminated composite plates," *Engineering with Computers*, vol. 35, no. 2, pp. 619–626, 2019.

[14] M. H. Qais, H. M. Hasanien, and S. Alghuwainem, "Identification of electrical parameters for three-diode photovoltaic model using analytical and sunflower optimization algorithm," *Applied Energy*, vol. 250, pp. 109–117, 2019.

[15] M. A. M. Shaheen, H. M. Hasanien, S. F. Mekhamer, and H. E. A. Talaat, "Optimal power flow of power systems including distributed generation units using sunflower optimization algorithm," *IEEE Access*, vol. 7, pp. 109289–109300, 2019.

[16] S. Kola Sampangi and J. Thangavelu, "Optimal allocation of renewable distributed generation and capacitor banks in distribution systems using salp swarm algorithm," *International Journal of Renewable Energy Resources*, vol. 9, pp. 96–107, 2019.

[17] H. Faris, S. Mirjalili, I. Aljarah, M. Mafarja, and A. A. Heidari, "Salp swarm algorithm: theory, literature review, and

application in extreme learning machines," *Nature-Inspired Optimizers*, vol. 811, pp. 185–199, 2020.

[18] M. Tolba, H. Rezk, A. A. Z. Diab, and M. Al-Dhaifallah, "A novel robust methodology based salp swarm algorithm for allocation and capacity of renewable distributed generators on distribution grids," *Energies*, vol. 11, no. 10, p. 34, 2018.

[19] H. Abdel-mawgoud, S. Kamel, J. Yu, and F. Jurado, "Hybrid Salp Swarm Algorithm for integrating renewable distributed energy resources in distribution systems considering annual load growth," *Journal of King Saud University—Computer and Information Sciences*, vol. 34, no. 1, pp. 1381–1393, 2022.

[20] A. Tharwat and T. Gabel, "Parameters optimization of support vector machines for imbalanced data using social ski driver algorithm," *Neural Computing & Applications*, vol. 32, no. 11, pp. 6925–6938, 2020.

[21] A. K. Das and D. K. Pratihar, "A new bonobo optimizer (BO) for real-parameter optimization," in *Proceedings of the 2019 IEEE Region 10 Symposium*, Kolkata, India, June 2019.

[22] S. Li, H. Chen, M. Wang, A. A. Heidari, and S. Mirjalili, "Slime mould algorithm: a new method for stochastic optimization," *Future Generation Computer Systems*, vol. 111, pp. 300–323, 2020.

[23] C. Kumar, T. D. Raj, M. Premkumar, and T. D. Raj, "A new stochastic slime mould optimization algorithm for the estimation of solar photovoltaic cell parameters," *Optik*, vol. 223, p. 165277, 2020.

[24] R. T. Bhimarasetti and A. Kumar, "Distributed generation placement in unbalanced distribution system with seasonal load variation," in *Proceedings of the 2014 Eighteenth National Power Systems Conference (NPSC)*, Guwahati, India, December 2014.

[25] L. R. de Araujo, D. R. R. Penido, S. Carneiro, and J. L. R. Pereira, "Optimal unbalanced capacitor placement in distribution systems for voltage control and energy losses minimization," *Electric Power Systems Research*, vol. 154, pp. 110–121, 2018.

[26] F. Yang and Z. Li, "Effects of balanced and unbalanced distribution system modeling on power flow analysis," in *Proceedings of the 2016 IEEE Power & Energy Society Innovative Smart Grid Technologies Conference (ISGT)*, Minneapolis, MN, USA, September 2016.

[27] P. V. K. Babu and D. Swarnasri, "Novel technique for optimal placement and sizing of DG in 3-phase unbalanced radial secondary distribution system," *International Journal of Innovative Technology and Exploring Engineering*, vol. 9, no. 4, pp. 1756–1760, 2020.

[28] M. Kumawat, N. Gupta, N. Jain, and R. C. Bansal, "Optimally allocation of distributed generators in three-phase unbalanced distribution network," *Energy Procedia*, vol. 142, pp. 749–754, 2017.

[29] M. Reno and K. Coogan, *Grid Integrated Distributed PV (GridPV)*, Sandia National Laboratories SAND2013-6733, Albuquerque, NM, USA, 2013.

[30] A. Verma, A. Tyagi, and L. K. Panwar, "Optimal placement and sizing of distributed generation in an unbalance distribution system using gray wolf optimization method," *International Journal of Power and Energy Conversion*, vol. 1, no. 1, pp. 1–224, 2018.

[31] P. Ramsami and R. T. F. Ah King, "Multi-objective optimisation of distributed generation units in unbalanced distribution systems," *Lecture Notes in Electrical Engineering*, vol. 561, pp. 70–81, 2019.

[32] M. J. Hadidian-Moghaddam, S. Arabi-Nowdeh, M. Bigdeli, and D. Azizian, "A multi-objective optimal sizing and siting of distributed generation using ant lion optimization technique," *Ain Shams Engineering Journal*, vol. 9, no. 4, pp. 2101–2109, 2018.

[33] G. Srinivasan and S. J. E. P. Visalakshi, "Application of AGPSO for power loss minimization in radial distribution network via DG units, capacitors and NR," *Energy Procedia*, vol. 117, pp. 190–200, 2017.

[34] S. J. Rudresha and S. G. Ankaliki, "Voltage stability improvement with integration of dg into the distribution system," *International Journal of Rmerging Tend & Technology in Computer Science*, vol. 6, pp. 196–200, 2017.

[35] M. M. Othman, Y. G. Hegazy, and A. Y. Abdelaziz, "A modified firefly algorithm for optimal sizing and siting of voltage controlled distributed generators in distribution networks," *Periodica Polytechnica Electrical Engineering and Computer Science*, vol. 59, no. 3, pp. 104–109, 2015.

[36] K. M. S. Alzaidi, O. Bayat, and O. N. Uçan, "Multiple DGs for reducing total power losses in radial distribution systems using hybrid WOA-SSA algorithm," *International Journal of Photoenergy*, vol. 2019, Article ID 2426538, 20 pages, 2019.

[37] R. C. Dugan, *The Open Distribution System Simulator (OpenDSS)*, Electric Power Research Institute, Palo Alto, CA, USA, 2016.

[38] S. Pukhrem, M. Conlon, K. Sunderland, and M. Basu, "Analysis of voltage fluctuation and flicker on distribution networks with significant PV installations," in *Proceedings of the European PV Solar Energy Conference*, Hamburg, Germany, September 2015.

[39] J. C. Mendieta, "Intelligent distribution voltage control with distributed generation," Doctoral dissertation, École de Technologie Supérieure, Quebec, Canada, 2016.

[40] "IEEE PES, 123-bus feeder," https://site.ieee.org/pes-testfeeders/resources/.

[41] T. T. Nguyen, T. D. Pham, L. C. Kien, and L. Van Dai, "Improved coyote optimization algorithm for optimally installing solar photovoltaic distribution generation units in radial distribution power systems," *Complexity*, vol. 2020, Article ID 1603802, 34 pages, 2020.

[42] K. R. Devabalaji, T. Yuvaraj, and K. Ravi, "An efficient method for solving the optimal sitting and sizing problem of capacitor banks based on cuckoo search algorithm," *Ain Shams Engineering Journal*, vol. 9, no. 4, pp. 589–597, 2018.

[43] A. Anwar and H. R. Pota, "Optimum allocation and sizing of DG unit for efficiency enhancement of distribution system," in *Proceedings of the 2012 IEEE International Power Engineering and Optimization Conference*, pp. 165–170, Melaka, Malaysia, June 2012.

[44] S. Dahal and H. Salehfar, "Impact of distributed generators in the power loss and voltage profile of three phase unbalanced distribution network," *International Journal of Electrical Power & Energy Systems*, vol. 77, pp. 256–262, 2016.

[45] A. F. A. Kadir, A. Mohamed, H. Shareef, M. Z. C. Wanik, and A. A. Ibrahim, "Optimal sizing and placement of distributed generation in distribution system considering losses and THDv using gravitational search algorithm," *Przeglad Elektrotechniczny*, vol. 4, pp. 1–5, 2013.

[46] F. G. Montoya, R. Baños, C. Gil, A. Espín, A. Alcayde, and J. Gómez, "Minimization of voltage deviation and power losses in power networks using Pareto optimization methods," *Engineering Applications of Artificial Intelligence*, vol. 23, no. 5, pp. 695–703, 2010.

[47] K. Deb, "Multi-objective optimisation using evolutionary algorithms: an introduction," in *Multi-Objective Evolutionary Optimisation for Product Design and Manufacturing*Wiley, New York, NY, USA, 2011.

Hindawi
Complexity
Volume 2022, Article ID 3755754, 23 pages
https://doi.org/10.1155/2022/3755754

Research Article

An Improved Equilibrium Optimizer for Optimal Placement of Distributed Generators in Distribution Systems considering Harmonic Distortion Limits

Thai Dinh Pham,[1] **Thang Trung Nguyen**,[2] **and Le Chi Kien**[1]

[1]*Faculty of Electrical and Electronics Engineering, Ho Chi Minh City University of Technology and Education, Ho Chi Minh City, Vietnam*
[2]*Power System Optimization Research Group, Faculty of Electrical and Electronics Engineering, Ton Duc Thang University, Ho Chi Minh City, Vietnam*

Correspondence should be addressed to Thang Trung Nguyen; nguyentrungthang@tdtu.edu.vn

Received 27 June 2022; Revised 26 September 2022; Accepted 25 November 2022; Published 13 December 2022

Academic Editor: Giacomo Fiumara

This paper proposes an improved equilibrium optimizer (IEO) for determining optimal location and effective size of distributed generation units (DGUs) in the distribution systems in order to minimize the total power loss on distribution branches, investment cost, and operation and maintenance cost. In a good obtained solution, limits of voltage, current, and harmonic flows are also seriously considered, exactly satisfying predetermined ranges. Especially, individual harmonic distortion (IHD) and total harmonic distortion (THD) of bus voltage must fall into IEEE Std. 519. The proposed IEO is developed from the original equilibrium optimizer (EO), which was motivated by control volume mass balance models. This novel algorithm can effectively expand the search area and avoid the premature convergence to low-quality solution spaces. With the determined solutions from IEO, not only are the voltages well improved but also the harmonics are mitigated from the violated values down to the allowable values of IEEE Std. 519. Moreover, the total power loss is significantly reduced from 0.2110 MW to 0.0815 MW, 0.2245 MW to 0.07197 MW, and 0.3161 MW to 0.1515 MW for IEEE 33-bus, IEEE 69-bus, and IEEE 85-bus radial distribution systems, respectively. Not only that, the total cost of DGUs is also more economical and consumes only $3.4753 million, $3.2840 million, and $3.0593 million corresponding to the three systems for a 20-year planning period. The performance of the proposed algorithm is compared to three other implemented methods consisting of artificial bee colony (ABC) algorithm, salp swarm algorithm (SSA), and EO and eight previously published methods for the three test systems. The comparisons of results imply that IEO is better than other methods in terms of performance, stability, and convergence characteristics.

1. Introduction

Nowadays, it is very common to integrate distributed generation sources into distribution systems due to the development of renewable energies. Properly determining the location and capacity of DGUs in the integrated systems can reach great achievement such as minimizing the losses on the lines, improving the voltage quality of the system, mitigating the harmonic distortions, and reducing the operation and maintenance costs [1]. On the contrary, if the installation of DGUs is not appropriately planned, it can cause undesirable effects such as increasing power losses, decreasing voltage quality, increasing operation costs and other costs, and so on [2]. Thus, optimal planning strategy of DGUs in the distribution systems is essential to maximize the economic and technical achievements.

The achieved benefits derived from the installation of DGUs in distribution systems mainly depend on the placement locations and the rated power of DGUs in which optimization algorithms are utilized for determining the planning of DGUs in the integrated system. In [3–5], the authors used GA for determining the two factors of DGUs

with intent to reduce losses on transmission sectors and boost the bus voltage to the best stable region in the distribution systems. GA is a simple optimization technique, and it is known as a local search method reaching ineffective solutions for the optimization problem. To overcome the disadvantages of GA, other authors in [6–8] proposed hybrid methods which divide tasks of each phase in the considered problem to apply the most appropriate algorithm to each phase. Those authors applied the hybrid methods between GA and other techniques such as fuzzy, PSO, and RNN to search more favorable solutions for the proper integration of DGUs in 33-bus, 51-bus, and 69-bus distribution systems. In addition to GA, PSO is also a commonly selected method for finding the effective solution in solving the problem of determining placement and capacity of DGUs [9–11]. These authors optimally determined the penetration of multiple DGUs into distribution systems. As a result, the voltage profile was greatly improved and losses on branches were effectively cut. However, this algorithm has reached a low convergence rate and unguaranteed stability. Thus, many researchers have sought to improve the original PSO. The studies [12, 13] proposed improvements by integrating uniform distribution, exponential attenuation inertia weight, cubic spline interpolation function, and learning factor of enhanced control. These studies have significantly contributed to a high efficiency of the improved algorithms. In addition to the abovementioned methods, ABC is also widely used for optimizing the installation of DGUs [14, 15]. The authors have proved the effects of different types of DGUs to the loss reduction target in the distribution system, and they have successfully found a suitable planning strategy for DGU's installation with low total losses.

Likewise, the studies in [16, 17] also proposed efficient hybrid methods for optimal installation of DGUs such as VSA-CBGA and BPSO-SLFA, respectively. By properly connecting DGUs, the voltage as well as power loss has changed positively with guaranteed energy balance in the system. Additionally, another strong method is applied in solving the same problem, named BBO [18]. The authors demonstrated the obtained multi-benefit for the grid connected DGU system. This study considered the multi-objective function of minimizing the electricity purchase cost from the distribution company and maximizing the profitability of the DGU's owners. Similarly, in [19, 20], with the same applied optimization method, the authors examined harmonic distortions on 33 and 69-bus systems. The results from simulation have also proved that harmonic distortions could be significantly mitigated to IEEE Std. 519 after integrating DGUs into the considered systems. Besides, with the goal of enhancing distribution system capacity without causing adverse effects, revised IEEE Std. 1547-2018 has introduced the smart functions of interfacing photovoltaic inverter [21], and recent studies have also suggested to connect inverters which have smart functions in controlling voltage, frequency, and power flow in the DGU integrated system [22, 23]. In addition, a few other studies have analyzed the benefits for voltage regulation, loss reduction, and congestion mitigation through integrating photovoltaic inverter to generate reactive power [24, 25]. In the DGU integrated system, the inverter can be used for injecting or absorbing reactive power to maximize the achieved economic and technical welfare [26]. For the optimization problem in generating the active and reactive powers, the power factor of DGUs needs to be considered and parameter should be inserted accordingly [27]. About the environmental aspect, several researchers have looked at reducing annual operation costs and pollutant gas emissions [28]. These authors have suggested the multi-objective evolutionary algorithm which is based on the Pareto optimality, called SPEA2, to solve the optimization problem of network reconfiguration and connection of DGUs. Not only that, the fuzzy set theory is also used for selecting the best compromise solution among achieved Pareto solution set in the distribution system under the consideration of many electrical stability criteria and variation of loads. Similarly, another positive method has recently been created for finding the optimal solutions, named SSA [29]. SSA is developed based on the swarming behaviors of salps in oceans. In the mathematical model of the algorithm, the salp population is divided into two groups, the leader and the followers. The leader is the leading salp and stands in front of the chain. Other remaining salps are considered as the followers. The leader determines the direction of movement for followers. By comparing the obtained results with some other metaheuristic algorithms, the study [29] showed the superior effectiveness of SSA in solving the single and multi-objective functions. Additionally, SFO is also recently developed for solving the optimization problems [30]. It was known as a nature-inspired optimization algorithm that was inspired by sunflowers' motion toward the sun to get the radiation. Sunflowers that are located near the sun are calmer because greater heat is received in this space. Conversely, flowers that are further away from the sun tend to move closer to the sun because they receive less heat. This cycle is repeated daily in the morning [31]. Based on this natural feature, the algorithm has been built and applied in finding the optimal solutions effectively. Besides, a recently effective method, called EO, was also published in 2020 [32]. This algorithm is developed based on control volume mass balance models that are applied to predict equilibrium state and dynamic state. In the mathematical model, each particle with its concentration is responsible for finding the feasible solution in the space, and they are considered as the search agents. The concentration of these agents is updated with respect to the current best solution to reach the equilibrium state. EO's strengths are in exploration and local minima avoidance. Its effectiveness has been demonstrated by comparing it with many other existing powerful methods. EO is really a great method in solving optimization problems with high stability. However, the performance of the EO can be enhanced with an improvement in the update equation, and this has been demonstrated in this study.

In this paper, an improvement in the original algorithm (EO) is implemented, called improved equilibrium optimizer (IEO). The suggested IEO can inherit the strengths of EO and effectively avoid disadvantages of EO to reach a greater performance than EO. Thus, IEO is employed to find

the optimal solution in determining the sitting and sizing of solar photovoltaic distributed generation units in three distribution systems of 33 buses, 69 buses, and 85 buses. To satisfy many aspects of the technical and economic problems in the grid integrated DGU system, this study has considered the multi-objective function under various constraints. The main objective of the study is to reduce the power loss, enhance the voltage stability, and minimize the costs of DGUs while the branch current, bus voltage, and harmonic distortions in the systems operating nonlinear loads are kept within the allowable limits. In addition, to solve harmonic power flow, the backward/forward sweep technique (BW/FWST) has been used and the detailed description is clearly presented in [33]. Moreover, the weighted sum method is applied to decide the compromise solution for the multi-objective function [31]. In this technique, each weighting coefficient is assigned to each single objective function and the value of the weighting coefficient depends on the importance of each component in the multi-objective function. Overall, this study includes the following major contributions:

(1) For a project of DGU installation in distribution system, two major factors that should be calculated to evaluate the effectiveness are power loss and costs of investment, operation, and maintenance for the installed DGUs. Therefore, this study proposes to consider the multi-objective function under constraints of voltage profile, branch current, and harmonic distortions in different distribution systems of IEEE 33-bus, IEEE 69-bus, and IEEE 85-bus radial distribution systems. The two objectives included in the multi-objective function are as follows:

Minimize power loss on distribution lines in systems.
Minimize the sum of investment cost, operation cost, and maintenance cost for DGUs, which are integrated in distribution systems during a 20-year project.

(2) When DGUs are installed at buses in distributions systems, four key parameters including current of branches, power loss on branches, voltage of loads, and harmonic distortions will vary negatively or positively due to the power supply from installed DGUs. Hence, this paper analyzes the four parameters for two cases, before and after the installation of DGUs. As a result, proper determination of the sitting and sizing for DGUs can reach the reduction of power loss, the enhancement of voltage quality, the reduction of the costs of DGUs, and the mitigation of harmonic distortions.

(3) The gained benefits from integrating DGUs in a distribution system greatly depend on the found optimal solutions by applied algorithms. In other words, the selection or development of an efficient and stable optimal method will contribute to the both economic and technical benefits. Therefore, this paper has developed a novel algorithm (called IEO) based on modifications on equations updating solutions in the original algorithm (EO). Thereby, IEO has significant improvements in finding feasible solutions with high quality while EO is less effective when testing them on IEEE 33-bus, IEEE 69-bus, and IEEE 85-bus radial distribution systems.

The rest of the paper is organized as follows.

Firstly, section of the problem formulation (Section 2) describes the objective functions and constraints of this research. Secondly, section of the proposed algorithm (Section 3) shows the structure of EO and improvements of IEO on mechanism of EO. Thirdly, section of application of IEO for the DGUs problem (Section 4) presents computation steps to apply IEO for the problem. Next, section of simulation results (Section 5) analyzes the obtained results from integrating DGUs into IEEE 33-bus, IEEE 69-bus, and 85-bus radial distribution systems. Besides, the discussion of the performance of the proposed method and compared methods is also covered in this section. The shortcomings of the proposed method and research expansion are also discussed in Section 5. Finally, Section 6 presents the summary of results, contributions, and future work of the study.

2. Problem Formulation

2.1. Objective Function. Total power loss reduction on conductors is one of the key factors that mainly affect the economic and technical problems of distribution systems. Thus, it is important to take into account the minimization of the loss. Besides, when investing in a new integrated distribution system, the investors are always interested in the optimal strategy which can help to decrease costs on investments, maintenance, and operation. Thus, in order to satisfy the important criteria as mentioned above, the multi-objective function is proposed for use and it includes total active power loss (TAPL) and total cost of DGUs (TCDG).

2.1.1. Total Active Power Loss (TAPL). In the distribution system, the total active power loss is increasing more and more due to the development of loads as well as the extension of grid. Therefore, determining the optimal strategy in connecting DGUs to the system is a great way for the power loss minimization. The reduction of power loss mainly contributes to the effectiveness of the power grid in terms of technical as well as economic factors in saving energy and reducing operation costs. Hence, in this study, TAPL is considered as the first target in the multi-target problem. When performing the integration of DGUs into the grid, the mathematical equation of TAPL is described as follows [12]:

$$\mathrm{TAPL}_{\mathrm{DGU}} = \sum_{bh=1}^{N_{bh}} I_{bhDGU}^{2} R_{bh}, \tag{1}$$

where $\mathrm{TAPL}_{\mathrm{DGU}}$ is the total power loss after connecting DGUs to the system.

However, the compromise solution in the multi-objective function is difficult to determine because the single

objective values have large deviations. Therefore, it is necessary to convert the objectives to the same considered range. Specifically, in the first single objective, we suggest the normalization equation and it is presented as equation (2) for determining the best compromise solution [20].

$$\text{Minimize OF}_I = \frac{\text{TAPL}_{\text{DGU}}}{\text{TAPL}_{\text{NoDGU}}}, \tag{2}$$

where $\text{TAPL}_{\text{NoDGU}}$ is the total power loss of the original system without DGUs and it can be found by using the equation below [17]:

$$\text{TAPL}_{\text{NoDGU}} = \sum_{bh=1}^{N_{bh}} I_{bh}^2 R_{bh}. \tag{3}$$

If DGUs are successfully integrated into the distribution system, the value of TAPL_{DGU} will be smaller than the value of $\text{TAPL}_{\text{NoDGU}}$. In other words, the value of OF_{I} will vary in the range from 0 to 1 and the small value of the objective is expected. This demonstrates the positive effect of connecting DGUs in the system in reducing the total power loss.

2.1.2. Total Cost of DGUs (TCDG). In order to improve technical efficiency and maximize profits during the operation in a long period, it is necessary to minimize the related costs. In this case, the sum of investment cost and the cost of operation and maintenance is considered and becomes the second target in the multi-objective function. The initial investment cost of all DGUs ($\text{IC}_{\text{DGU},d}^{\text{opt}}(\$)$) and the total cost of maintenance and operation sector ($\text{MOC}_{\text{DGU},d}^{\text{opt}}(\$)$) are mainly influenced by the penetration level of DGUs ($\text{AP}_{\text{DGU},d}^{\text{opt}}(MW)$). The larger the penetration level is, the higher the above costs are. In addition, $\text{IC}_{\text{DGU},d}^{\text{opt}}(\$)$ and $\text{MOC}_{\text{DGU},d}^{\text{opt}}(\$)$ also depend on the current market on the investment price ($C_d^{\text{inv}}(M/MW)$) as well as maintenance and operation price ($C_d^{m\&o}(/MWh)$) for each connected DGU, respectively. $IC_{\text{DGU},d}^{\text{opt}}(\$)$ and $\text{MOC}_{\text{DGU},d}^{\text{opt}}(\$)$ can be found by [34]

$$\text{IC}_{\text{DGU},d}^{\text{opt}} = \sum_{d=1}^{N_{dg}} \left(C_d^{\text{inv}}.\text{AP}_{\text{DGU},d}^{\text{opt}}\right), \tag{4}$$

$$\text{MOC}_{\text{DGU},d}^{\text{opt}} = 8760.\sum_{y=1}^{PP}\sum_{d}^{N_{dg}} \left(\alpha_y.C_d^{m\&o}.\text{AP}_{\text{DGU},d}^{\text{opt}}\right). \tag{5}$$

In equation (5), $\text{MOC}_{\text{DGU},d}^{\text{opt}}(\$)$ is considered for a 20-year planning period (i.e., $PP = 20$) and α_y is the cumulative present value factor and obtained by

$$\alpha_y = \left(\frac{1}{1+dr}\right)^y, \tag{6}$$

where dr is the discount rate and y is the considered year varying from 1 to 20 (years).

Finally, the total cost of DGUs is the sum of initial investment cost and maintenance and operation cost as the following equation:

$$\text{TCDG}_{\text{DGU}}^{\text{opt}} = IC_{\text{DGU},d}^{\text{opt}} + \text{MOC}_{\text{DGU},d}^{\text{opt}}. \tag{7}$$

Similar to the first objective, the second objective (OF_{II}) must be also converted into the same range from 0 to 1 for evaluating the multi-objective function correctly. Thus, the second objective can be normalized as follows:

$$\text{Minimize OF}_{II} = \frac{\text{TCDG}_{\text{DGU}}^{\text{opt}}}{\text{TCDG}_{\text{DGU}}^{\text{max}}}. \tag{8}$$

Here, $\text{TCDG}_{\text{DGU}}^{\text{max}}$ is the total cost of the maximum generated power of DGUs in the distribution system. The value of $\text{TCDG}_{\text{DGU}}^{\text{max}}$ can be found by using equations (9)–(11) [34]:

$$\text{IC}_{\text{DGU},d}^{\text{max}} = \sum_{d=1}^{N_{dg}} \left(C_d^{\text{inv}}.\text{AP}_{\text{DGU},d}^{\text{max}}\right), \tag{9}$$

$$\text{MOC}_{\text{DGU},d}^{\text{max}} = 8760.\sum_{y=1}^{PP}\sum_{d}^{N_{dg}} \left(\alpha_y.C_d^{m\&o}.AP_{\text{DGU},d}^{\text{max}}\right), \tag{10}$$

$$\text{TCDG}_{\text{DGU}}^{\text{max}} = \text{IC}_{\text{DGU},d}^{\text{max}} + \text{MOC}_{\text{DGU},d}^{\text{max}}, \tag{11}$$

where $\text{IC}_{\text{DGU},d}^{\text{max}}(\$)$ is the maximum initial investment cost of all DGUs and $\text{MOC}_{\text{DGU},d}^{\text{max}}$ is the maximum total cost of maintenance and operation.

In the considered optimization problem, the optimal generation of each DGU is searched within the minimum and maximum limits of the output power, which are given. Therefore, OF_{II} always varies in the range from 0 to 1. The smaller OF_{II} is, the more profitable the distribution system is.

As mentioned, this study considers the multi-objective function consisting of two objectives as the power loss and the costs of DGUs. To determine the best compromise solution for the multi-objective function, the weighted sum method is used [31]. Lastly, the multi-objective function is established as follows:

$$\text{Minimize OF} = \omega_I.\text{OF}_I + \omega_{II}.\text{OF}_{II}, \tag{12}$$

where OF_{I} and ω_I are the first normalized single target and the weighting factor associated to the target. OF_{II} and ω_{II} are the second normalized single target and the weighting factor associated to the target, respectively. In equation (12), the two weighting factors are constrained by [20]

$$\omega_I + \omega_{II} = 1 \text{ and } 0 \le \omega_I, \omega_{II} \le 1. \tag{13}$$

The values of ω_I and ω_{II} are chosen dependent on the importance of the components (single objective) in the multi-objective function [34]. These values can be adjusted by user. The larger the weighting factor is, the greater its significance in the multi-objective function is.

2.2. Constraints

2.2.1. Power Balance Constraints. The power balance is a key factor in keeping the stability for system frequency. If the power generation is more or less than the total power consumption, the frequency of the system will be increased

or decreased, respectively [35]. Thus, it is necessary to take the power balance between power generation and power consumption sides into account. The power generation side includes the supplied power from the grid (AP_{gr}) and the injected power by connected DGUs ($AP_{DGU,d}$); meanwhile, the total power consumption side is comprised of the consumed power by loads ($AP_{ld,b}$) and the power losses ($AP_{ls,bh}$). These two power sides should be balanced as follows [31]:

$$AP_{gr} = \sum_{b=1}^{N_{ld}} AP_{ld,b} + \sum_{bh=1}^{N_{bh}} AP_{ls,bh} - \sum_{d=1}^{N_{dg}} AP_{DGU,d}. \quad (14)$$

2.2.2. Voltage Limits. The voltage profile plays a major role in evaluating quality power of the operating systems. However, when we consider the penetration of DGUs as another power source in the distribution system, the voltage has variations and its range is expanded. Thus, the voltage should be considered to keep in the limits. According to IEC and European EN 50160 standards, the allowable voltage limits are from 0.90 pu to 1.10 pu. However, in 33-bus, 69-bus, and 85-bus radial distribution systems, the best range for the bus voltage is maintained within the minimum limit (V^{min}) and the maximum limit (V^{max}) of 0.95 pu and 1.05 pu, respectively. Obviously, the limit can also satisfy the standard of IEC and European EN 50160, but it is more serious than the two organizers. The bus voltage and voltage limits are considered at the fundamental frequency and constrained as follows [17]:

$$V^{min} \le V_b \le V^{max}, \quad b = 1, \ldots, N_b. \quad (15)$$

2.2.3. Total Voltage Harmonic Distortion and Individual Voltage Harmonic Distortion Limits. Harmonic distortions are considered a prime concern in the electrical power system because it can cause overheating (for capacitors, generators, and transformers), disoperation (for electronics, relays, and switchgear), reduction of life time of the connected devices in the system, and so on. Harmonic distortions can be defined as the deformation of a waveform by integer multiples of a fundamental frequency. As shown in Figure 1, they are the distorted waveforms of the 12-pulse converter, AC voltage regulator, and fluorescent lighting [35].

Harmonic distortions are caused by nonlinear load's operations (saturated electric machines or rectifiers), and they can be minimized by using passive and active filters. To evaluate the power quality of the systems, the two parameters including total harmonic distortion and individual harmonic distortion must satisfy allowable ranges in Table 1 [36, 37].

The two factors which indicate the harmonic noise level of the system are total voltage harmonic distortion ($THD_b(\%)$) and individual voltage harmonic distortion ($IHD_b^h(\%)$). Their values can be obtained by voltage values

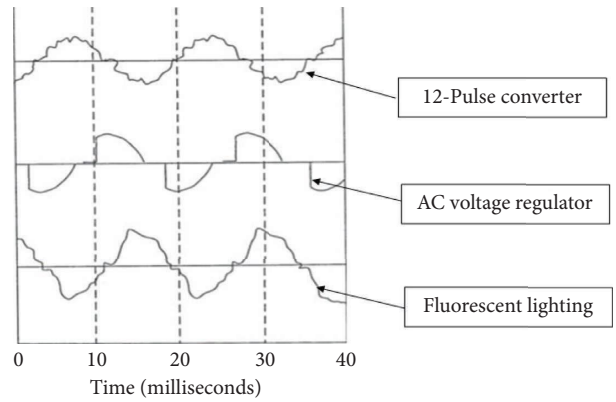

Figure 1: The waveform of some disturbing loads.

at the fundamental frequency (V_b^1) and other higher order frequencies (V_b^h) as follows [20]:

$$THD_b(\%) = \left[\frac{\sqrt{\sum_{h\neq 1}^{H}\left(V_b^h\right)^2}}{V_b^1}\right] \times 100 \le THD^{max}(\%), \quad (16)$$

$$IHD_b^h(\%) = \left[\frac{V_b^h}{V_b^1}\right] \times 100 \le IHD^{max}(\%). \quad (17)$$

By applying the IEEE Std. 519 of harmonic limits as shown in Table 1, $THD^{max}(\%)$ and $IHD^{max}(\%)$ in equations (16) and (17) are set to 5% and 3%, respectively, because the voltage level at the point of common coupling in the considered systems is less than 69 kV [33].

2.2.4. DGU's Capacity Limits. Before photovoltaic strategy planning, for each DGU, the lower and upper bounds of location (L_{DGU}^{min} and L_{DGU}^{max}) as well as capacity (AP_{DGU}^{min} and AP_{DGU}^{max}) should be predetermined and imposed on DGUs as shown in equations (18) and (19), respectively [4]. In other words, the selection of location ($L_{DGU,d}$) and rated power ($AP_{DGU,d}$) of the d^{th} DGU is performed by applying the predetermined allowed regions. Moreover, the total generating capacity of all DGUs must not exceed 80% of the total load demand (AP_{ld}) as equation (20) for this study [12, 20].

$$L_{DGU}^{min} \le L_{DGU,d} \le L_{DGU}^{max}, \quad (18)$$

$$AP_{DGU}^{min} \le AP_{DGU,d} \le AP_{DGU}^{max}, \quad (19)$$

$$\sum_{d=1}^{N_{dg}} AP_{DGU,d} \le 80\% \times AP_{ld}. \quad (20)$$

2.2.5. Branch Current Limits. When DGUs are connected to the distribution system, the current in the branches can be significantly increased depending on the location and power of DGUs. This can disrupt the original structure of the grid and cause damage to existing conductors and other electric components. Therefore, the branch current limit should be

Table 1: The harmonic voltage limits for power producer.

Bus voltage at PCC	Individual harmonic distortion (IHD) (%)	Total harmonic distortion (THD) (%)
69 kV and below	3.0	5.0
69 kV to 161 kV	1.5	2.5
169 kV and above	1.0	1.5

considered as one of the most serious constraints in systems after integrated DGUs as follows [28]:

$$I_{bhDGU} \le I_{bh}^{\max}, \quad bh = 1, \ldots, N_{bh}. \tag{21}$$

3. The Proposed Method

3.1. Equilibrium Optimization (EO). A strong optimization algorithm based on the mass balance control models was published in 2020 called equilibrium optimizer (EO) [32]. In this algorithm, each particle along with its concentration works as a search agent. These search agents update their concentration randomly with the desire of finding the best quality solution. In other words, each solution represents an internal concentration and the adjustment variables in the solutions are the concentration parameters of EO. The quality of the solution entirely depends on the fitness function value under the constraints, and the use of the fitness function result is intended to evaluate the mass-concentration balance within the adjusted volume. Overall, EO is an ideal algorithm for exploration, finding high-quality optimal solutions and avoiding local traps. The algorithm is expressed as follows.

3.1.1. Initial Population Generation. In EO, each solution F_i in the population contains a set of adjustment variables and there must be a predetermined range for the variables. The lower and upper bounds of the variables are called the minimum solution ($F^{\min}$) and the maximum solution ($F^{\max}$), respectively. During the application of EO, each solution F_i is always kept within these limits. The mentioned solutions and the boundary solutions are formulated as follows:

$$F_i = \left[Va_{ji}\right]; j = 1, 2, 3, \ldots, N_{ad} \& i = 1, 2, 3, \ldots, N_c, \tag{22}$$

$$F^{\min} = \left[Va_j^{\min}\right] \& F^{\max} = \left[Va_j^{\max}\right]; j = 1, \ldots, N_{ad}. \tag{23}$$

The generation of initial solution set or initial population is implemented by [32]

$$F_i = F^{\min} + \text{rand}(0, 1).\left(F^{\max} - F^{\min}\right); i = 1, \ldots, N_c. \tag{24}$$

3.1.2. Calculation Process for Updating Concentration. Quality of all solutions is calculated to rank the solutions in population in which solution with the smallest fitness value is the best and other solutions with worse fitness values are from the second-best solution to the worst solution. After obtaining the fitness values of solutions, the top four best solutions are collected and assigned to $F_{L\text{best1}}$, $F_{L\text{best2}}$, $F_{L\text{best3}}$, $F_{L\text{best4}}$ for the calculation of the arithmetic mean ($F_{L\text{mean}}$). The new solution (F_i^{new}) is updated through a combination of three components. The first component (F_s) is randomly selected from the solution set including $F_{L\text{best1}}$, $F_{L\text{best2}}$, $F_{L\text{best3}}$, $F_{L\text{best4}}$, and $F_{L\text{mean}}$. Clearly, the selection of a solution in the good group can contribute to a positive orientation for reaching the next generation. For the second component, it is the difference between the selected solution (F_s) and the considered old solution (F_i). This component is regarded as a part of distance between the current candidate solution and the new found solution. Another component is also another part of distance between old and new solutions, but it is built without the experience of the current solution. The three components are useful in finding better solutions, which are not close to the current good solutions. Finally, the new solution (F_i^{new}) can be calculated by applying the following equation [32].

$$F_i^{\text{new}} = F_s + (F_i - F_s)ET + \frac{GR}{l}(1 - ET). \tag{25}$$

In equation (25), two important terms, which mainly affect the quality of produced new solutions, are the exponential term (ET) and the generation rate (GR). ET and GR values can be found by solving complex equations.

For the exponential term (ET), it can be calculated by applying the following equation [32].

$$ET = \beta_1 \text{sign}(\mu - 0.5)\left(e^{-tc.l} - 1\right). \tag{26}$$

Its main purpose is built to create the suitable balance between exploration and exploitation. Practically, the turnover rate will be changed in the real control volume with time. So, l is added in the equation to represent random variation over time in the range of (0, 1). In equation (26), the constant (β_1) is selected to be 2 and the integer number (μ) is randomly taken between 0 and 1. Besides, the time coefficient (tc) is a value that changes with each iteration, and its value depends entirely on the maximum iteration number (It^{Max}) and the current iteration number (It). The value of tc can be found by applying the following equation [32].

$$tc = \left(1 - \frac{\text{It}}{\text{It}^{\text{Max}}}\right)^{\beta_2\left(\text{It}/\text{It}^{\text{Max}}\right)}, \tag{27}$$

where β_2 is a constant and it is selected to be 1 for the sake of simplicity.

For the generation rate (GR), it is the most important item in the algorithm of EO to suggest efficient solutions through enhancing the exploitation phase and GR can be determined by using the following equation [32].

$$GR = ET.Gq.(F_s - l.F_i), \tag{28}$$

where

$$Gq = \begin{cases} \dfrac{\theta_1}{2}, & \text{if } \theta_2 \geq q, \\ 0, & \text{else.} \end{cases} \tag{29}$$

In equation (28), Gq is considered as the control coefficient of GR. It positively contributes to the process of creating new solutions. Its value depends on random generated variables in the range of (0, 1) such as θ 1 and θ 2 and generation probability (q). Obviously, once Gq takes on zero, the update equation (25) will no longer exist the exploitation rate term. Therefore, the value of q is important in determining the existence of this term and q should be chosen to be 0.5 to achieve a good balance [32].

3.1.3. New Concentration Correction and Update. Each new concentration is always checked for determining the violation in the predetermined limits, and the found violation will be corrected according to the rule below:

$$F_i^{\text{new}} = \begin{cases} F^{\min}, & \text{if } F_i^{\text{new}} < F^{\min}, \\ F^{\max}, & \text{if } F_i^{\text{new}} > F^{\max}, \\ F_i^{\text{new}}, & \text{else.} \end{cases} \tag{30}$$

By calculating fitness function, the quality of each concentration is determined. Solutions with better quality (i.e., concentrations with better mass balance) are retained. Therefore, new concentration quality ($\text{Fit}_i^{\text{new}}$) should be compared with the current concentration quality (Fit_i) for storing better ones. The explanation can be formulated as follows:

$$\text{Fit}_i = \begin{cases} \text{Fit}_i^{\text{new}}, & \text{if } \text{Fit}_i \geq \text{Fit}_i^{\text{new}}, \\ \text{Fit}_i, & \text{else,} \end{cases} \tag{31}$$

$$F_i = \begin{cases} F_i^{\text{new}}, & \text{if } \text{Fit}_i \geq \text{Fit}_i^{\text{new}}, \\ F_i, & \text{else.} \end{cases} \tag{32}$$

3.1.4. Improved Equilibrium Optimizer Algorithm (IEO). By substituting equation (28) into equation (25), new solutions can be obtained:

$$F_i^{\text{new}} = F_s + (F_i - F_s).ET + (F_s - l.F_i).\frac{Gq.ET}{l}.(1 - ET). \tag{33}$$

Equation (33) has three terms including F_s, $[(F_i - F_s).ET]$, and $[(F_s - l.F_i)Gq.ET/l.(1 - ET)]$ in which the second term and third term are the updated jumping steps to make the new solution F_i^{new} different from the old solution F_s. In this case, the scaling factor of the first jumping step is ET. Similarly, the scaling factor of the second jumping step is $Gq.ET.(1 - ET)/l$ and it is set to ET′ for the sake of simplicity. The values of ET and ET′ are investigated to avoid the incorrect evaluation for ET and ET′ due to the missing values from randomization in the range of 0 to 1. Thus, in this case, to minimize the randomization that can affect the evaluation results, l is run from 0 to 1 with a step size of 0.0001, which is equivalent to 10,000 steps. In other words, 10,000 values of l will be produced for evaluation. ET and ET′ will be found with respect to l values for determining their operating regions. The operating regions of ET and ET′ are plotted in Figures 2 and 3.

Through Figure 2, the obtained results clearly indicate that the values of ET completely fluctuate in the range of [−0.6, 0.6], and this implies that the scaling factor of the first jumping step is only suitable for finding local solutions. Besides, as presented in Figure 3, the limits of ET′ are in the range of [−1.2, 0.9]. However, only 806/10,000 values (corresponding to 8.06%) are out of range [−0.6 0.6] and 5,014/10,000 values (corresponding to 50.14%) are zero as counted. Therefore, most of the scaling factor values make the second jumping step fall into the local trap, and more than half the chance of existence of ET′ is completely eliminated. In other words, most of operating ranges of ET and ET′ are only concentrated in the narrow margins. So, the use of ET and ET′ leads to a difficulty to expand the search space. Clearly, equation (33) restricts the expansion of search spaces by the impact of the two scaling factors and this makes the performance of the algorithm low. Hence, the original algorithm (EO) is only considered appropriate for finding the optimal solutions in the local search space. In this study, equation (33) has been improved to extend the search area.

$$F_i^{\text{new}} = F_{L\text{best1}} + (F_i - F_{L\text{best1}}).ET + (F_{r1} - F_{r2}).\gamma. \tag{34}$$

In the first jumping step, the current solution (F_i) should be moved to a new location near the location of the best current solution ($F_{L\text{best1}}$) to inherit the best current solution's experience at the previous generation. This will contribute to increase the probability of finding better quality solutions. In summary, the position of the best current solution is chosen instead of random selection from a group that contains the top four best solutions and an average solution of them at the previous generation. Additionally, two randomly selected solutions (F_{r1} and F_{r2}) by taking variables in the F_s solution will bring many advantages in approaching a higher quality solution. As a result, $(F_{r1} - F_{r2})$ is always greater than zero and $(F_{r1} - F_{r2})$ is multiplied by a randomization vector (γ) which is comprised of terms between 0 and 1. The results of multiplication facilitate the expansion of the search space to avoid local traps. Generally, equation (33) has advantages in finding solutions in the local space, and equation (34) is useful in expanding the search area. Therefore, the great combination of equations (33) and (34) will improve the performance of EO significantly. In this research, the choice of the update equation depends on the quality of the current solution (Fit_i) and the mean fitness of all solutions (Fit_{mean}). If the quality value of Fit_i is better than the value of Fit_{mean}, equation (33) is used for generating new solutions. For other cases, equation (34) is applied for new solution update.

The implementation process of IEO for a typical problem is shown in Figure 4.

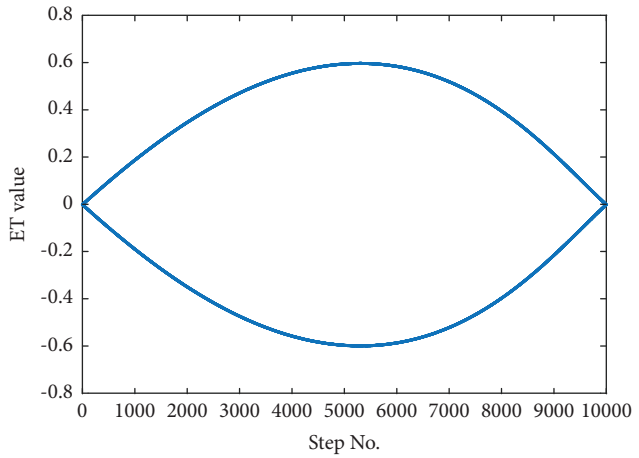

Figure 2: The maximum and minimum values of ET.

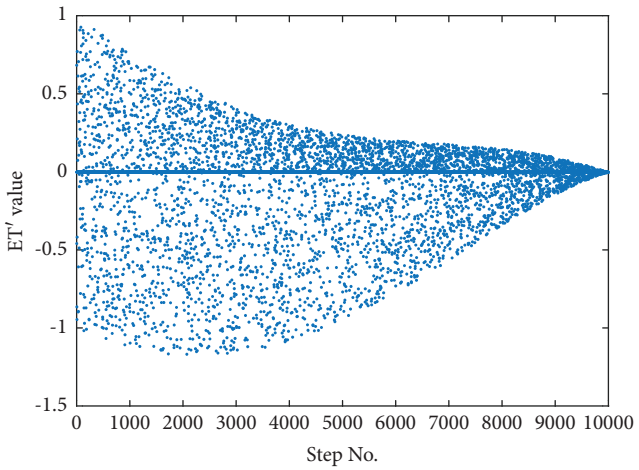

Figure 3: The maximum and minimum values of ET′.

3.2. Application of Improved Equilibrium Optimization

3.2.1. Selection of Decision Variables. In this paper, three DGUs are considered for connecting to IEEE 33-bus, IEEE 69-bus, and IEEE 85-bus radial distribution systems. In this paper, five harmonic flows are simultaneously injected into several linear loads and the harmonic currents affect the entire system. In this study, FW/BWST is chosen to compute power flows at the fundamental frequency and other higher order frequencies. After reaching the power flows, the obtained parameters such as the branch current and the bus voltage at the order frequencies are used to compute the fitness function. Among the input data, the location and capacity of the DGUs are the elements to be determined by using IEO. Thus, each solution (F_i) will consist of location ($L_{\mathrm{DGU},d,i}$) and capacity ($\mathrm{AP}_{\mathrm{DGU},d,i}$) as follows:

$$F_i = \left[L_{DGU,d,i}, AP_{DGU,d,i}\right]; d = 1, \ldots N_{d,g} \text{ and } i = 1, \ldots, N_c. \tag{35}$$

In equation (35), $L_{\mathrm{DGU},d,i}$ and $\mathrm{AP}_{\mathrm{DGU},d,i}$ are the location and capacity of the d^{th} DGU of the i^{th} solution with the limitations as follows:

$$L_{DGU}^{\min} \le L_{DGU,d,i} \le L_{DGU}^{\max}, \tag{36}$$

$$AP_{DGU}^{\min} \le AP_{DGU,d,i} \le AP_{DGU}^{\max}. \tag{37}$$

The two parameters of DGUs will be randomly generated by

$$L_{DGU,d,i} = \mathrm{round}\left(L_{DGU}^{\min} + rand\left(L_{DGU}^{\max} - L_{DGU}^{\min}\right)\right), \tag{38}$$

$$AP_{DGU,d,i} = AP_{DGU}^{\min} + rand\left(AP_{dgu}^{\max} - AP_{DGU}^{\min}\right). \tag{39}$$

3.2.2. Penalty Term for Violation. After the i^{th} new solution is generated, voltage, current, and the harmonic violations are checked as follows:

$$\Delta V_{b,i} = \begin{cases} \left|V^{\min} - V_{b,i}\right|, & \text{if } V_{b,i} < V^{\min}, \\ \left|V^{\max} - V_{b,i}\right|, & \text{if } V_{b,i} < V^{\max}, \\ 0, & \text{else}, \end{cases} \tag{40}$$

$$\Delta I_{bh,i} = \begin{cases} \left|I_{bh}^{\max} - I_{bhDGU,i}\right|, & \text{if } I_{bhDGU,i} > I_{bh}^{\max}, \\ 0, & \text{else}, \end{cases} \tag{41}$$

$$\Delta \mathrm{THD}_{b,i} = \begin{cases} \left|\mathrm{THD}^{\max} - \mathrm{THD}_{b,i}\right| \text{if } \mathrm{THD}_{b,i} > \mathrm{THD}^{\max} \\ 0 \text{ else} \end{cases}, \tag{42}$$

$$\Delta \mathrm{IHD}_{b,i}^{h} = \begin{cases} \left|\mathrm{IHD}^{\max} - \mathrm{IHD}_{b,i}^{h}\right| \text{if } \mathrm{IHD}_{b,i}^{h} > \mathrm{IHD}^{\max} \\ 0 \text{ else} \end{cases}. \tag{43}$$

3.2.3. Fitness Function. The fitness function is a combination of objective function and penalty functions. It is used to evaluate the quality of each solution. In this paper, the fitness function of the i^{th} solution is constructed as follows:

$$\mathrm{Fit}_i = \mathrm{OF} + \sigma_v \cdot \sum_{b=1}^{N_b} \left(\Delta V_{b,i}\right)^2 + \sigma_1 \cdot \sum_{bh=1}^{N_{bh}} \left(\Delta V_{bh,i}\right)^2 + \sigma_{THD} \cdot \sum_{b=1}^{N_b} \left(\Delta \mathrm{THD}_{b,i}\right)^2 + \sigma_{1HD} \sum_{b=1}^{N_b} \left(\Delta \mathrm{IHD}_{b,i}^{h}\right)^2. \tag{44}$$

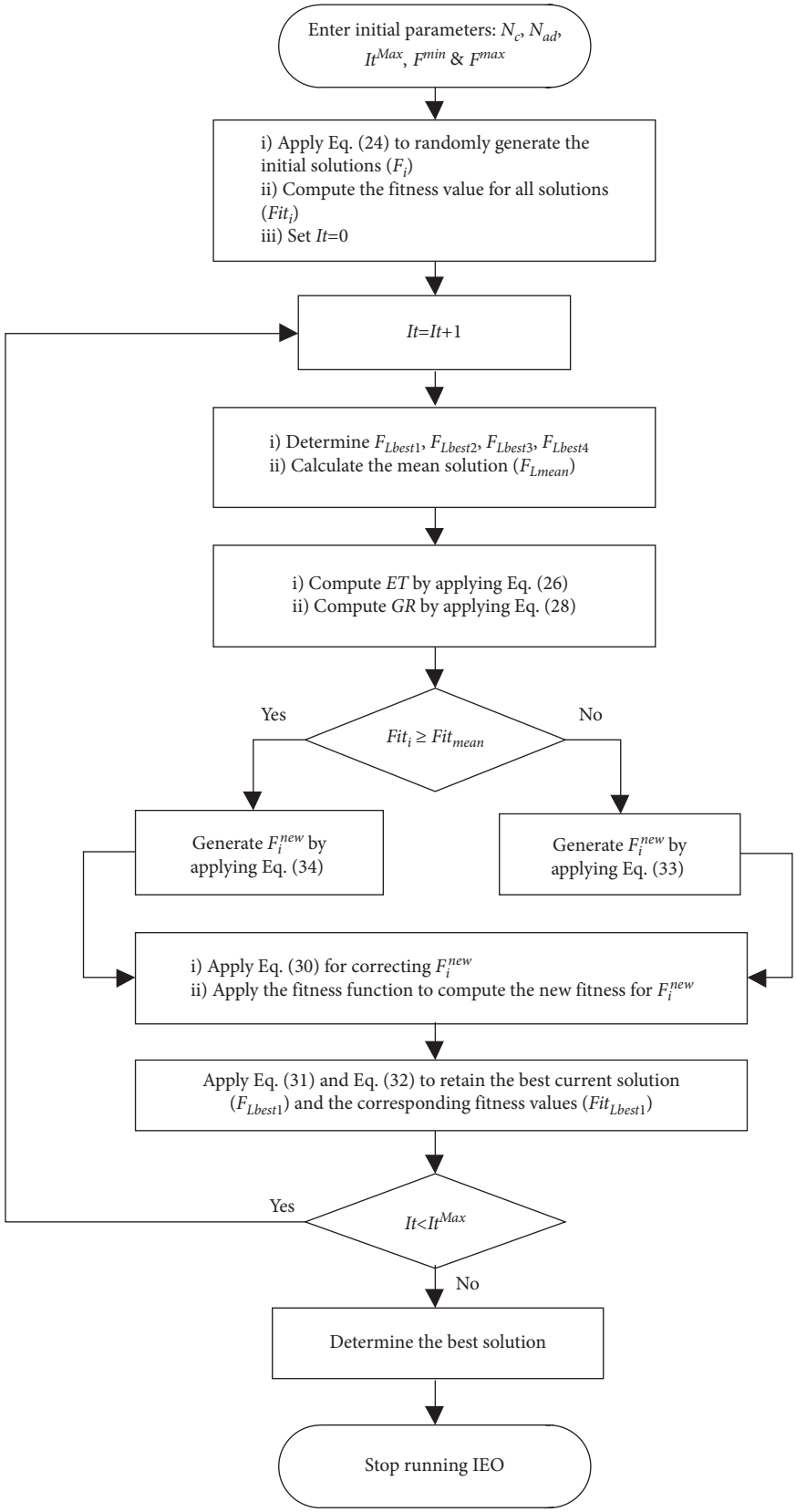

Figure 4: The implementation process for the whole of IEO for the typical problem.

3.2.4. Correction for the Violated Variables. When a new solution (i.e., the new location and the new capacity of DGUs) is produced, it has to be checked and adjusted throughout the search for the optimal solution as follows:

$$L_{\mathrm{DGU},d,i} = \begin{cases} L_{\mathrm{DGU}}^{\max} \text{ if } L_{DGU,d,i} > L_{\mathrm{DGU}}^{\max} \\ L_{\mathrm{DGU}}^{\min} \text{ if } L_{DGU,d,i} > L_{\mathrm{DGU}}^{\min}, \\ L_{\mathrm{DGU},d,i} \text{ else} \end{cases} \tag{45}$$

$$\mathrm{AP}_{\mathrm{DGU},d,i} = \begin{cases} \mathrm{AP}_{\mathrm{DGU}}^{\max}, & \text{if } \mathrm{AP}_{\mathrm{DGU},d,i} > \mathrm{AP}_{\mathrm{DGU}}^{\max}, \\ \mathrm{AP}_{\mathrm{DGU}}^{\min}, & \text{if } \mathrm{AP}_{\mathrm{DGU},d,i} > \mathrm{AP}_{\mathrm{DGU}}^{\min}, \\ \mathrm{AP}_{\mathrm{DGU},d,i}, & \text{else.} \end{cases} \tag{46}$$

3.2.5. Implementation Process of the Whole IEO for DGU's Problem. The process of searching location and capacity of DGUs in the distribution systems by using IEO is briefly presented in Figure 5, and the implemented steps are as follows:

Step 1: survey and select parameters of proposed method.

The survey is implemented to select the appropriate number of concentrations and the maximum number of iterations. Besides, the parameters of the proposed algorithm are also selected.

Step 2: generate the initial solutions at random.

The initial solutions of the placement and sizing of DGUs are randomly created within the allowable limits, which are predetermined by using equations (38) and (39). For each newly generated solution, all constraints are checked to calculate the penalty terms for bus voltage, branch current, total harmonic distortion, and individual harmonic distortion by applying equations (40)–(43), respectively. After that, the sum of these penalty terms and the objective function are determined to calculate the fitness function as equation (44). The function value is also quality of each solution.

Step 3: start loop in the algorithm.

The first iteration is started to perform the promising solution search iterative algorithm.

Step 4: determine the group of solutions with high quality.

Based on their fitness values in Step 2, the four most effective solutions are determined and assigned to $F_{L\mathrm{best1}}$, $F_{L\mathrm{best2}}$, $F_{L\mathrm{best3}}$, $F_{L\mathrm{best4}}$ for the calculation of the arithmetic mean ($F_{L\mathrm{mean}}$). The selection of good solutions contributes significantly in improving the quality of the next generation.

Step 5: calculate important terms for the new solution generation equation.

Two important terms with a high influence on the performance of the proposed algorithm are the exponential term (ET) and the generation rate (GR). ET and GR can be found by solving complex equations (26) and (28), respectively. They are important terms of the new solution generation equation.

Step 6: check the conditions for selecting the method of new solution generation.

Compare the fitness value of each solution (Fit_i) with the mean fitness value ($\mathrm{Fit}_{\mathrm{mean}}$) to select the equation for creating the next generation (F_i^{new}).

Step 7: create the new solution generation.

Either equation (33) or equation (34) is employed to calculate the i^{th} new solution. If $\mathrm{Fit}_i \geq \mathrm{Fit}_{\mathrm{mean}}$ occurs, the i^{th} new solution is found by utilizing equation (34). For another case, equation (33) is used.

Step 8: check the violation for correction and calculate the fitness value for each new solution.

Each created new solution should be checked for limit violations and corrected as the rules in equations (45)–(46). Penalty and objective values of these corrected solutions are calculated by using equations (40)–(43). Then, fitness value in equation (44) is obtained for each new solution.

Step 9: find the best current solution.

Through the evaluation of the fitness values, the best current solution ($F_{L\mathrm{best1}}$) and its fitness value ($\mathrm{Fit}_{L\mathrm{best1}}$) are retained by applying the rules in equations (31) and (32).

Step 10: check the termination condition.

The condition for stopping the iteration is checked by comparing It and $\mathrm{It}^{\mathrm{Max}}$. If $\mathrm{It} = \mathrm{It}^{\mathrm{Max}}$ happens, stop implementing the proposed method and report the best results. For other cases, It is increased to (It + 1) and go back to Step 4.

4. Simulation Results

This section presents the applications of EO, ABC, SSA, and the proposed IEO for minimizing power loss on all distribution branches and costs of DGUs while satisfying all constraints including branch current, voltage profile, and harmonic distortions. In addition to the comparison with EO, ABC, and SSA, the proposed IEO is also compared to other published methods such as GA, PSO, GA/PSO, SA, HSA, BFOA, and BSOA via the simulation for three IEEE distribution systems with 33, 69, and 85 buses.

In this paper, each implemented method is independently run 50 times on a personal computer with a 1.8 GHz processor and 8.0 GB RAM in MATLAB environment. To get a fair evaluation for the implemented methods, the population is surveyed from 20 to 40 with step size of 10, and the suitable population is selected as 30. Besides, ItMax is set to 200, 230, and 250 iterations for 33, 69, and 85 buses systems, respectively. Moreover, the parameters for methods are also taken appropriately. For ABC algorithm, the colony size, which is the sum of employed bees and onlooker bees, is set to the population, and employed bees and onlooker bees have the same quantity [38]. For SSA, the coefficient of c_1 is the obtained result from function of $2.e^{-(4.It/It^{Max})^2}$, and the

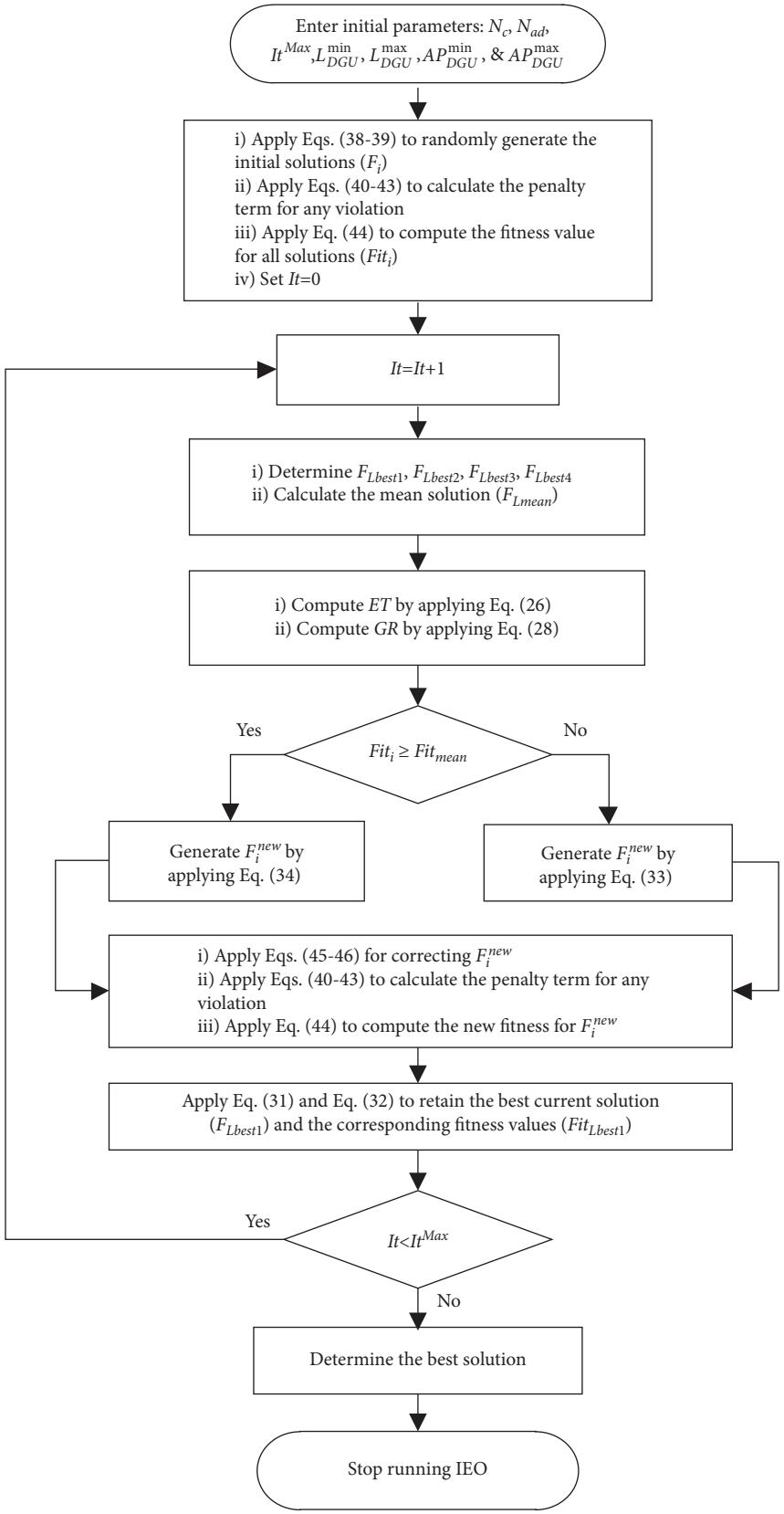

Figure 5: The implementation process of IEO for placing DGUs in radial distribution networks.

coefficients of c_2 and c_3 are generated numbers randomly from 0 to 1 [29]. To run the proposed IEO and EO, parameters of α_1, α_2, and GP are set to 2, 1, and 0.5, respectively [32]. For calculating the costs of DGUs in the multi-objective function, investment and maintenance and operation costs are, respectively, 770 ($/kW) and 0.01 ($/kWh) [4] while the discount rate is selected to be 9% for a 20-year plan. Besides, this study applied the weighted sum method to decide the best compromise solution. Thus, the value of each weighting coefficient depends on the importance of each element in the multi-objective function [31]. Its value can be adjusted by user. The larger value of a weighting coefficient, the greater its significance in the multi-objective function. In this study, the authors considered minimizing of power loss to be more important than the costs of DGUs in the distribution system. Thus, the total power loss receives significant weight (ω_I) of 0.8 and light weight of the cost (ω_{II}) of 0.2. Furthermore, all test systems are evaluated in the case of harmonic distortions. Hence, the five harmonic flows are simultaneously injected to linear loads, and the detailed information is presented in Table 2 [20].

4.1. Case 1: IEEE 33-Bus Radial Distribution System. The configuration of the 33-bus distribution system is shown in Figure 6. The load and line data of the system are collected from [31]. The basic system has total power loss of 0.2110 MW and total load demand of 3.715 MW and 2.300 MVar. In this case, three DGUs can be installed at three different buses from bus 2 to bus 33, and the capacity of each DGU can be chosen from 0.0 MW to 2.0 MW [34]. Furthermore, harmonic flows are also injected simultaneously into six buses 9, 15, 20, 24, 29, and 32.

After 50 trial runs are implemented, the worst, average, and best fitness values are collected and clearly presented in Table 3. According to the presented results in Table 3, the best fitness value of the implemented methods such as ABC, SSA, EO, and IEO is 0.3866, 0.3837, 0.3832, and 0.3828, respectively. The value of the proposed method (IEO) is lower than that of ABC, SSA, and EO. In other words, IEO can find a more optimal solution than ABC, SSA, and EO. Moreover, the mean and worst fitness values of IEO are smaller than those of others. For a clearer view of performance comparison, fitness values of 50 trial runs of these methods are sorted and plotted in Figure 7. All points on the curve of IEO are located at the lower positions than those of others, and the fluctuation of IEO is very small in the range of [0.3828, 0.3896]. Thus, IEO is the most stable method.

Table 4 shows the objective values in the multi-objective function for comparison. The first objective and the corresponding power loss of IEO are 0.3863 and 0.0815 MW, which are equal to those of SSA and better than those of others. About the contribution to power loss, the proposed solution of IEO can drastically reduce losses in the system from 0.2110 MW to 0.0815 MW, while others can reduce the loss to 0.0816 MW (the second-best method, EO) and 0.1061 MW (the worst method, GA [39]). The power loss on branches in the base system and the hybrid system with DGUs by using optimal solution of IEO is plotted in Figure 8. The figure indicates that the power loss on branches in the IEEE 33-bus system before and after placing DGUs has a relatively high deviation and approximately all branches of the system with the installation of DGUs have lower power losses than those in the system without DGUs. Especially, the loss reduction is very high for branches close to slack bus 1, including branches 1, 2, 3, 4, 5, 7, and 27. Other branches cannot reach the same high power loss reduction, but the loss reduction is still relatively high, for example, from branches 8 to 12 and from branches 25 to 30. The loss reduction on other remaining branches is not significant, but there are still small values. The very small reduction cannot be identified in the figure due to the constraint of figure size. In general, the installation of DGUs can bring high benefits to the system in reducing power loss.

Table 2: The detailed information of five harmonic flows.

Harmonic order	Magnitude (%)	Angle (°)
5	0.765	28
7	0.627	−180
11	0.248	−59
13	0.127	79
17	0.071	−253

The second objective and the corresponding cost of IEO are 0.3690 and $3.4753 million, which are smaller than those of others excluding BFOA [41], BSOA [42], and ABC. Clearly, the solution from IEO can save $1.2246 million and $0.0021 million in comparison to the worst method (GA [39]) and the original method (EO), respectively. So, it can lead to a conclusion that the proposed IEO is more effective than GA [39], PSO [39], GA-PSO [39], LSF-SA [40], SSA, and EO. For the comparison with BFOA [41], BSOA [42], and ABC, the proposed IEO cannot reach better cost, but it reaches much better power loss. This is a trade-off in solving multi-objective function problem. This result is due to the selection of weighting coefficients, and it cannot be avoided when comparing a proposed method to many other methods. However, the proposed IEO has reached better fitness function than the three methods; meanwhile, fitness function is also the multi-objective function and used to evaluate performance of methods. As a result, the proposed IEO is also more effective than the compared methods in solving the problem of DGU placement in the IEEE 33-bus distribution system.

In this research, harmonic distortions and voltage profile are considered as the two constraints of the multi-objective function. According to IEEE Std. 519, THD and IHD should not exceed 5% and 3%, respectively. However, the modified system with nonlinear loads and without DGU connection has exceeded the limitations of both THD and IHD as shown in Figure 9. Specifically, the largest values of THD and IHD at frequency orders are 7.2504% and 4.7037%, respectively. But the violation of harmonic distortions is solved after placing three DGUs by using IEO, and these factors are reduced to 4.6203% and 3.0%, respectively.

Similarly, the voltage profile of the modified system before and after placing three DGUs is also plotted in Figure 10. In the system without DGUs, many buses have

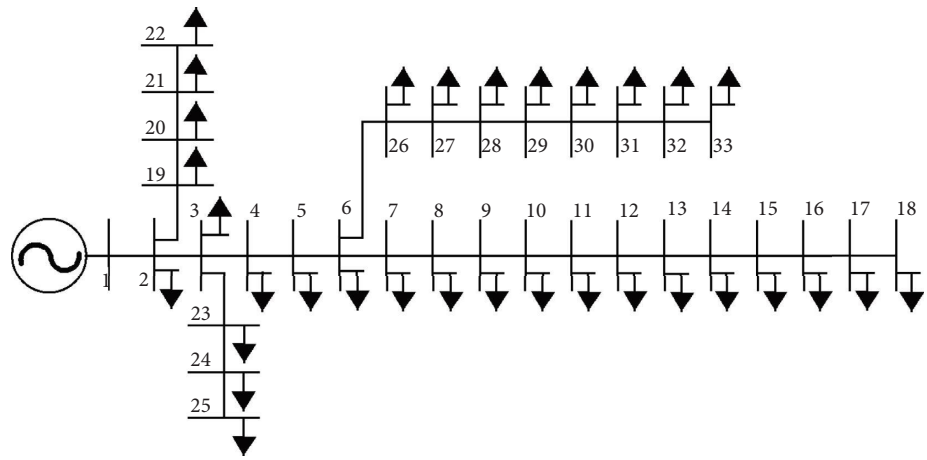

Figure 6: IEEE 33-bus radial distribution system.

Table 3: The comparison of fitness values found by four implemented methods for case 1.

Method	ABC	SSA	EO	IEO
The worst fitness value	0.4141	0.4198	0.3969	0.3896
The mean fitness value	0.3980	0.3951	0.3861	0.3856
The best fitness value	0.3866	0.3837	0.3832	0.3828

lower voltage than 0.95 pu and the worst voltage is 0.9038 pu. But in the system with three placed DGUs, the voltage is significantly improved and it has the range from 0.9613 pu to 1.0 pu. Clearly, DGUs can improve the voltage of the system effectively.

Optimal solutions of the applied system are reported in Table S1 in Supplementary Materials.

4.2. Case 2: IEEE 69-Bus Radial Distribution System. Figure 11 shows the structure of the IEEE 69-bus radial distribution system, and data of the system can be taken from [20]. In addition, general information of the system is comprised of total power loss of 0.2245 MW and total loads of 3.8019 MW and 2.6941 MVar. In this system, three DGUs can be installed from buses 2 to 69 and the power of each DGU can be chosen to be from 0.0 MW to 2.0 MW. Since this research is being considered under harmonic conditions, the harmonic flows shown in Table 2 are injected simultaneously into nine buses 12, 18, 19, 22, 25, 34, 46, 56, and 65.

The worst, mean, and best fitness values for the 50 trial runs are clearly presented in Table 5. According to the collected data from Table 5, the best fitness values for ABC, SSA, EO, and IEO are 0.3279, 0.3267, 0.3264, and 0.3262, respectively. The best fitness value of IEO is smaller than that of all other methods. Clearly, the modifications carried out on IEO have a positive impact on the effectiveness of the method and they support IEO reach the most optimal solution among the four run methods. To prove the high stability of IEO, the mean of fifty trial runs and the fifty runs in detail are also reported in Table 5 and Figure 12. The mean value of IEO is 0.3267, and it is smaller than 0.3317, 0.3298, and 0.3269 from ABC, SSA, and EO, respectively. In Figure 12, the fifty fitness values of the methods are re-sorted and the curve of IEO is almost below the curves of other methods. Furthermore, this curve has very small fluctuations while others have significant fluctuations. In summary, IEO can reach the best performance and the most stable search ability among the four run methods.

Table 6 shows a summary of two objectives and corresponding power loss and cost obtained by implemented and compared methods. The first objective and the corresponding power loss of IEO are 0.3206 and 0.07197 MW, whereas those of the second-best method (EO) and the worst method (GA [39]) are (0.3207 and 0.0720 MW) and (0.3962 and 0.0889 MW), respectively. The power loss on branches in the base system and the hybrid system with DGUs by applying the optimal solution from IEO is clearly presented in Figure 13. It has been shown that the power loss in the IEEE 69-bus system before and after the integration of DGUs is significantly different. Specifically, the power loss reduction is greater on branches 4 to 9, 11 to 14, and 52 to 60. The loss reduction on other remaining branches is much smaller than these branches. Overall, thanks to the proper installation of DGUs, branch losses are drastically reduced for more economic and technical benefits.

The second objective and the corresponding cost of IEO are 0.3487 and $3.2840 million, respectively. These values are higher than those of MOBA [34], BFOA [41], HSA [43], and SSA but lower than other methods such as GA [39], PSO [39], GA-PSO [39], LSF-SA [40], ABC, and EO. Excluding the comparison with MOBA [34], BFOA [41], HSA [43], and SSA, IEO can save up to $1.4209 million and $0.0028 million when compared to the worst method (GA [39]) and the second-best method (EO). Comparing IEO with MOBA, BFOA, HSA, and SSA, the optimal solution from the proposed IEO method cannot achieve better cost, but it can get much better power loss reduction. As mentioned, this is a trade-off in solving the multi-objective function problem. The results are affected by the selected weighting factors, and it is unavoidable when compared with many other methods.

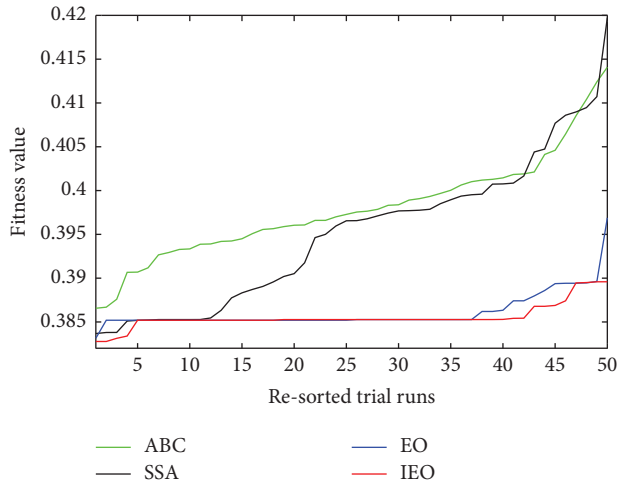

Figure 7: The fitness values of 50 trial runs in increasing arrangement for the IEEE 33-bus system.

Table 4: The comparison of the objective function values for the IEEE 33-bus system.

Method	OF_I	OF_{II}	OF	Real loss (MW)	Cost of DGUs (million $)
GA [39]	0.5028	0.4990	0.5021	0.1061	4.6999
PSO [39]	0.4993	0.4980	0.4990	0.1054	4.6903
GA-PSO [39]	0.4900	0.4980	0.4916	0.1034	4.6901
LSF-SA [40]	0.3889	0.4113	0.3933	0.0820	3.8735
BFOA [41]	0.4659	0.2784	0.4284	0.0983	2.6234
BSOA [42]	0.4221	0.2780	0.3933	0.0891	2.6182
ABC	0.3941	0.3565	0.3866	0.0832	3.3572
SSA	0.3863	0.3733	0.3837	0.0815	3.5161
EO	0.3867	0.3692	0.3832	0.0816	3.4774
IEO	0.3863	0.3690	0.3828	0.0815	3.4753

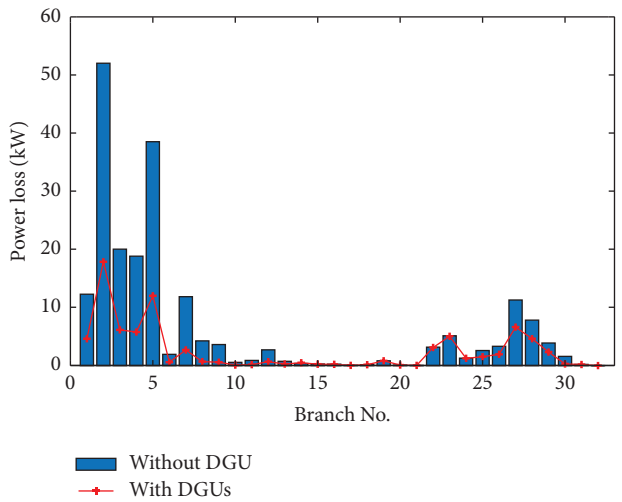

Figure 8: Power loss on distribution lines in IEEE 33-bus radial distribution system before and after placing DGUs.

However, the multi-objective function of IEO with 0.3262 is smaller than these methods with 0.3281, 0.3376, 0.3684, and 0.3267. Thus, IEO is actually more effective than others in solving the problem of the location of DGUs in the IEEE 69-bus system.

Using the optimal solution obtained by the proposed IEO method, THD and IHD of each bus in the base system without DGUs and modified system with DGUs are plotted in Figure 14. Data from the figure indicate that the maximum values of THD and IHD of the base system are 5.4287% and 3.5087%, but those from the modified system with the application of IEO are 3.0232% and 1.9495%, respectively. In addition, the view on THD and IHD of the whole 69 buses also sees the significant improvement of the modified system from buses 5 to 28 and from buses 51 to 69. In another view, the improvement of voltage is also presented in Figure 15. The minimum bus voltage is 0.9092 pu for the base system but is much higher and equal to 0.9761 pu for the modified system with DGU connection. Voltage values at buses 5 to 28 and 51 to 69 in the modified system with DGUs are much higher than those in the base system without DGUs. Clearly, the installation of DGUs in the distribution system can reach an extra benefit in reducing harmonic distortions and improving voltage profile.

Optimal solutions of the applied system are reported in Table S2 in Supplementary Materials.

4.3. Case 3: IEEE 85-Bus Radial Distribution System. Figure 16 shows the configuration of the IEEE 85-bus radial distribution system. The load data and line data of the system

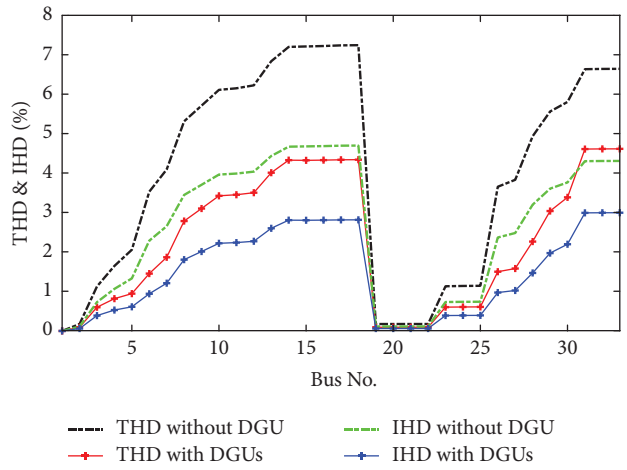

Figure 9: THD (%) and IHD (%) of the IEEE 33-bus system before and after DGUs connection.

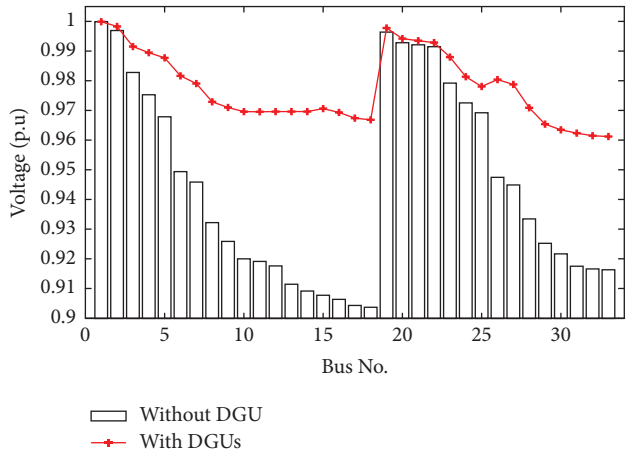

Figure 10: Voltage profile of the IEEE 33-bus system before and after DGUs connection.

are collected from [31]. The system has the total loss of 0.3161 MW and the total loads of 2.5703 MW and 2.6221 MVar. For reducing loss and cost, location and size of three DGUs are selected from bus No. 2 to bus No. 85 and from 0.0 MW to 2.0 MW. To produce distortion of voltage wave, five harmonic flows in Table 2 are also injected to seven buses 5, 12, 25, 34, 56, 65, and 77.

The best, mean, and worst fitness values of ABC, SSA, EO, and IEO are presented in Table 7. IEO is also still the best method with all smallest values excluding the comparison of the worst fitness value with EO. The fifty runs are also presented in detail in Figure 17 by sorting fitness from the smallest to the highest values shown in different color curves. Almost all points on red curve of IEO are lower than other points on three other curves of ABC, SSA, and EO. So, IEO is the most powerful method among the four applied ones for the system.

Table 8 presents the results obtained by the four methods in detail. There are no comparisons with other published methods for the system because there were no studies regarding the IEEE 85-bus system before. The first objective and the corresponding power loss of IEO are, respectively, 0.4792 and 0.1515 MW, which are better than those of others. In other words, the solution of IEO can reduce the power loss from 0.3161 MW to 0.1515 MW while ABC, SSA, and EO can reduce the loss to a higher value, 0.1553 MW, 0.1524 MW, and 0.1521 MW, respectively. It has been strongly proven that the solution from IEO is more effective in terms of power loss reduction than others. To see the effectiveness of loss reduction thanks to the solution obtained by IEO, the power losses on all branches in the IEEE 85-bus system for two cases, with and without DGUs, are plotted in Figure 18. There is outstanding power loss reduction on the first branches, from branch 1 to branch 7. Especially, the highest loss reduction is reached on branch 7 and the loss reduces from higher than 100 kW to under 50 kW. Although the loss reduction on branches 1 to 6 is not as effective as on branch 7, the reduction is relatively high, from some kW to 20 kW. The loss reduction on other branches is not as effective or even there is no loss reduction on some branches. The loss reduction on branches 24 to 29, branch 56, and branch 57 is still high while the reduction on other remaining branches is not identified. In general, power loss reduction is effective in all branches, but the total loss reduction is still high, from 0.3161 MW to 0.1515 MW. The high loss reduction is only for one hour, and it indicates that the placement of DGUs in distribution system is very useful.

The second objective and the corresponding cost of IEO are 0.3248 and $3.0593 million, which are slightly better than other compared methods. As presented, this is a trade-off in solving the multi-objective function problem.

By applying the best solution from IEO, THD and IHD of each bus and voltage profile in the base system without DGUs and modified system with DGUs are plotted in Figures 19 and 20, respectively. The maximum values of THD and IHD in the base system are 6.1504% and 3.9840%, but those from the modified system with the application of IEO are 4.0445% and 2.6233%, respectively. Approximately all buses in the modified system can reach much better THD and IHD than those in the base system. The base system has the smallest voltage with 0.8713 pu, which is much smaller than the permissible voltage limits with [0.95, 1.05] pu. However, after the three DGUs are connected to the system, the voltage profile is improved drastically with the lowest voltage value of 0.9500 pu. The view on voltage of all buses in the two cases can indicate that the modified system can have a much better voltage profile than the base system. Clearly, the installation of three DGUs can cut the harmonic distortion and increase the voltage of buses for the IEEE 85-bus system. Finally, these outstanding results show that the proposed method (IEO) is indeed more powerful than others in solving the problem of DGU placement in the considered distribution system.

Optimal solutions of the applied system are reported in Table S3 in Supplementary Materials.

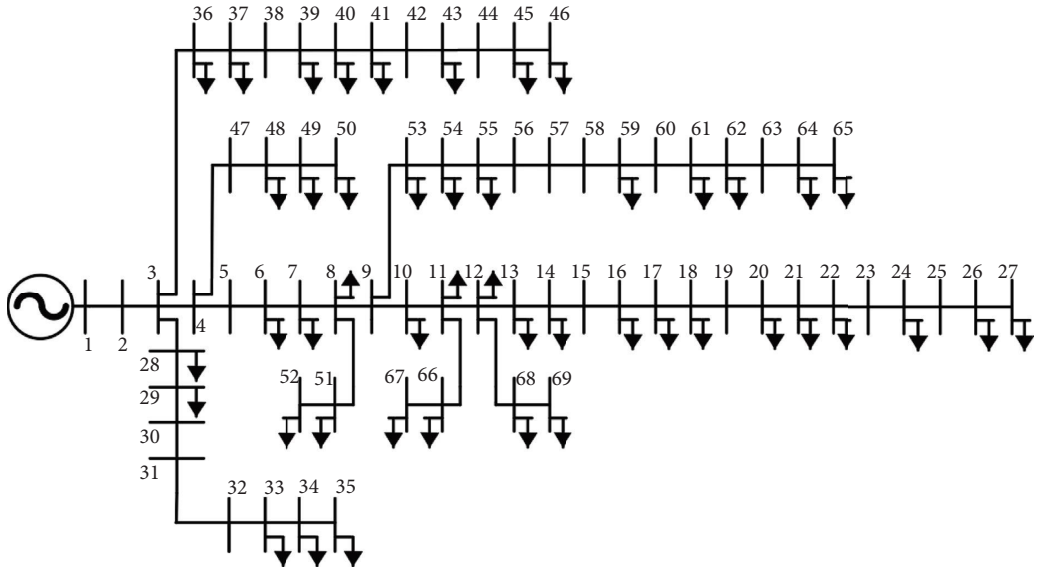

Figure 11: The IEEE 69-bus radial distribution system.

Table 5: The comparison of fitness values found by four implemented methods for the IEEE 69-bus system.

Method	ABC	SSA	EO	IEO
The worst fitness value	0.3396	0.3454	0.3283	0.3282
The mean fitness value	0.3317	0.3298	0.3269	0.3267
The best fitness value	0.3279	0.3267	0.3264	0.3262

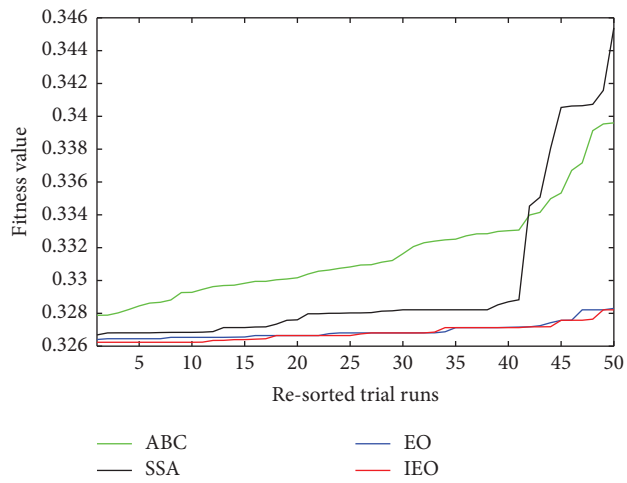

Figure 12: The fitness values of 50 trial runs in increasing arrangement for the IEEE 69-bus system.

5. Shortcomings of the Proposed Method and Research Expansion

In this paper, the proposed method (IEO) has outstanding performance over EO, ABC, and SSA. As shown in Figures 7, 12, and 17, IEO can reach many better solutions than EO, ABC, and SSA. Furthermore, IEO also has very small fluctuations, but the fluctuations from ABC, SSA, and EO are very high. As compared to previous methods in other studies, Tables 4 and 6 indicate that the proposed IEO also reaches better solutions with smaller cost and loss. For the three test systems, IEO is really effective, but it cannot avoid shortcomings such as solving larger and more complicated systems. In fact, IEO is successful in finding optimal solutions of the problems because the number of control variables is not high. It is 6 for all three test systems, including three locations and three rated powers. In addition, the variable boundaries are not large. The location can be from 2 to 33 for the first system, to 69 for the second system, and to 85 for the last system, and the rated powers can be from 0 to 2.0 MW. IEO is based on four best solutions to update new solutions, and almost all newly obtained solutions are near the four best solutions. So, local search has a huge contribution to the promising results obtained by IEO. This feature can be the highest limitation of IEO when it is applied for large-scale problems with a high number of control variables and very large search spaces. The second limit of IEO is convergence speed to high-quality solutions. Although IEO is tested on the three test systems with only six control variables and small search space, it needs high enough values for control parameters. Population size is set to 30 while iteration number is 200 for the first system, 230 for the second system, and 250 iterations for the last system. Due to the two limitations, IEO can be ineffective for larger and more complicated problems, and it may need more improvements. Additionally, in this study, we supposed the highest power of DGUs is 2.0 MW, and DGUs can change in the range between 0 and 2.0 MW. This assumption may not be true in practice. So, in the future, the authors will consider

Table 6: The comparison of the objective function values for the IEEE 69-bus system.

Method	OF_I	OF_{II}	OF	Real loss (MW)	Cost of DGUs (million $)
MOBA [34]	0.3268	0.3333	0.3281	0.0734	3.1393
GA [39]	0.3962	0.4996	0.4168	0.0889	4.7049
PSO [39]	0.3715	0.4980	0.3968	0.0834	4.6900
GA-PSO [39]	0.3612	0.4980	0.3886	0.0811	4.6901
LSF-SA [40]	0.3434	0.3635	0.3474	0.0771	3.4239
BFOA [41]	0.3350	0.3480	0.3376	0.0752	3.2776
HSA [43]	0.3866	0.2955	0.3684	0.0868	2.7833
ABC	0.3225	0.3493	0.3279	0.0724	3.2893
SSA	0.3216	0.3472	0.3267	0.0723	3.2699
EO	0.3207	0.3490	0.3264	0.0720	3.2868
IEO	0.3206	0.3487	0.3262	0.07197	3.2840

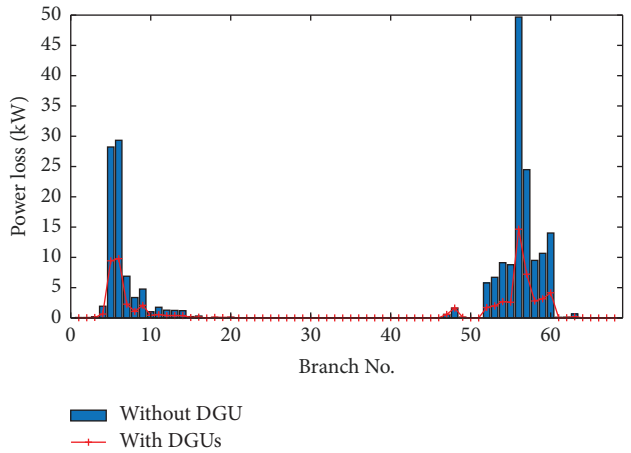

Figure 13: Power loss on distribution lines in IEEE 69-bus radial distribution system before and after placing DGUs.

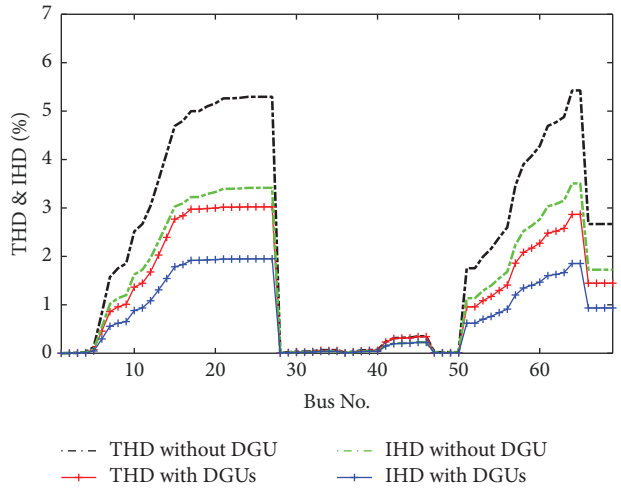

Figure 14: THD (%) and IHD (%) of the IEEE 69-bus system before and after DGUs connection.

the uncertainties of solar radiation as well as wind speed for solar photovoltaic units and wind turbines. Realistically, the power of solar photovoltaic units and wind turbines mainly depends on the primary energies [44, 45]. For considering these uncertainties, they can be based on recorded historical data and combined with the probability density function to predict the power for solar photovoltaic units and wind turbines [46].

For the cases that systems change topology because of expansion or reconfiguration, the application of the proposed IEO or other metaheuristic algorithms to solve the optimization problem is the same as long as the grid data

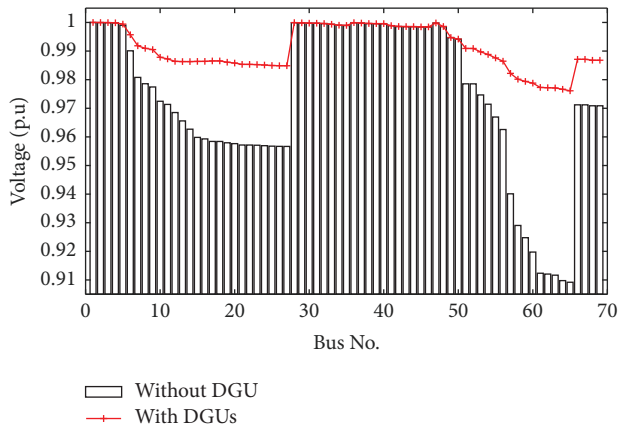

Figure 15: Voltage profile of the IEEE 69-bus system before and after DGUs connection.

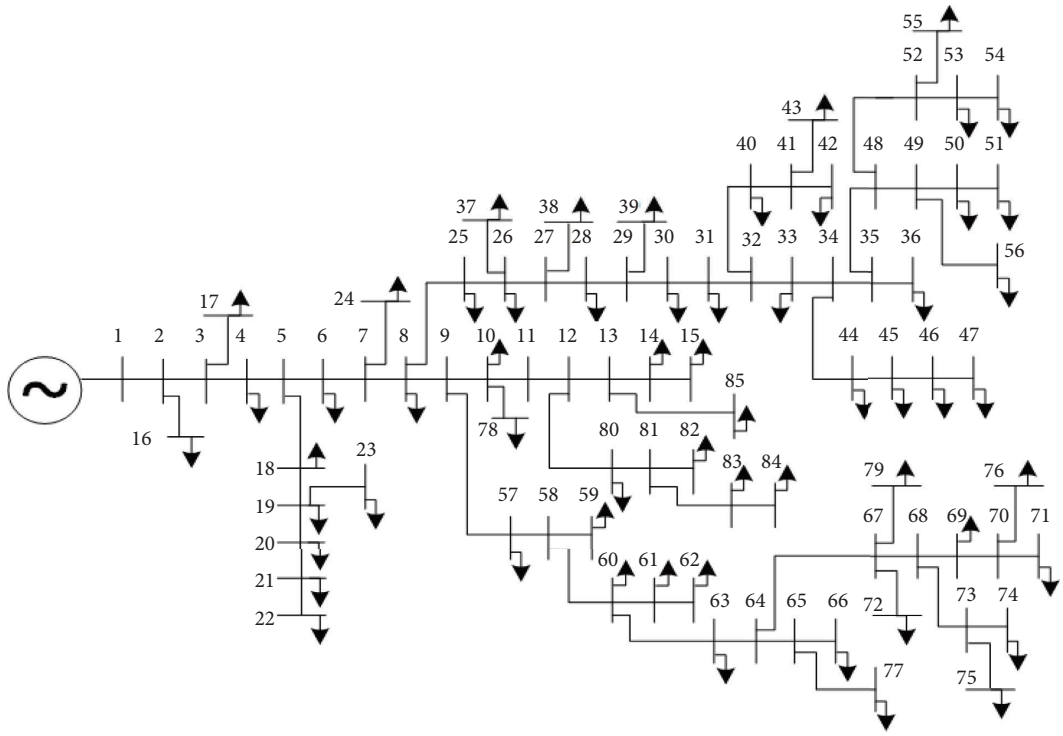

Figure 16: The IEEE 85-bus radial distribution system.

Table 7: The comparison of fitness values found by four implemented methods for the IEEE 85-bus system.

Method	ABC	SSA	EO	IEO
The worst fitness value	0.5381	0.5608	0.4819	0.4842
The mean fitness value	0.4860	0.4733	0.4633	0.4614
The best fitness value	0.4546	0.4492	0.4489	0.4483

such as load and line data are given or calculated at each computation iteration. For other cases that the systems need the installation of capacitors and/or wind turbines, the problem will have more control variables, including the location and rated power of the capacitors and/or wind turbines. It is noted that rated power of capacitors is reactive power while that of wind turbines is comprised of active and reactive power [45]. Then, the additional control variables are put in the data and the forward/backward sweep technique is run to reach dependent variables as those in the current problem, including current, voltage, and individual and total harmonic distortions. These independent variables are checked and penalized if they are beyond predetermined boundaries. The objective function and the penalty terms

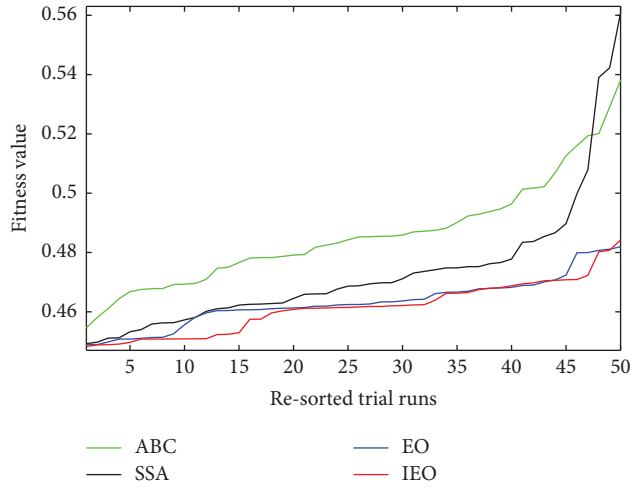

Figure 17: The fitness values of 50 trial runs in increasing arrangement for the IEEE 85-bus system.

Table 8: The comparison of the objective function values for the IEEE 85-bus system.

Method	OF_I	OF_{II}	OF	Real loss (MW)	Cost of DGUs (million $)
ABC	0.4912	0.3083	0.4546	0.1553	2.9036
SSA	0.4822	0.3176	0.4492	0.1524	2.9915
EO	0.4812	0.3198	0.4489	0.1521	3.0115
IEO	0.4792	0.3248	0.4483	0.1515	3.0593

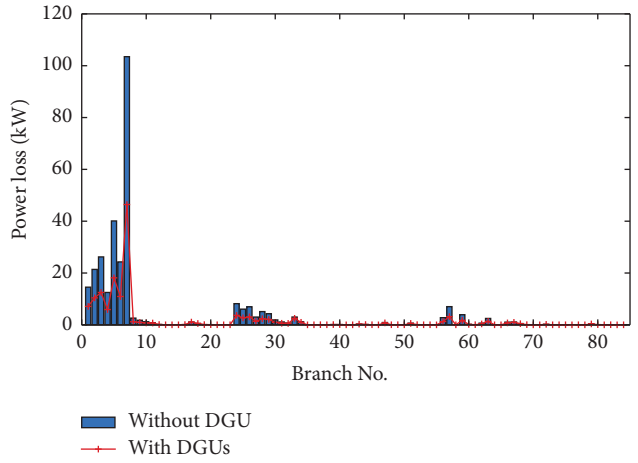

Figure 18: Power loss on distribution lines in IEEE 85-bus radial distribution system before and after placing DGUs.

become fitness function to evaluate the performance of IEO as well as other metaheuristic algorithms. In summary, a higher number of installed DGUs lead to a higher number of considered control variables, and the implementation of IEO for optimally placing separately or simultaneously different types of DGUs is the same.

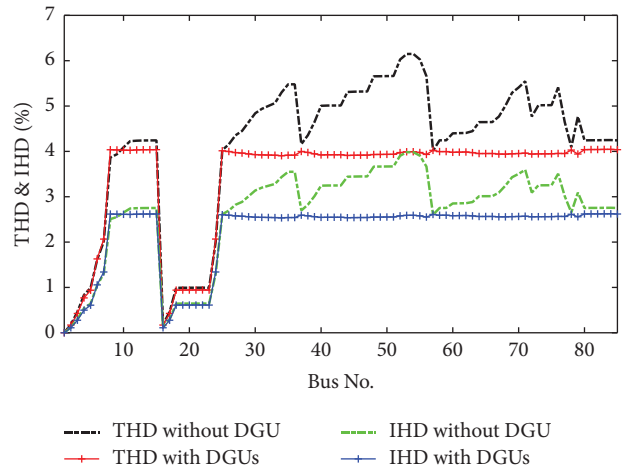

Figure 19: THD (%) and IHD (%) of the IEEE 85-bus system before and after DGUs connection.

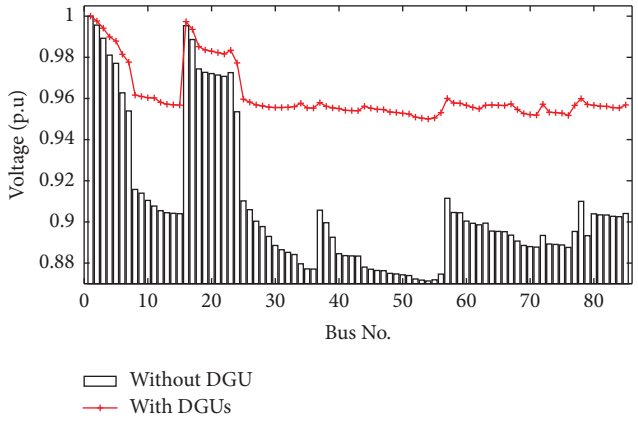

Figure 20: Voltage profile of the IEEE 85-bus system before and after DGUs connection.

6. Conclusions

This research proposed improved equilibrium optimizer (IEO) to reach higher solutions and more stable search performance than other methods in solving the optimization problem of installing DGUs in three distribution systems for maximizing the economic and technical benefits. Overall, the main contributions of the study can be briefly summarized as follows:

(i) The proposed method could reach more promising solutions for the problem than conventional EO. Realistically, the average values of the fitness function of IEO for the three systems were 0.3856, 0.3267, and 0.4614 while these values of the second-best method (EO) were 0.3861, 0.3269, and 0.4633, respectively. As compared from the obtained results, the proposed method is not only better than the original method but also better than other implemented methods (ABC, SSA, and EO) and previously published methods (MOBA, GA, PSO, GA-PSO, LSF-SA, HSA, BFOA, and BSOA). This proves that the improvements in IEO have been remarkably effective.

(ii) For the first objective of minimizing power loss, by applying the optimal solution of IEO, it could reduce the loss from 0.2110 MW to 0.0815 MW for the first system, from 0.2245 MW to 0.07197 MW for the second system, and from 0.3161 MW to 0.1515 MW for the third system. In addition, the second objective was also optimized effecitvely. The total cost over 20 years was only $3.4753 million, $3.2840 million, and $3.0593 million for the three systems, respectively.

(iii) The proposed solutions from IEO also satisfied all the constraints. It has given excellent optimal solutions for placing DGUs that can mitigate harmonic distortions and keeps it in IEEE Std. 519. In addition, the voltage profiles were also significantly enhanced with the voltage range from [0.9038, 1.0] pu to [0.9613, 1.0] pu, from [0.9092, 1.0] pu to [0.9761, 1.0] pu, and from [0.8713, 1.0] pu to [0.95, 1.0] pu for three systems, respectively.

Clearly, the contributions of the placement of DGUs are significant for distribution systems. However, DGUs will bring more benefits to the systems if DGUs are combined with smart inverters and battery energy store system (BESS). Smart inverters can stabilize the operation of DGUs, meanwhile BESS can store energy for the case that the solar- or wind-based DGUs produce higher power than load demand. The optimization operation of the distribution systems with the presence of DGUs, smart inverters, and BESS problem is an upcoming direction of the study.

Abbreviations

ABC:	Artificial bee colony algorithm
BBO:	Biogeography-based optimization
BFOA:	Bacterial foraging optimization algorithm
BPSO-SLFA:	Binary particle swarm optimization and shuffled frog leap algorithm
BSOA:	Backtracking search optimization algorithm
DGU(s):	Distributed generation unit(s)
GA:	Genetic algorithm
HSA:	Harmony search algorithm
LSF-SA:	Loss sensitivity factor and simulated annealing algorithm
MOBA:	Multi-objective bat algorithm
PCC:	Point at common coupling
PSO:	Particle swarm optimization
RNN:	Recurrent neural system
SFO:	Sunflower optimization algorithm
SPEA2:	Strength Pareto evolutionary algorithm 2
SSA:	Salp swarm algorithm
VS-CBGA:	Vortex search and Chu–Beasley genetic algorithm

Symbols

AP_{DGU}^{max} and AP_{DGU}^{min}:

Maximum and minimum capacities of DGUs, respectively
$AP_{DGU,d}$: Active power of the d^{th} DGU
$AP_{DGU,d,i}$: Active power of the d^{th} DGU at the i^{th} solution
$AP^{max}_{DGU,d}$: Maximum active power of DGU at the d^{th} DGU
$AP^{opt}_{DGU,d}$: Optimal active power of DGU at the d^{th} DGU
AP_{gr}: Amount of power from the grid
AP_{ld}: Total load capacity of the system
AP_{ls}: Total power loss of the system
$\Delta IHD^{h}_{b,i}$ and $\Delta THD_{b,i}$: Individual and total harmonic distortion violations at the b^{th} bus, respectively, of the i^{th} solution
$\Delta I_{bh,i}$: Current violation at the bh^{th} branch at the i^{th} solution
$\Delta V_{b,i}$: Voltage violation at the b^{th} bus at the i^{th} solution
$C^{m\&o}_{d}$: Maintenance and operation cost in \$/kWh at the d^{th} DGU
C^{inv}_{d}: Investment cost in \$/kVA at the d^{th} DGU
IHD^{h}_{b}: Individual voltage harmonic distortion of the "h^{th}" order harmonic at the b^{th} bus
$IHD^{h}_{b,i}$: Individual voltage harmonic distortion of the "h^{th}" order harmonic at the b^{th} bus of the i^{th} solution
IHD^{max}: Maximum limit of individual harmonic distortion
I_{bh}: Current magnitude of the bh^{th} branch before connecting DGUs
I_{bhDGU}: Current magnitude of the bh^{th} branch after connecting DGUs
$I_{bhDGU,i}$: Current magnitude of the bh^{th} branch after connecting DGUs at the i^{th} solution
I^{max}_{bh}: Maximum current at the bh^{th} branch
It^{Max}: Maximum number of iteration
$L_{DGU,d}$: Location of the d^{th} DGU
$L_{DGU,d,i}$: Location of the d^{th} DGU at the i^{th} solution
L^{max}_{DGU} and L^{min}_{DGU}: Maximum and minimum locations for installing DGUs, respectively
N_{ad}: Total number of adjustment variables
N_{b}: Total number of buses in the system
N_{bh}: Total number of branches in the system
N_{c}: Total number of concentrations
N_{dg}: Total number of DGUs
N_{ld}: Number of loads in the system
θ_1, θ_2 and l: Random numbers in the range of $(0, 1)$
R_{bh}: Resistance of the bh^{th} branch
S_i: The i^{th} solution
S^{new}_{i}: The i^{th} new solution
$TCDG^{max}_{DGU}$: Total cost of maximum sizing of DGUs
$TCDG^{opt}_{DGU}$: Total cost of optimal sizing of DGUs
THD_b: Total voltage harmonic distortion at the b^{th} bus
$THD_{b,i}$: Total voltage harmonic distortion at the b^{th} bus at the i^{th} solution
THD^{max}: Maximum limit of total harmonic distortion
Va_{ji}: The j^{th} adjustment variable at the i^{th} solution
Va^{max}_{j} and Va^{min}_{j}: Maximum and minimum values of the j^{th} adjustment variables, respectively
V_b: Voltage at the b^{th} bus
$V_{b,i}$: Voltage at the b^{th} bus at the i^{th} solution
V^{1}_{b}: Fundamental voltage at the b^{th} bus
V^{h}_{b}: The h^{th} order harmonic voltage at the b^{th} bus
V^{max} and V^{min}: Maximum and minimum voltage magnitudes, respectively
$\beta_1$andβ_2: Constant values which are selected as 2 and 1, respectively
σ_V,σ_I,σ_{THD}, andσ_{IHD}: Penalty factors of the voltage, current, individual, and total harmonic distortions in the fitness function, respectively
ω_I: Weighting coefficient of OF_I
ω_{II}: Weighting coefficient of OF_{II}
H: Maximum number of the order harmonic distortions
It: Current iteration number
OF: Multi-objective function
OF_I and OF_{II}: Two objectives.

Data Availability

Data of the employed systems were extracted from [20, 31].

Conflicts of Interest

The authors declare that there are no conflicts of interest.

Acknowledgments

This research was funded by Ho Chi Minh City University of Technology and Education, Vietnam, under project no. T2022-03NCS.

Supplementary Materials

Table S1, Table S2, and Table S3: optimal solutions of the applied systems. (*Supplementary Materials*)

References

[1] A. S. Abbas, R. A. El-Sehiemy, A. Abou El-Ela et al., "Optimal harmonic mitigation in distribution systems with inverter based distributed generation," *Applied Sciences*, vol. 11, no. 2, p. 774, 2021.

[2] E. E. Elattar and S. K. Elsayed, "Optimal location and sizing of distributed generators based on renewable energy sources using modified moth flame optimization technique," *IEEE Access*, vol. 8, pp. 109625–109638, 2020.

[3] M. Mosbah, S. Arif, R. Zine, R. D. Mohammedi, and S. H. Oudjana, "Optimal size and location of PV based DG-unit in transmission system using GA method for loss reduction," *Journal of Electrical Engineering*, vol. 17, pp. 330–339, 2017.

[4] S. R. Gampa and D. Das, "Optimum placement and sizing of DGs considering average hourly variations of load," *International Journal of Electrical Power & Energy Systems*, vol. 66, pp. 25–40, 2015.

[5] S. Das, D. Das, and A. Patra, "Operation of distribution network with optimal placement and sizing of dispatchable DGs and shunt capacitors," *Renewable and Sustainable Energy Reviews*, vol. 113, Article ID 109219, 2019.

[6] S. R. Gampa and D. Das, "Simultaneous optimal allocation and sizing of distributed generations and shunt capacitors in distribution networks using fuzzy GA methodology," *Journal of Electrical Systems and Information Technology*, vol. 6, pp. 4–8, 2019.

[7] V. J. Mohan and T. A. Albert, "Optimal sizing and sitting of distributed generation using particle swarm optimization guided genetic algorithm," *Advances in Computational Sciences and Technology*, vol. 10, pp. 709–720, 2017.

[8] T. C. Subramanyam, S. T. Ram, and J. B. Subrahmanyam, "Optimal placement and sizing of DG in a distributed generation environment with comparison of different techniques," in *Artificial Intelligence and Evolutionary Computations in Engineering Systems*, pp. 609–619, Springer, Singapore, 2018.

[9] K. M. Lin, P. L. Swe, and K. Z. Oo, "Optimal distributed generator sizing and placement by analytical method and PSO algorithm considering optimal reactive power dispatch. World academy of science, engineering and Technology," *International Journal of Electronics and Communication Engineering*, vol. 13, 2019.

[10] R. Baghipour and S. M. Hosseini, "Optimal placement and sizing of DG in capacitor compensated distribution networks using binary particle swarm optimization," *Journal of Soft Computing and Information Technology*, vol. 3, no. 4, pp. 29–37, 2015.

[11] M. H. Paleba, L. M. Putranto, and S. P. Hadi, "Optimal placement and sizing distributed wind generation using particle swarm optimization in distribution system," in *Proceedings of the 2020 12th International Conference on Information Technology and Electrical Engineering (ICITEE)*, pp. 239–244, IEEE, Yogyakarta, Indonesia, 06-08 October 2020.

[12] N. Hantash, T. Khatib, and M. Khammash, "An improved particle swarm optimization algorithm for optimal allocation of distributed generation units in radial power systems," *Applied Computational Intelligence and Soft Computing*, vol. 20208 pages, 2020.

[13] X. Li, D. Wu, J. He, M. Bashir, and M. Liping, "An improved method of particle swarm optimization for path planning of mobile robot," *Journal of Control Science and Engineering*, vol. 2020, no. 1, 12 pages, 2020.

[14] F. Ratuhaji, A. Arief, and M. B. Nappu, "Determination of optimal location and capacity of distributed generations based on artificial bee colony," *Journal of Physics: Conference Series*, vol. 1341, no. 5, Article ID 052012, 2019.

[15] E. A. Al-Ammar, K. Farzana, A. Waqar et al., "ABC algorithm based optimal sizing and placement of DGs in distribution networks considering multiple objectives," *Ain Shams Engineering Journal*, vol. 12, no. 1, pp. 697–708, 2021.

[16] O. D. Montoya, W. Gil-González, and C. Orozco-Henao, "Vortex search and Chu-Beasley genetic algorithms for optimal location and sizing of distributed generators in distribution networks: a novel hybrid approach," *Engineering Science and Technology, an International Journal*, vol. 23, no. 6, pp. 1351–1363, 2020.

[17] A. S. Hassan, Y. Sun, and Z. Wang, "Multi-objective for optimal placement and sizing DG units in reducing loss of power and enhancing voltage profile using BPSO-SLFA," *Energy Reports*, vol. 6, pp. 1581–1589, 2020.

[18] M. R. Surya, R. Neela, and G. Radman, "Multi-objective optimization of DG sizing and placement using BBO technique," *International Journal of Engineering Research and Technology*, vol. 6, pp. 623–629, 2017.

[19] N. Ghaffarzadeh and H. Sadeghi, "A new efficient BBO based method for simultaneous placement of inverter-based DG units and capacitors considering harmonic limits," *International Journal of Electrical Power & Energy Systems*, vol. 80, pp. 37–45, 2016.

[20] M. Q. Duong, T. D. Pham, T. T. Nguyen, A. T. Doan, and H. V. Tran, "Determination of optimal location and sizing of solar photovoltaic distribution generation units in radial distribution systems," *Energies*, vol. 12, no. 1, p. 174, 2019.

[21] R. A. Jabr, "Robust volt/VAR control with photovoltaics," *IEEE Transactions on Power Systems*, vol. 34, no. 3, pp. 2401–2408, 2019.

[22] K. Mahmoud and M. Lehtonen, "Comprehensive analytical expressions for assessing and maximizing technical benefits of photovoltaics to distribution systems," *IEEE Transactions on Smart Grid*, vol. 12, no. 6, pp. 4938–4949, 2021.

[23] S. Singh, V. Babu Pamshetti, A. K. Thakur, and S. P. Singh, "Multistage multiobjective volt/var control for smart grid-enabled CVR with solar PV penetration," *IEEE Systems Journal*, vol. 15, no. 2, pp. 2767–2778, 2021.

[24] S. Vlahinić, D. Franković, V. Komen, and A. Antonić, "Reactive power compensation with PV inverters for system loss reduction," *Energies*, vol. 12, no. 21, p. 4062, 2019.

[25] K. Mahmoud, N. Yorino, and A. Ahmed, "Optimal distributed generation allocation in distribution systems for loss minimization," *IEEE Transactions on Power Systems*, vol. 31, no. 2, pp. 960–969, 2016.

[26] S. Souri, H. M. Shourkaei, S. Soleymani, and B. Mozafari, "Flexible reactive power management using PV inverter overrating capabilities and fixed capacitor," *Electric Power Systems Research*, vol. 209, Article ID 107927, 2022.

[27] D. Q. Hung, N. Mithulananthan, and K. Y. Lee, "Determining PV penetration for distribution systems with time-varying load models," *IEEE Transactions on Power Systems*, vol. 29, no. 6, pp. 3048–3057, 2014.

[28] I. Ben Hamida, S. B. Salah, F. Msahli, and M. F. Mimouni, "Optimal network reconfiguration and renewable DG integration considering time sequence variation in load and DGs," *Renewable Energy*, vol. 121, pp. 66–80, 2018.

[29] S. Mirjalili, A. H. Gandomi, S. Z. Mirjalili, S. Saremi, H. Faris, and S. M. Mirjalili, "Salp Swarm Algorithm: a bio-inspired optimizer for engineering design problems," *Advances in Engineering Software*, vol. 114, pp. 163–191, 2017.

[30] G. F. Gomes, S. S. da Cunha, and A. C. Ancelotti, "A sunflower optimization (SFO) algorithm applied to damage identification on laminated composite plates," *Engineering with Computers*, vol. 35, no. 2, pp. 619–626, 2019.

[31] T. D. Pham, T. T. Nguyen, and B. H. Dinh, "Find optimal capacity and location of distributed generation units in radial distribution networks by using enhanced coyote optimization algorithm," *Neural Computing & Applications*, vol. 33, no. 9, pp. 4343–4371, 2021.

[32] A. Faramarzi, M. Heidarinejad, B. Stephens, and S. Mirjalili, "Equilibrium optimizer: a novel optimization algorithm," *Knowledge-Based Systems*, vol. 191, Article ID 105190, 2020.

[33] M. Milovanović, J. Radosavljević, and B. Perović, "A backward/forward sweep power flow method for harmonic polluted radial distribution systems with distributed generation units," *International Transactions on Electrical Energy Systems*, vol. 30, no. 5, Article ID e12310, 2020.

[34] R. Prakash, B. Lokeshgupta, and S. Sivasubramani, "Multiobjective bat algorithm for optimal placement and sizing of DG," in *Proceedings of the 2018 20th National Power Systems Conference (NPSC)*, pp. 1–6, IEEE, Tiruchirappalli, India, 14-16 December 2018.

[35] D. Chen and K. Ding, "System stability and control technologies after large-scale wind power integration," in *Large-scale Wind Power Grid Integration*, W Ningbo, Ed., Academic Press, Cambridge, pp. 107–184, 2016.

[36] J. C. Das, "Harmonic Distortion Limits According to Standards. Power system harmonics and passive filter design," *Power System Harmonics and Passive Filter Designs*, pp. 427–451, 2015.

[37] T. M. Blooming and D. J. Carnovale, "Application of IEEE Std 519-1992 harmonic limits," in *Proceedings of the Conference Record of 2006 Annual Pulp and Paper Industry Technical Conference*, pp. 1–9, IEEE, Appleton, WI, USA, 18-23 June 2006.

[38] S. Sajeevan and N. Padmavathy, "Optimal allocation and sizing of distributed generation using artificial bee colony algorithm," *International Research Journal of Engineering and Technology (IRJET)*, vol. 3, 2016.

[39] M. H. Moradi and M. Abedini, "A combination of genetic algorithm and particle swarm optimization for optimal DG location and sizing in distribution systems," *International Journal of Electrical Power & Energy Systems*, vol. 34, no. 1, pp. 66–74, 2012.

[40] S. K. Injeti and N. Prema Kumar, "A novel approach to identify optimal access point and capacity of multiple DGs in a small, medium and large scale radial distribution systems," *International Journal of Electrical Power & Energy Systems*, vol. 45, no. 1, pp. 142–151, 2013.

[41] K. R. Devabalaji and K. Ravi, "Optimal size and siting of multiple DG and DSTATCOM in radial distribution system using bacterial foraging optimization algorithm," *Ain Shams Engineering Journal*, vol. 7, no. 3, pp. 959–971, 2016.

[42] A. El-Fergany, "Optimal allocation of multi-type distributed generators using backtracking search optimization algorithm," *International Journal of Electrical Power & Energy Systems*, vol. 64, pp. 1197–1205, 2015.

[43] R. S. Rao, K. Ravindra, K. Satish, and S. V. L. Narasimham, "Power loss minimization in distribution system using network reconfiguration in the presence of distributed generation," *IEEE Transactions on Power Systems*, vol. 28, no. 1, pp. 317–325, 2013.

[44] P. P. Biswas, P. N. Suganthan, and G. A. Amaratunga, "Optimal power flow solutions incorporating stochastic wind and solar power," *Energy Conversion and Management*, vol. 148, pp. 1194–1207, 2017.

[45] C. T. Hsu, R. Korimara, and T. J. Cheng, "Power quality analysis for the distribution systems with a wind power generation system," *Computers & Electrical Engineering*, vol. 54, pp. 131–136, 2016.

[46] D. Q. Hung, N. Mithulananthan, and R. C. Bansal, "Integration of PV and BES units in commercial distribution systems considering energy loss and voltage stability," *Applied Energy*, vol. 113, pp. 1162–1170, 2014.

Indonesian Journal of Electrical Engineering and Informatics (IJEEI)
Vol. 11, No. 1, March 2023, pp. 36~49
ISSN: 2089-3272, DOI: 10.52549/ijeei.v11i1.4103

Reduction of Emission Cost, Loss Cost and Energy Purchase Cost for Distribution Systems with Capacitors, Photovoltaic Distributed Generators, and Harmonics

Thai Dinh Pham[1], Hung Duc Nguyen[2,3] and Thang Trung Nguyen[4*]
[1]Faculty of Electrical and Electronics Engineering, Ho Chi Minh City University of Technology and Education, Ho Chi Minh City, Vietnam; thaipd.ncs@hcmute.edu.vn.
[2]Faculty of Electrical and Electronics Engineering, Ho Chi Minh City University of Technology, Ho Chi Minh City, (HCMUT) Vietnam;
[3]Vietnam National University Ho Chi Minh City, Linh Trung Ward, Thu Duc District, Ho Chi Minh City, Vietnam; hungnd@hcmut.edu.vn
[4]Power System Optimization Research Group, Faculty of Electrical and Electronics Engineering, Ton Duc Thang University, Ho Chi Minh City, Vietnam

Article Info

Article history:

Received Aug 26, 2022
Revised Jan 28, 2023
Accepted Feb 12, 2023

Keyword:

Bonobo optimizer
Capacitor
Emissions
Power loss
Harmonic
Voltage profile

ABSTRACT

In this paper, a bonobo optimizer (BO) and two other methods, particle swarm optimization (PSO) and salp swarm algorithm (SSA), are implemented to determine the location and sizing of photovoltaic distributed generators (PDGs) and capacitors (CPs) in IEEE 69-bus radial distribution system with many nonlinear loads. The objective of the study is to minimize the costs for purchasing energy from main grid for load demand and power loss on transmission lines as well as cost for emission fines from fossil fuel generation units of the grid under considering strict constraints on penetration, voltage, current and harmonic distortions. The results have shown that BO is the best and most stable method in solving the considered optimization problem. With the use of the optimal solution from BO, the total cost is significantly reduced up to 80.52%. As compared to base system without CPs and PDGs, the obtained solution can reduce power loss up to 94.48% and increase the voltage profile from the range of [0.9092 1.00] pu to higher range of [0.9907 1.0084] pu. In addition, total harmonic distortion (THD) and individual harmonic distortion (IHD) are also much improved and satisfied under the IEEE Std. 519. Thus, BO is a suitable method for the application of installing CPs and PDGs in distribution systems.

Corresponding Author:

Thang Trung Nguyen,
Power System Optimization Research Group,
Faculty of Electrical and Electronics Engineering,
Ton Duc Thang University, Ho Chi Minh City, Vietnam
Email: nguyentrungthang@tdtu.edu.vn

The list of symbols

$C_{TotalCost}$	Total cost in distribution systems ($)
$C_{emission}$	Emission cost ($)
C_{load}	Energy purchase cost for loads ($)
C_{loss}	Power loss cost ($)
E_{emi}	Emission produced by conventional power plants (kg/MWh)
IHD^{max}	Maximum individual harmonic distortion
IHD_s^h	Individual harmonic distortion at the h^{th} order of the s^{th} bus

I_b^{max}	Maximum thermal current limit of the b^{th} branch
I_b	The thermal current of the b^{th} branch
N_b	Number of branches
N_{cap}	Number of capacitors
N_l	Number of loads
N_{pv}	Number of photovoltaic distributed generators
N_s	Number of buses
$P_{load,l}$	Active power of load demand at the l^{th} load
$P_{loss,b}$	Active power loss at the b^{th} branch
$P_{pv,n}$	Active power produced from the n^{th} photovoltaic distributed generator
P_{sub}	Active power supplied by the main grid
$Price_{emission}$	Price of emissions ($/kg)
$Price_{load}$	Price for purchasing electricity from the substation ($/MWh)
$Price_{loss}$	Price for energy loss on transmission lines ($/MWh)
$Q_{load,l}$	Reactive power of load demand at the l^{th} load
$Q_{loss,b}$	Reactive power loss at the b^{th} branch
$Q_{cap,k}$	Reactive power produced from the k^{th} capacitor bank
Q_{sub}	Reactive power supplied by the main grid
THD^{max}	Maximum total harmonic distortion
THD_s	Total harmonic distortion at the s^{th} bus
V_s	The voltage magnitude at the s^{th} bus
V_s^1	The fundamental voltage magnitude at the s^{th} bus
V_s^h	The voltage magnitude at the h^{th} order harmonic of the s^{th} bus
H	Maximum harmonic order

1. INTRODUCTION

The use of non-renewable fossil fuels as oil, coal and fracked gas causes the release of carbon dioxide and global warming [1-2]. Thus, many countries have policies to encourage the development of renewable energy sources, which rely on the natural processes as wind, solar, hydropower, geothermal, bioenergy, etc. due to many obtained benefits [3-4]. Connection of renewable distributed generators (RDGs) to the distribution systems offers many great advantages in terms of technology, economy and environment [5]. Therefore, RDGs have received a lot of attention of energy researchers around the world. Realistically, the great benefit that the RDGs are integrated in distribution system is to improve the system reliability, reduce the power loss on the transmission line due to using local generation sources, enhance the voltage profile, support the voltage stability and reduce the greenhouse gas emissions [6]. However, obtained benefits mainly depend on the location and capacity of RDGs [7-9]. So, almost studies regarding the installation of RDGs are about the optimization of the two major factors of the RDGs and then evaluations are done by comparing different objective functions such as active power loss, energy loss, investment cost and operation cost for RDGs, etc.

In recent years, many researchers have proposed different algorithms for solving the problem of installing PDGs in distribution systems. Specifically, in [10], the authors have applied the moth flame optimization (MFO) for determining the installation location of RDGs with the aim of minimizing power loss with consideration of operating constraints. This algorithm was developed based on the observation of moth activity in the nature. This moth has a very special nocturnal movement and called directional lateral movement. However, it has many disadvantages that greatly affect its performance such as low accuracy, slow convergence and poor ability to expand the exploration area to find new solutions [11]. With the same objective function, the authors [12] proposed an algorithm, named manta ray foraging optimization (MRFO) to solve this problem. This algorithm is inspired by the food source search behavior of the manta rays. However, researchers have found that it is not very efficient due to slow convergence and easily falls into the local optimal region [13]. In addition to the new algorithms, other popular algorithms were also used to solve the problem to be considered. In [14], the authors have shown that connecting the suitable siting and sizing of RDGs to the distributed systems contribute to a dramatic reduction in losses and voltage drops by using the genetic algorithm (GA). GA is a fairly simple algorithm in implementation, but it is computationally expensive, and the performance is not high due to randomly generated operation of mutation process. In [15], for the multiple objectives of voltage improvement, harmonic mitigation and power loss reduction, the appropriate installation of RDGs is successfully found on two distribution systems 33 and 69 buses by applying biogeography-based optimization (BBO). This algorithm was developed based on the immigration

and migration of species between habitats. However, this algorithm is quite complicated, the convergence speed is relatively slow, and its performance is easily affected by the initial parameters. Moreover, there are other positive methods also used in the studies [16-17]. In [16], the optimal sizing of the photovoltaic system has also been proposed by using Lagrange Multipliers (LM). This work minimized the total energy loss during the daily insolation period in various scenarios with test system of 37 buses. Additionally, [17] also appropriately selected the placement for the photovoltaic system and energy store system with the consideration of power loss and voltage stability in the system. These authors proposed the crow search optimization algorithm (CSO) for finding the optimal solution in different radial distributed systems. Besides the traditional distribution systems that only combine with solar generators, some researchers have also focused on solving the problem of optimal installation for hybrid renewable energy systems. Specifically, the study [18] presented an optimal solution for distribution system integrating both photovoltaic and wind turbines by using a combined method of real power loss sensitivity index factor and artificial ecosystem-based optimization algorithm (RPLSI-AEO). The obtained results also proved the effectiveness of the proposed hybrid method with others for the loss reduction in a 33-bus system. Similarly, other researchers have succeeded in determining the size of photovoltaic, wind, battery and diesel generator integrated system [19]. By using grasshopper optimization algorithm (GOA), the cost of energy has been reduced highly, while a high reliability of power supply in the real grid in Nigeria has been still guaranteed. These hybrid systems had a great contribution in keeping stability for the power grid and reaching a big potential in replacing fossil fuel sources. In general, most studies only considered power loss reduction as primary goal and the most optimal capacity range of RDGs was not suggested [20]. However, it is extremely important to consider the reduction of the costs for purchasing electricity for load demand, power loss on transmission lines and generating emissions from fossil fuel generation units. But this has been ignored in most previous studies. Besides, it is necessary to consider the distribution systems with many nonlinear loads to keep the indicators related to harmonic distortions within standard limits. In order to overcome the mentioned disadvantages, this study searches the possible solution for optimal installing PDGs and CPs to minimize the costs of purchasing energy from main grid for load demand and losses as well as cost for emission fines from fossil fuel generation sources of the grid under considering strict constraints on penetration, bus voltage, branch current and harmonic distortions.

In addition, meta-heuristic algorithms have been used widely for different applications of integrating distributed generators, including ant lion optimization algorithm (ALOA) [21], equilibrium optimizer (EO) [22], multi-objective chaotic symbiotic organisms search algorithm (MCSOSA) [23], modified moth flame optimization technique (MMFOT) [24], improved whale optimization approach (IWOA) [25], atom search optimization (ASO) [26], tree growth algorithm (TGA) [27], etc. As a result, the group of meta-heuristic methods has many outstanding advantages in determining global solutions for solving optimization problems. However, these methods are outdated and their main disadvantages are easily fall into the local optimization trap and low stability. This has the effect to the performance of the algorithms in solving various optimization problems [28-29]. The search for a strong optimization algorithm capable of expanding the finding area as well as avoiding the problem of local minima trapping is always welcomed. In recent years, many efficient meta-heuristic algorithms have been introduced and bonobo optimizer (BO) is a good example. BO was first published in 2019 by A.K. Das and D.K. Pratihar [30]. This optimization algorithm was inspired by the social behavior and Bonobos' reproductive strategies. BO is an active method with high stability and quick convergence time, so it is widely applied to solve optimization problems. As in [31], the authors have demonstrated the superiority of BO over other meta-heuristic algorithms in finding the optimal solution for an off-grid hybrid renewable energy system. Besides, a few studies like [32, 33] also tried to combine BO with other techniques to enhance the performance. The authors in [32] proposed the chaotic bonobo optimizer (CBO) to solve the problem for minimizing the operating costs of the system with integrating the renewable energy sources. The effectiveness of the algorithm was improved significantly. This has contributed to CBO's ability in expanding the search area to find the positive optimal solutions and avoid local traps Additionally, the authors in [33] also succeeded in developing a new version of BO, called the improved quasi-oppositional BO (QOBO) algorithm. This improvement includes two techniques. The first is to rely on three leaders instead of the best solution in the original BO. The second is to apply opposition-based learning (OBL) to use candidate solution and its opposite at the same time. The combination between the three leader's section and quasi-opposition-based learning helped to avoid the stuck in the local minimum. On the other hand, authors of the original algorithm also introduced BO with self-adjusting parameters over continuous spaces for various situations in 2022 [34]. In that study, BO was checked on different test functions and it was also compared with many strong methods that have been published recently. The obtained results have demonstrated the superiority of BO in solving optimization problems.

Thus, for this work, BO is applied for determining the optimal location and sizing of PDGs and CPs without negatively affecting for reliable technical indicators of the distribution system. Besides, forward/

backward sweep technique (FW/BWST) was also applied for solving power flow and harmonic flow [35]. Two PDGs and two CPs are proposed for connecting to the test system of IEEE 69 bus radial distribution system. The main objective of this study is to minimize costs of purchasing electricity for load demand, power loss and emissions without any violation for the technical criteria of overvoltage, overcurrent, and harmonic limits in the radial distribution system. The novelties of the paper are as follows:

1) This paper calculates total costs of emissions from fossil fuel generation unit of the main grid, loss on transmission lines and energy purchase for load demand that most previous studies have not fully considered.
2) The study focused on determining the optimal integration of capacitors and photovoltaic distributed generators into a distribution system with nonlinear loads. This is considered a novelty because previous studies were limited in considering harmonic distortions in integrated systems.

After implementing three algorithms for the system and comparing the obtained results, the major contributions of the study can be stated as follows:

1) This research suggests a novel effective and highly stable algorithm, which is called bonobo optimizer (BO). The obtained results from the simulation under considering the same objective function and constraints. The suggested algorithm has superiority over the compared methods in solving optimization problem.
2) This paper shows the most suitable solution for the position and capacity of capacitors and photovoltaic distributed generators in the distribution system. The best obtained solution can strongly cut the emission cost, energy loss cost and energy purchase cost. The reduction is greater than 80% as compared to original scenario. In addition, the power loss on branches is reduced effectively, and the violation of voltage limits and harmonic distortion limits are also eliminated by using distributed generators in the system.

2. RESEARCH METHOD

2.1. Objective function

In this paper, two PDGs and two CPs are installed in the IEEE 69-node system to reduce the sum of emission cost, energy purchase cost and energy loss cost while satisfying all technical criterion, especially THD and IHD at each node. The objective function can be formulated as follows [24, 36]:

$$Minimize\ C_{TotalCost} = C_{load} + C_{loss} + C_{emission}\ (\$) \quad (1)$$

Where,

$$C_{load} = Price_{load} \times \sum_{l=1}^{N_l} P_{load,l}\ (\$) \quad (2)$$

$$C_{loss} = Price_{loss} \times \sum_{b=1}^{N_b} P_{loss,b}\ (\$) \quad (3)$$

$$C_{emission} = Price_{emission} \times E_{emi} \times P_{sub}\ (\$) \quad (4)$$

2.2. Constraints

2.2.1. The power balance constraints

Active power supply and active power demand should be equal as follows [15, 37]:

$$P_{sub} + \sum_{n=1}^{N_{pv}} P_{pv,n} = \sum_{l=1}^{N_l} P_{load,l} + \sum_{b=1}^{N_b} P_{loss,b} \quad (5)$$

Similarly, the equality constraint between reactive power supply and reactive power demand is formulated by [15]:

$$Q_{sub} + \sum_{k=1}^{N_{cap}} Q_{cap,k} = \sum_{l=1}^{N_l} Q_{load,l} + \sum_{b=1}^{N_b} Q_{loss,b} \quad (6)$$

2.2.2. The overvoltage limits

According to the Std. BS EN 50160, the voltage limit must be between 0.9 and to 1.1 pu [38]. However, many studies have shown that the best acceptable limit for voltage profile is from 0.95 pu to 1.05

pu [39-40]. Therefore, it is essential to keep the upper level (V^{max}) and lower level (V^{min}) of the bus voltage at the best limits, and the following inequality is applied for voltage of each node [41]:

$$V^{min} \leq V_s \leq V^{max}, s = 1, \dots, N_s \quad (7)$$

2.2.3. Total harmonic distortion limit

According to the IEEE Std. 519, total voltage harmonic distortion should not exceed the limit of 5% [2]. The distortion is determined and constrained by:

$$THD_s(\%) = \left[\frac{\sqrt{\sum_{h\neq 1}^{H}(V_s^h)^2}}{V_s^1}\right] \times 100 \leq THD^{max}(\%) \quad (8)$$

2.2.4. Individual harmonic distortion limit

Similarly, individual harmonic distortion should be followed the limit of 3% [15]. The distortion is determined and constrained by:

$$IHD_s^h(\%) = \left[\frac{V_s^h}{V_s^1}\right] \times 100 \leq IHD^{max}(\%) \quad (9)$$

2.2.5. The overcurrent limits

There is a line connecting each two nodes and this line is a conductor with a thermal limit. To satisfy the thermal limit, working current should not be higher than the maximum limit as shown in the inequality below [41]:

$$I_b \leq I_b^{max}, b = 1, \dots, N_b \quad (10)$$

2.2.6. The PDG capacity limits

The capacity limits of PDGs must be predetermined and it should be kept within the upper bound (P_{pv}^{max}) and lower bound (P_{pv}^{min}) as follows [42]:

$$P_{pv}^{min} \leq P_{pv,n} \leq P_{pv}^{max}, n=1, \dots, N_{pv} \quad (11)$$

Similarly, the maximum and minimum generating limits of the capacitors (Q_{cap}^{max} and Q_{cap}^{min}) are also predefined as follows:

$$Q_{cap}^{min} \leq Q_{cap,k} \leq Q_{cap}^{max}, k=1, \dots, N_{cap} \quad (12)$$

In addition, the total penetration of all PDGs and CPs in the integrated system must not exceed the load demand during the optimal solution search process. The two following constraints are applied to limit their penetration [43]:

$$\sum_{n=1}^{N_{pv}} P_{pv,n} \leq 80\% \times \sum_{l=1}^{N_l} P_{load,l} \quad (13)$$

$$\sum_{k=1}^{N_{cap}} Q_{cap,k} \leq 80\% \times \sum_{l=1}^{N_l} Q_{load,l} \quad (14)$$

3. THE APPLIED METHOD

In this study, bonobo optimizer (BO) is applied to find the placement and sizing of PDGs and CPs in the distribution system. BO was inspired by the social behavior of bonobos and breeding methods [30]. The community of bonobos adopted a social strategy that could be called a fission-fusion. Basically, it forms many groups with different sizes and different compositions in a community of bonobos. After a short time, it will reunite itself with the community. In BO, each solution is considered like a bonobo and bonobo with the best rank in society is called alpha-bonobo. At the end of each iteration, the verification and evaluation process for all bonobos are implemented. If alpha-bonobo is improved then it is called positive phase, where the most suitable conditions and vice versa is negative phase [30]. The process of applying BO to solve the optimization problem can be briefly summarized in the flowchart of Figure 1 and expressed in detail as follows:

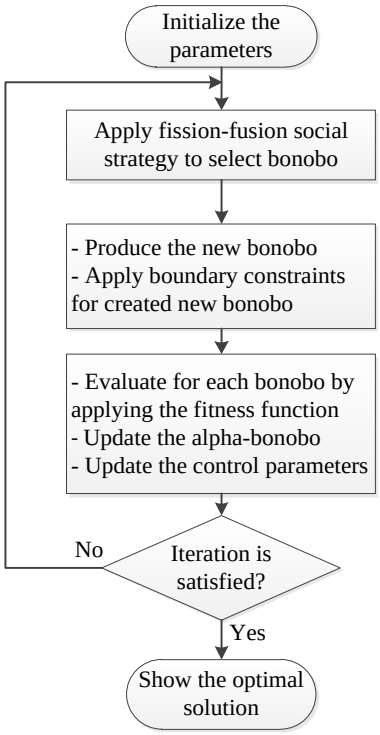

Figure 1. The flowchart of bonobo optimizer

Step 1:
- Initializing the non-user-defined parameters of the algorithm.

Step 2:
- Selecting the bonobo by using fission-fusion social strategy. Before updating, bonobos are determined for the mating based on the fission-fusion social strategy. Here, in a large community, individuals form temporary small groups of varying sizes. This size is unpredictable due to its random nature. The maximum size of a temporary sub-group size factor (tsg^{max}) depends on the population size (N_{pop}) and temporary subgroup size factor (tsg_{factor}). The value of tsg^{max} can be determined by [30]:

$$tsg^{max} = maximum(2, tsg_{factor} \times N_{pop}) \quad (15)$$

In this case, tsg_{factor} can be run from zero to the maximum value of temporary subgroup size factor (tsg_{factor}^{max}) to keep the right balance between exploration and exploitation in the algorithm.

Step 3:
- Producing the new bonobo ($Nbon_j$).

In this algorithm, the phase probability (p_p) is used to decide the mating strategy for generating a bonobo. The initial value of p_p is assigned as 0.5 and is will be updated after each iteration according to the phase count number and the current phase. The value of p_p will be decreased from 0.5 to 0.0 with a predefined rate (*rcpp*) during consecutive negative phases and vice versa, it should be increased from 0.5 to 1.0 for positive phases.

In the promiscuous and restrictive mating strategies, p_p is compared with a random number (rd_1) between zero and one, if p_p is greater than or equal to rd_1 then a new bonobo is produced by applying Eq. (16) as given below [34, 44]:

$$Nbon_j = bon_j^i + rd_1 \times s_1 \times \left(a_j^{bon} - bon_j^i\right) + \left(1 - rd_1\right) \times s_2 \times f \times \left(bon_j^i - bon_j^p\right), j = 1, \ldots, N_V \quad (16)$$

Where N_V is the decision variables number; s_1 and s_2 are defined as the sharing cofficient factors for alpha bonobo and selected bonobo; f is a flag (set with -1 or 1) and its value depends on restrictive mating types or promiscuous, respectively; bon_j^i and bon_j^p are the j^{th} variable value of the i^{th} and the p^{th} bonobos. $Nbon_j$ and a_j^{bon} are the j^{th} variable value of the offspring and alpha-bonobo in the current community, respectively.

In the consortship and extra-group mating strategies, the important factor for determing the new bonobo is the probability of extra- group mating strategy (p_{egms}). The value of p_{egms} should be updated at each iteration and it is used to compare with the random number (rd_2) in the range of [0, 1]. If p_{egms} is higher than or equal to rd_2, then Eqs. (19-22) are applying for creating the new bonobo. For this stage, the two interrmediate measured values (B_1 and B_2) for determining the equation of producing offspring ($Nbon_j^i$) can be defined by [30]:

$$B_1 = e^{(rd_4^2 + rd_4 - 2/rd_4)} \quad (17)$$

$$B_2 = e^{(-rd_4^2 + 2.rd_4 - 2/rd_4)} \quad (18)$$

The equations and accompanying conditions for generating new bonobo at this stage can be listed as follows [34]:

$$Nbon_j = bon_j^i + B_1 \times \left(cv_j^{max} - bon_j^i\right), \text{ if } (a_j^{bon} \geq bon_j^i \,\&\, p_p \geq rd_3) \quad (19)$$

$$Nbon_j = bon_j^i - B_2 \times \left(-cv_j^{min} + bon_j^i\right), \text{ if } (a_j^{bon} \geq bon_j^i \,\&\, p_p < rd_3) \quad (20)$$

$$Nbon_j = bon_j^i - B_1 \times \left(-cv_j^{min} + bon_j^i\right), \text{ if } (a_j^{bon} < bon_j^i \,\&\, p_p \geq rd_3) \quad (21)$$

$$Nbon_j = bon_j^i + B_2 \times \left(cv_j^{max} - bon_j^i\right), \text{ if } (a_j^{bon} < bon_j^i \,\&\, p_p < rd_3) \quad (22)$$

In the Eqs. (17-22), rd_3 and rd_4 are the random numbers in the range of [0, 1] ($rd_4 \neq 0$). cv_j^{max} *and* cv_j^{min} are the upper and lower limits of the *j*th decision variable, respectively.

In the case of p_{egms} is smaller than rd_2, the new bonobo is generated by using Eq. (23) [34].

$$Nbon_j = \begin{cases} bon_j^i + f \times e^{-rd_5} \times \left(bon_j^i - bon_j^p\right), if\ (f = 1 \,||\, p_p \geq rd_6) \\ bon_j^p, otherwise \end{cases} \quad (23)$$

In the Eq. (23), rd_5 *and* rd_6 are the random numbers from zero to one.

- Appling boundary limiting conditions. If the generated $Nbon_j$ is greater than cv_j^{max}, it is assigned as cv_j^{max}. Similarly, $Nbon_j$ does not change if it is not smaller than cv_j^{min}.

Step 4:

- Evaluating the quality of the *i*th solution by using the fitness function (F^i) below:

$$F^i = C_{TotalCost}^i + \partial.\Delta PE^i \quad (24)$$

Where $C_{TotalCost}^i$ is the objective function value of the *i*th solution which obtained by using Eq. (1), ∂ is the penalty factor and ΔPE^i is the sum of penalty elements of the *i*th solution which clearly descripted in [42].

- Determining the alpha-bonobo and updating the control parameters that process was clearly described in [34]. If the next generation can produce bonobos with a better fitness than the old alpha-bonobo, the created new bonobo is selected to be a new alpha-bonobo. Besides, the problem parameters are also updated in the specific fashion with updating alpha-bonobo.

Step 5:

- Repeating the above steps until the termination condition is satisfied.

4. THE SIMULATION RESULTS AND DISCUSSION

In this paper, two PDGs and two CPs are considered for connection into the IEEE-69 node distribution system. The single line diagram of the system is shown in Figure 2. Bus data and line data of the system were given in [39], and total load demand is respectively, 3.8019 MW and 2.6941 MVar. The locations that we can install the generators and capacitors are from Bus 2 to Bus 69 excluding slack bus 1. Capacity limits are within 0 and 2 MW for PDGs and within 0 to 2 MVar for CPs. This study establishes the limits for the fundamental bus voltage in the range of [0.95 1.05] (pu), and the maximum limits for THD and IHD is respectively 5% and 3% [2]. To generate harmonics, nonlinear loads are placed at Bus 8, Bus 12, Bus 18, Bus 22, Bus 24, Bus 34, Bus 46, Bus 55, and Bus 65. The detail of the nonlinear loads was given in the study [39]. For this paper, $Price_{load}$ and $Price_{loss}$are set to 96 $/MWh and 60 $/MWh, respectively [45]. Besides, $Price_{emission}$ is taken as 0.004 ($/kg) with emissions produced by conventional power plants (E_{emi}) is 724 kg/MWh [46].

To reach the best results for the system, three methods including PSO, SSA and BO are implemented. To compare objectively, the parameters for these algorithms are referenced from previously published studies. For running PSOs, the acceleration factors (c_a and c_b) are taken as 2, the weighting function (W) is set to 0.99 and the ramdom numbers (r_1 and r_2) are between 0 and 1 [15]. To implement SSA, the coefficient (c_1) is the most important and its value is taken from the function of $c_1 = 2e^{-(\frac{4l}{L})^2}$, where *l* and

L are defined as the current and maximum iteration. While, c_2 and c_3 are the random numbers in the interval of [0, 1] [47]. For operating the BO, s_1 and s_2 are set to 1.55 and 1.4, respectively; *rcpp* is selected as 0.0039; tsg_{factor}^{max} is set to 0.07 and the value of p_{egms} is updated at each iteration with its initial value is 0.001 for this study [34]. The code of BO which is developed for this study, is referenced from [34]. Finally, the total trial run number (*Tr*), the maximum number of iterations (It^{max}) and the population number (N_{po}) are selected to be 40, 180 and 30, respectively for all methods. The simulations are performed by coding program on MATLAB ver.2017 on a personal computer with 1.8 GHz and 8.0 GB.

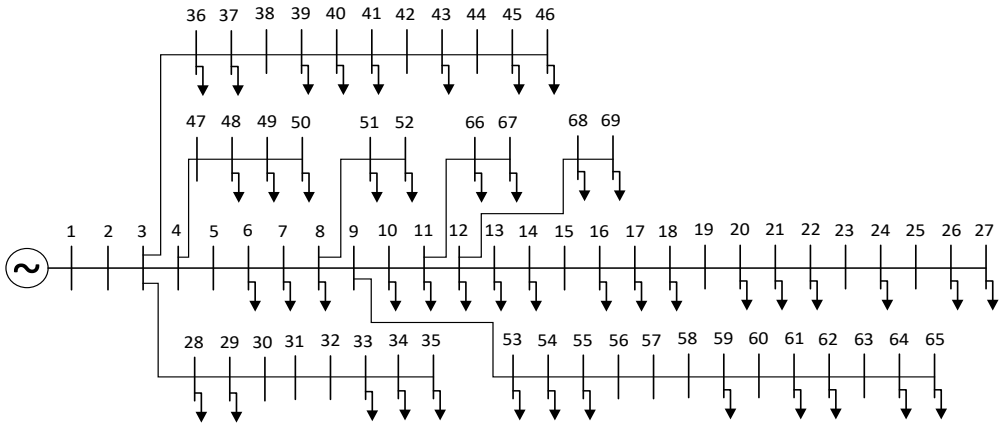

Figure 2. IEEE 69-bus radial distribution system

In addition to the use of proper update mechanisms, these algorithms are also based on randomization factors such as the use of random scaling factors from 0 to 1, and the use of randomly picked solutions from current population. Thus, one computation run is not high enough to reach the most optimal solution and obtained results from the sole run cannot reflect the performance of applied algorithms. But, 40 trial runs are enough and results from the runs are reported in Figure 3. Total costs from 40 runs are sorted from the lowest to the highest for the clear comparison. Red curve of BO is below than blue curve of SSA and green curve of PSO for all 40 runs. Like as counted, there are 33 solutions of the suggested method that are better than PSO, corresponding to 82.5% and there are 17 better solutions than SSA, accounting for 42.5%. This phenomenon indicates that the suggested method (BO) win compared methods (PSO and SSA) in reaching the best cost and the most stable cost.

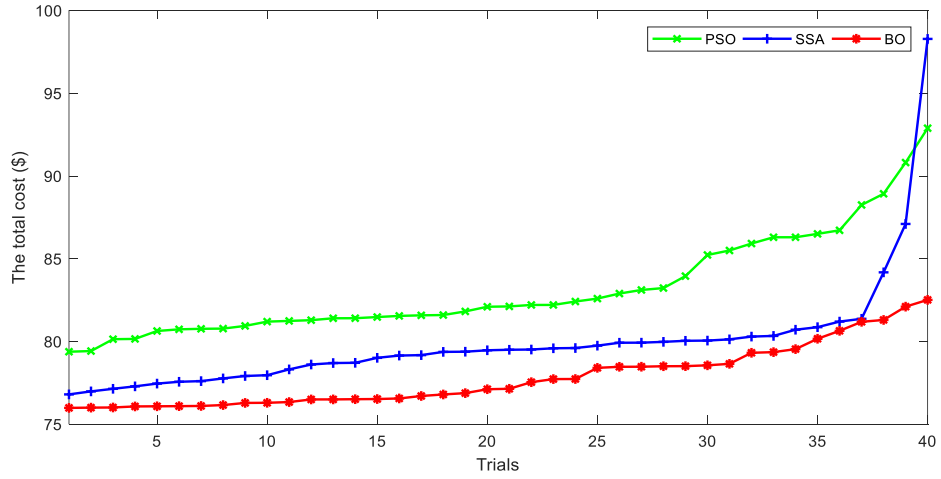

Figure 3. The objective function fitness values in 40 trials

Metaheuristic algorithms which are based on randomization need three comparison criteria to evaluate the performance including 1) Minimum fitness function is used to conclude the effectiveness of obtained solutions; 2) Average fitness function is used to evaluate the possibility of finding good solutions; and 3) Maximum fitness function is used to evaluate the fluctuation of algorithms. Among the three criteria, the minimum fitness function, which is also the total cost, is the most important factor to conclude the performance of algorithms. The comparison of the minimum total cost is to reflect the quality of the best run

from a number of trials, and the best solution with the smaller total minimum cost is adopted for the test system. So, the algorithm reaching the best run is the most effective ones among applied algorithms. However, there is a possibility to reach the best run and the possibility can be determined by using the average total cost. Algorithms with smaller average total cost will have a higher possibility to reach the best run. So, the average total cost is the second important factor. Finally, the maximum total cost is to reflect the fluctuation of the applied algorithms. The comparison criterion is not very necessary, but it can confirm the real superiority of algorithms. A method with smaller minimum fitness, smaller average fitness and smaller maximum fitness is the best. For another case, the method with smaller minimum fitness and smaller average fitness but higher maximum fitness is also the best. For the worst case, the method with smaller minimum fitness but higher average fitness and higher maximum fitness is also the best because the obtained solution with the lower minimum fitness is applied for the test system. To determine the best algorithm among PSO, SSA and BO, the best, average and worst total cost calculated from 40 trial runs are reported in Figure 4. BO can reach smaller best, mean and worst total cost than SSA and PSO. The best total costs of PSO, SSA and BO are \$79.3833, \$76.8041 and \$75.9889, while the worst total cost is \$92.8906, \$98.2851 and \$82.5147 for PSO, SSA and BO, respectively. Furthermore, the mean of 40 total cost values that can be relied on to evaluate the stability is calculated and it is \$83.1933 for PSO, \$79.9198 for SSA and \$77.8357 for BO. Clearly, BO can reach better all values than PSO and SSA. So, BO is superior to PSO and SSA.

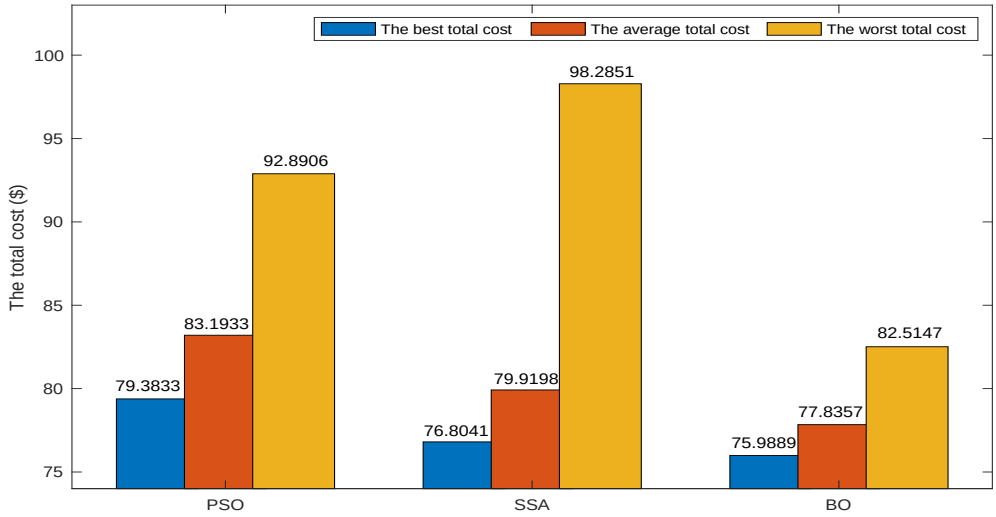

Figure 4. The best, the average and the worst total in 40 trials

The optimal position and capacity of two PDGs and two CPs are clearly reported in Table 1. Besides, the cost of purchasing energy for the load demand from the main grid (C_{load}), the cost to pay for the distribution energy loss (C_{loss}) as well as the cost of emission penalty from fossil fuel generator of the main grid ($C_{emission}$) are also presented in detail.

Table 1. The optimal solution from the implemented methods

Method	Optimal solution		C_{load}	C_{loss}	$C_{emission}$	$C_{TotalCost}$
	PDGs	CPs	(\$)	(\$)	(\$)	(\$)
Base	–	–	364.9814	13.4700	11.6604	390.1119
PSO	Bus 55 – 1.1290 MW Bus 58 – 1.9007 MW	Bus 63 – 1.5306 MVar Bus 50 – 0.4317 MVar	74.1302	2.8780	2.3752	79.3833
SSA	Bus 60 – 1.9858 MW Bus 11 – 1.0557 MW	Bus 60 – 1.2706 MVar Bus 10 – 0.3823 MVar	72.9974	1.5318	2.2760	76.8041
BO	Bus 61 – 1.8865 MW Bus 11 – 1.1549 MW	Bus 61 – 1.1948 MVar Bus 12 – 0.5386 MVar	73.0070	0.7465	2.2384	75.9889

As shown in Table 1, after connecting the PDGs and CPs, the C_{load} dropped drastically from \$364.9814 to \$74.1302 by using PSO, \$72.9974 by using SSA and \$73.0070 by using BO. The significant drops prove that the integration of PDGs and CPs has contributed greatly in reducing the electricity cost to supply energy to the loads. For comparing between implemented methods, this cost reduction for BO and SSA is 80.00% and it is higher than PSO of 79.68%. In terms of the C_{loss}, the three algorithms can reduce the energy loss cost effectively and their costs are smaller than the base system by \$12.7235 (BO), \$10.5920

(PSO) and \$11.9382 (SSA). Thereby, the solution from BO has the highest cost saving compared to other methods. In other words, BO is a more effective method than others in proposing the feasible solution to solve the problem of power loss cost on the transmission lines. About the $C_{emission}$, the base system suffers from the highest penalty with \$11.6604, but that is much smaller for the solutions from the three algorithms. The emission penalty cost is \$2.3752 for PSO, \$2.2760 for SSA, and \$2.2384 for BO. Clearly, BO's cost is the lowest, so it will be the best among three applied algorithms. As a result, the total cost saving from BO is the highest, \$314.1230, while this value for PSO and SSA is \$310.7286 and \$313.3078, respectively.

As pointed above, the suggested BO method is an effective method in solving the considered optimization problem. By using its optimal solution, the power loss, the voltage profile and the harmonic distortions in the system have been positively changed. As shown in Figure 5, the power loss on the transmission lines was markedly reduced from 0.2245 MW in the original system to 0.0124 MW in the modified system with PDGs and CPs. The loss is reduced by 94.48%. This has demonstrated the great advantage of integrating distributed sources in the distribution system to obtain both technical and economic benefits.

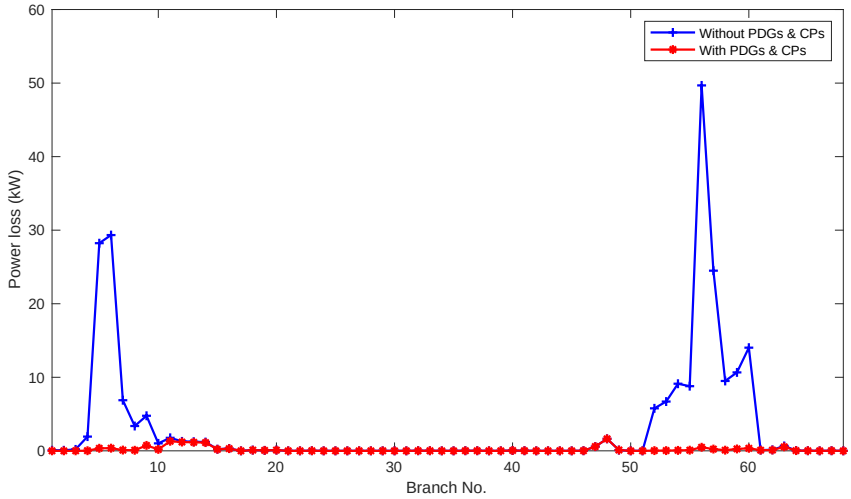

Figure 5. Power loss on distribution lines

Figure 6 is voltage profiles before and after applying the optimal solution from suggested method. For the original system, the lowest bus voltage is 0.9092 pu at Buses 65 and there are 9 buses with voltage beyond the allowable range of [0.95 1.05] pu. However, the voltage profile has been improved significantly in the modified system. The lowest bus voltage is 0.9907 pu at Bus 27 and the voltage of all buses voltages fluctuates in the range of [0.9907 1.0084] pu. Clearly, one more benefit of connecting PDGs and CPs in the distribution system is to enhance the voltage profile.

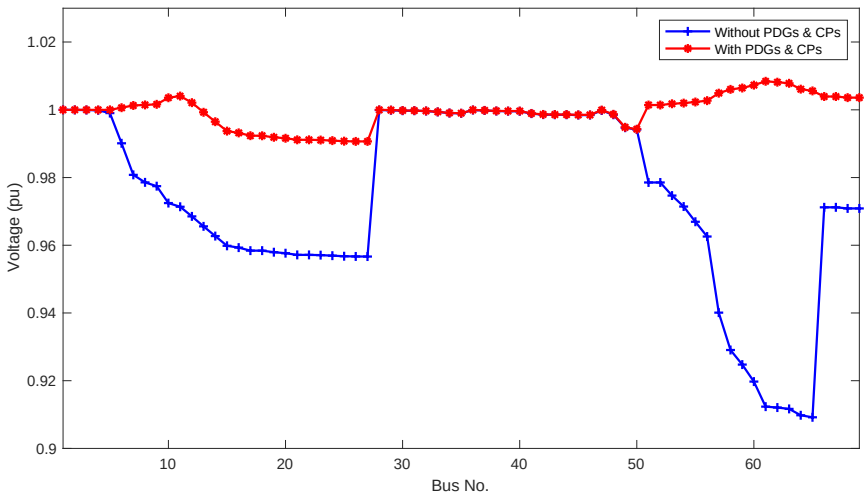

Figure 6. The voltage profile before and after connecting PDGs and CPs

Additionally, THD and IHD values representing for harmonic distortions are also changed positively when adding PDGs and CPs in the system. By implementing the proper connection, the maximum

THD value is drastically reduced from 5.265% to 2.766% as plotted in Figure 7. Similarly, as shown in Figure 8, the maximum IHD value is also mitigated to 1.786%, while that is 3.403% in the base system. As drawing a line of 5% in Figure 7 and another line of 3% in Figure 8, we can see some buses in the base system violating the THD and IHD limits. Clearly, the installation of distributed generators for supplying additional active and reactive power to distribution system, the IEEE Std. 519 about harmonic distortions is satisfied as expected.

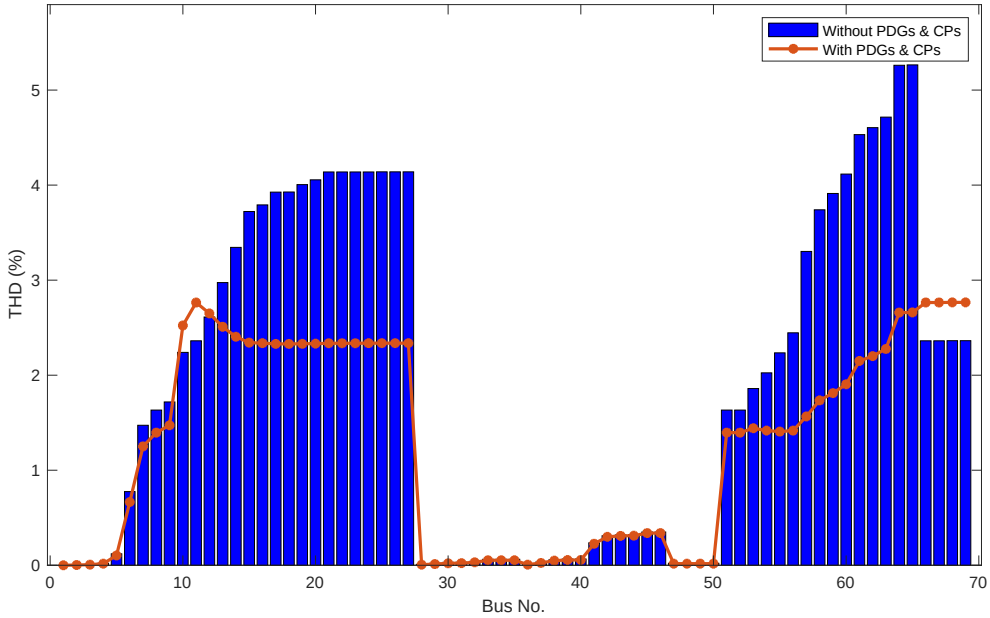

Figure 7. The THD before connecting PDGs and capacitors

Figure 8. The IHD after connecting PDGs and CPs

5. CONCLUSION

In this study, three metaheuristic methods, including of PSO, SSA and BO, were developed to search the optimal solutions for position and capacity of PDGs and CPs in IEEE 69-bus radial distribution system with many nonlinear loads for maximizing economic and technical benefits. The main objective was to minimize the total cost, including of the cost of purchasing energy to supply the load demand, power loss on the lines and emission fines from the generator of the main power source under consideration of constraints on voltage, current, harmonics, etc. Overall, this study has obtained the following achievements:

- The suggested method (BO) together with PSO and SSA were implemented for the same objective and the conditions. The achieved results have proved that BO is the best and most stable method compared

to the compared methods. By integrating BO's optimal solution, the total cost was significantly reduced from $390.1119 to $75.9889, equivalent to 80.52% in total cost reduction.

- In addition, the power loss was also reduced by 94.48%, the voltage variation range was also improved dramatically from the range of [0.9092 1.00] pu to [0.9907 1.0084] pu. This greatly contributes to enhance the power quality of the system.
- Besides, thanks to the optimal integration, harmonic distortions were actively mitigated and met IEEE Std. 519. Specifically, the maximum values of THD and IHD were reduced from 5.265% to 2.766% and from 3.403% to 1.786%, respectively.

In the future, the next work of this study is to consider the time-varying load and power output of renewable energy sources (RER) such as wind turbines and photovoltaic units. On the other hand, the time of charged and discharged energy to achieve the optimal total costs of the battery energy store system (BESS) will also be considered while still satisfying the technical criteria. Finally, a new version of BO modification will be developed for enhancing the performance and stability of the original BO after this work.

ACKNOWLEDGEMENTS

We acknowledge Ho Chi Minh City University of Technology (HCMUT), VNU-HCM for supporting this study.

REFERENCES

[1] S.S. Kola, "A review on optimal allocation and sizing techniques for DG in distribution systems", *International Journal of Renewable Energy Research (IJRER)*, vol.8, No.3, pp. 1236-1256, 2018.

[2] H. HassanzadehFard, and A. Jalilian, "Optimal sizing and location of renewable energy based DG units in distribution systems considering load growth", *International Journal of Electrical Power & Energy Systems*, vol.101, pp. 356-370, 2018.

[3] L. Che, X. Zhang, M. Shahidehpour, A. Alabdulwahab, and A. Abusorrah, "Optimal interconnection planning of community microgrids with renewable energy sources", *IEEE Transactions on Smart Grid*, vol.8, no.3, pp. 1054-1063, 2015.

[4] V. Kalkhambkar, B. Rawat, R. Kumar, and R. Bhakar, Optimal allocation of renewable energy sources for energy loss minimization. *Journal of Electrical Systems*, vol.13, no.1, 115-130, 2017.

[5] R.A. Kordkheili, B. Bak-Jensen, R. Jayakrishnan, and P. Mahat, "Determining maximum photovoltaic penetration in a distribution grid considering grid operation limits", In *2014 IEEE PES General Meeting| Conference & Exposition, IEEE*, pp.1-5, 2014.

[6] A. Hoke, R. Butler, J. Hambrick, and B. Kroposki, "Maximum photovoltaic penetration levels on typical distribution feeders (No. NREL/JA-5500-55094)", *National Renewable Energy Lab.(NREL), Golden, CO (United States)*, 2012.

[7] H.A. Abdel-Ghany, A.M Azmy, N.I. Elkalashy, and E.M. Rashad, "Optimizing DG penetration in distribution networks concerning protection schemes and technical impact", *Electric Power Systems Research*, vol.128, pp.113-122, 2015.

[8] P.R.P Dinakara, R.V.C Veera, and M.T. Gowri, "Ant Lion optimization algorithm for optimal sizing of renewable energy resources for loss reduction in distribution systems", *Journal of Electrical Systems and Information Technology*, vol.5, no.3, pp.663-680, 2018.

[9] A.F. Buitrago-Velandia, O.D. Montoya, and W. Gil-González, "Dynamic Reactive Power Compensation in Power Systems through the Optimal Siting and Sizing of Photovoltaic Sources". *Resources*, vol.10, no.5, 47, 2021.

[10] S. Settoul, R. Chenni, H.A. Hasan, M. Zellagui, and M.N. Kraimia, "MFO algorithm for optimal location and sizing of multiple photovoltaic distributed generations units for loss reduction in distribution systems", In *2019 7th International Renewable and Sustainable Energy Conference (IRSEC)*. IEEE, pp. 1-6, 2019.

[11] C. Chen, X. Wang, H. Yu, M. Wang, and H. Chen, "Dealing with multi-modality using synthesis of Moth-flame optimizer with sine cosine mechanisms", *Mathematics and Computers in Simulation*, vol.188, pp.291-318, 2021.

[12] M.G. Hemeida, A.A. Ibrahim, A.A.A. Mohamed, S. Alkhalaf, and A.M.B. El-Dine, "Optimal allocation of distributed generators DG based Manta Ray Foraging Optimization algorithm (MRFO)", *Ain Shams Engineering Journal*, vol. 12, no.1, pp.609-619, 2021.

[13] O.E. Turgut, "A novel chaotic manta-ray foraging optimization algorithm for thermo-economic design optimization of an air-fin cooler", *SN Applied Sciences*, vol.3, no.1, pp.1-36, 2021.

[14] A. Ymeri, and S. Mujović, "Optimal location and sizing of photovoltaic systems in order to reduce power losses and voltage drops in the distribution grid", *methods*, vol.3, no.4, 2017.

[15] I.J. Hasan, M.R. Ab Ghani, and C.K. Gan, :Optimum distributed generation allocation using PSO in order to reduce losses and voltage improvement", 3rd *IET Internatinal conference on clean energy and technology*, 1-6, 2014

[16] J. A. D. Costa, D.A. Castelo Branco, M.C. Pimentel Filho, M.F.D. Medeiros Júnior, and N.F.D. Silva, "Optimal sizing of photovoltaic generation in radial distribution systems using lagrange multipliers," *Energies*, vol.12, no.9, 1728, 2019.

[17] A.K. Pandey, and S. Kirmani, "Optimal location and sizing of hybrid system by analytical crow search optimization algorithm", *International Transactions on Electrical Energy Systems*, vol.30, no.5, e12327, 2020.

[18] M. Khasanov, S. Kamel, M. Tostado-Véliz, and F. Jurado, "Allocation of photovoltaic and wind turbine based DG units using artificial ecosystem-based optimization", In *2020 IEEE International Conference on Environment and Electrical Engineering and 2020 IEEE Industrial and Commercial Power Systems Europe (EEEIC/I&CPS Europe)*, IEEE, pp. 1-5, 2020.
[19] A.L. Bukar, A, C.W. Tan, and K.Y. Lau, "Optimal sizing of an autonomous photovoltaic/wind/battery/diesel generator microgrid using grasshopper optimization algorithm", *Solar Energy*, 188, pp.685-696, 2019.
[20] T.T. Nguyen, T.T. Nguyen, and N.A. Nguyen, "Maximum Penetration of Distributed Generations and Improvement of Technical Indicators in Distribution Systems", *Mathematical Problems in Engineering*, 2020.
[21] E.S. Ali, S.M. Abd Elazim, and A.Y. Abdelaziz, "Ant lion optimization algorithm for renewable distributed generations", *Energy*, vol.116, pp. 445-458, 2016.
[22] A. Faramarzi, M. Heidarinejad, B. Stephens, and S. Mirjalili, "Equilibrium optimizer: A novel optimization algorithm", *Knowledge-Based Systems*, vol.191, 105190, 2020.
[23] S. Saha, and V. Mukherjee, "A novel multiobjective chaotic symbiotic organisms search algorithm to solve optimal DG allocation problem in radial distribution system", *International Transactions on Electrical Energy Systems*, vol.29, No.5, e2839, 2019.
[24] E.E. Elattar, and S.K. Elsayed, "Optimal location and sizing of distributed generators based on renewable energy sources using modified moth flame optimization technique", *IEEE Access*, vol.8, pp.109625-109638, 2020.
[25] S.M. Abd Elazim, and E.S. Ali, "Optimal network restructure via improved whale optimization approach", *International Journal of Communication Systems*, vol.34, No.1, e4617, 2021.
[26] A. Al Khatib, and H. Shareef, "Optimal Placement and Sizing of Distributed Generation for Power Loss Mitigation and Voltage Profile Enhancement Using Atom Search Optimization", *5th splitech 2020*, 2020.
[27] M. Khasanov, K. Xie, S. Kamel, L. Wen, and X. Fan, "Combined Tree Growth Algorithm for Optimal Location and Size of Multiple DGs with Different Types in Distribution Systems", In *2019 IEEE Innovative Smart Grid Technologies-Asia (ISGT Asia)*, IEEE, pp. 1265-1270, 2019.
[28] K.S. Sambaiah, and T. Jayabarathi, "Optimal reconfiguration and renewable distributed generation allocation in electric distribution systems", *International Journal of Ambient Energy*, vol.42, no.9, pp.1018-1031, 2021.
[29] K. Bhumkittipich, and W. Phuangpornpitak, "Optimal placement and sizing of distributed generation for power loss reduction using particle swarm optimization", *Energy procedia*, vol.*34*, pp.307-317, 2013.
[30] A.K. Das, and D.K. Pratihar, "A new bonobo optimizer (BO) for real-parameter optimization", In *2019 IEEE Region 10 Symposium (TENSYMP), IEEE*, pp. 108-113, 2019.
[31] H.M. Farh, A.A. Al-Shamma'a, A.M. Al-Shaalan, A. Alkuhayli, A.M. Noman, and T. Kandil, "Technical and economic evaluation for off-grid hybrid renewable energy system using novel bonobo optimizer", *Sustainability*, vol.*14*, No.3, 1533, 2022.
[32] M.H. Hassan, S.K. Elsayed, S.K. Kamel, C. Rahmann, and I.B. Taha, "Developing chaotic Bonobo optimizer for optimal power flow analysis considering stochastic renewable energy resources", *International Journal of Energy Research*, vol. 46, No.8, pp. 11291-11325, 2022.
[33] M. Kharrich, O.H. Mohammed, S. Kamel, A. Selim, H.M. Sultan, M. Akherraz, and F. Jurado, "Development and implementation of a novel optimization algorithm for reliable and economic grid- independent hybrid power system", Applied Sciences, vol. 10, No. 18, 6604, 2020
[34] A.K. Das and D.K. Pratihar," Bonobo optimizer (BO): an intelligent heuristic with self-adjusting parameters over continuous spaces and its applications to engineering problems", *Applied Intelligence*, vol. *52*, No. 3, pp. 2942-2974, 2022.
[35] J.H. Teng, and C.Y. Chang, "Backward/forward sweep-based harmonic analysis method for distribution systems" *IEEE transactions on power delivery*, vol.22, no.3, pp.1665-1672, 2007.
[36] V. Janamala, and K. Radha Rani, "Optimal allocation of solar photovoltaic distributed generation in electrical distribution networks using Archimedes optimization algorithm", *Clean Energy*, vol.*6*, no.2, pp.271-287, 2022.
[37] L.C. Kien, T.T.B. Nga, T.M. Phan, T.T. Nguyen, "Coot Optimization Algorithm for Optimal Placement of Photovoltaic Generators in Distribution Systems Considering Variation of Load and Solar Radiation", *Mathematical Problems in Engineering, 2022*
[38] A. Navarro-Espinosa, and L.F. Ochoa, "Probabilistic impact assessment of low carbon technologies in LV distribution systems", *IEEE Transactions on Power Systems*, vol.31, no.3, pp.2192-2203, 2015.
[39] T.T. Nguyen, T.D. Pham, L.C. Kien, and L.V. Dai, "Improved coyote optimization algorithm for optimally installing solar photovoltaic distribution generation units in radial distribution power systems", *Complexity*, 2020.
[40] M. Madhusudhan, N. Kumar, and H. Pradeepa, "Optimal location and capacity of DG systems in distribution network using genetic algorithm", *International Journal of Information Technology*, vol.13, no.1, pp.155-162, 2021.
[41] S.M. Abd Elazim, and E.S. Ali, "Optimal locations and sizing of capacitors in radial distribution systems using mine blast algorithm", *Electrical Engineering*, vol.100, pp.1-9, 2018.
[42] T.D. Pham, T.T. Nguyen, and L.C. Kien, "An Improved Equilibrium Optimizer for Optimal Placement of Distributed Generators in Distribution Systems considering Harmonic Distortion Limits", *Complexity, 2022*.
[43] S.K. Dash, L.R. Pati, S. Mishra, P.K. Satpathy, "Multi-objective Optimal Location and Size of Embedded Generation Units and Capacitors Using Metaheuristic Algorithms," In Green Technology for Smart City and Society, Springer, Singapore, pp. 471-486, 2021.
[44] A. Eid, S. Kamel, M.H. Hassan, and B. Khan, "A Comparison Study of Multi-Objective Bonobo Optimizers for Optimal Integration of Distributed Generation in Distribution Systems", *Energy Res*, vol.10, 847495, 2022.

[45] E.S. Oda, A.M. Abd El Hamed, A. Ali, A.A. Elbaset, M. Abd El Sattar and M. Ebeed, "Stochastic optimal planning of distribution system considering integrated photovoltaic-based DG and DSTATCOM under uncertainties of loads and solar irradiance", IEEE access, vol. 9, pp. 26541-26555, 2021.
[46] M.S. Alam, and S.A. Arefifar, "Cost & emission analysis of different DGs for performing energy management in smart grids," In *2018 IEEE International Conference on Electro/Information Technology (EIT), IEEE*, pp. 0667-0672, 2018.
[47] S. Mirjalili, A.H. Gandomi, S.Z. Mirjalili, S. Saremi, H. Faris, and S.M. Mirjalili, "Salp Swarm Algorithm: A bio-inspired optimizer for engineering design problems", *Advances in engineering software*, vol.114, pp.163-191, 2017.

BIOGRAPHY OF AUTHORS

Thai Dinh Pham received M.S.E.E degree with an outstanding academic record from National Chung Cheng University in Taiwan, R.O.C in 2017. He is currently pursuing the Ph.D degree in electrical engineering with HCMC University of Technology and Education in Ho Chi Minh City, Vietnam. His favorite research areas include power quality, power system optimization and renewable energies.

Hung Duc Nguyen received the B.E. (2004), M.E. (2009) degrees in electrical engineering from Ho Chi Minh City University of Technology, Vietnam. His research interests include microgrid, optimization algorithms, power system optimization, low-cost inverter, and renewable energy, On-board Charger.

Thang Trung Nguyen received his M.Sc. and Ph.D degree in electrical engineering from Ho Chi Minh City University of Technology (HCMUT), in 2010 and 2018 respectively, Vietnam. Currently, he is a research and head of power system optimization research group at Faculty Electrical and Electronics Engineering, Ton Duc Thang university. He has published over one hundred papers. His research fields are power system optimization, optimization algorithms, and renewable energies.

Science & Technology Development Journal 2023, 26(2):2776-2790

Open Access Full Text Article

Engineering and Technology: Research Article

Optimization Planning Method of Renewable distributed Generation in Radial Distribution Systems

Thai Dinh Pham[1,*], Le Chi Kien[1], Tran Huu Tinh[2]

Use your smartphone to scan this QR code and download this article

ABSTRACT

Introduction: This study presents an effective method with high stability called the coyote optimization algorithm (COA) for the optimal integration of renewable distributed generation units (DGUs), including biomass units (BMs), wind turbine units (WTs) and photovoltaic units (PVs). The main aim of the study is to minimize the annual power loss cost considering three hybrid systems with the combination of PV and WT, BM and PV, and BM and WT in the time-varying load demand and operating condition of DGUs simultaneously under constraints of bus voltage, branch current and penetration of DGUs. **Methods**: Apply coyote optimization algorithm (COA) for determining the optimal integration of hybrid distribution systems to minimize the annual operating costs. **Results**: The obtained results in the IEEE 69-bus radial distribution system have demonstrated that determining the proper integration of DGUs can reduce power loss, save annual operating costs, and improve the voltage profile significantly. In addition, the introduced method (COA) and recently published methods such as the slime mould algorithm (SMA) and improved particle swarm optimization algorithm (IPSO) are also implemented and compared together in solving the optimization problem. Compared to a standard IEEE 69-node system, the hybrid systems with the implementation of COA can reduce the annual power loss cost by 83.84%, 91.27% and 92.74%, respectively. On the other hand, COA can reach smaller annual power loss cost than IPSO by 0.96%, 2.17% and 2.1% and SMA by 0.72%, 1.64%, and 1.6%, respectively. **Conclusions**: The results indicate that hybrid systems are operating more effectively than base systems without DGUs, and COA is a strong method providing good solutions for reduction of annual power loss cost.

Key words: Coyote optimization algorithm, wind turbine, photovoltaic, biomass, power loss, voltage profile

[1]*Faculty of Electrical and Electronics Engineering, Ho Chi Minh City University of Technology and Education, Ho Chi Minh City, Vietnam*

[2]*Faculty of Electricity - Electronics - Telecommunications, Can Tho University of Technology, Can Tho City, Viet Nam*

Correspondence

Thai Dinh Pham, Faculty of Electrical and Electronics Engineering, Ho Chi Minh City University of Technology and Education, Ho Chi Minh City, Vietnam

Email: thaipd.ncs@hcmute.edu.vn

History

- Received: 2023-05-27
- Accepted: 2023-07-20
- Published: 2023-7-31

DOI :

https://doi.org/10.32508/stdj.v26i2.4094

Check for updates

INTRODUCTION

In recent years, problems related to environmental pollution and instability in fuel prices have contributed significantly to increasing the penetration of DGUs in distribution systems [1]. The main purpose of integrating DGUs is to inject energy into the system. However, with a suitable integrated strategy, DGUs can provide other great benefits. In some typical examples of the benefits of DGUs [2–4], the power loss on the branches of the distribution system was strongly reduced thanks to the penetration of DGUs. In addition, the voltage quality and reliability of the system are also enhanced [5,6]. On the other hand, loss compensation, reactive power support and frequency control are also additional benefits of connecting DGUs [7]. Conversely, improper integration of DGUs into the distribution system can lead to an increase in power loss, overvoltage, and reverse power flow [8,9].

In the past, determining the DGU installation strategy for power loss minimization has attracted the attention of many researchers. For the most part, they focus on developing different optimization algorithms to reduce losses at the peak load and the fixed power output of DGUs [10,11]. Therefore, the found solution may not be optimal when the load demand and output condition of the DGUs change. Specifically, mixed integer programming [12,13], optimal power flow [14], and heuristic algorithms [15–17] are prime examples for such studies. Only a relatively limited number of papers have considered the variation in load demand and output conditions of DGUs, but these studies have not fully mentioned different types of DGUs and have ignored consideration of the power factor for DGUs [18,19]. In this paper, a study was implemented to overcome the existing shortcomings of previous studies. The optimization problem of the location and capacity as well as the operating power factor of individual DGUs are considered to minimize the annual power loss cost in the distribution system where constraints of the bus voltage, the branch current and the renewable energy penetration level are satisfied. Moreover, three different hybrid systems are also analyzed, including hybrid systems

Cite this article : Pham T D, Kien L C, Tinh T H. **Optimization Planning Method of Renewable dis-tributed Generation in Radial Distribution Systems**. *Sci. Tech. Dev. J. 2023;* 26(2):2776-2790.

of PV and WT, BM and PV, and BM and WT under consideration of time-varying load demand and their operating conditions simultaneously. In addition, a forward-backward sweep (FW-BWS)-based numerical technique is applied to solve the load flow problem and calculate power loss before and after connecting DGUs[20]. On the other hand, to obtain the maximum benefit from integrating DGUs into a distributed system, an efficient algorithm with high stability, named the coyote optimization algorithm (COA)[21], is suggested for solving the optimization problem. The obtained results of the COA are also compared with recently introduced methods in 2020 and 2021, such as the slime mould algorithm (SMA)[22] and improved particle swarm optimization (IPSO) algorithm[23], respectively, to show the superior effectiveness of the suggested method. In summary, the contributions of this study can be briefly presented as follows:

- The study considers the optimal integration of three hybrid systems, including BM and WT, WT and PV, and BM and WT, into the distribution system considering the time-varying load demand and generation under constraints of bus voltage, branch current and penetration level of connected units.
- The study successfully determines the optimal position and capacity of the BM, WT and PV in the distribution system to maximize the achieved economic benefit of annual power loss cost reduction for the three hybrid systems mentioned above while still satisfying the technical criteria.
- The study introduces an effective method with high stability, called the coyote optimization algorithm (COA), for solving the optimization problem of the installation of the BM, WT and PV. The study compares the COA with recently published robust methods such as SMA and IPSO to demonstrate the COA's superiority in handling optimization problems.

The rest of the paper is divided as follows: Section 2 describes the objective function and constraints. Section 3 introduces the suggested method. The flowchart of the suggested method for solving the optimization problem is presented in Section 4. Section 5 focuses on the analysis of the obtained results from the simulation. Finally, Section 6 is a summary of the whole paper.

PROBLEM FORMULATION

Objective function

Power loss in the distribution system plays an important role in evaluating power quality as well as the efficiency of system operation. The smaller the power loss on the branches, the greater the cost savings. The formulation for calculating total power loss on the j^{th} branches can be presented as[24]:

$$P_{LS} = \sum_{j=1}^{N_{br}} I_j^2 \times R_j \quad (1)$$

where R_j and I_j are the resistance and current magnitude of the j^{th} branch, respectively.

Assuming a year has 365 days, the annual energy loss cost ($Cost_{Ls}$) in the distribution system with a time duration (Δh) of 1 hour should be expressed by[7,24]:

$$Cost_{Ls} = 365 \times Price_{Ls} \times \sum_{h=1}^{N_{hr}} P_{Ls}^h \times \triangle h \quad (2)$$

Constraints

The power balance constraints

To ensure system frequency stability, total power generation needs to be equal to total power consumption. Thus, the power balance equation should be described in the mathematical model as[25]:

$$P_{Grid}^h + \sum_{i=1}^{N_{DGU}} P_{Gen,i}^h = \sum_{j=1}^{N_{br}} P_{Ls,j}^h + \sum_{k=1}^{N_{ld}} P_{Ld,k}^h \quad (3)$$

$$Q_{Grid}^h + \sum_{i=1}^{N_{DGU}} Q_{Gen,i}^h = \sum_{j=1}^{N_{br}} Q_{Ls,j}^h + \sum_{k=1}^{N_{ld}} Q_{Ld,k}^h \quad (4)$$

In the above equation, $Q_{Gen,i}^h$ can be determined by[26]:

$$Q_{Gen,i}^h = P_{Gen,i}^h \times \tan\left(\cos^{-1}\left(PF_{Gen,i}\right)\right) \quad (5)$$

In this research, $PF_{Gen,i}$ is the operating power factor of the DGUs.

The branch current limit

The current on the branches should not exceed the maximum allowable limit[27]:

$$I_j^{\square} \le I_j^{Max};\ j = 1,2,3...,N_{br} \quad (6)$$

The bus voltage limits

The bus voltage should be kept in the upper and lower bounds[28]:

$$V^{Min} \le V_b^{\square} \le V^{max},\ b = 1,2,3,...,N_{bu} \quad (7)$$

The penetration of DGUs

The rated capacity of individual DGUs needs to be predefined in the lower and upper bounds. In addition, total power generation does not exceed total power consumption to avoid undesirable effects such as overvoltage, system unreliability and reverse power flow in the distribution systems[29]:

$$P_{DGU}^{Min} \le P_{DGU,i}^{Rated} \le P_{DGU}^{Max};\ i = 1,2,3,...,N_{DGU} \quad (8)$$

$$\sum_{i=1}^{N_{DGU}} P_{Gen,i}^{h} \le \alpha \times \sum_{k=1}^{N_{ld}} P_{LD,k}^{h};\ h = 1,2,3,...,N_{hr} \quad (9)$$

COYOTE OPTIMIZATION ALGORITHM (COA)

In recent years, real-world optimization problems have been formulated as computational codes for almost all fields, such as mechanical, civil, aerospace, chemicals and health science. Thus, the quality of the found solution for solving the optimization problems depends on the performance of the algorithm. The development of novel optimization algorithms is always welcomed. In 2018, Pierezan and Coelho published a powerful algorithm called the coyote optimization algorithm (COA) for solving a variety of real problems[21]. This algorithm is inspired by the canis latrans species and has a high ability to find the global optimal solution with high stability. Based on the nature of canis latrans species, this community can be divided into groups ($N_{gr}^{\square}$), and each group consists of many members ($N_{ca}^{\square}$). Therefore, the result of ($N_{ca}^{\square} \times N_{gr}^{\square}$) is considered the population of this species[30].

To run the algorithm, the social condition and quality of social condition are assigned as two important factors that represent the proposed solution and its fitness, respectively, in solving the optimization problems. Similar to other metaheuristic algorithms, the initial solution of the COA is randomly generated within the predetermined limits, and the mathematical model can be presented as[30]:

$$So_{gr,ca}^{\square} = So_{\square}^{Min} + r\left(So_{\square}^{Min} + So_{\square}^{Max}\right);\ gr = 1,2,3,...,N_{gr}^{\square}\ \&\ ca = 1,2,3,...,N_{CA}^{\square} \quad (10)$$

where $So_{\square}^{Max}$ and $So_{\square}^{Min}$ are the upper and lower bounds of the control variables in the solution. r is defined as a random number in the interval of [0, 1]. After obtaining initial solutions, every solution will be evaluated by the fitness function, and the current best solution will be kept.

The next step is to update the solutions to their new positions by applying the first generation equation, which is formulated by[21]:

$$So_{gr,ca}^{New} = So_{gr,ca}^{\square} + r.\left(So_{best,gr}^{\square} - So_{r1,gr}^{\square}\right) + r.\left(So_{cent,gr}^{\square} - So_{r2,gr}^{\square}\right);\ gr = 1,2,3,...,N_{gr}^{\square}\ \&ca = 1,2,3,...,N_{ca}^{\square} \quad (11)$$

Obviously, in equation (11), there are two jumps, including ($So_{best,gr}^{\square} - So_{r1,gr}^{\square}$) and ($So_{cent,gr}^{\square} - So_{r2,gr}^{\square}$). While ($So_{best,gr}^{\square} - So_{r1,gr}^{\square}$) tends to search the possible solutions around the best solution in each group, ($So_{cent,gr}^{\square} - So_{r2,gr}^{\square}$) focuses on finding the good solution around the center point of the group. This greatly contributes to avoiding omitting good solutions, thereby significantly improving the performance of the algorithm. Similarly, each newly created solution is evaluated by the objective function, and the current best solution is updated through comparison. In addition, the second generation equation is also used in COA for generating a new solution in each group, and the equation is built on the randomization mechanism as[30]:

$$So_{gr}^{New} = \begin{cases} So_{gr,r1}^{\square},\ if\ r < 1/N_{cv} \\ So_{gr,r2}^{\square},\ if\ 1/N_{cv} \le r < 5 + 1/N_{cv} \\ So_{gr,r}^{\square},\ otherwise \end{cases} \quad (12)$$

To extend opportunities for finding new solutions in the larger space and avoid missing good solutions, equation (12) is developed with three randomly produced solutions ($So_{gr,r1}^{\square}$, $So_{gr,r2}^{\square}$ and $So_{gr,r}^{\square}$) that are selected according to specific conditions. While $So_{gr,r1}^{\square}$ and $So_{gr,r2}^{\square}$ can be established for each group by incidentally selecting random variables from available solutions in each group, then $So_{gr,r}^{\square}$ is randomly generated within the allowable limits of predetermined control variables. At this stage, the created solution is qualitatively compared with the worst solution in the group, and the better solution is retained. This eliminated the worst quality solution in each group, leading to enhanced general quality for the proposed solutions. In addition, to simulate the movement of the coyotes from this group to other groups, the exchange action is performed. If the condition of equation (13) is satisfied, two solutions are randomly selected from two different random groups in the community to swap their positions[30].

$$\gamma < \frac{10^{-2}}{2} \times N_{ca}^{2} \quad (13)$$

Here, γ is a randomly generated number between 0 and 1. Clearly, the coyote migration rate is proportional to the population number in each group. The

larger the number of coyotes in the group, the greater the probability of coyote exchange action. Finally, the best solution in the community is also determined by comparing their fitness values.

FLOWCHART FOR APPLYING THE COA TO SOLVE THE CONSIDERED PROBLEM

This paper develops the integration of three hybrid systems of PV and WT, BM and WT, and BM and PV to minimize the annual energy cost by applying the coyote optimization algorithm. This algorithm executes iteratively until the maximum iteration value ($Iter_{\square}^{Max}$) is reached to solve the optimization problem. The flowchart for finding the global optimal solution is shown in Figure 1.

SIMULATION RESULTS

In this paper, three hybrid systems are considered for minimizing the annual power loss cost in the IEEE 69-bus radial distribution system considering the time-varying load demand and operating condition of DGUs. The structure of the system is presented in Figure 2 with a nominal voltage of 12.66 kV and a total power load of 3.802 MW and 2.694 MVar. The bus data and line data of the implemented system are taken from [25].

For the simulation of applied methods, initial parameters were investigated, and the obtained results were $Iter_{\square}^{Max}$ and $N_{\square}^{Run} = 30$. In this research, IPSO is implemented as one of the compared methods with the parameters of the inertia weight ($a = 0.9$ and $b = 0.5$) and the acceleration factor ($c_{1i} = 2.5$, $c_{1f} = 0.5$, $c_{2i} = 0.5$ and $c_{2f} = 2.5$) clearly described in [23]. For running SMA, in the formula for updating the location, the condition value (z) is set as 0.05, and r is a random number in the range of [0,1] [23]. The population (N_{pop}) of IPSO and SMA is selected through a survey, and its value is assigned as 30. On the other hand, the setting parameters for COA, including $N_{ca}^{\square}$ and $N_{gr}^{\square}$, are the same value, equal to 5. Additionally, this study has assumed that the BM is simulated as a synchronous machine with the output power of the BM being constant and generating at its rated power during 24 hours of a day. PV and WT apply converters for integration with the output powers that change over time and are plotted in Figure 3. The load data and output power data used for both PV and WT are presented in Table 2 in APPENDIX [7]. As mentioned, the study is implemented for three different cases as follows:

(1) Case 1: Hybrid system with PV and WT

(2) Case 2: Hybrid system with BM and PV

(3) Case 3: Hybrid system with BM and WT

To determine the optimal size of DGUs, the capacity of the BM is varied from 0 MW to 2.0 MW, and the minimum and maximum numbers for PV and WT are (2,000 modules and 30,000 modules) and (01 turbine and 20 turbines), respectively. The rated capacity of the PV module is also assumed to be 75 W [31], and the rated capacity of each turbine is 200 kW [32]. Moreover, this paper chose the operating power factor of the PV, WT and BM to be 0.9 (lagging) [7,33].

The optimal solutions from IPSO, SMA and COA for three different hybrid systems are reported in Table A.2, APPENDIX, and the obtained results regarding power loss are presented in Table 1. Obviously, when DGUs are connected, the annual power loss is significantly reduced compared to the system without DGUs. Specifically, the annual loss has fallen from 1756.5174 MW of the base system to 286.5806 MW, 285.8858 MW and 283.8602 MW (in case 1) to 156.6442 MW, 155.8214 MW and 153.266 MW (in case 2) and to 130.8121 MW, 127.9270 MW and 127.5543 MW (in case 3) for IPSO, SMA and COA, respectively. The loss reduction has greatly contributed to reducing the cost of operating the distribution system, and this is considered one of biggest benefits for integrating DGUs into the system in addition to supplying power to load demand as the primary purpose. Assuming the electricity price for the power loss is \$60/MWh [25], the annual cost was strongly decreased thanks to the integration of DGUs, and the amount of annual cost reduction for the three cases is reported in detail in Figure 4. Figure 8 in APPENDIX serves as a good example of loss reduction after connecting DGUs to the system by applying the optimal solution from COA. This resulted in annual loss cost reductions of 83.84%, 91.27% and 92.74% for case 1, case 2 and case 3, respectively. Obviously, the PV and WT hybrid system is the least efficient, and the BM and WT hybrid system is the most efficient. This is due in part to the capacity factor that can represent the individual characteristic for the output stability of each unit. That value is defined as the ratio of the actual amount of electricity generated to the energy that can be generated at full capacity for the same period of time [34]. In addition to the capacity factor, the solution of the location and sizing of DGUs also contributes significantly to improving the efficiency of the hybrid systems. Compared, the optimal solution from COA is more positive than the remaining methods. Specifically, in case 3, the cost reduction of annual power loss from COA occupies 92.74%, corresponding to only \$7,653/year, while IPSO and

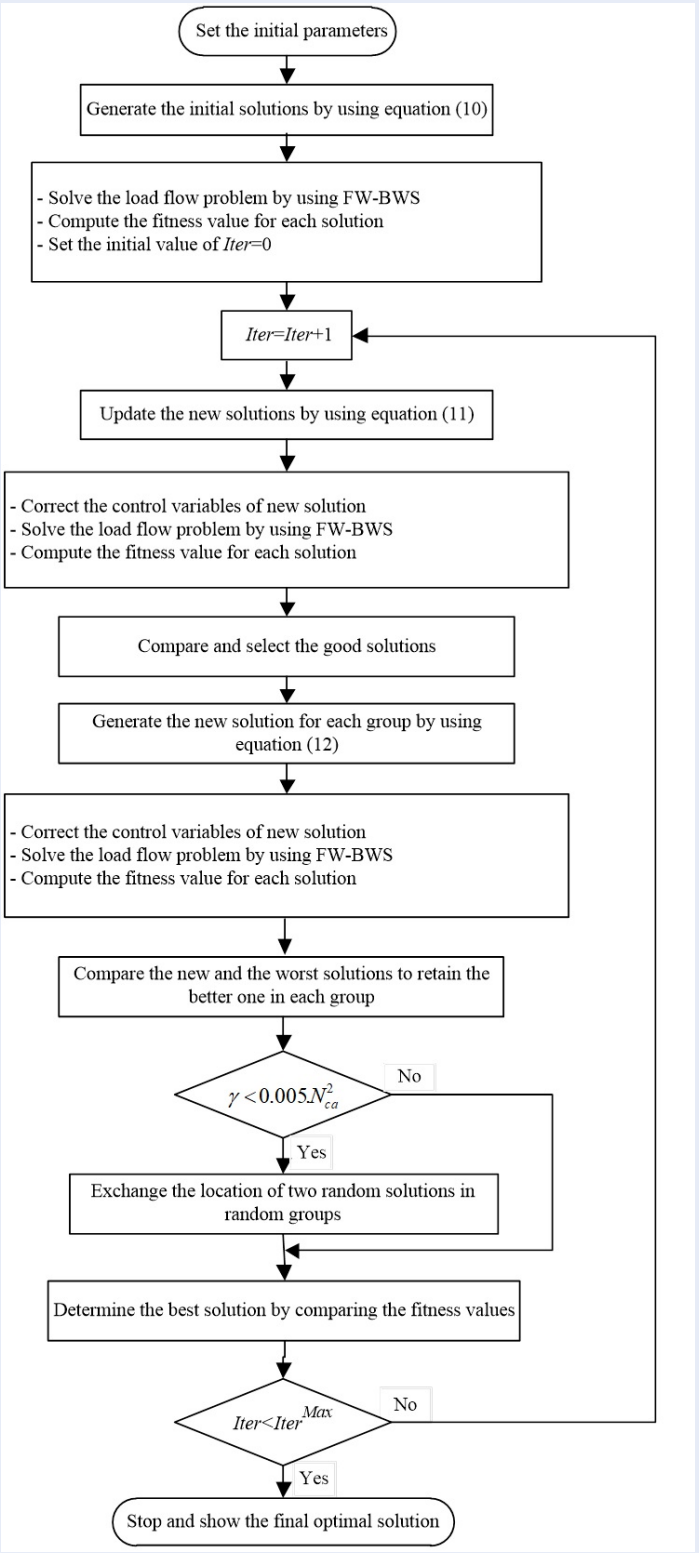

Figure 1: Flowchart for finding the optimal solution in the considered problem

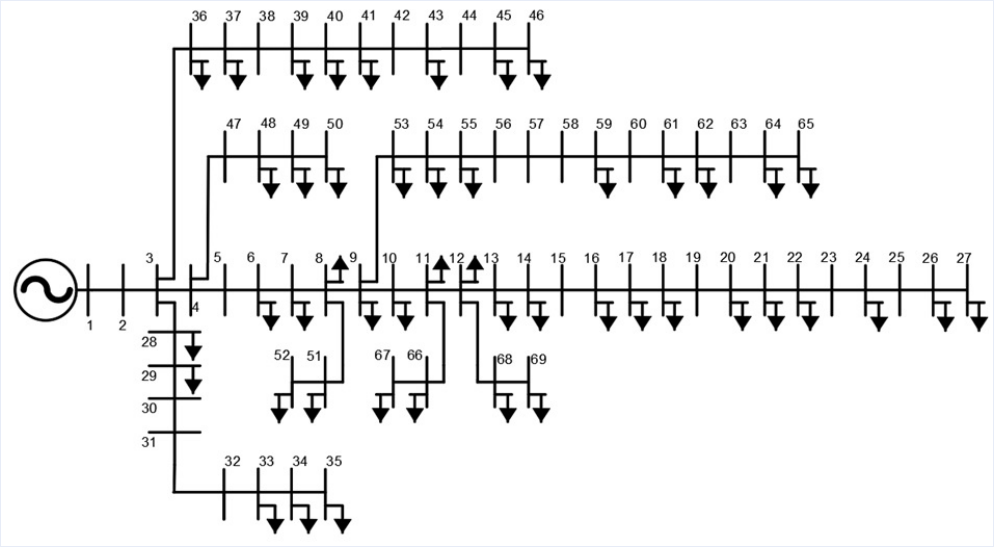

Figure 2: **The IEEE 69-bus radial distribution system**.

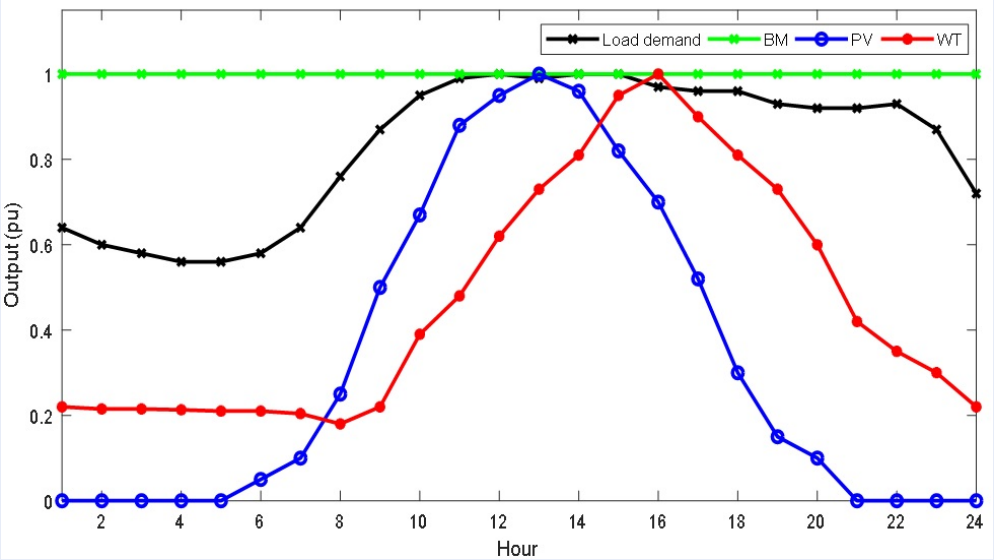

Figure 3: **The daily load demand, BM, PV, and WT output curves**.

SMA are 92.55% and 92.72%, corresponding to up to $7,849/year and $7,680/year, respectively. For an exact performance comparison, the annual cost savings of COA are calculated. COA can reach smaller annual costs than IPSO by $165, $204 and $165 and SMA by $123, $153, and $123 for Case 1, Case 2 and Case 3, respectively. The saving cost values are equal to the 0.96%, 2.17%, and 2.1% annual costs of IPSO and the 0.72%, 1.64%, and 1.6% annual costs of SMA for Case 1, Case 2 and Case 3, respectively. This indicates that COA is a higher performance method than IPSO and SMA for the problem.

Figure 5 presents the actual output power of DGUs considering the time-varying load demand and operating condition of DGUs simultaneously for the three cases. The total amount of load demand power in a day requires 75.66 MW, while the DGUs only provide 37.05 MW, 44.84 MW and 46.31 MW for case 1, case 2 and case 3, respectively, as shown Figure 6. Therefore, the remaining power of 38.61 MW, 30.82

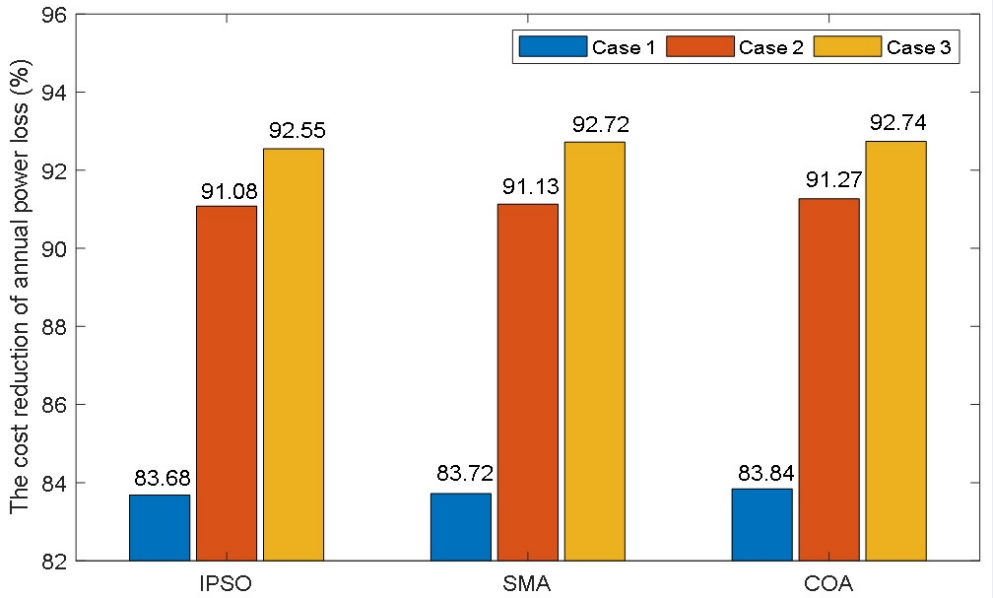

Figure 4: **The cost reduction of annual power loss (%) in three cases for implemented methods.**

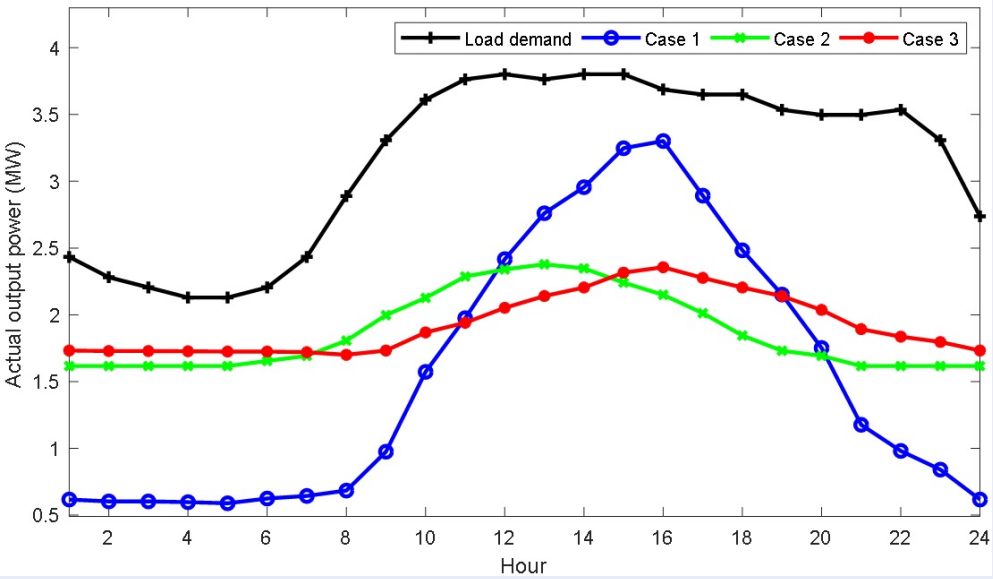

Figure 5: **The actual output power of implemented cases and load demand.**

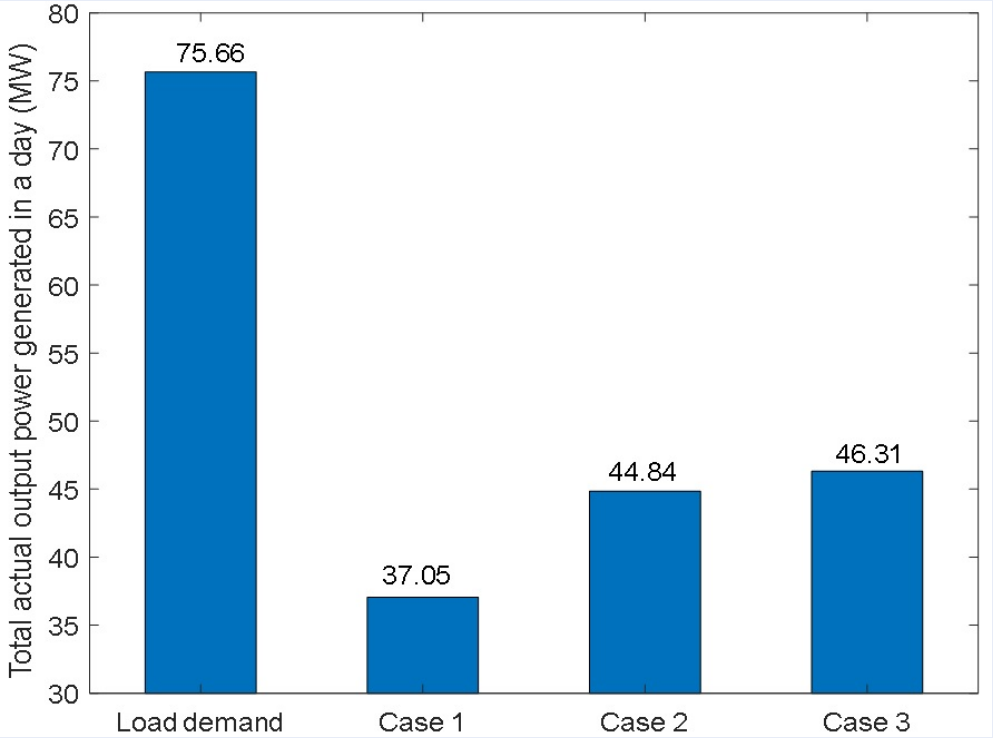

Figure 6: **Total actual output power of DGUs for cases in a day.**

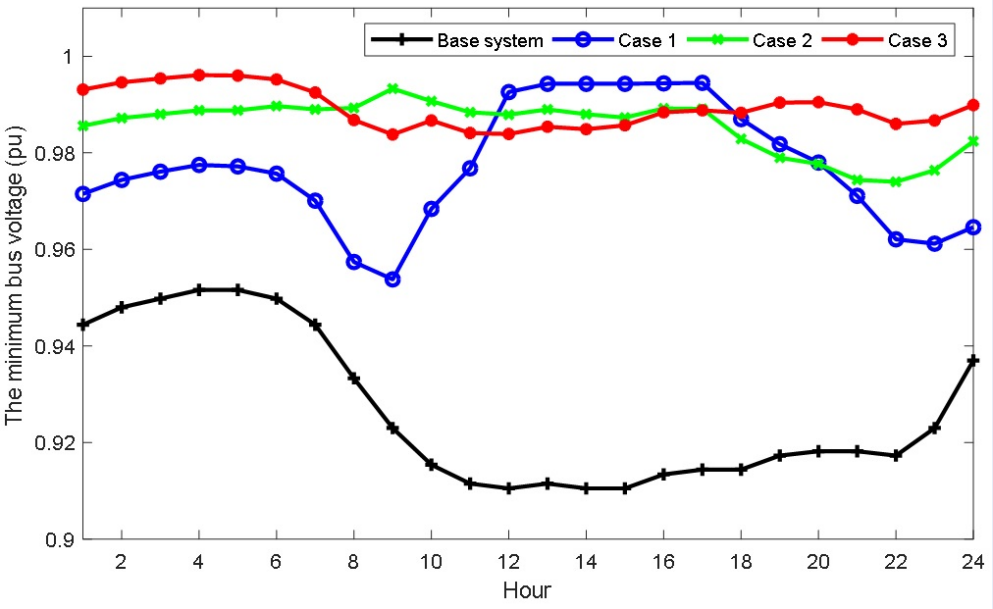

Figure 7: **The minimum bus voltage of cases.**

Table 1: The obtained results from implemented methods for three cases

Applied method	Case 1		Case 2		Case 3	
	The annual power loss (MW)	The annual cost for power loss ($)	The annual power loss (MW)	The annual cost for power loss ($)	The annual power loss (MW)	The annual cost for power loss ($)
IPSO	286.5806	17,195	156.6442	9,400	130.8121	7,849
SMA	285.8858	17,153	155.8214	9,349	127.9270	7,680
COA	283.8602	17,030	153.2660	9,196	127.5543	7,653

MW and 29.35 MW for three cases that are not yet supplied by DGUs will be supplied by the main grid through the substation. In addition, at each time , the generated power did not exceed the load demand. This completely satisfies the constraint of the penetration level from DGUs to avoid undesirable effects such as overvoltage, system unreliability and reverse power flow. Moreover, another important constraint of the bus voltage is also considered and analyzed in this section. Figure 7 plots the minimum bus voltage values at each time h of the cases before and after connecting DGUs by the suggested method. For the base system, the minimum voltage value is 0.909 (pu) and falls on peak load times at the 12^{th}, 14^{th} and 15^{th} hours. In addition, the voltage profile without DGUs at each time h is also shown in Figure 9, APPENDIX. Clearly, many voltage values are out of the allowable voltage range of [0.95 1.05] (pu). However, by properly connecting the DGUs, the voltage profile of the distribution system is enhanced drastically and satisfies the bounds of the bus voltage. For example, in the COA, by connecting suitable DGUs, the voltage profile is improved well, with minimum voltages of 0.954 (pu), 0.974 (pu) and 0.984 (pu) for case 1, case 2 and case 3, respectively. The voltage profiles with DGUs are also presented in Figures 10, 11 and 12 in APPENDIX for the three cases. Compared, the voltage profile of case 3 is better than the others, which contributed to the claim of case 3's effectiveness over the two compared cases. From the above arguments, it can be affirmed that determining the optimal DGU installation strategy can reduce power loss on distribution lines, cut operating costs and significantly enhance voltage.

CONCLUSIONS

In this study, the cost of annual power loss is minimized and compared between three effective methods, including IPSO, SMA, and COA, in the IEEE 69-bus radial distribution system. The paper considered the hybrid systems of PV and WT, BM and PV, and BM and WT in the time-varying load demand and operating conditions of DGUs simultaneously. The obtained solutions have proven the superior effectiveness of the COA in solving the optimization problem of the location and sizing of DGUs.

- The annual loss has cut from 1756.5174 MW of the original system to 286.5806 MW, 285.8858 MW and 283.8602 MW in case 1 to 156.6442 MW, 155.8214 MW and 153.266 MW in case 2 and to 130.8121 MW, 127.9270 MW and 127.5543 MW in case 3 for IPSO, SMA and COA, respectively. Clearly, by integrating suitable distributed generation units, the power loss can be greatly reduced, and economic well-being can be improved.
- In addition, by comparing the implemented methods in the best case (case 3), COA is better than the others since the cost reduction can reach 92.74%, while this value is 92.55% and 92.72% for IPSO and SMA, respectively. In summary, determining a suitable installation for DGUs can reduce loss, reduce system operating costs, and enhance the voltage profile.

In this study, harmonic distortions in the distribution system that are caused by nonlinear loads and inverters of the PV, WT and BM are ignored. Therefore, in the future, harmonics will be considered to ensure compliance with IEEE Std. 519. In addition, to minimize the discrepancy between the predicted and actual generation powers of DGUs, more hours should be considered. Specifically, 96 hours, which represent the typical 4 days of 4 seasons (spring, summer, autumn and winter) in a year, will be implemented in future works.

AUTHOR'S CONTRIBUTIONS

Thai Dinh Pham: Programming and writing entire paper. Le Chi Kien: Contributing ideas, supervising and editing paper. Tran Huu Tinh: Contributing ideas and collecting results.

FUNDING

This research has not received any funding.

COMPETING INTERESTS

The authors declare that they have no competing interests.

LIST OF SYMBOLS

$\triangle V^{\square}_{b,gr,ca}, \triangle V^{\square}_{j,gr,ca}$ The penalty amounts of the b^{th} bus voltage and the j^{th} branch current at the ca^{th} solution of the gr^{th} group

$FF^{\square}_{gr,ca}$, $OF^{\square}_{gr,ca}$ The fitness and objective function values at the ca^{th} solution of the gr^{th} group

$FF^{New}_{gr,ca}$ The new fitness of the ca^{th} solution of the gr^{th} group

I_j, I^{Max}_j Current magnitude and maximum allowable current magnitude at the i^{th} branch

L^{Min}_i, L^{Max}_i The maximum and minimum limits of the location for DGUs

$N^{\square}_{hr}$, $N^{\square}_{cv}$ The number of considered hours and control variables, respectively

$N^{\square}_{br}$, $N^{\square}_{bu}$, $N^{\square}_{ld}$, $N^{\square}_{DGU}$ The number of branches, buses, loads and DGUs

$P^{Rated}_{DGU,i}$ The rated power of the i^{th} DGU

P^{Min}_{DGU}, P^{Max}_{DGU} The minimum and maximum rated power of the DGU

$PF_{Gen,i}$ The operating power factor of the i^{th} DGU

$PF^{h}_{Gen,i}$, $Q^{h}_{Gen,i}$ The actual active and reactive power of the i^{th} DGU at the h^{th} hour

$P^{\square}_{Grid}$, $Q^{\square}_{Grid}$ The active and reactive power supplied by the main grid through the substation

$P^{h}_{L,d,k}$, $Q^{h}_{L,d,k}$ The active and reactive power load of the k^{th} load at the h^{th} hour

$P^{h}_{Ls,j}$, $Q^{h}_{Ls,j}$ The active and reactive power loss of the j^{th} branch at the h^{th} hour

$P^{\square}_{Ls}$ The active power loss of the system

P^{h}_{Ls} The active power loss at the h^{th} hour

$Price^{\square}_{Ls}$ The electricity price ($/MW.h)

Si^{Max}_i, Si^{Min}_i The maximum and minimum limits of the capacity for DGUs

$So^{Max}_{\square}$, $So^{Min}_{\square}$ The upper and lower bounds of solutions

$So^{\square}_{best,gr}$, $So^{\square}_{cent,gr}$ The best solution and the central solution of the gr^{th} group

$So^{\square}_{gr,ca}$, $So^{New}_{gr,ca}$ The ca^{th} solution and the ca^{th} new solution of the gr^{th} group

So^{New}_{gr} The new solution is generated at the gr^{th} group

$So^{\square}_{r1,gr}$, $So^{\square}_{r2,gr}$ The randomly taken solutions of the gr^{th} group

$Va^{New}_{cv,gr,ca}$ The created new control variable at the ca^{th} solution of the gr^{th} group

$Va^{Max}_{cv}, Va^{Min}_{cv}$ The upper and lower bounds of the control variables

V_b, $V^{Min}_{\square}$, $V^{Max}_{\square}$ The voltage magnitude at the b^{th} bus, minimum and maximum allowable voltage magnitudes of the system, respectively

ρ_v, ρ_l The penalty factors of the bus voltage and branch current, respectively

α The penetration level of DGUs

APPENDIX

Tables 2 and 3 and Figures 8, 9, 10, 11 and 12

REFERENCES

1. Adefarati T, Bansal RC. Integration of renewable distributed generators into the distribution system: a review. IET Renew Power Gener. 2016;10(7):873-84;Available from: https://doi.org/10.1049/iet-rpg.2015.0378.
2. ChithraDevi SA, Lakshminarasimman L, Balamurugan R. Stud Krill herd Algorithm for multiple DG placement and sizing in a radial distribution system. Eng Sci Technol An Int J. 2017;20(2):748-59;Available from: https://doi.org/10.1016/j.jestch.2016.11.009.
3. Azad S, Amiri MM, Heris MN, Mosallanejad A, Ameli MT. A novel analytical approach for optimal placement and sizing of distributed generations in radial electrical energy distribution systems. Sustainability. 2021;13(18):10224;Available from: https://doi.org/10.3390/su131810224.
4. Ogunsina AA, Petinrin MO, Petinrin OO, Offornedo EN, Petinrin JO, Asaolu GO. Optimal distributed generation location and sizing for loss minimization and voltage profile optimization using ant colony algorithm. SN Appl Sci. 2021;3:1-10;Available from: https://doi.org/10.1007/s42452-021-04226-y.
5. Kumar M, Nallagownden P, Elamvazuthi I. Optimal placement and sizing of distributed generators for voltage-dependent load model in radial distribution system. Renew Energy Focus. 2017;19-20:23-37;Available from: https://doi.org/10.1016/j.ref.2017.05.003.
6. Al Abri RS, El-Saadany EF, Atwa YM. Optimal placement and sizing method to improve the voltage stability margin in a distribution system using distributed generation. IEEE Trans Power Syst. 2012;28(1):326-34;Available from: https://doi.org/10.1109/TPWRS.2012.2200049.
7. Hung DQ, Mithulananthan N, Bansal RC. Analytical strategies for renewable distributed generation integration considering energy loss minimization. Appl Energy. 2013;105:75-85;Available from: https://doi.org/10.1016/j.apenergy.2012.12.023.
8. Reddy GH, Koundinya AN, Gope S, Raju M, Singh KM. Optimal sizing and allocation of DG and FACTS device in the distribution system using fractional Lévy flight bat algorithm. IFAC PapersOnLine. 2022;55(1):168-73;Available from: https://doi.org/10.1016/j.ifacol.2022.04.028.
9. Elattar EE, Elsayed SK. Optimal location and sizing of distributed generators based on renewable energy sources using modified moth flame optimization technique. IEEE Access. 2020;8:109625-38;Available from: https://doi.org/10.1109/ACCESS.2020.3001758.
10. Prakash P, Khatod DK. Optimal sizing and siting techniques for distributed generation in distribution systems: a review. Renew Sustain Energy Rev. 2016;57:111-30;Available from: https://doi.org/10.1016/j.rser.2015.12.099.

Table 2: The data used for simulating the load and output power of the BM, PV and WT

Hour No.	Load (pu)	Output power of BM (pu)	Output power of PV (pu)	Output power of WT (pu)
1	0.64	1.0	0	0.220
2	0.60	1.0	0	0.215
3	0.58	1.0	0	0.215
4	0.56	1.0	0	0.213
5	0.56	1.0	0	0.210
6	0.58	1.0	0.050	0.210
7	0.64	1.0	0.100	0.204
8	0.76	1.0	0.250	0.180
9	0.87	1.0	0.500	0.220
10	0.95	1.0	0.670	0.390
11	0.99	1.0	0.880	0.480
12	1.00	1.0	0.950	0.620
13	0.99	1.0	1.000	0.730
14	1.00	1.0	0.960	0.810
15	1.00	1.0	0.820	0.950
16	0.97	1.0	0.700	1.000
17	0.96	1.0	0.520	0.900
18	0.96	1.0	0.300	0.810
19	0.93	1.0	0.150	0.730
20	0.92	1.0	0.100	0.600
21	0.92	1.0	0	0.420
22	0.93	1.0	0	0.350
23	0.87	1.0	0	0.300
24	0.72	1.0	0	0.220

Table 3: The optimal solutions from implemented methods for three cases

Applied method	Case 1		Case 2		Case 3	
	PV	WT	PV	BM	WT	BM
IPSO	Bus 18 – 10,092 modules	Bus 61 – 14 turbines	Bus 13 – 13,080 modules	Bus 61 – 1.6058 MW	Bus 15 – 05 turbines	Bus 61 – 1.5653 MW
SMA	Bus 22 – 8,418 modules	Bus 61 – 14 turbines	Bus 21 – 9,667 modules	Bus 61 – 1.6213 MW	Bus 17 – 04 turbines	Bus 61 – 1.5976 MW
COA	Bus 17 – 9,558 modules	Bus 61 – 14 turbines	Bus 17 – 10,160 modules	Bus 61 – 1.6161 MW	Bus 17 – 04 turbines	Bus 61 – 1.5562 MW

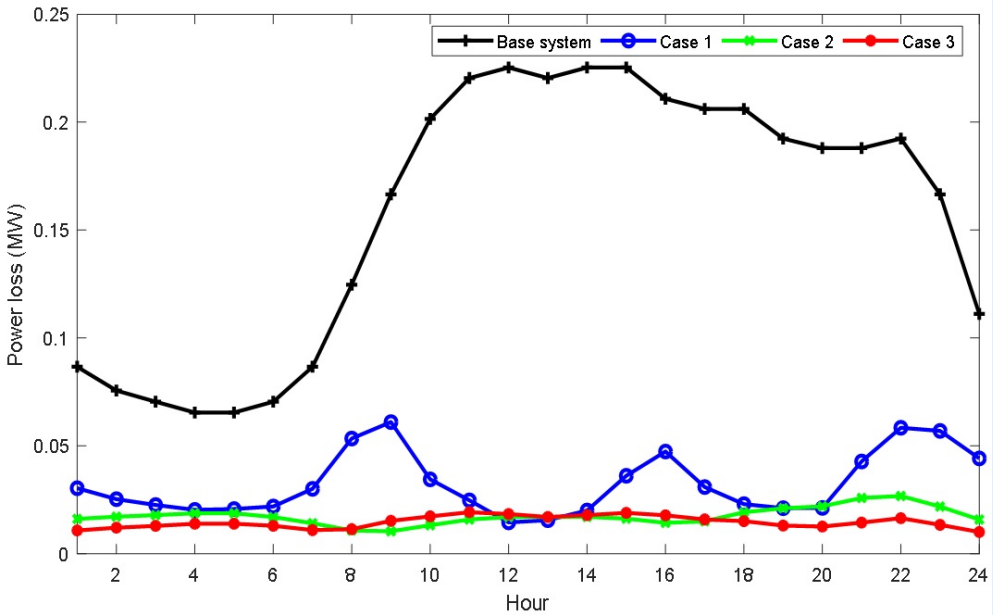

Figure 8: The power loss before and after connecting DGUs by using COA's solution at cases

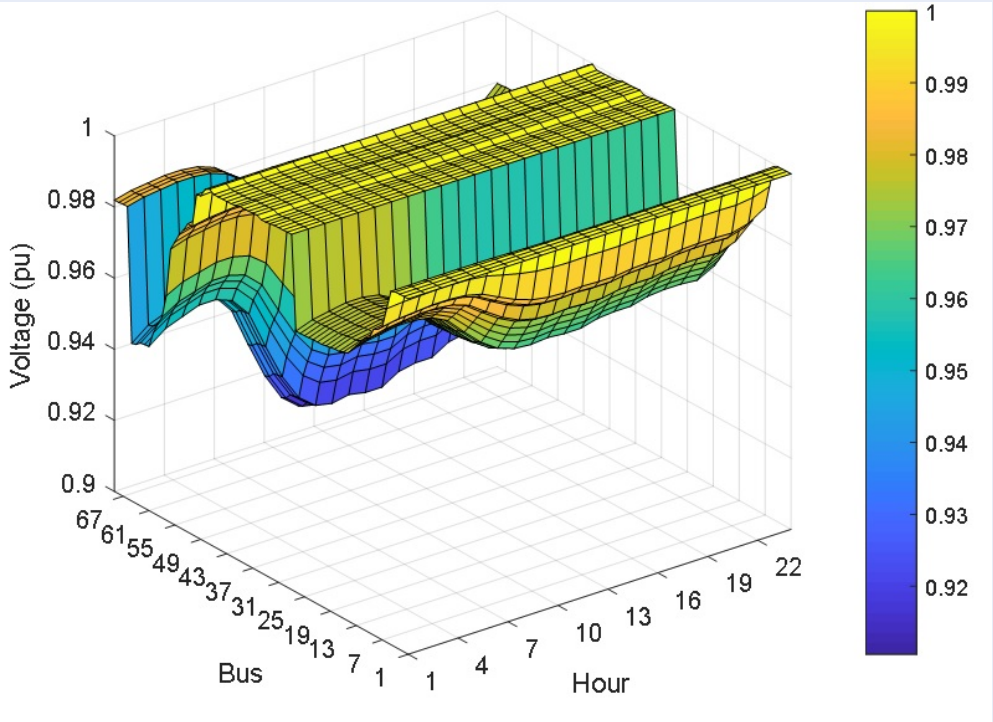

Figure 9: The voltage profile without DGUs

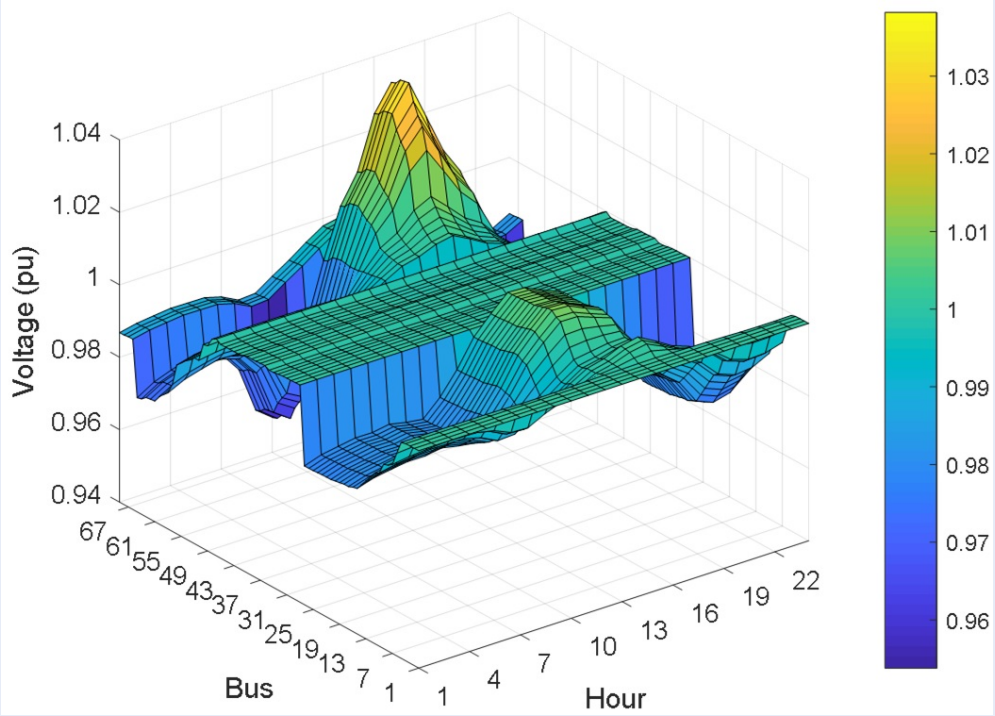

Figure 10: The voltage profile with DGUs from COA's solution at case 1

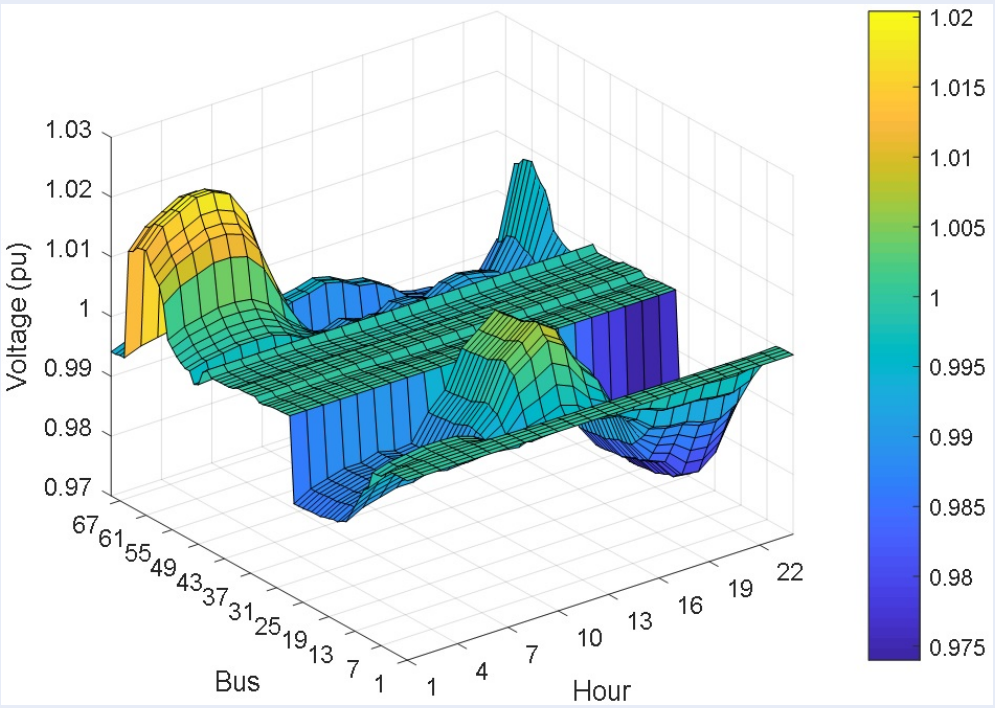

Figure 11: The voltage profile with DGUs from COA's solution at case 2

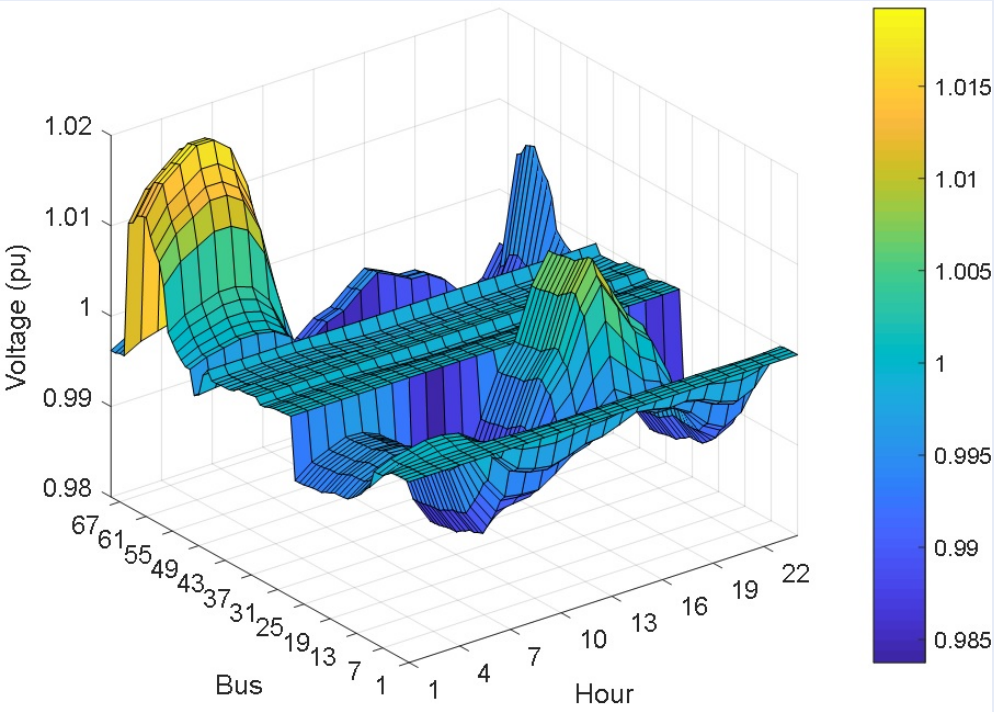

Figure 12: The voltage profile with DGUs from COA's solution at case 2

11. Siddiqui AS, Prashant. Optimal location and sizing of conglomerate DG-FACTS using an artificial neural network and heuristic probability distribution methodology for modern power system operations. Prot Control Mod Power Syst. 2022;7(1):9;Available from: https://doi.org/10.1186/s41601-022-00230-5.
12. Sandhu KS. Optimal location of WT based distributed generation in pool based electricity market using mixed integer non-linear programming. Mater Today Proc. 2018;5(1):445-57;Available from: https://doi.org/10.1016/j.matpr.2017.11.104.
13. Mashayekh S, Stadler M, Cardoso G, Heleno M. A mixed integer linear programming approach for optimal DER portfolio, sizing, and placement in multienergy microgrids. Appl Energy. 2017;187:154-68;Available from: https://doi.org/10.1016/j.apenergy.2016.11.020.
14. Bolfek M, Capuder T. An analysis of optimal power flow based formulations regarding DSO-TSO flexibility provision. Int J Electr Power Energy Syst. 2021;131:106935;Available from: https://doi.org/10.1016/j.ijepes.2021.106935.
15. Ayodele TR, Ogunjuyigbe ASO, Akinola OO. Optimal location, sizing, and appropriate technology selection of distributed generators for minimizing power loss using genetic algorithm. J Renew Energy. 2015;2015:1-9;Available from: https://doi.org/10.1155/2015/832917.
16. Mahmoud K, Yorino N, Ahmed A. Optimal distributed generation allocation in distribution systems for loss minimization. IEEE Trans Power Syst. 2015;31(2):960-9;Available from: https://doi.org/10.1109/TPWRS.2015.2418333.
17. Sanjay R, Jayabarathi T, Raghunathan T, Ramesh V, Mithulananthan N. Optimal allocation of distributed generation using hybrid grey wolf optimizer. IEEE Access. 2017;5:14807-18;Available from: https://doi.org/10.1109/ACCESS.2017.2726586.
18. HassanzadehFard H, Jalilian A. Optimal sizing and location of renewable energy based DG units in distribution systems considering load growth. Int J Electr Power Energy Syst. 2018;101:356-70;Available from: https://doi.org/10.1016/j.ijepes.2018.03.038.
19. Pham LH, Dinh BH, Nguyen TT. Optimal power flow for an integrated wind-solar-hydro - thermal power system considering uncertainty of wind speed and solar radiation. Neural Comput Appl. 2022;34(13):10655-89;Available from: https://doi.org/10.1007/s00521-022-07000-2.
20. Hota AP, Mishra S. A forward-backward sweep based numerical approach for active power loss allocation of radial distribution network with distributed generations. Int J Numer Modell Electron Netw Devices Fields. 2021;34(1):e2788;Available from: https://doi.org/10.1002/jnm.2788.
21. Pierezan J, Coelho LDS. Coyote optimization algorithm: a new metaheuristic for global optimization problems. In: IEEE congress on evolutionary computation (CEC). Vol. 2018. IEEE Publications 1; 2018, July. p. 8;Available from: https://doi.org/10.1109/CEC.2018.8477769.
22. Li S, Chen H, Wang M, Heidari AA, Mirjalili S. Slime mould algorithm: A new method for stochastic optimization. Future Gener Comput Syst. 2020;111:300-23;Available from: https://doi.org/10.1016/j.future.2020.03.055.
23. Xu L, Song B, Cao M. An improved particle swarm optimization algorithm with adaptive weighted delay velocity. Syst Sci Control Eng. 2021;9(1):188-97;Available from: https://doi.org/10.1080/21642583.2021.1891153.
24. Khan MH, Ulasyar A, Khattak A, Zad HS, Alsharef M, Alahmadi AA et al. Optimal sizing and allocation of distributed generation in the radial power distribution system using honey badger algorithm. Energies. 2022;15(16):5891;Available from: https://doi.org/10.3390/en15165891.
25. Oda ES, Hamed AMAE, Ali A, Elbaset AA, Sattar MAE, Ebeed M. Stochastic optimal planning of distribution system considering integrated photovoltaic-based DG and DSTATCOM under uncertainties of loads and solar irradiance. IEEE Ac-

cess. 2021;9:26541-55;Available from: https://doi.org/10.1109/ACCESS.2021.3058589.
26. Hung DQ, Mithulananthan N, Lee KY. Determining PV penetration for distribution systems with time-varying load models. IEEE Trans Power Syst. 2014;29(6):3048-57;Available from: https://doi.org/10.1109/TPWRS.2014.2314133.
27. Kumar M, Soomro AM, Uddin W, Kumar L. Optimal multi-objective placement and sizing of distributed generation in distribution system: A comprehensive review. Energies. 2022;15(21):7850;Available from: https://doi.org/10.3390/en15217850.
28. Navesi RB, Nazarpour D, Ghanizadeh R, Alemi P. Switchable capacitor bank coordination and dynamic network reconfiguration for improving operation of distribution network integrated with renewable energy resources. J Mod Power Syst Clean Energy. 2021;10(3):637-46;Available from: https://doi.org/10.35833/MPCE.2020.000067.
29. Selim A, Kamel S, Alghamdi AS, Jurado F. Optimal placement of DGs in distribution system using an improved harris hawks optimizer based on single-and multiobjective approaches. IEEE Access. 2020;8:52815-29;Available from: https://doi.org/10.1109/ACCESS.2020.2980245.
30. Janamala V, Sreenivasulu Reddy DS. Coyote optimization algorithm for optimal allocation of interline-Photovoltaic battery storage system in islanded electrical distribution network considering EV load penetration. J Energy Storage. 2021;41:102981;Available from: https://doi.org/10.1016/j.est.2021.102981.
31. Ghaitaoui T, Slimane L, Maouedj R, Touahri T. Advance control of a Isofotón-75 W photovoltaic module under MATLAB-Simulink. In: 6th International Renewable and Sustainable Energy Conference (IRSEC) IEEE 1-4. Vol. 2018; 2018, December;Available from: https://doi.org/10.1109/IRSEC.2018.8703003.
32. Radosavljević J, Arsić N, Milovanović M, Ktena A. Optimal placement and sizing of renewable distributed generation using hybrid metaheuristic algorithm. J Mod Power Syst Clean Energy. 2020;8(3):499-510;Available from: https://doi.org/10.35833/MPCE.2019.000259.
33. Masaud TM, El-Saadany EF. Optimal wind DG integration for security risk-based line overload enhancement: A two stage approach. IEEE Access. 2020;8:11939-47;Available from: https://doi.org/10.1109/ACCESS.2020.2965157.
34. Owolabi AB, Yakub AO, Li HX, Suh D. Performance evaluation of two grid-connected solar photovoltaic systems under temperate climatic conditions in South Korea. Energy Rep. 2022;8:12227-36;Available from: https://doi.org/10.1016/j.egyr.2022.09.053.